



**MEDRC**

**MEDRC Series of R&D Reports  
MEDRC Project: 07-AS-003**

# **Environmental planning, prediction and management of brine discharges from desalination plants**

*Final report*

**Principal Investigators**

**Dr.-Ing. Tobias Bleninger & Prof. G.H. Jirka, Ph.D.**  
Institute for Hydromechanics, Karlsruhe Institute of Technology, Germany

**Middle East Desalination Research Center  
Muscat, Sultanate of Oman**

**December 2010**

# Project Participants

## Project coordination / principle investigators:

*Dr.-Ing. Tobias Bleninger*  
*Prof. G.H. Jirka, Ph.D.*<sup>1</sup> Institute for Hydromechanics (IfH), Karlsruhe Institute of Technology, 76128 Karlsruhe, Germany  
Tel.: +49 - 721 / 608-2200, Fax: +49 - 721 / 608-2202  
E-mail: bleninger@kit.edu , URL: www.ifh.uni-karlsruhe.de

*Dipl.-Ing. Anne Niepelt* Research assistant at the IfH

*Dipl.-Wi.-Ing. Frank Münk* Diploma student of Engineering Economics in cooperation with the IfH at the Karlsruhe Institute of Technology

## Project partners:

*Prof. Anton Purnama &*  
*Prof. Hamdi H. Al-Barwani* Sultan Qaboos University (SQU),  
Department of Mathematics and Statistics  
P.O. Box 36, Al-Khod PC 123, Muscat, Sultanate of Oman  
Tel: +968 2414 1425, Fax: +968 2441 3415  
E-mail: hamdi@squ.edu.om, URL: www.squ.edu.om/sci/Math/

*Prof. Robert L. Doneker* MixZon Inc. and Department of Civil and Environmental  
Engineering, Portland State University, Oregon, USA  
1033 SW Yamhill Street, Suite 301  
Portland, Oregon 97205-2539, USA  
Tel.: +1 - 503 222 1022, Fax: +1 - 503 296 2354  
E-mail: doneker@mixzon.com, URL: www.mixzon.com

*Dr. Sabine Lattemann, M.Sc.* ARSU - Regional Planning and Environmental  
*Prof. Dr. Thomas Höpner* Research group, Escherweg 1, 26121 Oldenburg, Germany  
*Dipl.biol.H.Brunken-Winkler* Tel.: +49 - 441 / 97174 - 97, Fax: +49 - 441 / 97174 - 73  
E-mail: sabine.lattemann@icbm.de, URL: www.arsu.de

**Project web-page:** [www.brinedis.net.ms](http://www.brinedis.net.ms)

---

<sup>1</sup> Prof. G.H. Jirka died the 14.02.2010 following a strong heart attack. All project participants are deeply lamenting this enormous loss.

# CONTENTS

<b>LIST OF TABLES .....</b>	<b>4</b>
<b>LIST OF FIGURES .....</b>	<b>5</b>
<b>ABSTRACT .....</b>	<b>14</b>
<b>ACKNOWLEDGEMENTS.....</b>	<b>15</b>
<b>EXECUTIVE SUMMARY .....</b>	<b>16</b>
<b>Nomenclature.....</b>	<b>18</b>
<b>1. Introduction .....</b>	<b>19</b>
<b>2. Intake-, treatment-, disposal-Systems.....</b>	<b>23</b>
2.1. Intake systems	23
2.2. Treatment systems	25
2.3. Process related effluent characteristics	29
2.4. Disposal systems	31
2.4.1. Surface water discharge systems .....	32
<b>3. Environmental Impacts.....</b>	<b>44</b>
3.1. Installed capacities - discharge loads and concentrations	44
3.2. Literature review on environmental impacts	60
3.3. Literature review of socio-economic aspects	61
3.3.1. MENA region.....	61
3.3.2. USA, Spain, Australia.....	64
3.3.3. Socio-economic effects .....	69
3.4. Environmental standards	70
3.4.1. Temperature .....	72
3.4.2. Salinity .....	72
3.4.3. Residual chemicals – effluent standards (ES).....	73
3.4.4. Residual chemicals – ambient standards (AS).....	74
3.4.5. Regulatory mixing zone regulations .....	75
3.4.6. Omani regulations on mixing zones .....	80
3.5. Summary and recommendations for mitigation measures	81
<b>4. Mixing Processes of Brine Discharges .....</b>	<b>84</b>
4.1. Near-field processes	87
4.2. Intermediate-field processes	89
4.3. Far-field processes	95
<b>5. Brine discharge models .....</b>	<b>99</b>
5.1. Brine discharge design objectives	99
5.2. Screening equations - nomograms	102
5.2.1. Density and viscosity calculator .....	102
5.2.2. Discharge calculator.....	105
5.2.3. Length scale analysis and flow classification .....	108
5.2.4. Nomograms and screening equations (RO) .....	113
5.2.5. Empirical dilution equations (MSF) .....	119
5.3. Near-field models	121
5.3.1. CORMIX system .....	121

5.3.2. VisJet.....	125
5.3.3. Model comparison and model choice .....	125
5.4. Far-field models .....	128
5.4.1. Model choice.....	129
5.4.2. Delft3D .....	129
5.5. Linked brine discharge modeling .....	132
5.5.1. Coupling step 1: Pre-processing.....	132
5.5.2. Coupling step 2: CorTime .....	140
5.5.3. Coupling step 3: Post-processing .....	143
5.5.4. Coupling step 4: Model linking.....	145
5.5.5. Coupling step 5: Delft3D-FLOW .....	153
<b>6. Case studies .....</b>	<b>156</b>
6.1. Case studies for discharge calculator and CORMIX modeling analysis .....	156
6.1.1. Overview of seawater desalination in Oman .....	156
6.1.2. Characteristics of Barka desalination plants .....	159
6.1.3. Barka intake and outfall system.....	161
6.1.4. Marine environment at Barka plants location.....	164
6.1.5. Oceanographic field data at Barka plant location.....	169
6.1.6. Application of discharge calculator for Barka plants .....	174
6.1.7. CORMIX simulation for Barka plants.....	179
6.2. Theoretical case study for coupling analysis .....	186
6.2.1. Results of the near-field modeling.....	186
6.2.2. Coupling configurations.....	189
6.2.3. Results of the (coupled) far-field modeling .....	190
<b>7. Conclusions.....</b>	<b>194</b>
<b>8. References.....</b>	<b>196</b>
<b>APPENDIX C: Project Profile Form .....</b>	<b>207</b>
<b>APPENDIX D: Desalination Technologies .....</b>	<b>210</b>
<b>APPENDIX E: Environmental Impacts.....</b>	<b>215</b>
<b>APPENDIX F: Review of Environmental Impact Assessments.....</b>	<b>225</b>
<b>APPENDIX G: Capacity Building Materials .....</b>	<b>237</b>

## LIST OF TABLES

Table 1: Comparison of properties of MSF and RO plants (following Goebel, 2005). Discharge characteristics are assumed for a typical MSF plant (recovery: 10 %, $\Delta T = 10$ °C) and a RO plant (recovery: 32 %) with a fresh water production of $Q_{fresh} = 345$ ML/d = 4 m <sup>3</sup> /s according to Lattemann and Höpner (2003). "o" indicates the effluent characteristics. Ambient properties: $\rho = 1023.5$ kg/m <sup>3</sup> ; $Sal = 36.3$ ; $T = 27.7$ °C. $Q$ = flow rate, $T$ = temperature, $Sal$ = salinity, $\rho$ = density. (Figure 11) .....	29
Table 2: Comparison of brine disposal options for desalination plants (based on Alameddine and El-Fadel, 2007; Moch, 2007; Department of Natural Resources and Mines, 2003).....	32
Table 3: Intake pretreatment and discharge design of major SWRO plants (source: Consultants Intl. (2006) Environmental Literature Review and Position Paper for Perth Seawater Desalination Plant Two and Sydney Seawater Reverse Osmosis Plant) .....	41

Table 4: Effluent properties of RO, MSF and MED plants, assuming conventional process design (WHO, 2008; Lattemann and Höpner, 2008) .....	45
Table 5: Maximum values for <i>effluents</i> from thermal power plants (World Bank Group, 1998).....	74
Table 6: Maximum values for selected parameters for <i>effluent discharges</i> into the marine environment (Sultanate of Oman, 2005).....	74
Table 7: US EPA National Recommended Water Quality Criteria for selected pollutants .....	75
Table 8: Examples for emission standards (ES) and ambient standards (AS) for two selected pollutants.....	75
Table 9: Proposed indexes for defining N (reproduced from Freire, 2008) .....	79
Table 10: Omani discharge limits for selected effluent pollutants (based on Decision No. 159/2005) .....	80
Table 11: Environmental impact of RO and MSF effluents .....	82
Table 12: Potential harmfulness of major pollutants in MSF and RO effluents .....	83
Table 13: Environmental benefits and costs of major technologies in reference to conventional desalination systems.....	83
Table 14: Overview of dominant processes for coastal submerged multipoint discharges .....	86
Table 15: Feature comparison table amongst different CORMIX 6.0 versions is as follows:.....	124
Table 16: Structure of the CorTime input document <i>CorTimeInput.txt</i> , parameter definitions .....	133
Table 17: Coupling step 1: Pre-processing.....	140
Table 18: Coupling step 2: CorTime (CorTime, 2008).....	140
Table 19: Structure of CorTime output document <i>CorTime-Status Report.txt</i> , parameter definitions	142
Table 20: Coupling step 3: Post-Processing.....	143
Table 21: Coupling step 4: Model linking.....	146
Table 22: Structure of the flow rate input document <i>flowrate.dis</i> of Delft3D-FLOW. The header block.....	148
Table 23: <i>Left</i> : Structure of the input document <i>xy2mminp.txt</i> for conversion of Cartesian coordinates .....	150
Table 24: Coupling step 5: Delft3D-FLOW.....	154
Table 25: Projected water demands in Oman.....	158
Table 26: Quantities of seawater intake and outfall discharge during normal plant operation .....	163
Table 27: Barka I plant water characteristics during normal plant operation.....	163
Table 28: Comparison between sample concentrations collected from Barka I plant (Abdul-Wahab and Jupp, 2009).....	169
Table 29: Meteorological data for Seeb for the year 2002 (HMR, 2007) .....	171
Table 30: The surface seawater data collected annually at the Barka I plant.....	173
Table 31: Input data for the application of the discharge calculator to the Barka plants .....	177
Table 32: Input data for the CORMIX simulation of scenario I .....	180
Table 33: NRF characteristics of scenario I .....	181
Table 34: RMZ characteristics of scenario I .....	181
Table 35: Input data for the CORMIX simulation of scenario II .....	183
Table 36: NRF characteristics of scenario II.....	184
Table 37: RMZ characteristics of scenario II.....	184

## LIST OF FIGURES

Figure 1: Al Ghubrah desalination plant (largest in Oman, capacity 191,000 m <sup>3</sup> /d): Brine discharge through an open channel at the coast into the Gulf of Oman (photo: H.H. Al-Barwani).....	19
Figure 2: Mixing characteristics and substance distributions for different brine discharge configurations and effluents (Bleninger et al., 2006). <i>a</i> ) RO plant (dense effluent) shoreline discharge via channel or weir, <i>b</i> ) Thermal plant (dense effluent mixed with buoyant cooling water) shoreline discharge via channel or weir, <i>c</i> ) submerged discharge (dense effluent) via pipeline and nozzle or diffuser.....	21
Figure 3: Open intake tower with "velocity cap". Reproduced from Cannesson et al. (2009).....	24

Figure 4: Sub-seabed intake via Horizontal Directional Drilling (California American Water, 2004).....	24
Figure 5: Several horizontal subseabed drills with filtration region shown in light blue (Neodren system, Peters and Pinto, 2006).....	25
Figure 6: Typical pretreatment steps for MSF (above) and RO plants (below) (Höpner and Lattemann, 2008).....	25
Figure 7: Range of filtration systems and membrane processes (Passavant Roedinger, 2008).....	27
Figure 8: Comparison of flow rates in the conventional SWRO system with 35 % recovery (above) and in the NF-SWRO system with 60 % recovery each (below) (based on Hassan et al., 1998).....	28
Figure 9: Desalination effluent characteristics. Top: RO-effluent, down: MSF-effluent.....	30
Figure 10: Capital costs of major concentrate disposal options depending on the concentrate flow rate (Mickley, 2006).....	31
Figure 11: Brine discharge characteristics of desalination plants .....	33
Figure 12: Shoaiba (KSA), MSF Plant, Red Sea, 1.58 million m <sup>3</sup> /d, positively buoyant discharge (Source: Google Earth).....	33
Figure 13: Carlsbad RO plant, USA, positively/negatively buoyant discharge (Source: Poseidon Resources).....	34
Figure 14: Al Jubail (KSA), MSF plant, Arabian Gulf, 1.54 million m <sup>3</sup> /d, positively buoyant discharge (Source: Google Earth).....	34
Figure 15: Ashkelon (Israel), RO plant with negatively buoyant brine discharge during backwash through an open channel at the coast into the Mediterranean (Courtesy of Rani Amir, Director of the Marine and Coastal Environment Division, Israel Ministry of the Environment) besides positively buoyant cooling water effluents. ....	35
Figure 16: Al Gubrah (Oman), MSF plant, 191,000 m <sup>3</sup> /d, Gulf of Oman, positively buoyant discharge (Source: Google Earth).....	35
Figure 17: Jebel Ali MSF plant, UAE, power and water cogeneration plant with desalination capacity of 1.64 Mm <sup>3</sup> /d, positively buoyant discharge (Source: Google Earth).....	36
Figure 18: Taweelah MSF plant, Arabian Gulf, 1.12 mio m <sup>3</sup> /d, positively buoyant discharge (Source: Google Earth).....	36
Figure 19: Layout of an outfall pipeline with multiport diffuser (Bleninger, 2007) .....	37
Figure 20: Typical construction details for multiport diffusers in water bodies: (a) Diffuser pipe on bottom with port holes, (b) diffuser pipe buried in trench with short risers, (c) deep tunnel construction with long risers .....	37
Figure 21: Antalya wastewater outfall (Turkey) during installation in 1997. <i>Top</i> : Diffuser section assembling on shore. <i>Down</i> : Feeder section ( $L_F = 5$ km, HDPE pipe, $D = 1600$ mm) while sinking with attached concrete weights on the seabed (PipeLife Company).....	38
Figure 22: Boston outfall during installation in 1998. <i>Left</i> : View into tunnel section (16 km with 8 m diameter). <i>Right</i> : One out of 55 riser caps with eight outlets each in rosette-like configuration (Roberts and Snyder, 1993).....	38
Figure 23: Schematic designs for Sydney (Australia) RO plant, 125,000-500,000 m <sup>3</sup> /d, similarly applied for Perth RO plant, 140.000m <sup>3</sup> /d. Open intake towers located 200-300m offshore in a depth of approximately 20-30m. Outfall diffuser located 250-350m offshore in a water depth of approximately 20-30m. 20 risers spaced 25m discharging through 2 ports with an angle of 60° to the horizontal, (Source: Sydney Water and Fichtner, 2005).....	39
Figure 24: Operating diffuser outfall port of Australian RO plants. Left: Diver behind discharging outfall port (Source: Alspach et al., 2009). Right: Diver besides discharging diffuser port during tracer experiment to measure dilution characteristics (Source: Christie and Bonnélye, 2009). Bottom: Results of model studies and measurements showing salinity concentrations in certain distances of discharge point, being in compliance with the water quality criteria (WQC) of 1ppt above ambient within 75m distance from the discharge (Source: Sydney Water and Fichtner, 2005).....	40
Figure 25: Global desalination capacity (in Mm <sup>3</sup> /d and %) by source water type (top row), by process and source water type (2nd row), by use type and source water type (3rd row) and by plant size and source water type (last row). Abbreviations: reverse osmosis (RO),	

- multi-stage flash distillation (MSF), multi-effect distillation (MED), nanofiltration (NF), electro dialysis (ED), XL>50,000m<sup>3</sup>/d, L>10,000m<sup>3</sup>/d, M>1,000m<sup>3</sup>/d (IDA, 2008)..... 47
- Figure 26: Global desalination capacity in m<sup>3</sup>/d and %. For example, the installed capacity in Southern Europe is 4,405,024 m<sup>3</sup>/d. This figure includes all source water types. Seawater desalination accounts for most of the production in Southern Europe, brackish water for about 1/4 of the production and waste water desalination plays a relatively minor role (pie diagram). The figures next to the pie diagram give the contribution to the global production, i.e., the seawater desalination capacity in Southern Europe represent 10.6% of the global seawater desalination capacity. The brackish water capacity - though it is less than half the seawater desalination capacity in Southern Europe - represents 12.8% of the global brackish water desalination capacity (IDA, 2008) ..... 48
- Figure 27: Capacity: Cumulative MSF, MED and RO capacities in m<sup>3</sup>/day by site location (dots) and by country (triangles). The map shows all sites with an installed capacity ≥ 1,000 m<sup>3</sup>/d and displays sites with a capacity ≥ 100,000 m<sup>3</sup>/d by name and capacity. The map was first published in Lattemann and Höpner (2003) and updated using raw data from IDA and GWI (2008) ..... 49
- Figure 28: Chlorine: Estimated discharge of chlorine from MSF and MED distillation plants in kg/day. The figures were calculated from the installed desalination capacity, assuming a product recovery rate of 10 % for MSF and 20 % for MED plants (i.e. waste water flows of 90 % and 80 %, respectively), and assuming a residual chlorine concentration of 0.25 mg/l in the combined waste water of the MSF and MED process (i.e. concentrate and cooling water), resulting in a specific chlorine load of 2.3 kg/day for MSF and 1 kg/day for MED for every 1,000 m<sup>3</sup>/d. The estimated total load for the Arabian Gulf is 22.2 tons of chlorine from MSF plants and 1.5 tons from MED plants per day. The map shows all sites with an installed capacity ≥ 1,000 m<sup>3</sup>/d and displays the chemical load for all sites with a chlorine load ≥ 100 kg/d. The map does not take chlorine discharges from co-located power plants into account ..... 50
- Figure 29: Antiscalant: Estimated discharge of antiscalants from MSF and RO plants in kg/day. The figures were calculated from the installed desalination capacity, assuming a product recovery rate of 10 % for MSF and 33.3 % for RO plants, and assuming an antiscalant dosage of 2 mg/l to the make-up water in the MSF plant / respectively to the feedwater in the RO plant (for the given assumptions, the specific antiscalant loads are identical for MSF and RO plants, i.e. 6 kg/day for every 1,000 m<sup>3</sup>/d installed capacity). The estimated total load for the Arabian Gulf is 59.1 tons of antiscalants from MSF plants and 5.8 tons from RO plants per day. The map shows all sites with an installed capacity ≥ 1,000 m<sup>3</sup>/d and displays the chemical load for all sites with an antiscalant load ≥ 500 kg/d ..... 51
- Figure 30: Copper: Estimated discharge of copper from MSF plants in kg/day. The figures were calculated from the installed desalination capacity, assuming a product recovery rate of 10 % and a residual copper level of 15 µg/l in the concentrate of the MSF plant, resulting in a specific copper load of 0.03 kg/day for every 1,000 m<sup>3</sup>/d. The estimated total load for the Arabian Gulf is 296 kg of copper from MSF plants per day. The map shows all sites with an installed capacity ≥ 1,000 m<sup>3</sup>/d and displays the chemical load for all sites with a copper load ≥ 10 kg/day. The map does not take copper discharges from cooling water discharges (neither from the distillation plant nor from co-located power plants) into account ..... 52
- Figure 31: Ecosystems. Most of the desalination plants are located on the south-western shoreline of the Arabian Gulf which is characterized by shallow waters (< 25 m), bays fringed with coral reefs, mangroves and seagrasses. It can be estimated that the combined discharge of all MSF plants (9.9 million m<sup>3</sup>/day) amounts to a waste water flow of more than 1000 m<sup>3</sup>/s, which is the equivalent of a large river. This waste water is characterised by increased salinity and temperature and loaded with residual additives, including chlorine and antiscalants, as well as corrosion products such as copper. Daily discharge loads of these compounds from desalination plants into the Arabian Gulf are estimated to be at about 24 tons of chlorine, 65 tons of antiscalants and 0.3 tons of copper per day. Residual chlorine and chlorination by-products such as trihalomethanes,

chlorophenols and chlorobenzenes are detectable near desalination plants, and chlorine pollution has been reported to affect two mud flat areas in the Bay of Kuwait, which is probably caused by the Doha power and desalination plant. Nothing is known about the environmental fate and effects of the antiscalant discharges, and signals of copper contamination in water, sediment and organisms attributed to desalination activity are also missing, possibly due to a lack of consequent monitoring. To date, no impact assessment study has been published which is based on field investigations and comprehensively investigates the single or cumulative impacts of desalination plants on the Arabian Gulf's ecosystem..... 53

- Figure 32: Capacity: Cumulative MSF, MED and RO capacities in m<sup>3</sup>/day by site location (dots) and by country (triangles). The map shows all sites with an installed capacity ≥ 1,000 m<sup>3</sup>/d and displays sites with a capacity ≥ 50,000 m<sup>3</sup>/d by name and capacity. The map was first published in Lattemann and Höpner (2003) and updated using raw data from IDA and GWI (2008)..... 54
- Figure 33: Chlorine: Estimated discharge of chlorine from MSF and MED distillation plants in kg/day. The figures were calculated from the installed desalination capacity, assuming a product recovery rate of 10 % for MSF and 20 % for MED plants (i.e. waste water flows of 90 % and 80 %, respectively), and assuming a residual chlorine concentration of 0.25 mg/l in the combined waste water of the MSF and MED process (i.e. concentrate and cooling water), resulting in a specific chlorine load of 2.3 kg/day for MSF and 1 kg/day for MED for every 1,000 m<sup>3</sup>/d. The estimated total load for the Mediterranean is 1,356 kg of chlorine from MSF plants and 588 kg from MED plants per day. The map shows all sites with an installed capacity ≥ 1,000 m<sup>3</sup>/d and displays the chemical load for all sites with a chlorine load ≥ 50 kg/d. The map does not take chlorine discharges from co-located power plants into account..... 55
- Figure 34: Antiscalant: Estimated discharge of antiscalants from MSF and RO plants in kg/day. The figures were calculated from the installed desalination capacity, assuming a product recovery rate of 10 % for MSF and 33.3 % for RO plants, and assuming an antiscalant dosage of 2 mg/l to the make-up water in the MSF plant / respectively to the feedwater in the RO plant (for the given assumptions, the specific antiscalant loads are identical for MSF and RO plants, i.e. 6 kg/day for every 1,000 m<sup>3</sup>/d installed capacity). The estimated total load for the Mediterranean is 3.6 tons of antiscalants from MSF plants and 19.4 tons from RO plants per day. The map shows all sites with an installed capacity ≥ 1,000 m<sup>3</sup>/d and displays the chemical load for all sites with an antiscalant load ≥ 50 kg/d..... 56
- Figure 35: Copper: Estimated discharge of copper from MSF plants in kg/day. The figures were calculated from the installed desalination capacity, assuming a product recovery rate of 10 % and a residual copper level of 15 µg/l in the concentrate of the MSF plant, resulting in a specific copper load of 0.03 kg/day for every 1,000 m<sup>3</sup>/d. The estimated total load for the Mediterranean is 18 kg of copper from MSF plants per day. The map shows all sites with an installed capacity ≥ 1,000 m<sup>3</sup>/d and displays the chemical load for all sites with a copper load ≥ 1 kg/day. The map does not take copper discharges from cooling water discharges (neither from the distillation plant nor from co-located power plants) into account..... 57
- Figure 36: Capacity: Cumulative MSF, MED and RO capacities in m<sup>3</sup>/day by site location (dots) and by country (triangles). The map shows all sites with an installed capacity ≥ 1,000 m<sup>3</sup>/d and displays sites with a capacity ≥ 100,000 m<sup>3</sup>/d by name and capacity. The map was first published in Lattemann and Höpner (2003) and updated using raw data from IDA and GWI (2008)..... 58
- Figure 37: Chlorine: Estimated chemical discharges from MSF, MED and RO plants in kg/day. The figures were calculated from the installed desalination capacity, assuming a product recovery rate of 10 % for MSF, 20 % for MED plants and 33.3 % for RO plants. The chlorine estimate is based on a residual chlorine concentration of 0.25 mg/l in the combined waste water of the MSF and MED process (i.e. concentrate and cooling water), resulting in a specific chlorine load of 2.3 kg/day for MSF and 1 kg/day for MED for every 1,000 m<sup>3</sup>/d. The estimated total load for the Red Sea is 5.5 tons of

chlorine from MSF plants and 144 kg from MED plants per day. The copper estimate is based on a residual copper level of 15 µg/l in the concentrate of the MSF plant, resulting in a specific copper load of 0.03 kg/day for every 1,000 m<sup>3</sup>/d. The estimated total load for the Red Sea is 74 kg of copper from MSF plants per day. The antiscalant estimate is based on an antiscalant dosage of 2 mg/l to the make-up water in the MSF plant / respectively to the feedwater in the RO plant (for the given assumptions, the specific antiscalant loads are identical for MSF and RO plants, i.e. 6 kg/day for every 1,000 m<sup>3</sup>/d installed capacity). The estimated total load for the Red Sea is 14.7 tons of antiscalants from MSF plants and 6 tons from RO plants per day. The maps show all sites with an installed capacity ≥ 1,000 m<sup>3</sup>/d and display the chemical load for all sites with a chlorine and antiscalant loads ≥ 50 kg/d and a copper load ≥ 10 kg/d. It does not take chlorine and copper discharges from co-located power plants into account..... 59

Figure 38: Assessment of environmental problems according to respondents in MENA countries (Tolba and Saab, 2006) .....	62
Figure 39: Results of an opinion poll on seawater desalination in San Diego County (San Diego County Water Authority, 2004) .....	65
Figure 40: Environmental concerns about seawater desalination in San Diego County (San Diego County Water Authority, 2004) .....	66
Figure 41: Result of a community consultation on the question: which factor is the most important when considering the location of a desalination plant (Reproduced from Cannesson et al., 2009) .....	69
Figure 42: Example of regulatory mixing zone specification for offshore submerged coastal discharges: The horizontal extent of the mixing zone is defined by some multiple N of the average water depth $H_{ave}$ at the sea outfall.....	78
Figure 43: Schematic view of an operating multiport diffuser outfall merged with a laboratory picture of a trapped waste plume in stratified ambient (modified from Domenichini et al., 2002) .....	84
Figure 44: Laboratory studies showing a dense discharge, having a density difference scaled to a difference resulting from an RO effluent with 50% recovery. The ambient conditions are equal for all experiments with a constant flow from left to right. The ratio of the discharge velocity to the ambient velocity has been chosen according to real values $R = 5\text{m/s} / 0.2\text{m/s} = 25$ . For the discharge conditions only the vertical discharge angle varied from 0° (horizontal discharge) to 60°. The images show the side views on the left and the top views on the right side for each discharge angle.....	85
Figure 45: Typical temporal and spatial scales for transport and mixing processes related to coastal wastewater discharges (Jirka et al., 1976; Fischer et al., 1979) .....	87
Figure 46: Schematized figures and visualizations from laboratory experiments showing different positively buoyant jet trajectories influenced by <i>a</i> ) ambient density, <i>b</i> ) ambient current $u_a$ , and <i>c</i> ) ambient stratification (Jirka et al., 1996; pictures from G.H. Jirka; L. Fan).....	87
Figure 47: Schematization and visualization of laboratory experiment for merging of jets discharged unidirectional by multiport diffusers (reproduced from Jirka, 2006) .....	88
Figure 48: Schematization of merging jets discharged by a multiport diffusers with an alternating port arrangement in stagnant conditions and in crossflow (reproduced from Jirka, 2006)..	89
Figure 49: Submerged buoyant slot jet discharging into stagnant water of finite depth (Jirka, 1982). <i>a</i> ) Deep water discharge with stable discharge configuration, <i>b</i> ) shallow water discharge with unstable recirculation zone (reproduced from Jirka et al., 1996).....	90
Figure 50: Laboratory experiment for a dense jet discharge into a density stratified and flowing environment. Left image: slow ambient velocity. Right image: higher ambient velocity (courtesy of G.H. Jirka, L. Fan, Keck Lab, CIT) .....	90
Figure 51: Pictures of laboratory experiments showing boundary interactions with the surface, the bottom and the pycnocline (courtesy of G.H. Jirka, L. Fan, Keck Lab, CIT).....	91
Figure 52: Examples of boundary interactions for submerged positively buoyant jets in finite depth (reproduced from Jirka et al., 1996).....	91
Figure 53: Submerged negatively buoyant single port discharge into a flowing unstratified receiving water on a sloping bottom (source: Doneker et al., 2004) .....	92

Figure 54: Buoyant spreading processes after near-field region (upstream and lateral spreading), superimposed on the transport by ambient currents (reproduced from Jirka and Akar, 1991)	93
Figure 55: Measured concentration maps for salinity (left) and turbidity (right) at the seabed (top) and the surface (down) for two negatively buoyant RO discharges in Spain (Reproduced from Perez Talavera and Quesada Ruiz, 2001)	94
Figure 56: Measured vertical velocity distributions close to dense RO discharge in Spain (Reproduced from Payo et al., 2009)	94
Figure 57: Examples of <i>a</i> ) wake attachment and <i>b</i> ) Coanda attachment conditions for jets discharging near boundaries (reproduced from Jirka et al., 1996)	95
Figure 58: Surface plume in a long shore coastal current produced by a submerged sea outfall. The infrared image shows the plume produced by the cooling water discharge from a power plant at the western coast of Florida.	96
Figure 59: Left: Buoyant spreading process, right: passive ambient diffusion process (modified from: Doneker and Jirka, 2007)	96
Figure 60: Example showing far-field waste plume transport and dispersion. The transport is governed by the tidal current and mixing is governed by the wind shear stress (courtesy of Torben Larsen, Denmark)	97
Figure 61: Typical temporal and spatial scales for transport and mixing processes related to coastal wastewater discharges and model capabilities (Jirka et al., 1976; Fischer et al., 1979)	101
Figure 62: Screenshot of density calculator (download under: <a href="http://www.brinedis.net.ms">www.brinedis.net.ms</a> )	103
Figure 63: Differences in density calculation between different calculators for varying salinities and temperatures	103
Figure 64: Nomogram for defining the effluent or seawater density and viscosity for different salinities and temperatures using the relationship from El-Dessouky and Ettouny (2002)	104
Figure 65: First table of the RO-discharge-calculator to compute the final effluent characteristics	106
Figure 66: First table of the MSF-discharge-calculator to compute the final effluent characteristics	107
Figure 67: Jet to plume transition length scale $L_M$ for a single jet allows distinguishing between a jet like or plume like single jet behavior (reproduced from Jirka et al, 1996)	109
Figure 68: Table 2 of the RO-discharge-calculator to compute characteristic discharge parameters	110
Figure 69: Table 2 of the MSF-discharge-calculator to compute characteristic discharge parameters	111
Figure 70: CORMIX flow classification tree for bottom attachment (reproduced from Jirka et al., 1996)	112
Figure 71: CORMIX flow classification tree for a near-surface negatively buoyant multipoint discharge into stratified ambient water (reproduced from Jirka et al., 1996)	112
Figure 72: Flow classification tree within CORMIX, for a buoyant multipoint discharge in stratified ambient waters (reproduced from Jirka et al., 1996)	113
Figure 73: 3-dimensional horizontal buoyant jet trajectories for a single port discharge in stagnant ambient. Comparison between predictions and experimental data. <i>Left</i> : normalized with port diameter. <i>Right</i> : normalized with momentum length scale $L_M$ (reproduced from Jirka, 2006)	114
Figure 74: Schematic side view of negatively buoyant jet discharging into stagnant ambient with sloping bottom (Jirka, 2008)	114
Figure 75: Jet trajectories. Negatively buoyant jet behavior for a complete range of discharge angles $0^\circ \leq \theta_0 \leq 90^\circ$ and with variable offshore slopes $\theta_B$ from $0^\circ$ to $30^\circ$ . A zero discharge height, $h_0 = 0$ , is assumed.	116
Figure 76: Bulk dilutions $S_i$ at impingement point as a function of discharge angle $\theta_0$ . Negatively buoyant jet behavior for complete range of discharge angles $0^\circ \leq \theta_0 \leq 90^\circ$ and with variable offshore slopes $\theta_B$ from $0^\circ$ to $30^\circ$ . A zero discharge height, $h_0 = 0$ , is assumed.	116
Figure 77: Jet properties at maximum level of rise. Comparison of CorJet model with experimental data. (a) Geometric properties, (b) Minimum centerline dilution, both as a function of discharge angle $\theta_0$	117
Figure 78: Table 3 of the RO-discharge-calculator to analyze jet discharge characteristics and dilution values	118

Figure 79: Displacement of impingement point due to increasing port height .....	119
Figure 80: Comparison of jet and mixing models .....	127
Figure 81: Schematic illustration of the range of model applicability in regulatory discharge zone analysis (source: www.cormix.info) .....	127
Figure 82: Depth averaged ambient velocity $U_a$ and its direction $\phi$ measured clockwise from the north, .....	135
Figure 83: Determination of the magnitude of the depth averaged ambient velocity $U_a$ and its direction $\phi$ measured clockwise from the north (field data: velocity $Vel$ , direction $\Phi$ ).....	135
Figure 84: Discharge geometry: a) submerged single port (CORMIX1), b) multiport diffuser (CORMIX2) (modified from: Doneker and Jirka, 2007).....	136
Figure 85: Definition of the alignment angle $\gamma$ , examples for three orientation angles: $\alpha = 0^\circ, 90^\circ, 180^\circ$ .....	136
Figure 86: Different approximations for representing the ambient density stratification within CORMIX (source: Doneker and Jirka, 2007) .....	137
Figure 87: Approximations for ambient density distribution: uniform (defined by $\rho_{a,m}$ ) or linear stratified (defined by $\rho_{a,s}$ and $\rho_{a,b}$ ). <i>Left</i> : constant water level, <i>right</i> : variable water level	137
Figure 88: Example plot for CorTime input parameters $Q_o, C_o, U_a, H_a$ , and $\rho_{a,m}$ indicating $\rho_{a,b}$ and .	138
Figure 89: Example plots for current direction parameters $\phi, \sigma$ and $\gamma$ plotted on a circular grid.....	139
Figure 90: Example plot: Statistical analysis (relative frequency and cumulative distribution) of the	139
Figure 91: The graphic user interface for CORMIX v5.0 with active <i>Ambient</i> tab .....	140
Figure 92: Cross-sectional distributions of CORMIX predicted jet/plume sections (source: CORMIX user manual (Doneker and Jirka, 2007)).....	142
Figure 93: Example plot for CorTime output parameters: dilution, plume thickness, and plume elevation at the end of the near-field.....	144
Figure 94: Example scatter plot: endpoints of the near-field and the RMZ indicating the corresponding.....	144
Figure 95: Example plot: Statistical analysis (relative frequency and cumulative distribution) for ...	145
Figure 96 Transformation of CORMIX plume coordinates (NFRX, NFRY, NFRZ) into corresponding grid cells (M, N, K) of Delft3D via global coordinates ( $x, y, z$ ). Division of the flow rate $Q_o$ in $i$ parts ( $i =$ number of cells): $Q_o = \sum Q_i$ , $Q_i$ depends on the cell size. Concentration $C$ , salinity $Sal$ , temperature $T$ remain the same since they are properties of $Q$ : $C_i = C_o, Sal_i = Sal_o, T_i = T_o$ .....	146
Figure 97: Transformation of coordinates of the plume at the end of the near-field:.....	149
Figure 98: The GUI of the FLOW input processor of Delft3D with active data group 'Discharge'....	155
Figure 99: Location and installed capacities of major seawater desalination plants in Oman (Munk, 2008).....	157
Figure 100: Al-Ghubrah power generation and seawater desalination plant (file photo: HMR Consultants) .....	157
Figure 101: Impact of the RO plant near Sur effluent on a nearby coral reef: Transition to the impact zone (left) and close-up view of dead corals within the impact zone (right) (courtesy of Michel Claereboudt) .....	159
Figure 102: Boat landing by fishermen at Barka beach (file photo: HMR Consultants) .....	160
Figure 103: AES Barka I power generation and seawater desalination plant (file photo: HMR Consultants) .....	160
Figure 104: The intake and outfall systems of Barka I plant. Barka II will share the intake and outfall structures with Barka I. The other structures are for future installations (modified HMR, 2007).....	161
Figure 105: Velocity cap intake terminal (left) and fish community inside the velocity cap (right) (file photo: HMR Consultants) .....	162
Figure 106: The intake and outfall system of Barka I plant (modified Abdul-Wahab and Jupp, 2009).....	162
Figure 107: Multiport diffusers at the end of the outfall pipes.....	163
Figure 108: Bathymetry contour of the Barka plants location site (modified Wallingford, 2001) .....	164
Figure 109: Location of field survey by the HMR Consultants (HMR, 2007).....	165

Figure 110: (a) Barnacles found at an inspection valve (left). (b) Reef scallops found on the rock piles around an inspection valve (right) (file photo: HMR Consultants).....	165
Figure 111: Fish community found on the rock piles stabilising an inspection valve (file photo: HMR Consultants) .....	166
Figure 112: Outfall diffuser for discharge of brine (file photo: HMR Consultants) .....	166
Figure 113: Fish community around the outfall diffuser (file photo: HMR Consultants).....	167
Figure 114: Sediment sampling stations in the vicinity of Barka I plant (Abdul-Wahab and Jupp, 2009).....	168
Figure 115: Distribution of temperature and salinity in surface seawater around the Barka I plant (modified Abdul-Wahab and Jupp, 2009).....	168
Figure 116: Distribution of heavy metals in sediment associated with the outfall discharges from Barka I plant (modified Abdul-Wahab and Jupp, 2009).....	168
Figure 117: Tidal characteristics at Wudam station (plotted from the National Hydrographic Office, 2008) relative to the lowest astronomical tide. ....	170
Figure 118: Water elevation measured by a tide gauge at Barka I (plotted from Wallingford, 2001) 170	170
Figure 119: Statistical analysis of wind directions and speed for the year 2002 (HMR, 2007).....	171
Figure 120: Wind speed (top) and direction (bottom) measured at the Barka plant I (plotted from Wallingford, 2001).....	172
Figure 121: Coastal currents along the coast of Oman (Purnama and Barwani, 2006).....	172
Figure 122: Current speed (top) and direction (bottom) measured at the proposed location of the Barka plant I outfall (plotted from Wallingford, 2001) .....	173
Figure 123: Spring (top row) and neap (bottom row) tides mean values of current, temperature and salinity measured at the proposed location of the Barka plant I outfall (plotted from Wallingford, 2001).....	174
Figure 124: The first sheet of the discharge calculator for the Barka I (MSF) plant.....	175
Figure 125: The second sheet of the discharge calculator for the Barka I (MSF) plant.....	176
Figure 126: The first sheet of the discharge calculator for the Barka II (RO) plant.....	177
Figure 127: The second sheet of the discharge calculator for the Barka II (RO) plant.....	178
Figure 128: The third sheet of the discharge calculator for the Barka II (RO) plant .....	179
Figure 129: 3D view of the near field positively buoyant plume of scenario I.....	181
Figure 130: 3D view of the far field positively buoyant plume of scenario I .....	182
Figure 131: Temperature distribution (left) and dilution (right) downstream of scenario I.....	182
Figure 132: 3D view of the near field negatively buoyant plume of scenario II (origin is located at the surface).....	184
Figure 133: 3D view of the far field negatively buoyant plume of scenario II (origin is located at the surface).....	185
Figure 134: Concentration distribution (left) and (dilution) downstream of scenario II.....	185
Figure 135: Sketch of the applied outfall design.....	186
Figure 136: Computational domain of the far-field model. <i>Left</i> : Plan view of the numerical grid. <i>Right</i> : Cross-sectional views of the numerical grid: west ↔ east cross-section along N51 ( <i>top</i> ), south ↔ north cross-section along M49 ( <i>bottom</i> ).....	187
Figure 137: CORMIX plume visualizations for the time step I (left) and II (right).....	188
Figure 138: Scatter plot of the predicted endpoints of the near-field with their concentrations .....	188
Figure 139: Distribution of the discharge locations for the three coupling configurations. Left: plan views, middle: south↔north cross-sections, right: east↔west cross-sections •: discharge locations, ×: grid points where layer 7 to 13 are affected separately.....	189
Figure 140 and Figure 141 show maps for the three coupling configurations at the time steps I and II. Figure 141 shows the concentration distribution in layer 11 in which the outfall is located. Figure 142 displays cross-sectional views of the concentration distribution along the grid line M49. In the case of no coupling, a larger concentration scale is used. Figure 143 shows concentration profiles over the depth at the observation points outfall, A and B. Regarding the plan views given in Figure 141 at one time step, the plume looks similar for all coupling cases. The plume is travelling in the mean flow direction. Unsteady variations cause slight deflections and stretching of the plumes. ....	190

Figure 141: Plan views of the concentration distributions in layer 11 (height of outfall) for the three coupling configurations at time step I (top) and II (bottom). In the case of no coupling a larger concentration scale is used .....	190
Figure 142: Concentration distributions in the cross-section along M49 for the three coupling configurations at time steps I and II. In the case of no coupling a larger concentration scale is used .....	192
Figure 143: Concentration profiles at the observation points outfall, A and B for the three coupling configurations no, vertical and full coupling. Time steps: I and II .....	193
Figure 144: Global distribution of installed desalination capacity by technology (based on Höpner and Lattemann, 2008) .....	210
Figure 145: Global distribution of installed seawater desalination capacity by technology (based on Glade, 2005).....	210
Figure 146: Schematic of the Multi Stage Flash process with four stages (Lahmeier Int., 2003).....	211
Figure 147: Schematic of the Multi Effect Distillation process with three effects (Buros, 2000) .....	212
Figure 148: Major components of an RO desalination system (Munk, 2008) .....	214
Figure 149: Schematic of the Electrodialysis process (Miller, 2003) .....	214

# ABSTRACT

A modelling framework for the environmental-hydraulic design of the outfall system for desalination plants is described. It is based on five main items: first, the identification of environmental impacts, regulatory frameworks and public concerns regarding brine effluent discharges; second, the elaboration of easily applicable design nomograms and design recommendations as a basis for the first screening process within the assessment of brine discharges; third, the development of hydrodynamic model interfaces for predicting brine effluent concentrations of key parameters in the marine environment by coupling the near-field mixing model CORMIX for outfall design optimization with the far-field transport model Delft3D for optimized outfall siting; fourth, the model application and validation for typical case studies for the compilation of design recommendations with parallel improvement of design oriented input/output features; and fifth, the management and realization of capacity building activities.

The developed model package allows analyzing, improving, and controlling the outfall siting and design. Resulting designs reduce environmental impacts and also operational costs by reducing negative effects from effluent accumulation and recirculation to the intake. Furthermore, the resulting concentration distributions can be used to develop sustainable concentrate management plans for desalination technologies to protect the environment and improve related technological solutions. This issue may in addition reduce costs related to delays in plant commissioning due to badly prepared proposals for outfall permits.

Capacity building materials are integrated in this text and available as free download on the projects website ([www.brinedis.net.ms](http://www.brinedis.net.ms)). Design engineers, regulators and authorities, as well as plant operators and consultants have advantages using the developed tools and best-practice manual (this document).

## **ACKNOWLEDGEMENTS**

The authors would like to thank the Middle East Desalination Research Center (MEDRC) for its financial support and technical guidance, and for organizing professional workshops related to our activities.

Furthermore, we are grateful that the European Desalination Society (EDS) sponsored our workshop activities.

We thank the consultant Dr. Paul Akar (Oman and Lebanon) and the student John Bandas (University Texas A&M, USA) for their continuous support of the project without direct financial involvement. Their contributions improved the results and directly supported this document.

For data on the Barka I plant, we also would like to thank Dr. Sabah Abdul-Wahab (Sultan Qaboos University), Dr. Barry Jupp (Ministry of Environment and Climate Affairs, Sultanate of Oman), Mr. Mohammed Al Weshahi (Shinas College of Technology, Oman; and formerly the operation and maintenance engineer at AES Barka, Oman), Mr. Salim Al Hatmi (the operation and maintenance engineer, AES Barka, Oman), and Mr. Ahmed Al Subhi (The Wave, Oman, and formerly the operating manager of AES Barka, Oman).

## EXECUTIVE SUMMARY

The impacts of a seawater desalination plant discharge on the marine environment depend on the physical and chemical properties of the desalination plant reject streams and the susceptibility of coastal ecosystems to these discharges depending on their hydrographical and biological features. Therefore, a good knowledge of both the effluent properties and the receiving environments is required in order to evaluate the potential impacts of desalination plants on the marine environment. This can be achieved by carrying out site- and project-specific environmental impact assessment (EIA) studies. This document, entitled "**Environmental planning, prediction and management of brine discharges from desalination plants**" provides required background information for the discharge related impact analysis. It supports the *planning* process by providing *prediction* tools to simulate and predict the distribution and fate of substances discharged from desalination plants. It furthermore improves the *management* of such discharges by providing recommendations on improved discharge regulations, improved designs for discharge structures and improved methods to define their siting.

The document provides background information on the *intake, treatment and disposal systems* of the main desalination technologies (Chapter 2). It summarizes detailed information on potential *environmental impacts* of desalination plant discharges in the form of descriptions of effluent characteristics, estimates of chemical discharge loads on the basis of installed seawater desalination capacities for different sea regions (Section 3.1), a literature review on related environmental impacts and impact assessments (Section 3.2) and socio-economic issues (Section 3.3) of the two most common seawater desalination processes. A summary of existing *environmental quality standards* is given in Section 3.4. Waste water discharges are usually regulated by limiting pollutant levels in the reject streams at the point of discharge (effluent standards) and in the receiving environment (ambient standards). Furthermore, total allowable emission loads may be specified for certain pollutants, especially those that have a tendency for accumulating in the environment, taking the pollutant concentration and the waste water flow rate into account. Recommendations for the implementation of a *regulatory mixing zone approach* are described. General *mitigation measures* are briefly summarized in Section 3.5.

The various density differences between the brine and the receiving water represented by the buoyancy flux causes different flow characteristics of the discharge. The dense RO (reverse osmosis) effluent flow has the tendency to fall as a negatively buoyant plume. The MSF (multi-stage-flash) effluent is distinguished by a neutral to positive buoyant flux causing the plume to rise. *Discharge technologies* aim for enhanced effluent dispersion in the receiving environment and adequate discharge siting to avoid pollutant accumulation, to protect sensitive regions and to utilize natural purification processes. *Submerged, offshore, multiport diffuser outfalls* designed as efficient mixing devices installed at locations with high transport and purification capacities are capable to reduce environmental impacts significantly. However, modelling techniques are needed for design and optimization of such installations.

The relevant mixing processes and the related modeling techniques are described in Chapter 4 and 5, including a spreadsheet calculator to define effluent properties and first screening equations to define the initial dilution of a chosen system. Two different hydrodynamic models are used for the prediction of either the near-field mixing (CORMIX) and/or the transport processes in the far-field (Delft3D). An optimized approach to couple both model types for brine discharge analysis has been developed. The coupling interface algorithm

includes the transformation of the output data of the near-field model CORMIX into the input data for the far-field model Delft3D-FLOW based on a comprehensive flow classification system. Calculations indicate that the far-field model alone (without coupling) can not simulate the vertical concentration distribution of the plume in contrast to the near-field model. Thus, a model coupling is unavoidable for an environmental assessment. The coupling methodology, though simple, allows for a considerably improved discharge assessment and an optimized environmental hydraulic design of the outfall structure.

The developed screening equations, spreadsheets and model coupling algorithms have been tested first for a theoretical but detailed case study (Section 6.2). The final applicability has been shown for case studies for the modern Barka plants in Oman, using discharge calculators and the alpha-version of the herein extended CORMIX system (Sections 6.1.2 and 6.1.6). Barka I represents the distillation based technologies with a total installed capacity of 91000 m<sup>3</sup>/d (commissioned in 2003), and Barka II the membrane based technologies, with a total installed capacity of 120000 m<sup>3</sup>/d (under construction). Both plants use and share the same existing seawater intake and outfall systems. The Barka I plant withdraws seawater up to a maximum flow rate of 67500 m<sup>3</sup>/h (53% of the installed intake capacity) and discharges brine up to a maximum flow rate of 61500 m<sup>3</sup>/h (50% of the installed outfall capacity). The cooling water from the power generation Barka I plant is mixed with reject brine (and other effluents) and is discharged into the sea through the existing outfall pipelines.

The results showed that the tools are readily applicable and improve the current state of the art for desalination brine discharge analysis. Dischargers, consultants and regulators are encouraged to apply these tools and to discuss the proposed modifications of existing regulations on one hand and existing discharge systems on the other hand. Ongoing analysis showed that "cleaner" desalination is possible and feasible.

# Nomenclature

Parameter	Dimension	Definition
$b$	m	jet width (radial distance from centerline where 1/e of centerline quantity)
$C$	mg/l, kg/m <sup>3</sup>	substance concentration
$D$	m	internal pipe diameter
$F_o$	-	initial (source) densimetric Froude number
$g$	m/s <sup>2</sup>	gravitational acceleration
$g'$	m/s <sup>2</sup>	reduced gravity, $g' = \Delta\rho/\rho g$
$H$	m	head above datum / water depth
$j_o$	m <sup>3</sup> /s <sup>2</sup>	buoyancy flux per diffuser length, $j_o = g' q_o$
$J_o$	m <sup>4</sup> /s <sup>3</sup>	buoyancy flux
$h_o$	m	height of discharge port
$\ell$	m	riser spacing
$L$	m	length of the considered pipe section
$L_M$	m	momentum length scale
$\ell_M$	m	slot jet / plume transition length scale $\ell_M = m_o/j_o^{2/3}$
$\ell_m$	m	crossflow length scale $\ell_m = m_o/u_a^2$
$\ell_m'$	m	stratification length scale $\ell_m' = m_o^{1/3}/\varepsilon^{1/3}$
$\ell_b'$	m	stratification / plume length scale $\ell_b' = j_o^{1/3}/\varepsilon^{1/2}$
$\ell_a$	m	stratification / crossflow length scale $\ell_a = u_a/\varepsilon^{1/2}$
$m$	m <sup>3</sup> /s <sup>2</sup>	momentum flux per diffuser length
$M$	m <sup>4</sup> /s <sup>2</sup>	momentum flux
$Q$	m <sup>3</sup> /s	total flow through outfall system
$q$	m <sup>2</sup> /s	mass flux per diffuser length
$Re$	-	Reynolds number $Re = VD/\nu$
$S$	-	dilution, $S = C_o/C$
$t$	s	time
$t_M$	s	jet / plume time scale $t_M = m_o/j_o$
$t_m$	s	jet / crossflow time scale $t_m = m_o/u_a^3$ [s]
$T_{90}$	h	the time taken for 90% of the bacteria to die-off
$u, v, w$	m/s	velocity
$U, V, W$	m/s	mean velocity
$x, y, z$	m	Cartesian coordinates

## Greek symbols

$\mu$	Ns/m <sup>2</sup>	dynamic viscosity
$\nu$	m <sup>2</sup> /s	kinematic viscosity
$\varepsilon$		stratification parameter, $\varepsilon = -(g/\rho_a)(d\rho_a/dz)$
$\theta$	°	slope or discharge angle
$\rho$	kg/m <sup>3</sup>	density

## Indices

$a$	ambient
$b$	background
$B$	bottom / bed
$c$	centerline
$e$	effluent
$ff$	far-field
$i$	impingement point
$min$	minimal
$max$	maximum
$nf$	near-field
$o$	initial quantity
$tot$	total

# 1. INTRODUCTION

The trend is clear for the 21<sup>st</sup> century: worldwide water consumption is growing, driven by an increasing population combined with increasing industrial and agricultural production. In arid zones and other water-scarce areas, this consumptive demand must largely be met through desalination plants using a variety of technological processes, e.g. thermal processes such as multistage flash (MSF) plants, or membrane processes such as reverse osmosis (RO) plants. In 2005, the total world installed capacity for seawater desalination was about 27.8 Mill. m<sup>3</sup>/d (IDA, 2006; 2008) of which about 75% was situated in the Middle East and North Africa (MENA) regions (Goebel, 2005). Some states depend on desalinated water for more than 50% of their domestic use, where other drinking water sources are close to depletion. To avert the real threat to resource sustainability and to satisfy the immediate need to increase the production and supply of potable water, desalination is a key focus for governments across the region, generating massive investment and creating demand for global expertise plus the latest advanced systems and technologies. In the period up to 2015, the countries of the MENA region are expected to spend US\$24 billion in desalination costs (www.middleeastelectricity.com). Also noteworthy are the increasing plant sizes for these large scale industrial size installations (Figure 1), such as the Al-Jubail (Saudi Arabia) MSF plant with 1.54 Mill. m<sup>3</sup>/d capacity (IDA, 2006; 2008).

But also outside the MENA region desalination is a growing market where new desalination hot-spots in Australia, Southeast-Asia, Spain and California are emerging (Höpner and Lattemann, 2008). For example, the Spanish government informed that production has doubled in the last five years and predicts that it will double again in another five years (Technology Review, 2006). The US Bureau of Reclamation (2003) also states: “By 2020, desalination and water purification technologies will contribute significantly to ensuring a safe, sustainable, affordable, and adequate water supply for the United States”. For the Mediterranean, an increase in water demands of 32% has been predicted for the period 2003-2010 (UNEP, 2003), mainly satisfied by non-conventional resources.



Figure 1: Al Ghubrah desalination plant (largest in Oman, capacity 191,000 m<sup>3</sup>/d): Brine discharge through an open channel at the coast into the Gulf of Oman (photo: H.H. Al-Barwani)

Due to the increasing desalination activities and the concentration of activities on a small number of regions and water bodies, it is necessary to deal with the possible adverse environmental effects of the technology and to develop mitigation strategies at an early stage. The main impacts are regarding land use, energy consumption and brine disposal.

The problem of land usage is connected with every major industrial project. Seawater desalination plants are situated at coastal sites which are particularly sensitive environmental habitats with many social, economic, ecological and recreational functions. The search for an appropriate plant location has to be carried out with great care in order to minimise differing interests.

Despite great achievements in reducing the overall energy consumption, RO desalination plants remain an energy-intensive process. Since most of the energy is taken from fossil sources, the CO<sub>2</sub>-emission from desalination plants is another important environmental problem. Research projects are currently on-going to find the efficient and reliable solutions for solar-driven desalination (DLR, 2007). The main objective of these projects is to reduce the emissions of CO<sub>2</sub> and other air pollutants.

Besides the impacts regarding energy consumption and land use, a major impact is related to the marine environment, especially to coastal water quality problems caused by brine discharges (Einav et al., 2003, e.g. Figure 1).

The brine (or concentrate) is the waste stream produced by desalination plants and is usually discharged into the sea. The brine flow rates are large, generally up to 40 % (RO) and up to 90 % (MSF, including cooling water) of the intake flow rate, thus either almost as large or even considerably larger than the required drinking water flow rate. The brine is characterized by its high concentration of substances taken out of marine waters (i.e. salt). Furthermore, and often more critical, the brine contains additives and corrosion products. Additives are chemicals used for biofouling control (e.g. chlorine), scale control (antiscalants), foam reduction, and corrosion inhibition that are added during the desalination process and discharged into the coastal waters as contaminants (Lattemann and Höpner, 2003). In addition, next to the high salinity and contaminants, the brine effluent might also show increased turbidity and temperature (the former mainly applies to RO, the latter mainly applies to MSF plants). Main problems arise due to the strongly limited mixing behavior in the receiving waters, which is significantly influenced by the effluent density, which is dominated by the varying effluent salinity and temperature (Figure 2a,b). The impacts of these pollutants and brine characteristics on the marine environment can be diverse and must be mitigated by technical measures.

Depending on the physical and ecological characteristics, effluent substances can have a harmful impact on the local environment. Especially vulnerable are areas such as mangrove forests, salt marshes, coral reefs, or low energy intertidal areas and shallow coasts, while exposed rocky coasts with high energy wave action may be less susceptible (Höpner and Windelberg, 1996). Enclosed seas, like the Arabian Gulf or the Red Sea have limited water exchange capacities and are generally shallow and less energetic, thus more sensitive to effluent discharges. Potential impacts on local fisheries or tourism resources with considerable economic consequences are some of the conflict points that arise when planning desalination plants. In particular, increased plant capacities increase impact concentrations of effluent constituents to levels that can become harmful to the marine environment.

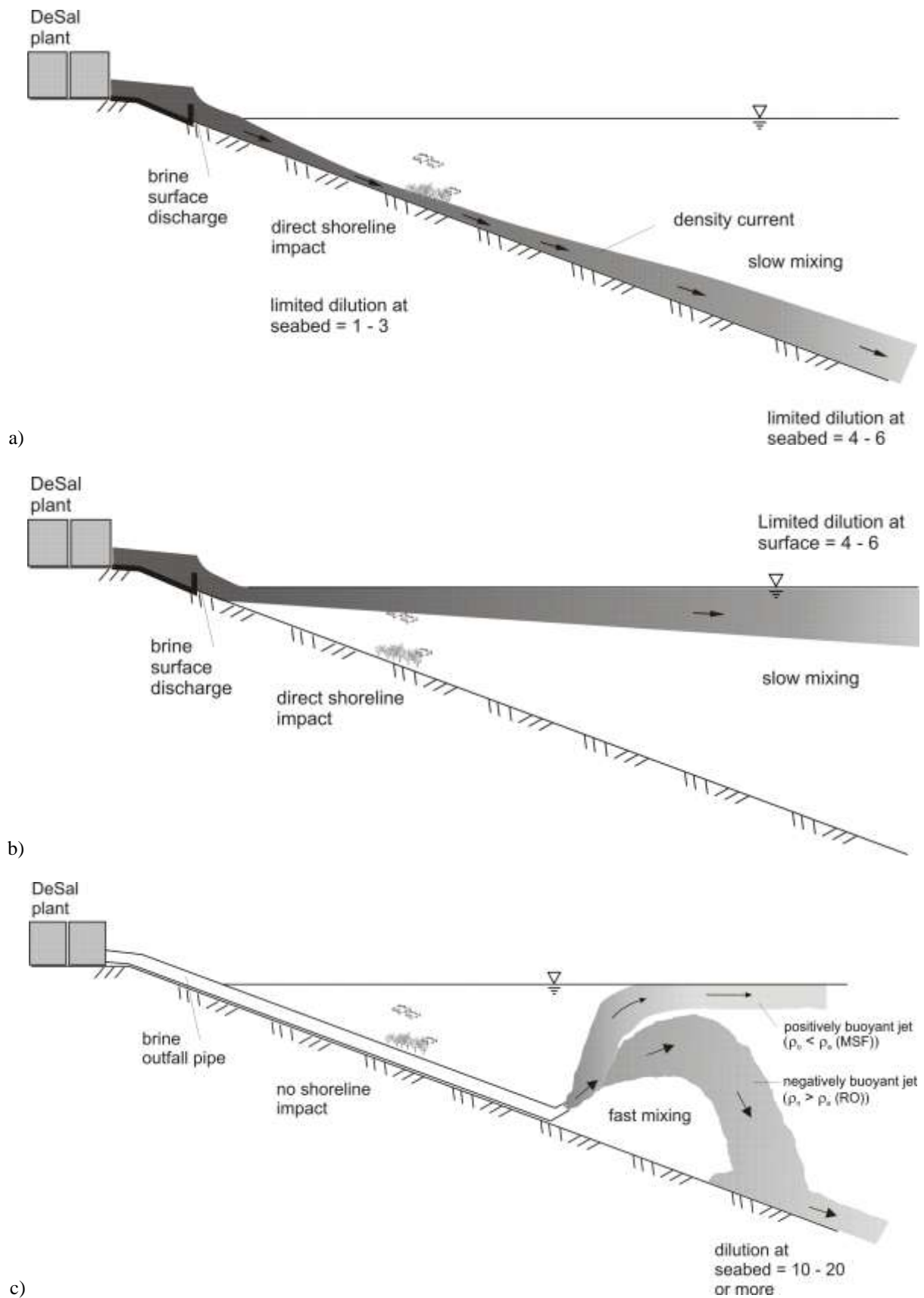


Figure 2: Mixing characteristics and substance distributions for different brine discharge configurations and effluents (Bleninger et al., 2006). *a*) RO plant (dense effluent) shoreline discharge via channel or weir, *b*) Thermal plant (dense effluent mixed with buoyant cooling water) shoreline discharge via channel or weir, *c*) submerged discharge (dense effluent) via pipeline and nozzle or diffuser

Genthner (2005) notes that there is increased public concern and scientific awareness on the environmental impact of desalination plants. For example, objections in Australia and the USA regarding environmental impacts have already become key issues for project permits, often considerably influencing plant commissioning and design (e.g. Huntington Beach, 2006 or Carlsbad, [www.carlsbaddesal.com](http://www.carlsbaddesal.com)), and thus overall project costs. The necessity of sound environmental impact studies and public involvement will further increase because several countries define new regulatory strategies on protection and conservation of the marine environment (e.g. WFD, 2000).

From a regulatory viewpoint, many countries (e.g. USA or European Union countries) restrict the levels of aquatic pollutants both at the discharge point (“effluent standards”) as well as within the receiving water (“ambient standards”). The former encourages source control principles, effluent treatment and recycling technologies. The latter demands for the consideration of the ambient response often associated with the concept of the “mixing zone”, an allocated impact zone in which the numerical water quality standards can be exceeded (Jirka et al., 2004). In order to meet these regulations, properly sited outfalls with optimized high efficiency mixing designs are needed for the brine discharges (Figure 2c), embedded overall in a sustainable concentrate management plan.

In comparison to municipal wastewater discharges, there is a major lack of basic knowledge on brine discharges, which is made evident by the fact that there is frequently insufficient information on the physical characteristics of the brine effluent as well as the receiving seawater, especially density and velocity variations, which are crucial conditions for mixing and substance distribution. In the case of desalination facilities combined with power plants for energy production, the problems are even more complicated as the brine effluent is mixed with the cooling water of the power plant before discharge. In these cases, mixing characteristics can be many (compare Figure 2a,b).

Unfortunately, brine outfall systems are often not properly sited and not at all optimized regarding the mixing conditions and substance distribution, thus leading to unnecessary environmental impacts or even operational problems. If there is a potential for recirculation to the plant intake, badly sited outfalls may reduce overall system efficiency, especially for larger plants or plant complexes. Scientifically validated and efficient planning tools in the form of nomograms, predictive models and expert systems are needed to assist desalination plant designers and plant managers in designing and operating the intake-outfall scheme so that environmental impacts on the marine environment can be controlled and minimized.

The description and application of such tools is the overall objective of this report. A modelling framework for the environmental-hydraulic design of the outfall system for desalination plants has been developed. It is based on five main objectives: the identification of environmental impacts, regulatory frameworks and public concerns regarding brine effluent discharges; the elaboration of easily applicable design nomograms and design recommendations as basis for the first screening process within the assessment of brine discharges; the development of hydrodynamic model interfaces for predicting brine effluent concentrations of key parameters in the marine environment by coupling a near-field mixing model for outfall design optimization with a far-field transport model for optimized outfall siting; the model application and validation for typical case studies for the compilation of design recommendations with parallel improvement of design oriented input/output features; and lastly, the management and realization of capacity building activities.

## 2. INTAKE-, TREATMENT-, DISPOSAL-SYSTEMS

The state of the desalination technology has been sufficiently described in the literature (e.g. NRC, 2008; WHO, 2008) and is therefore only briefly summarized in this document (Appendix D). Further considerations will focus on the three commonly applied technologies, namely Reverse Osmosis (RO) and Multi Stage Flash (MSF) Distillation or Multi Effect Distillation (MED).

The key elements of a desalination plant that have the highest relevance in terms of environmental impacts are the intake structures, the pretreatment and cleaning system, the design of the desalination process in terms of energy, water and material use causing different effluent characteristics, and the concentrate disposal system.

### 2.1. Intake systems

Seawater contains substances and particles which are potentially harmful for the desalination plant components. Biological substances can create fouling, solid particles can cause coagulation and deposition, dissolved solids can cause scaling and material corrosion can be accelerated. Therefore, plant operators carefully choose the intake system, position the intake at the site with the best water quality and look for the most robust materials. In most cases, the raw water quality is not sufficient for plant operation and technical cleaning systems need to be installed. Filters are integrated to purify the water as far as possible and chemicals are dosed to ensure the right water parameters.

*Open water intakes* take the water directly from the sea via pipes, which enable a theoretically unlimited raw water stream. The strong water suction poses a risk of impingement and entrainment for fish and other animals. Species do not survive a passage through a desalination plant (entrainment) and can be harmed at the intake structure (impingement). In addition particles and organisms small enough to pass through the screens are sucked into the plant and significantly deteriorate the feed water quality (Cooley et al., 2006). Mitigation measures to minimize those effects are siting the intake in deep, offshore waters, using designs with small intake velocities, fine meshed screens and fish handling systems. A design criterion is usually keeping the intake velocities smaller than 0.1m/s, thus being smaller than ambient velocities (California Coastal Commission, 2004). In addition, designs are recommended causing mainly horizontal intake velocities, as fish can more easily swim against horizontal flows. This can be achieved by having velocity caps as applied at Australian desalination plant intakes (Figure 3).

The hydrodynamic design of such structures is rather simple compared to the complex hydraulics involved in outfall designs. This is due to the almost passive and low velocity flow induced by the intake structure, compared to the active and high velocity flow induced by discharge structures. A first design can be made by applying the continuity equation,  $Q_i = U_{crit} A_i$ , where  $Q_i = Q/n$  is the the individual intake flowrate of  $n$  intake structures ( $n = 1$ , if only one intake),  $U_{crit} = 0.1\text{m/s}$ , and  $A_i = \pi D h$ , being the flow efficient inflow area of acircular inflow tower of diameter  $D$  and flow efficient height  $h$ . For given flowrates and limiting inflow geometry  $D$  or  $h$  one can easily compute the resulting inflow geometry  $D$  or  $h$  respectively using  $D = Q_i / (U_{crit} \pi h)$  or  $h = Q_i / (U_{crit} \pi D)$ . Further hydrodynamic or physical modeling of the internal flow allows improving the preferably smooth geometry variation within the intake tower to obtain a uniform velocity distribution at the intake tower screens.



Figure 3: Open intake tower with "velocity cap". Reproduced from Cannesson et al. (2009)

*Subsurface intakes* are either vertical bore holes constructed on the beach side (beach wells) or horizontally drilled systems. They make use of the sandy soil as natural prefiltration and thus deliver a better feed water quality. The danger of impingement and entrainment is avoided. However, subsurface intakes strongly depend on geological conditions and can only provide limited water volumes which are generally not enough for large plants. Higher intake volumes can be delivered by applying several Horizontal Directional Drilling (HDD) lines. This technique installs several pipelines under the seabed (Figure 4 and Figure 5). The water, prefiltered by the geological layers, can therefore collect in sufficient quantities, independent of waves, currents and tides. A further advantage is the reduced environmental impact due to reduced construction activities on land and the seabed. A commercial implementation of sub-seabed intakes via HDD is the *Neodren* system (Figure 5). It enables to deliver intake flows of 80,000m<sup>3</sup>/d to 400,000m<sup>3</sup>/d (Peters and Pinto, 2006). A desalination plant in San Pedro del Pinatar in Spain with a capacity of 172,800m<sup>3</sup>/d is entirely fed by a Neodren intake. All Neodren systems are currently used in RO plants. Application in MSF plants is theoretically possible but as thermal plants do not need highly pure feed water, the operational need for Neodren is less strong than for RO. Additionally, lower recovery rates and higher average capacities in MSF plants require higher intake volumes which could pose design problems and add to the capital costs of Neodren.

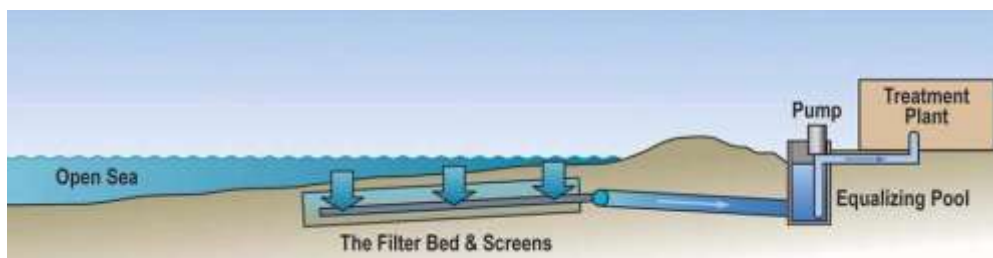


Figure 4: Sub-seabed intake via Horizontal Directional Drilling (California American Water, 2004)



Figure 5: Several horizontal subseabed drills with filtration region shown in light blue (Neodren system, Peters and Pinto, 2006).

## 2.2. Treatment systems

When the raw water quality is bad and does not meet the quality criteria of the plant, pretreatment has to be carried out in order to avoid operational problems.

**Chemical pretreatment** is the most commonly used technique for seawater desalination plants (Lattemann and Höpner, 2003). Chemical treatment is applied to reduce and avoid suspended particles, fouling, scaling, corrosion, and foaming. Figure 6 illustrates the typical chemical pretreatment steps of MSF and RO plants.

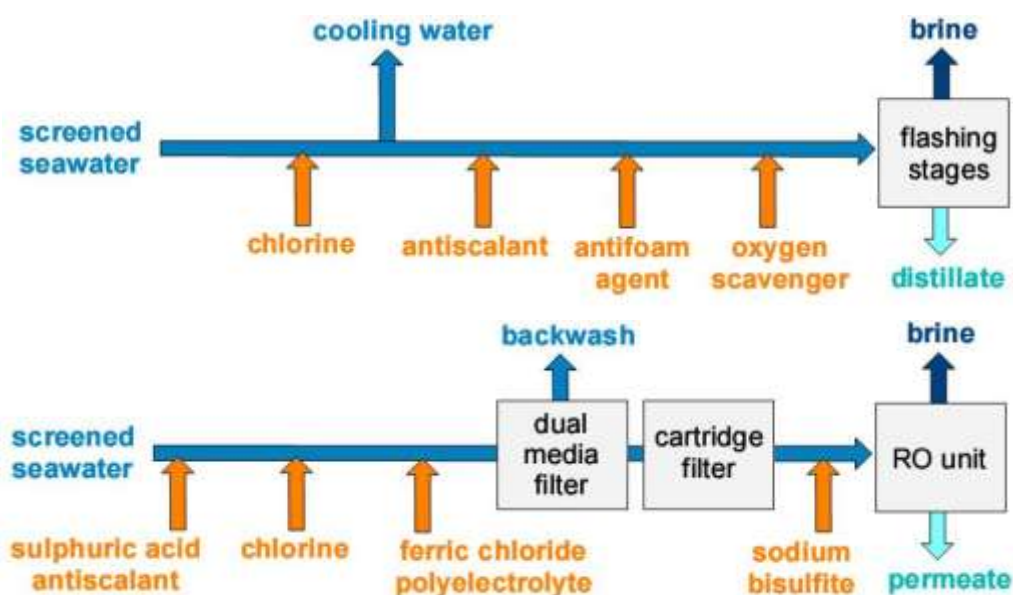


Figure 6: Typical pretreatment steps for MSF (above) and RO plants (below) (Höpner and Lattemann, 2008)

*Suspended particles* in the feed water contaminate and block the RO membranes. The particles have to be forced to form bigger agglomerations so that they can be filtered with dual media and cartridge filters (Figure 6). This is usually done by adding *coagulation chemicals* like ferric chloride or polyelectrolytes to the water. Turbines or propellers can also be used to achieve mechanical *flocculation* through slow mixing (UN ESCWA, 2001).

*Fouling* is caused by organic material in the feed water, most likely fine unfiltered particles and bacteria which settle on surfaces and start growing. They cause blockage and destruction of RO membranes and reduce the heat transfer and the process efficiency in MSF plants. Fouling is usually fought by continuously adding biocides, most commonly *chlorine*, to the feed water, which restricts biological growth. In order to stop all biological activity, *shock-chlorination* with higher dosages is carried out in regular intervals.

*Scaling* occurs when the solubility of dissolved salts is exceeded and the salts start to precipitate. As a result of the desalination process, the concentrations of salts rise and eventually reach the solubility limits. Calcium carbonate scales form the quickest. Solubility levels decrease with rising temperatures, which poses an additional problem for thermal plants. Scale formation reduces the RO membrane performance and supports fouling. In MSF plants, scale formation promotes corrosion, and reduces the heat transfer and thus the overall operating efficiency. In order to control scale formation, *acids* and *antiscalant chemicals* are dosed. When calcium sulphate scales form, they cannot be easily removed by antiscalants. Due to this reason, the MSF process temperatures are restricted to about 115 °C.

Fouling and scaling cannot be completely avoided by means of regular pretreatment; fine films will form eventually. Therefore, regular *chemical cleaning* with acids and a mix of other chemicals has to be carried out additionally.

*Corrosion* is a major problem in MSF plants. It is promoted by high temperatures, high salinity, oxygen and chlorine. Copper-nickel alloys in particular, which are applied due to their good heat transfer capacities, are vulnerable to corrosion. In order to maximise the protection of the sensitive metals, *anti-corrosive chemicals* are dosed and the feed water can be depleted of oxygen by using a so-called oxygen scavenger.

*Foaming* is an exclusive problem of MSF plants. It occurs when dissolved organics concentrate on the water surface due to the water movement. Foam increases the danger of salt intrusion into the distillate and is therefore tried to be avoided through the use of *antifoaming agents*. These reduce the tension in the surface water and destroy the surface films.

New approaches to pretreatment are **membrane filtration systems** (Van der Bruggen and Vandecasteele, 2002). Depending on the pore sizes of the membranes, different sizes of particles can be filtered and different pressures have to be applied (Figure 7). Membrane filtration systems have the potential to replace conventional chemical pretreatments, but operating systems are not chemically free, since the pretreatment membranes often require periodical chemical enhanced backwashing (CEB) and cleaning in place (CIP) or use in-line coagulation instead of conventional coagulation-flocculation.

*Microfiltration* (MF) removes particles of down to 0.1 µm. This includes suspended solids, algae, emulsions and some bacteria. The energy consumption is relatively low as only small pressures are applied.

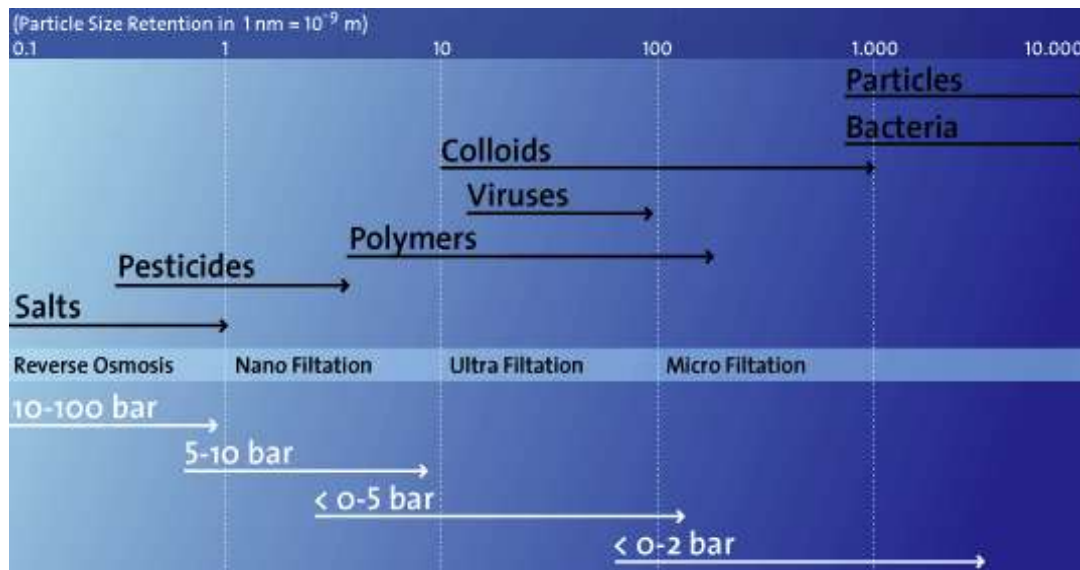


Figure 7: Range of filtration systems and membrane processes (Passavandt Roedinger, 2008)

*Ultrafiltration* (UF) removes substances down to  $0.01\ \mu\text{m}$  which comprises of dissolved macromolecules, colloids, viruses and smaller bacteria. Pressures of up to 5 bars have to be applied. UF membranes are physically cleaned by regular water backwashes. The removed deposits are filtered by a backwash filter and discharged to the sea. If operated in ‘dead end mode’, which is a maximum flux mode with regular backwashes, the energy consumption of UF membranes can be kept as low as  $0.1\text{-}0.3\ \text{kWh/m}^3$  (Peters, 2005). Similar to RO membranes, there exist spiral wound and hollow fibre configurations. In spiral wound configurations, accumulating particles between the layers can cause heavy fouling and scaling problems. The hollow fibre configuration somehow lacks the mechanical stability for an efficient backwash of the filtrate. The newly developed Multibore membranes combine stability with good cleanability as well as good fouling and scaling resistance, and thus are the best choice for UF pretreatment. Multibore membranes consist of a bundle of small fiber cables which are inserted into a collecting tube. Each fibre cable consists of seven capillaries with pore diameters of  $0.02\ \mu\text{m}$ . The seawater enters the capillaries and is desalinated by being pushed through the fibre cables into the collecting tube. The duration between backwashes usually varies between 15 and 30 minutes.

All reviewed studies agree that UF membranes are a reliable and efficient pretreatment option for seawater RO plants and outclass current conventional pretreatment systems by providing far superior feed water quality and operational advantages. The potential ecological benefits need to be proven since there is conflicting information on the actual chemical use of Integrated Membrane Systems (IMS). However, the technology offers the potential to significantly reduce or even avoid chemical use if the system is well-designed. Though adding another costly process to the plant UF pre-treatment already has financial advantages, due to savings for the RO membranes for poor and highly varying raw water qualities (Wolf et al., 2005).

UF pretreatment for MSF plants, however, has not been reported in any study. Similar to sub-seabed intakes, this might be due to the fact that MSF does not require highly pure feed water and that many more UF membranes would be necessary for the high MSF intake volumes. Nevertheless, application of UF pretreatment in MSF plants could have similar environmental advantages like in RO plants.

*Nanofiltration* (NF) has the finest pores of down to 0.001  $\mu\text{m}$ . NF even removes hardness ions (e.g. Ca, Mg), dissolved organic carbon and a fraction of the salts. It works similar to RO units, but at significantly lower pressures. In contrast to UF, NF membranes cannot be backwashed due to their technical layout. Thus, particles can accumulate on the surface and make NF susceptible to fouling and scaling, similar to RO membranes (Violleau et al., 2005).

Hassan et al. (1998) analysed the first set-ups of RO and MSF pilot plants with nanofiltration pretreatment. No chemicals, or only reduced dosages, were used during the test runs. However, it is uncertain if chemicals could be removed from the NF feed water. Most likely, the reduction of chemicals only referred to the RO feed water. RO membrane performance in the NF-SWRO process was found to be superior to that of conventional pretreatment. Due to the excellent NF permeate quality, the RO membranes could only be operated at 20-30 bars, without any deterioration in RO permeate quality. At RO pressures of 40 bars, the recovery ratio was increased to 48 %, compared to 16.7 % with conventional pretreatment. A NF-MSF system was safely operated for 66 days at a top brine temperature of 120 °C without the addition of any antiscaling or antifoaming chemicals. The concentrations of the important scale forming ions  $\text{Ca}^{++}$  and  $\text{SO}_4^-$  in the feed water were reduced by 81 % and 93 % respectively. This would enable plants to operate at higher top brine temperatures of up to 160 °C, and thus have higher overall plant efficiency.

Applied to the 56.800  $\text{m}^3/\text{d}$  Jeddah SWRO plant, the NF pretreated RO membranes achieved a 60 % recovery rate compared to only 35 % in standard operation. RO membrane output increased from 2370  $\text{m}^3/\text{h}$  in the conventional system to 4056  $\text{m}^3/\text{h}$  (Figure 8). The overall energy consumption dropped by 25 % with NF pretreatment.

As the NF membranes cannot be operated with low chemical dosages, the ecological advantage of chemical savings in the RO unit is clearly undermined. The amount of necessary antifouling or antiscaling additives seems to depend on the flow rates and on the pressures of the NF modules. Only coagulants and antifoaming agents which are low priority pollutants can definitely be removed when using NF pretreatment. Resistant NF membranes have to be developed before they can replace conventional pretreatment.

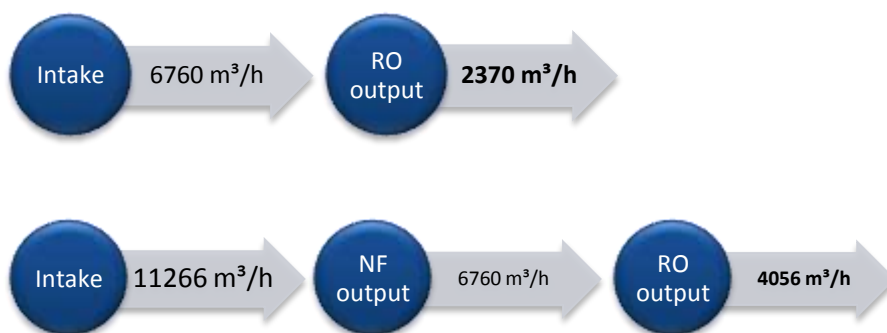


Figure 8: Comparison of flow rates in the conventional SWRO system with 35 % recovery (above) and in the NF-SWRO system with 60 % recovery each (below) (based on Hassan et al., 1998)

It is concluded that NF pretreatment is economical in cases with poor raw water quality where RO membranes with conventional pretreatment experience excessive fouling and have poor performance. In order to minimise the unit costs, NF-SWRO should be operated with high RO recovery rates.

## Post-treatment

Chlorine is one of the most hazardous pretreatment chemicals. In cases where its application cannot be prevented, dechlorination is a simple and effective method to avoid adverse effects. This step should be a compulsory part of the environmental strategy and not only an operational necessity in RO plants in order to protect the membranes. A harmless neutraliser is sulphur dioxide. Although overdosage can lead to pH reduction in the treated water, the acidic products are quickly neutralised by seawater alkalinity (Lattemann and Höpner, 2003; Höpner and Lattemann, 2008).

## 2.3. Process related effluent characteristics

The brine (or concentrate) is the waste stream produced by desalination plants. The brine is characterized by its high concentration of substances taken out of marine waters (i.e. salt). Furthermore, and often more critical, the brine contains additives and corrosion products. A sharp distinction in brine characteristics exists between the two major desalination processes. RO plants have a recovery rate from 20 to 50 %. In contrast, MSF plants have lower recovery rates (10-20 %) because of additionally having large cooling water demands (Goebel, 2005). Thus, the effluent flow rate is 4-5 times higher for thermal desalination than for RO processes referring to the same amount of produced fresh water (Table 1). In the case of a MSF plant coupled with a power plant, the drinking water flow is only about 4 % of the total intake flow (Lattemann and Höpner, 2003), which is illustrated generally in (Figure 9). A simple discharge calculator is described in section 0 to compute the effluent and discharge characteristics for different plant configurations and ambient characteristics.

Table 1: Comparison of properties of MSF and RO plants (following Goebel, 2005). Discharge characteristics are assumed for a typical MSF plant (recovery: 10 %,  $\Delta T = 10$  °C) and a RO plant (recovery: 32 %) with a fresh water production of  $Q_{fresh} = 345$  Ml/d = 4 m<sup>3</sup>/s according to Lattemann and Höpner (2003). "o" indicates the effluent characteristics. Ambient properties:  $\rho = 1023.5$  kg/m<sup>3</sup>;  $Sal = 36.3$ ;  $T = 27.7$  °C.  $Q$  = flow rate,  $T$  = temperature,  $Sal$  = salinity,  $\rho$  = density. (Figure 11)

	MSF	RO
driving force	increased temperature	pressure
energy demand	thermal (95 %) ≡ 13 -18 kWh <sub>el</sub> plus thermal energy in the form of steam	electrical 4-5 kWh <sub>el</sub>
recovery rate ( $Q_{fresh}:Q_{intake}$ )	10-20 %	20-50 %
cooling required	yes	no
$\Delta T = T_o - T_a$	5-15 °C	ca. 0 °C
<i>example study:</i>		
$Q_{fresh}$	4 m <sup>3</sup> /s	4 m <sup>3</sup> /s
$Q_{intake}$	39 m <sup>3</sup> /s	12.5 m <sup>3</sup> /s
$Q_{cool}$	27 m <sup>3</sup> /s	-
$Q_{brine}$	8 m <sup>3</sup> /s	8.5 m <sup>3</sup> /s
$Q_o = Q_{brine} + Q_{cool}$	35 m <sup>3</sup> /s	8.5 m <sup>3</sup> /s
$T_o$	37.7 °C	27.7 °C
$Sal_o$	40.4	65.3
$\rho_o$	1022.9 kg/m <sup>3</sup>	1045.5 kg/m <sup>3</sup>

Salinity and temperature are essential properties that differ between the two processes. This causes differences in the effluent density since it varies with salinity and temperature - the higher the salinity, the higher the density; the higher the temperature, the lower the density ( $T > 4\text{ }^{\circ}\text{C}$ ). In the case of RO, the salt concentration of brine can reach almost twice the concentration of seawater. No heating or phase change takes place in RO (Buros, 2000). This results in a strongly increased effluent density. The brine of MSF plants is extremely hot ( $T > 100\text{ }^{\circ}\text{C}$ ) but is blended with cooling water from the MSF process, which reduces the overall effluent temperature to about  $10\text{ }^{\circ}\text{C}$  above the receiving water temperature. The increased effluent temperature minimizes the density difference arising from the elevated salt content (increased by 15%). Usually coupled with power generation plants, the effluent produced by MSF is additionally mixed with cooling water from the power plant. As a result, the effluent is lighter than the receiving water (Lattemann and Höpner, 2003). Summarized, this means that in contrast to a MSF plant, a RO plant rejects less water with a higher salinity and a higher density as illustrated in (Figure 9).

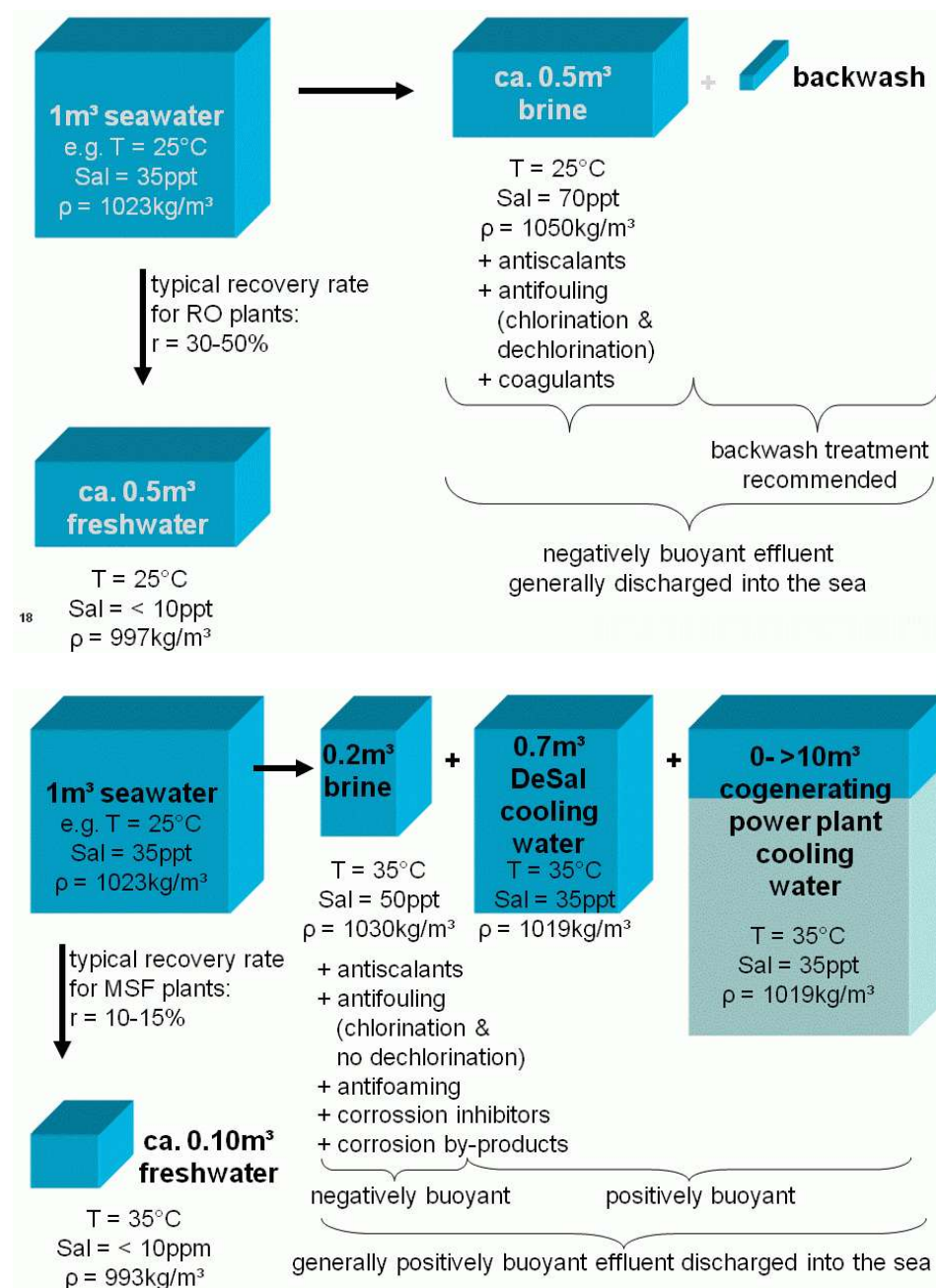


Figure 9: Desalination effluent characteristics. Top: RO-effluent, down: MSF-effluent.

## 2.4. Disposal systems

Conventional disposal methods of desalination plants comprise of:

- *Disposal to surface water*, which comprises of discharge to rivers, lakes, the ocean and other water bodies. It is the most common practice since most plants are situated next to surface water.
- *Sewer disposal* uses the existing infrastructure of a waste water treatment plant. The discharged brine must comply with the maximum sewer and plant treatment capacity as well as the wastewater quality characteristics.
- *Deep well injection* means the insertion of brine into a deep aquifer under the groundwater layers and depends on suitable geological conditions.
- *Evaporation ponds* are areas of land where brine is disposed of and evaporated by solar heat, leaving the salts behind.
- *Land application* enables the reuse of desalination effluents for irrigating lawns, parks and agriculture. It depends on the tolerance of plants towards salinity and the conformance with water quality standards for irrigation.
- The *zero liquid discharge (ZLD)* systems converts all feed water into drinking water or evaporates the residual water during the process, leaving only dry, solid constituents behind. ZLD incorporates the potential of providing desalinated water without any brine discharges and impacts on the marine environment. Solid wastes, however, need to be treated and disposed of in landfills. Recovery and commercial use of salts and other valuable minerals might also be taken into consideration. According to Mickley (2006), zero liquid discharge is the most costly of all disposal options. Furthermore, it remains to be proven if the system can really be efficiently applied to any existing seawater desalination plant of any capacity. It is also unclear if salts can be commercially used if they are extracted from chemically contaminated brine, and it is unknown how useless solid waste or residual constituents denominated as ‘other products’ would be disposed. However, a study issued by MEDRC underlines the advantages of ZLD for small home-use water treatment systems in the MENA region.

Figure 10 gives an illustrative comparison of the approximate capital costs of typical discharge options, depending on the effluent volumes. It can be seen that surface water and sewer discharge have the least capital costs and that these costs only slightly increase with the effluent flow rates.

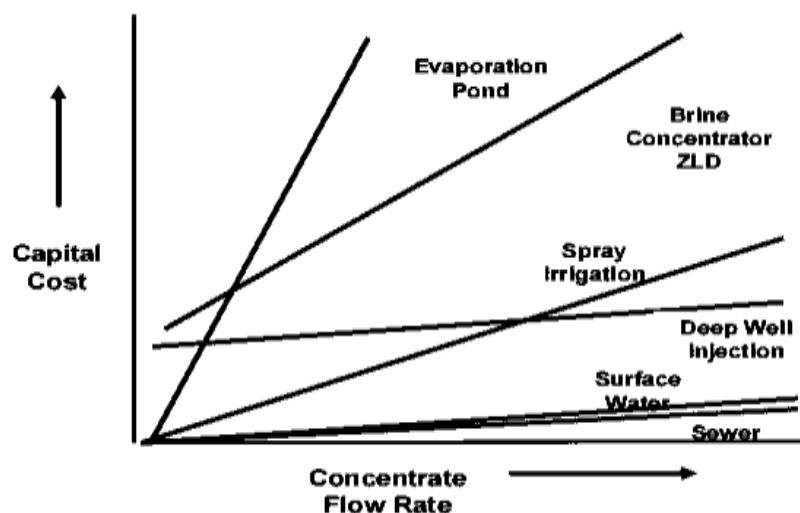


Figure 10: Capital costs of major concentrate disposal options depending on the concentrate flow rate (Mickley, 2006)

Factors like plant size, increasing regulations and public concerns are limiting the disposal options and challenging the search for a technically, environmentally and financially feasible method. The discharge volumes are a particularly limiting parameter for seawater desalination plants. The advantages and disadvantages of typical concentrate management options are summed up in Table 2.

Table 2: Comparison of brine disposal options for desalination plants (based on Alameddine and El-Fadel, 2007; Moch, 2007; Department of Natural Resources and Mines, 2003)

Disposal method	Advantages	Disadvantages
<b>Surface water discharge</b>	<ul style="list-style-type: none"> <li>- Can handle large volumes</li> <li>- Natural processes promote degradation</li> <li>- Water body promotes dilution</li> <li>- Often least expensive option</li> <li>- Possible dilution and blending with power plant discharge</li> </ul>	<ul style="list-style-type: none"> <li>- Limited natural assimilation capacities causing adverse impacts on marine environment if exceeded</li> <li>- Dilution depends on local hydrodynamic conditions</li> <li>- Good knowledge and monitoring of receiving waters required</li> </ul>
<b>Sewer disposal</b>	<ul style="list-style-type: none"> <li>- Dilution through waste stream</li> <li>- Uses existing infrastructure</li> <li>- Possible beneficial treatment</li> </ul>	<ul style="list-style-type: none"> <li>- Restricted capacity depending on sewage plant</li> <li>- Must meet sewer quality standards</li> <li>- Final disposal generally still to surface water</li> </ul>
<b>Deep well injection</b>	<ul style="list-style-type: none"> <li>- No marine impacts</li> <li>- Good option for smaller inland plants</li> </ul>	<ul style="list-style-type: none"> <li>- Only cost efficient for larger volumes</li> <li>- Maximum capacity hard to assess</li> <li>- Dependent on suitable, isolated aquifer structure</li> <li>- Danger of groundwater pollution</li> </ul>
<b>Evaporation ponds</b>	<ul style="list-style-type: none"> <li>- No marine impacts</li> <li>- Possible commercial salt exploitation</li> <li>- Low technological and managing efforts</li> </ul>	<ul style="list-style-type: none"> <li>- Strongly restricted capacity</li> <li>- Large areas of land necessary</li> <li>- Only in dry climate with high evaporation</li> <li>- Risk of soil and groundwater pollution</li> <li>- Disposal of unusable salts needed</li> </ul>
<b>Land application</b>	<ul style="list-style-type: none"> <li>- No marine impacts</li> <li>- Alternative water source for irrigation of tolerant species</li> </ul>	<ul style="list-style-type: none"> <li>- Only for smaller discharge flows</li> <li>- Possible adverse impact of chemicals and pollutants on plants</li> <li>- Risk of soil and groundwater pollution</li> <li>- Storage and distribution system needed</li> </ul>
<b>Zero liquid discharge</b>	<ul style="list-style-type: none"> <li>- No liquid waste disposal</li> <li>- Recovery of salt and minerals</li> </ul>	<ul style="list-style-type: none"> <li>- Still not feasible on industrial scale</li> <li>- Solid residuals</li> <li>- High energy need</li> <li>- Expensive</li> </ul>

According to the WHO guidance paper on desalination, more than 90 % of all large seawater desalination plants dispose of the concentrate into the ocean via an own outfall system (WHO, 2007), consequently being the option considered in the following chapters. This applies particularly to seawater desalination plants with large discharge volumes (Mickley, 2006).

### 2.4.1. Surface water discharge systems

The various density differences between the brine and the receiving water represented by the buoyancy flux causes different flow characteristics of the discharge (Figure 2). The dense RO effluent flow has the tendency to fall as a negatively buoyant plume. The MSF effluent is distinguished by a neutral to positive buoyant flux causing the plume to rise. Figure 11 illustrates the typical behaviour of positively or negatively buoyant jet discharging into the receiving water through a submerged single port outfall.

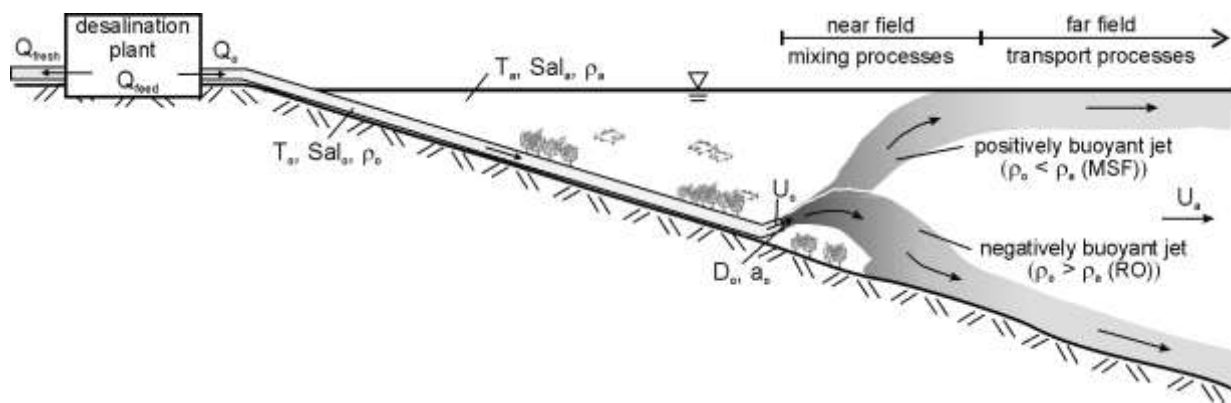


Figure 11: Brine discharge characteristics of desalination plants

Ocean outfalls are classified according to their location (onshore surface discharges / offshore submerged discharges), their mixing features (single port / multiport) and their effluent characteristics (positively buoyant, or negatively buoyant).

Onshore surface discharges have traditionally been installed due to their low costs. Examples are shown in Figure 12 to Figure 18. However, such discharges should be analyzed carefully and generally be avoided due to their limited mixing characteristics, high visibility, their need for large scale coastal constructions, and thus generally larger impacts (Figure 2).



Figure 12: Shoaiba (KSA), MSF Plant, Red Sea, 1.58 million m<sup>3</sup>/d, positively buoyant discharge (Source: Google Earth)



Figure 13: Carlsbad RO plant, USA, positively/negatively buoyant discharge (Source: Poseidon Resources)



Figure 14: Al Jubail (KSA), MSF plant, Arabian Gulf, 1.54 million m<sup>3</sup>/d, positively buoyant discharge (Source: Google Earth)



Figure 15: Ashkelon (Israel), RO plant with negatively buoyant brine discharge during backwash through an open channel at the coast into the Mediterranean (Courtesy of Rani Amir, Director of the Marine and Coastal Environment Division, Israel Ministry of the Environment) besides positively buoyant cooling water effluents.



Figure 16: Al Gubrah (Oman), MSF plant, 191,000 m<sup>3</sup>/d, Gulf of Oman, positively buoyant discharge (Source: Google Earth)



Figure 17: Jebel Ali MSF plant, UAE, power and water cogeneration plant with desalination capacity of 1.64 Mm<sup>3</sup>/d, positively buoyant discharge (Source: Google Earth)



Figure 18: Taweelah MSF plant, Arabian Gulf, 1.12 mio m<sup>3</sup>/d, positively buoyant discharge (Source: Google Earth)

Shoreline discharges may cause shoreline impacts by causing high concentrations accumulating in the near-shore region due to the limited mixing characteristics of these discharges. Further direct impacts are caused by the often necessary large scale discharge and

protection structures (wave protection, stilling basins, etc.), and their effect on coastal currents and sediment transport characteristics.

Therefore, it is recommended to apply modern efficient mixing devices, which overcome the limitations of the traditional surface onshore discharges. Such single or multiport submerged diffuser systems are characterized by their flexible location and their high mixing rates (Figure 19). These discharge technologies follow two main principles, aiming for *enhanced effluent dispersion* in the receiving environment and providing an *adequate discharge siting* to avoid pollutant accumulation, to protect sensitive regions and to utilize natural purification processes.

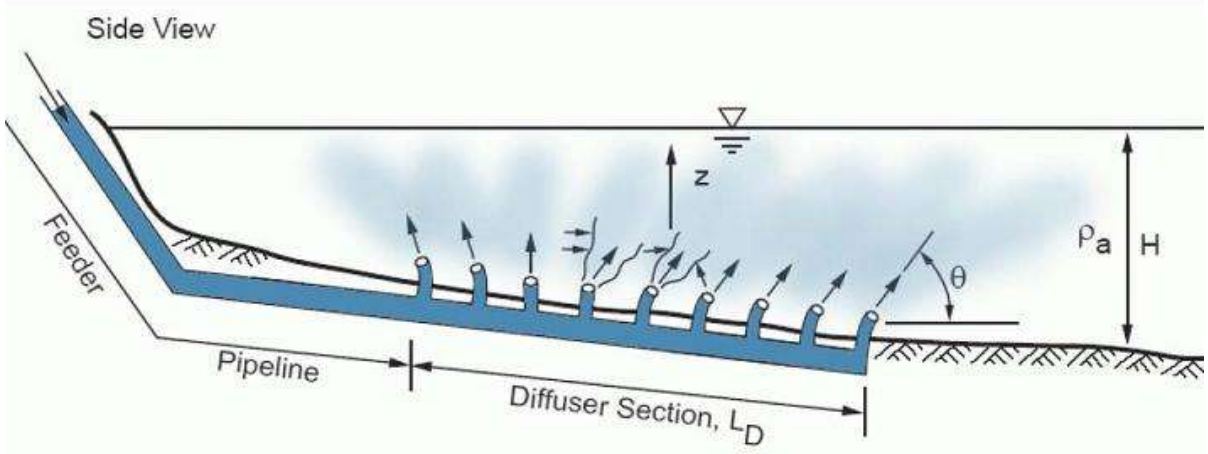


Figure 19: Layout of an outfall pipeline with multiport diffuser (Bleninger, 2007)

There are different materials and designs available, depending on the construction method (Figure 20) applied, and the prevailing ambient conditions. Images from the medium size Antalya wastewater outfall in Turkey (Figure 21) and the large size Boston wastewater outfall in USA (Figure 22) illustrate the type of these structures.

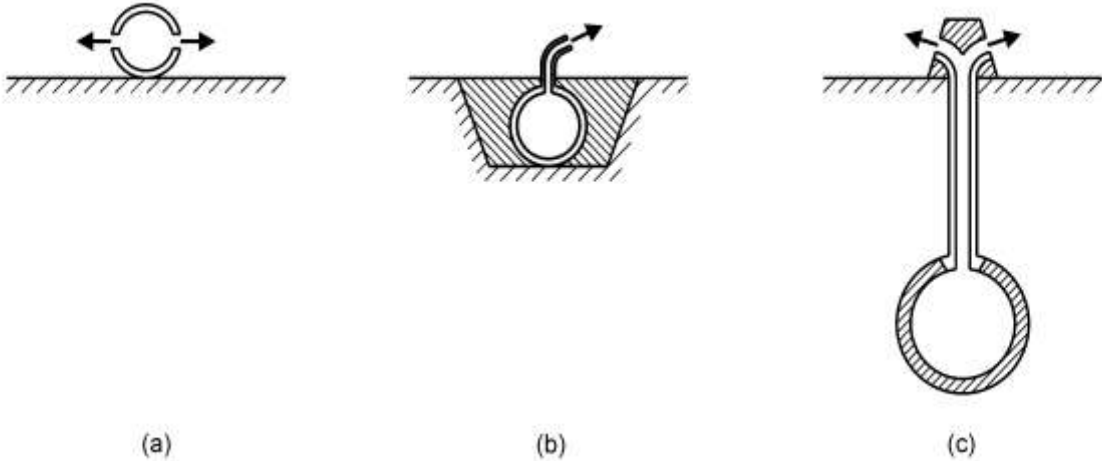


Figure 20: Typical construction details for multiport diffusers in water bodies: (a) Diffuser pipe on bottom with port holes, (b) diffuser pipe buried in trench with short risers, (c) deep tunnel construction with long risers



Figure 21: Antalya wastewater outfall (Turkey) during installation in 1997. *Top*: Diffuser section assembling on shore. *Down*: Feeder section ( $L_F = 5$  km, HDPE pipe,  $D = 1600$  mm) while sinking with attached concrete weights on the seabed (PipeLife Company)



Figure 22: Boston outfall during installation in 1998. *Left*: View into tunnel section (16 km with 8 m diameter). *Right*: One out of 55 riser caps with eight outlets each in rosette-like configuration (Roberts and Snyder, 1993)

Good examples for such mixing systems applied for large scale desalination plants are illustrated in Figure 23 and Figure 24, as well as in the case study for the Barka outfall in Oman (section 6).

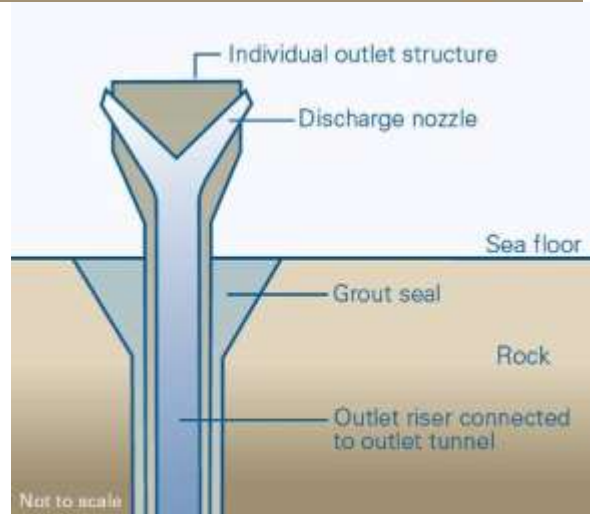
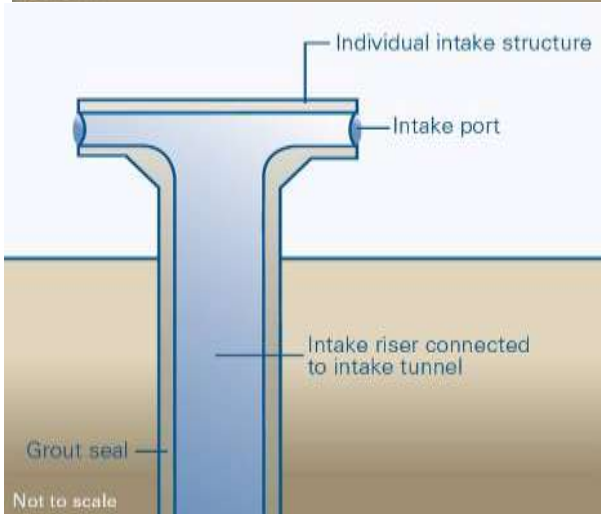
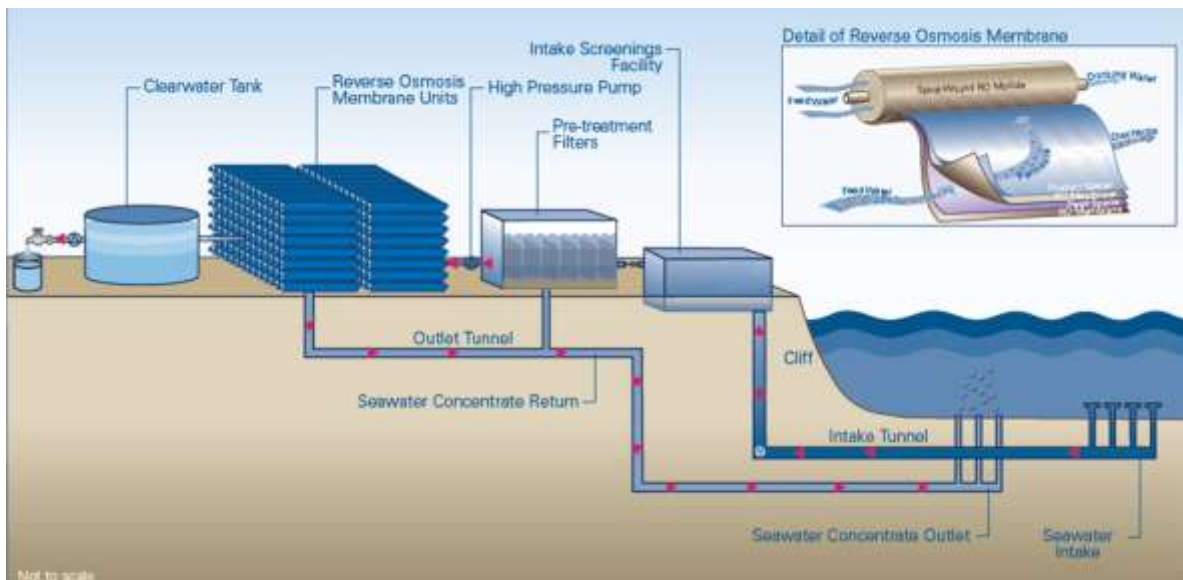


Figure 23: Schematic designs for Sydney (Australia) RO plant, 125,000-500,000 m<sup>3</sup>/d, similarly applied for Perth RO plant, 140,000m<sup>3</sup>/d. Open intake towers located 200-300m offshore in a depth of approximately 20-30m. Outfall diffuser located 250-350m offshore in a water depth of approximately 20-30m. 20 risers spaced 25m discharging through 2 ports with an angle of 60° to the horizontal, (Source: Sydney Water and Fichtner, 2005).

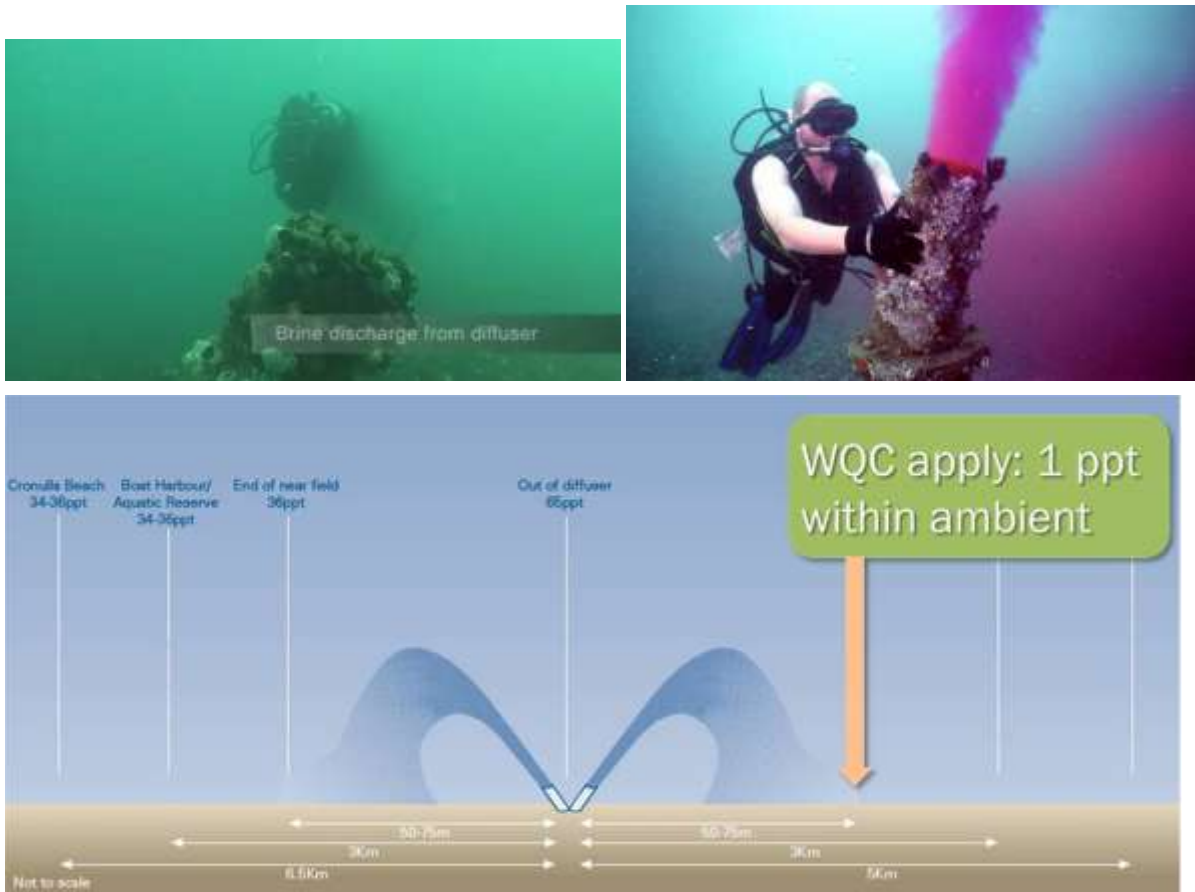


Figure 24: Operating diffuser outfall port of Australian RO plants. Left: Diver behind discharging outfall port (Source: Alspach et al., 2009). Right: Diver besides discharging diffuser port during tracer experiment to measure dilution characteristics (Source: Christie and Bonn elye, 2009). Bottom: Results of model studies and measurements showing salinity concentrations in certain distances of discharge point, being in compliance with the water quality criteria (WQC) of 1ppt above ambient within 75m distance from the discharge (Source: Sydney Water and Fichtner, 2005).

Unfortunately, still shoreline discharges dominate the market and brine outfall systems are furthermore often not properly sited and not at all optimized regarding the mixing conditions and substance distribution, thus leading to unnecessary environmental impacts or even operational problems. In comparison to conventional structures applied for either wastewater or cooling water outfalls (both positively buoyant), brine discharges require for an additional more complex analysis due to the often strong density effects, causing negatively buoyant effluents. If there is furthermore potential for recirculation to the plant intake, badly sited outfalls may reduce overall system efficiency especially, for larger plants or plant complexes.

This report focuses on the improvement of brine discharge systems for surface waters with an efficient multiport diffuser installation showing considerable advantages against the traditional surface discharges on the shore.

An overview of the characteristics of typical intake-outfall schemes is shown in Table 3. It illustrates the variety of applied solutions and the complexity of combinations and sizes, thus showing that no standard solutions apply, nor can be developed. But design and analysis tools will allow mitigating negative effects.

Table 3: Intake pretreatment and discharge design of major SWRO plants (source: Consultants Intl. (2006) Environmental Literature Review and Position Paper for Perth Seawater Desalination Plant Two and Sydney Seawater Reverse Osmosis Plant)

Plant Location	South Europe I	South Europe II	South Europe III	South Europe IV	South Europe V	South Europe VI
Total capacity, m <sup>3</sup> /d	42,750	120,000	65,000	65,000	54,000	40,000
<b>RO product recovery, %</b>	<b>50.0 %</b>	<b>45.0 %</b>	<b>45.0 %</b>	<b>53.0 %</b>	<b>50.0 %</b>	<b>50.0 %</b>
Commissioning year	1989	2002	2000	Under Const	2001	2009
<b>Intake salinity</b>	<b>38.3</b>	<b>39.0</b>	<b>39.0</b>	<b>39.0</b>	<b>36.0</b>	<b>40.6</b>
Intake description	Open intake	Open sea	Horizontal well	Open intake	Open sea, offshore	Open sea, offshore
Pretreatment description	DM Gravity Filter Precoat Filter	Degrit DM pressure filter	1-stage horizontal pressure filter	2-stage pressure filter	DM Gravity Filter	DM Gravity Filter
Coagulant	FeCl <sub>3</sub> , DE	FeCl <sub>3</sub>	FeCl <sub>3</sub>	FeCl <sub>3</sub>	FeSO <sub>4</sub>	FeCl <sub>3</sub>
<b>Brine flow, m<sup>3</sup>/d</b>	<b>42,750</b>	<b>146,667</b>	<b>79,444</b>	<b>57,642</b>	<b>54,000</b>	<b>40,000</b>
<b>Concentrate salinity</b>	<b>76.6</b>	<b>71.0</b>	<b>71.0</b>	<b>83.0</b>	<b>72.0</b>	<b>81.1</b>
<b>Dilution water source</b>	<b>none</b>	<b>PPWC</b>	<b>none</b>	<b>none</b>	<b>none</b>	<b>none</b>
<b>Dilution water, m<sup>3</sup>/d</b>	<b>0</b>	<b>n/a</b>	<b>0</b>	<b>0</b>	<b>0</b>	<b>0</b>
<b>Final discharge salinity</b>	<b>76.6</b>	<b>n/a</b>	<b>70.9</b>	<b>83.0</b>	<b>72.0</b>	<b>81.1</b>
<b>Discharge distance offshore</b>		<b>150 m</b>	<b>4650 m</b>	<b>5100 m</b>	<b>1500 m</b>	<b>250 m</b>
<b>Discharge elevation</b>		<b>-13 m</b>			<b>-18 m</b>	<b>-3.5 m</b>
<b>Discharge description</b>		<b>CC and filter BW blended with PPCW</b>	<b>Subsea outfall with multiple diffusers</b>	<b>Subsea outfall with multiple diffusers</b>		<b>10 diffusers, pipe on seabed/buried</b>
<b>BW blended with CC</b>	<b>Y</b>	<b>Y</b>	<b>Y</b>	<b>Y</b>	<b>Y</b>	<b>Y</b>
BW sludge blended CC	Y	Y	Y	Y	Y	Y
Is discharge plume visible?	N/R	N/R	N/R	N/R	N	infrequently
Energy demand kWh/m <sup>3</sup>	6.16	4.08	4.25	4.3	4.5	5.3
Power source	Grid	Grid	Grid	Grid	Grid	Grid
Receiving body type	Open sea	Open Sea	Open Sea	Open Sea	Open Sea	Open Sea

(PPCW: Power plant cooling water, BW: filter backwash, CC: concentrate, WW: wastewater plant, DM: dual media, DE: Diatomaceous Earth)

Plant Location	North America I	North America II	North America III	North America IV	Caribbean I
Total capacity, m <sup>3</sup> /d	108,820	189,250	189,250	75,700	119,000
<b>RO product recovery, %</b>	<b>41.8%</b>	<b>50.0%</b>	<b>50.0%</b>	<b>45.0%</b>	<b>50.0%</b>
Commissioning year	not comm.	Proposed	Proposed	Proposed	2002
<b>Intake salinity</b>	<b>32.0</b>	<b>34.0</b>	<b>33.5</b>	<b>34.0</b>	<b>29.0</b>
Intake description	Open intake	Open sea, 550m offshore	tbd	tbd	Open intake
Pretreatment description	Flocculation SM Gravity Filter Precoat filter	tbd	tbd	tbd	Flocculation/settle, deep bed gravity filter
Coagulant	FeSO <sub>4</sub> , DE	tbd	tbd	tbd	FeCl <sub>3</sub>
<b>Brine flow, m<sup>3</sup>/d</b>	<b>151,515</b>	<b>189,250</b>	<b>189,250</b>	<b>92,522</b>	<b>119,000</b>
<b>Concentrate salinity</b>	<b>55.0</b>	<b>68.0</b>	<b>67.0</b>	<b>61.8</b>	<b>58.0</b>
<b>Dilution water source</b>	<b>PPCW</b>	<b>PPCW</b>	<b>PPCW</b>	<b>PPCW</b>	<b>Industrial plant CW</b>
<b>Dilution water, m<sup>3</sup>/d</b>	<b>8,553,600</b>	<b>480,700</b>	<b>1,022,000</b>	<b>4,640,000</b>	n/a
<b>Final discharge salinity</b>	<b>32.4</b>	<b>43.6</b>	<b>38.8</b>	<b>34.5</b>	n/a
<b>Discharge distance offshore</b>	<b>at shoreline</b>	<b>518 m</b>	<b>at shoreline</b>	<b>1370 m</b>	<b>At shoreline</b>
<b>Discharge elevation</b>	<b>0</b>	<b>-10 m</b>	<b>0</b>		<b>0</b>
<b>Discharge description</b>	<b>Filter BW settled, sludge to landfill; CC blended with PPCW</b>	<b>Pipe buried under seabed, single port discharge</b>	<b>Discharged with PPCW</b>	<b>Pipe laid or anchored to seabed, 10+ omni- directional diffusers</b>	<b>Filter backwash settled, sludge to landfill</b>
<b>BW blended with CC</b>	<b>Y</b>	<b>Y</b>	<b>Y</b>	<b>Y</b>	<b>Y</b>
BW sludge blended CC	N	Y	Y	Y	N
Is discharge plume visible?	N/R	N/A	N/A	N/A	N/R
Energy demand kWh/m <sup>3</sup>	2.96				3.8
Power source	Co-located	Co-located	Co-located	Co-located	Grid
Receiving body type	Bay	Open Sea	Open Sea	Open Sea	Bay

(PPCW: Power plant cooling water, BW: filter backwash, CC: concentrate, WW: wastewater plant, DM: dual media, DE: Diatomaceous Earth)

Plant Location	Asia I	Asia II	Mid East I	Mid East II	Mid East III	Mid East IV	Mid East V	Mid East VI
Total capacity, m <sup>3</sup> /d	136,360	50,000	170,465	326,144	56,800	56,800	90,900	127,500
<b>RO product recovery, %</b>	<b>38.5 %</b>	<b>60.0 %</b>	<b>43.0 %</b>	<b>40.7 %</b>	<b>35.0 %</b>	<b>35.0 %</b>	<b>35.0 %</b>	<b>35.0 %</b>
Commissioning year	2005	2005	2004	2005	1989	1994	2001	1998
<b>Intake salinity</b>	<b>35.0</b>	<b>35.0</b>	<b>40.0</b>	<b>40.7</b>	<b>43.3</b>	<b>43.3</b>	<b>45.0</b>	<b>43.8</b>
Intake description	Open sea, offshore	Infiltration gallery	Open sea, offshore	Open sea, 1 km offshore	Open intake	Open intake	Open sea	Open sea, offshore
Pretreatment description	DAF, Gravity filter	Spiralwound UF	DM Gravity Filter	DM Gravity Filter	DM Gravity Filter	DM Gravity Filter	DM Gravity Filter	DM Gravity Filter
Coagulant	FeCl <sub>3</sub>	n/a	FeCl <sub>3</sub>	FeSO <sub>4</sub>	FeCl <sub>3</sub>	FeCl <sub>3</sub>	FeCl <sub>3</sub>	
<b>Brine flow, m<sup>3</sup>/d</b>	<b>217,822</b>	<b>33,333</b>	<b>225,965</b>	<b>475,193</b>	<b>105,486</b>	<b>105,486</b>	<b>168,814</b>	<b>236,786</b>
<b>Concentrate salinity</b>	<b>57.0</b>	<b>87.5</b>	<b>70.2</b>	<b>68.6</b>	<b>66.6</b>	<b>66.6</b>	<b>69.2</b>	<b>67.3</b>
Dilution water source	none	WW effluent	PPCW	none	PPCW	PPCW		
Dilution water, m <sup>3</sup> /d	0	33,000	1,409,160	0				
<b>Final discharge salinity</b>	<b>56.9</b>	<b>61.4</b>	<b>44.2</b>	<b>68.6</b>	<b>66.6</b>	<b>66.6</b>	<b>69.2</b>	<b>67.3</b>
Discharge distance offshore	120 m	360 m	at shoreline	at shoreline				
Discharge elevation	≈ -3 m		0	0				
Discharge description	DAF float, BW with CC, pipe laid on seabed, discharge angled for better mixing	with WW effluent onshore, gravity discharge to sea via multi-port diffuser	Blend with PPCW, discharge from channel at shoreline	BW and concentrate discharge at shoreline adjacent to PPCW	CC and BW blended with PPCW	CC and BW blended with PPCW	BW blended with CC discharged to sea	
<b>BW blended with CC</b>	<b>Y</b>	<b>Y</b>	<b>Y</b>	<b>Y</b>	<b>Y</b>	<b>Y</b>	<b>Y</b>	<b>Y</b>
BW sludge blended CC	Y	Y	Y	Y	Y	Y	Y	Y
Is discharge plume visible?	Infrequently	N/R	No	Infrequently	N/R	N/R	N/R	N/R
Energy demand kWh/m <sup>3</sup>	4.34	5.5	<5.3	3.9	4.8		7.5	7.0
Power source	Grid	Grid	Co-located/ Hybrid	Co-located	Co-located	Co-located	Co-located	Co-located
Receiving body type	Open Sea	Open Sea	Open Sea	Open Sea	Open Sea	Open Sea	Open Sea	Open Sea

(PPCW: Power plant cooling water, BW: filter backwash, CC: concentrate, WW: wastewater plant, DM: dual media, DE: Diatomaceous Earth)

### **3. ENVIRONMENTAL IMPACTS**

The impacts of a desalination plant discharge on the marine environment depend on the physical and chemical properties of the desalination plant reject streams, and the susceptibility of coastal ecosystems to these discharges depending on their hydrographical and biological features. Therefore, a good knowledge of both the effluent properties and the receiving environments is required in order to evaluate the potential impacts of desalination plants on the marine environment. This can be achieved by carrying out site- and project-specific environmental impact assessment (EIA) studies.

This chapter provides background information on the potential environmental impacts of desalination plant discharges in the form of: descriptions of effluent characteristics (Table 4), estimates of chemical discharge loads, calculated on the basis of installed seawater desalination capacities for different sea regions (Section 3.1), a literature review on related environmental impacts and impact assessments (Section 3.2) and socio-economic impacts (Section 3.3) of the two most common seawater desalination processes. A summary of existing environmental quality standards is given in Section 3.4. Though the report is focused on the brine discharge system, general mitigation measures for the whole system are also briefly described in Section 3.5.

#### **3.1. Installed capacities - discharge loads and concentrations**

The worldwide installed capacity for desalination of seawater is increasing at a rapid pace. The latest figures from the 20th IDA Worldwide Desalting Plant Inventory indicate that about 28 million cubic meters per day ( $\text{Mm}^3/\text{d}$ ) are presently produced from seawater sources (IDA, 2008), which is comparable to the average discharge of the Seine River in Paris. Three quarters of this water is produced in three sea areas: the Arabian Gulf, the Red Sea, and the Mediterranean Sea. Due to their semi-enclosed natures, cumulative effects on the sea areas as a whole need to be evaluated in addition to the localized effects on coastal ecosystems. The following maps present installed capacity by sea region and estimated chemical discharge loads for three pollutants (chlorine, copper and antiscalants), based on typical effluent properties. A detailed description of effluent characteristics has been given in previous publications, e.g. Hodgkiess et al. (2003), Lattemann and Höpner (2003).

The maps presented here were first published in Lattemann and Höpner (2003) and later updated on the basis of the 19th IDA Worldwide Desalting Plant Inventory (IDA, 2006). The maps showing installed capacities were published in Lattemann and Höpner (2008). An update on the basis of the 20th IDA has been prepared for the present report.

Table 4: Effluent properties of RO, MSF and MED plants, assuming conventional process design (WHO, 2008; Lattemann and Höpner, 2008)

	Reverse Osmosis	Multi Stage Flash (MSF)	Multi Effect Distillation (MED)
<b>Physical parameters</b>	no use of cooling water in the process, but RO plants may receive their intake water from cooling water discharges	assuming that the two waste streams from the desalination process are combined, i.e. the brine is diluted with major amounts of cooling water from the desalination process; further dilution with cooling water from power plants may occur but is not considered here.	
Salinity (S) (depending on ambient salinity and recovery rate)	<ul style="list-style-type: none"> <li>SWRO: 65–85 g/l</li> <li>BWRO: 1–25 g/l</li> </ul>	<ul style="list-style-type: none"> <li>cooling water: ambient salinity (e.g. 40 g/l)</li> <li>brine: 60–70 g/l</li> <li>combined: 45–50 g/l</li> </ul>	<ul style="list-style-type: none"> <li>cooling water: ambient salinity</li> <li>brine: 60–70 g/l</li> <li>combined: 50–60 g/l</li> </ul>
Temperature (T)	<ul style="list-style-type: none"> <li>if subsurface intakes: may be below ambient T due to a lower T of source</li> <li>if open intakes used: close to ambient</li> <li>if mixed with cooling water of power plants: may be above ambient</li> </ul>	<ul style="list-style-type: none"> <li>brine: 3–5°C above ambient</li> <li>cooling water: 8–12°C above ambient</li> <li>combined: ~ 5–10°C above ambient</li> </ul>	<ul style="list-style-type: none"> <li>brine: 5–25°C above ambient</li> <li>cooling water: 8–12°C above ambient, up to 20 °C possible</li> <li>combined: ~ 10–20°C above ambient</li> </ul>
Plume density ( $\rho$ )	<ul style="list-style-type: none"> <li>higher than ambient (negatively buoyant plume)</li> </ul>	<ul style="list-style-type: none"> <li>plume can be positively, neutrally or negatively buoyant depending on the process design and mixing with cooling water before discharge, typically positively buoyant</li> </ul>	
Dissolved Oxygen (DO)	<ul style="list-style-type: none"> <li>if subsurface intake: may be below ambient due to lower DO of source</li> <li>if open intakes used and if oxygen scavengers for dechlorination are not overdosed: close to ambient</li> </ul>	<ul style="list-style-type: none"> <li>brine: below ambient because of deaeration and use of oxygen scavengers</li> <li>cooling water: close to ambient (minor effects on DO because of changes in temperature)</li> <li>combined: mixing of brine with cooling water increases the DO content of the combined effluent close to ambient; turbulent mixing allows oxygen take-up from air</li> </ul>	
<b>Biofouling control additives and by-products</b>			
Oxidants <ul style="list-style-type: none"> <li>mainly chlorine</li> <li>chlorine dioxide used in some plants</li> </ul>	<ul style="list-style-type: none"> <li>typically dosage of 1–2 ppm to the feed water in all plants operating on open seawater</li> </ul>	<ul style="list-style-type: none"> <li>discharge level is about 10–25 % of dosage due to chlorine demand of the seawater</li> <li>both the brine and the cooling water contain residual chlorine</li> <li>chlorine typically not removed by a dechlorination step inside the plant</li> </ul>	
	<ul style="list-style-type: none"> <li>oxidants removed to prevent membrane damage, using sodium bisulfite (2–4 times higher dosage than oxidizing agent dose)</li> </ul>		
Halogenated organic by-products such as trihalomethanes (THMs)	<ul style="list-style-type: none"> <li>use of chlorine dioxide reduces the risk of by-product formation</li> </ul>	<ul style="list-style-type: none"> <li>chlorination of seawater results in varying composition and concentrations of halogenated (chlorinated and brominated) organic by products, mainly THMs such as bromoform</li> </ul>	
	<ul style="list-style-type: none"> <li>may form during chlorination, but levels low due to dechlorination</li> </ul>		
<b>Removal of turbidity (suspended solids)</b>			
Coagulants <ul style="list-style-type: none"> <li>dosage 1–30 mg/l</li> <li>often iron-III-salts</li> </ul>	<ul style="list-style-type: none"> <li>if filter backwash is discharged to surface waters: may cause turbidity and sedimentation in the discharge site and iron salts may cause effluent coloration (“red brines”)</li> </ul>	treatment not applied	treatment not applied
Coagulant aids <ul style="list-style-type: none"> <li>dosage 0.1–5 mg/l</li> <li>e.g. polyacrylamide</li> </ul>			

<b>Scale control additives</b> (used in all desalination processes, can be a blend of several different antiscalants in combination with acid treatment)			
Polymeric antiscalants (e.g. polymaleic acids) and phosphonates ▪ dosage: 1–2 ppm	▪ mainly used in RO	▪ antiscalant only present in the brine, but not in the cooling water	
	<ul style="list-style-type: none"> <li>▪ dosage/discharge concentration below toxic levels to invertebrate and fish species; some products are classified as being harmful to algae, presumably due to a nutrient inhibition effect</li> <li>▪ slow degradation (some products classified as ‘inherently’ biodegradable) with presumably increased residence times in surface waters</li> </ul>		
Phosphates ▪ dosage: 2 ppm	▪ still used at a limited scale	▪ not stable at high temp. (blends of polymeric antiscalants and phosphonates preferred )	
	▪ may cause eutrophication near outlets, as easily hydrolyzed to orthophosphate, a major nutrient for primary producers		
Acid (H <sub>2</sub> SO <sub>4</sub> ) ▪ dosage: 30–100 ppm	<ul style="list-style-type: none"> <li>▪ lowers the pH from around 8.3 (natural pH of seawater) to pH 6–7</li> <li>▪ effective against calcium carbonate scales but not against sulphate scale, therefore more effective in seawater RO and MED processes where calcium carbonate is the main scale forming species</li> <li>▪ the acidity is quickly consumed by the natural alkalinity of seawater, so that the pH quickly returns to normal</li> </ul>		
<b>Foam control additives</b>			
Antifoaming agents (e.g. polyglycol)	▪ treatment not applied	<ul style="list-style-type: none"> <li>▪ typically low dosage (0.1 ppm) below harmful levels</li> <li>▪ used in all distillation processes, but primarily in MSF</li> <li>▪ antifoam only present in the brine, but not in the cooling water</li> </ul>	
<b>Corrosion</b>			
Heavy metals	<ul style="list-style-type: none"> <li>▪ metallic equipment made from corrosion-resistant stainless steel</li> <li>▪ concentrate may contain low levels of iron, chromium, nickel, molybdenum if low-quality steel is used</li> </ul>	<ul style="list-style-type: none"> <li>▪ metallic equipment made from carbon steel, stainless steel, copper nickel alloys</li> <li>▪ concentrate may contain iron and copper, copper levels can be an environmental concern</li> </ul>	<ul style="list-style-type: none"> <li>▪ metallic equipment made from carbon and stainless steel, aluminium and aluminum brass, titanium, or copper nickel alloys</li> <li>▪ lower corrosion rates than in MSF</li> <li>▪ no data on brine contamination available</li> </ul>
Corrosion prevention	▪ not necessary besides choice of materials	<ul style="list-style-type: none"> <li>▪ as the feed water is deaerated, the brine is also deaerated before mixing with cooling water, which is not deaerated</li> <li>▪ in MSF, the feed water (but not the cooling water) may also be treated with oxygen scavengers (e.g. sodium bisulfite), which may also remove residual chlorine</li> </ul>	
<b>Cleaning solutions (only present if cleaning solutions are discharged to surface waters)</b>			
Cleaning chemicals (used intermittently)	Alkaline (pH 11-12) or acidic (pH 2-3) solutions with additives, e.g.: – detergents (e.g. dodecylsulfate) – complexing agents (e.g. EDTA) – oxidants (e.g. sodium perborate) – biocides (e.g. formaldehyde)	Acidic (low pH) washing solution which may containing corrosion inhibitors such as benzotriazole derivates	

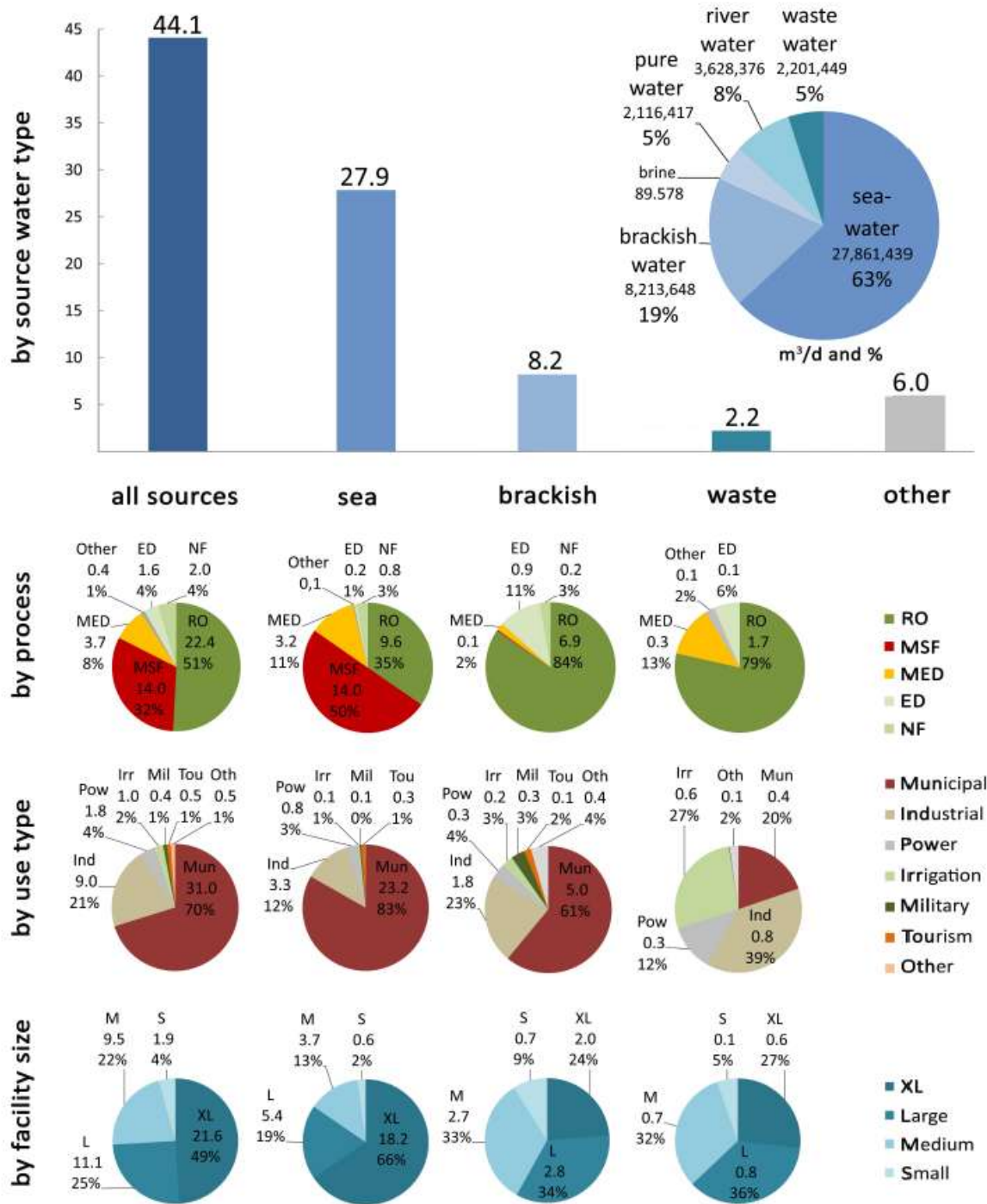


Figure 25: Global desalination capacity (in Mm<sup>3</sup>/d and %) by source water type (top row), by process and source water type (2nd row), by use type and source water type (3rd row) and by plant size and source water type (last row). Abbreviations: reverse osmosis (RO), multi-stage flash distillation (MSF), multi-effect distillation (MED), nanofiltration (NF), electrodialysis (ED), XL>50,000m<sup>3</sup>/d, L>10,000m<sup>3</sup>/d, M>1,000m<sup>3</sup>/d (IDA, 2008).

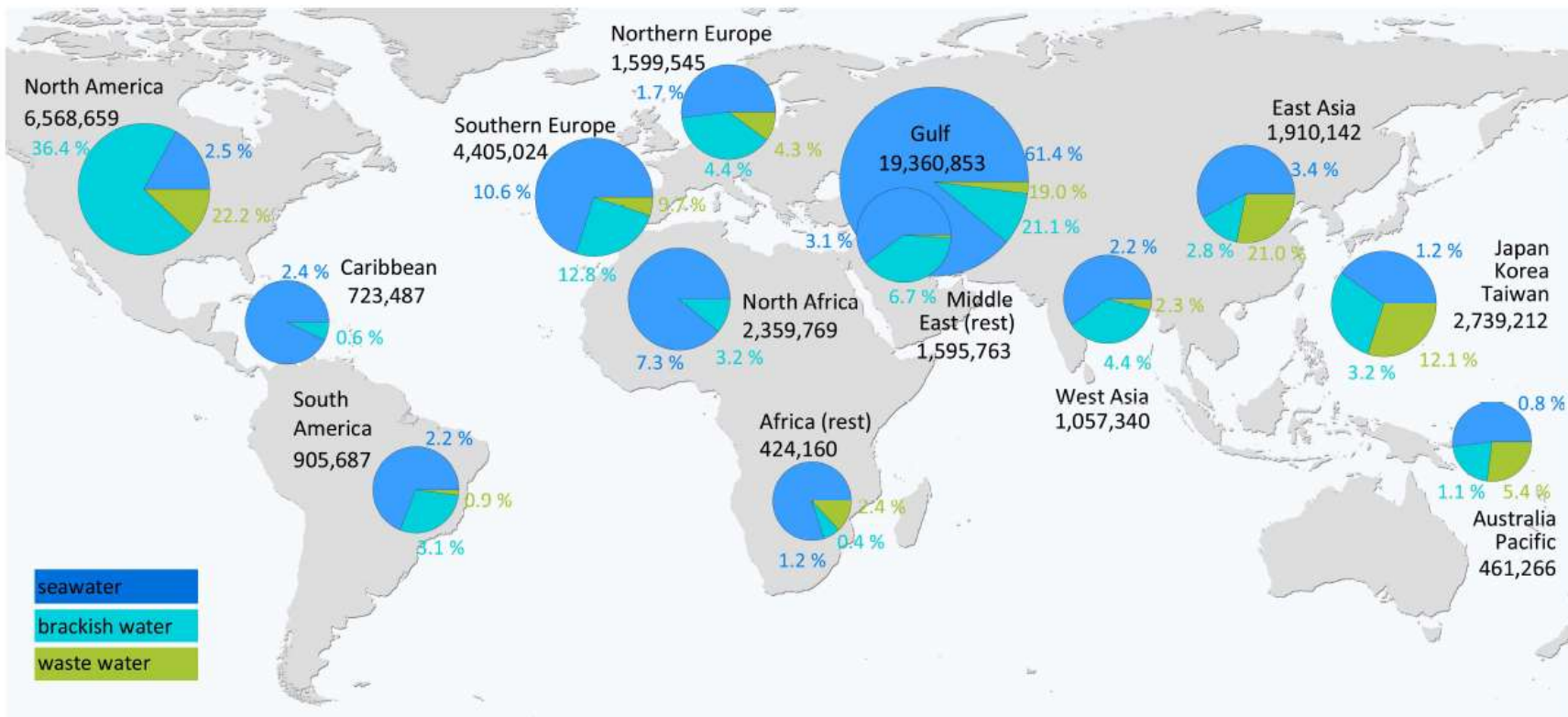


Figure 26: Global desalination capacity in m<sup>3</sup>/d and %. For example, the installed capacity in Southern Europe is 4,405,024 m<sup>3</sup>/d. This figure includes all source water types. Seawater desalination accounts for most of the production in Southern Europe, brackish water for about 1/4 of the production and waste water desalination plays a relatively minor role (pie diagram). The figures next to the pie diagram give the contribution to the global production, i.e., the seawater desalination capacity in Southern Europe represent 10.6% of the global seawater desalination capacity. The brackish water capacity - though it is less than half the seawater desalination capacity in Southern Europe - represents 12.8% of the global brackish water desalination capacity (IDA, 2008)

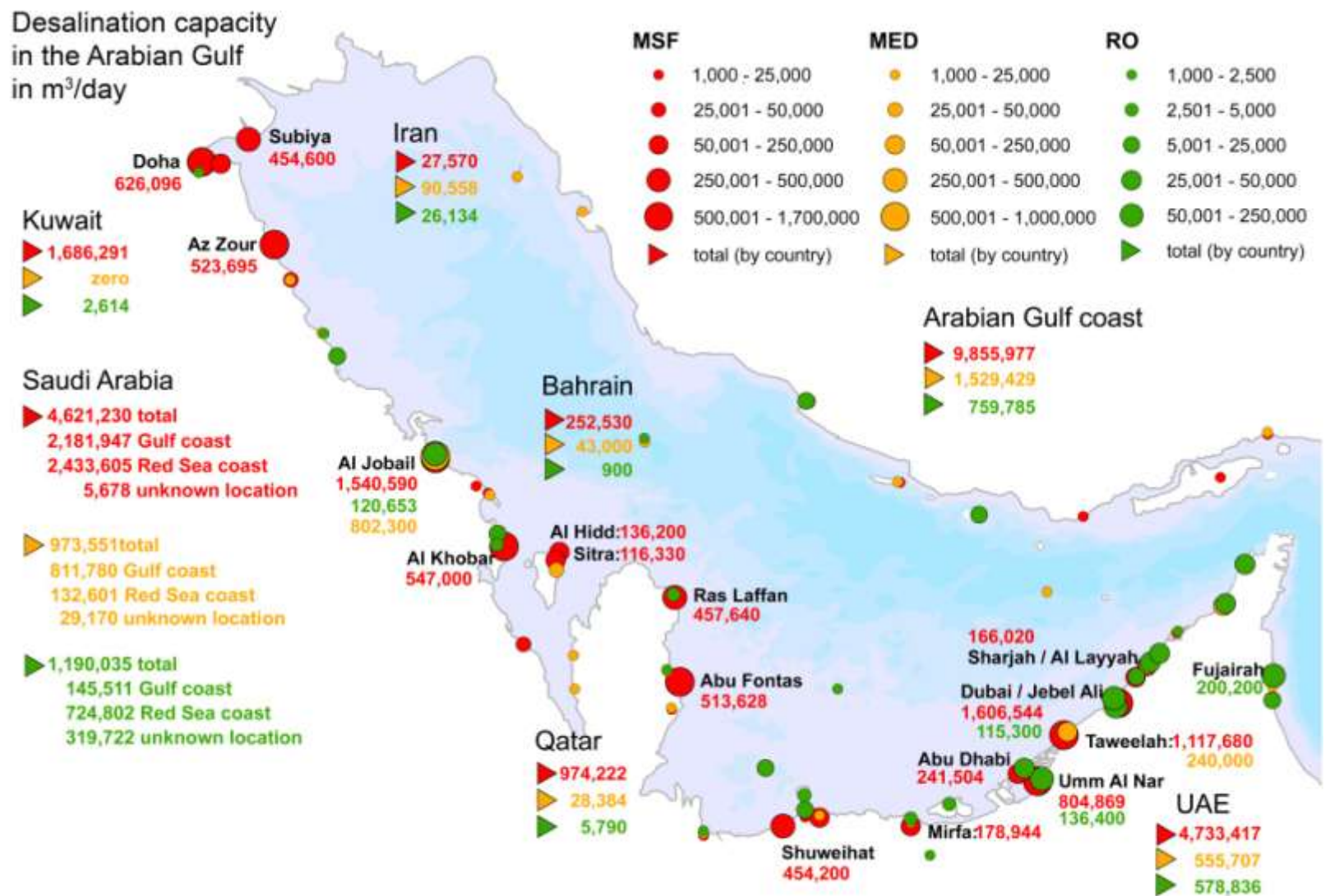


Figure 27: Capacity: Cumulative MSF, MED and RO capacities in m<sup>3</sup>/day by site location (dots) and by country (triangles). The map shows all sites with an installed capacity  $\geq 1,000$  m<sup>3</sup>/d and displays sites with a capacity  $\geq 100,000$  m<sup>3</sup>/d by name and capacity. The map was first published in Lattemann and Höpner (2003) and updated using raw data from IDA and GWI (2008)

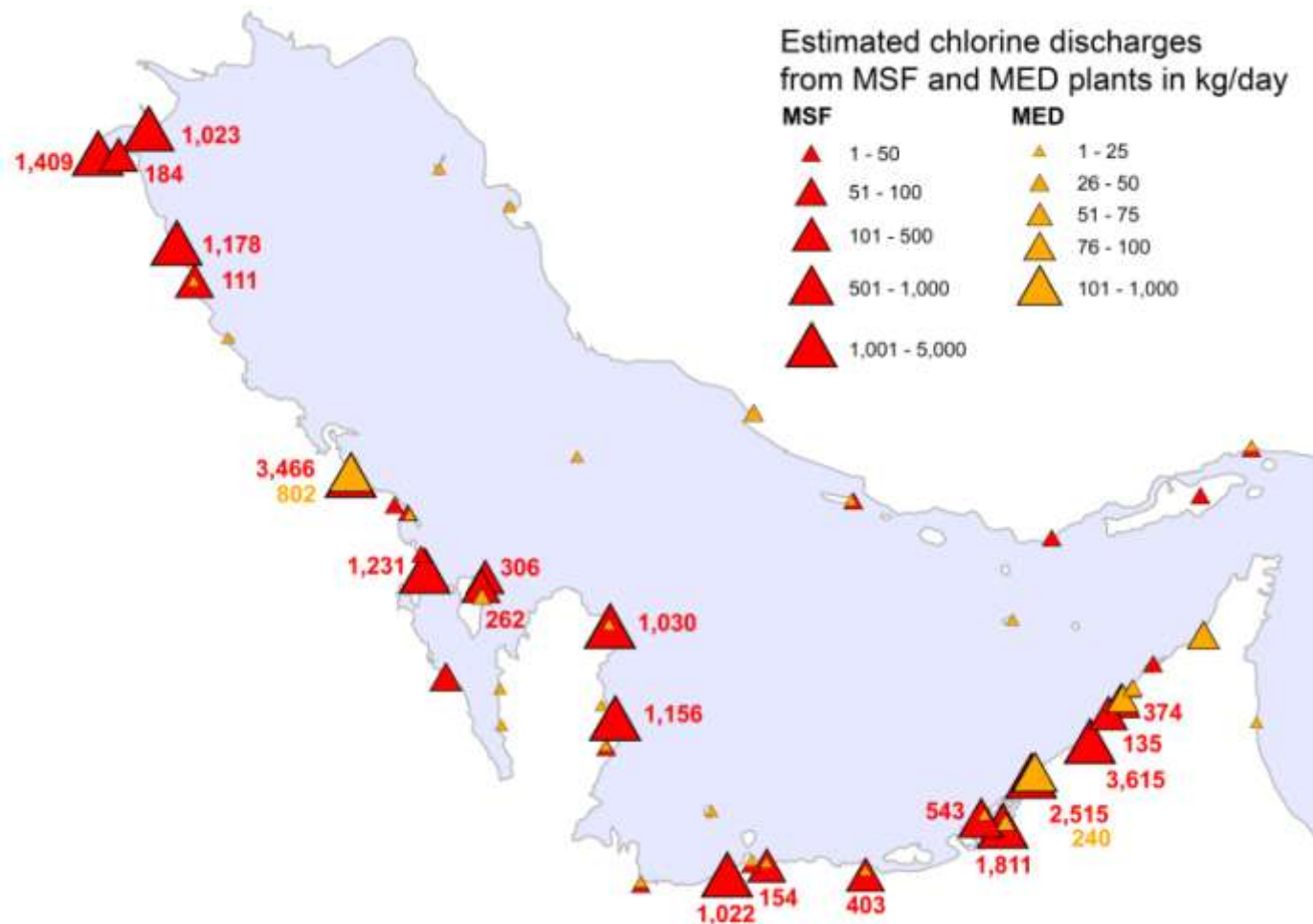


Figure 28: Chlorine: Estimated discharge of chlorine from MSF and MED distillation plants in kg/day. The figures were calculated from the installed desalination capacity, assuming a product recovery rate of 10 % for MSF and 20 % for MED plants (i.e. waste water flows of 90 % and 80 %, respectively), and assuming a residual chlorine concentration of 0.25 mg/l in the combined waste water of the MSF and MED process (i.e. concentrate and cooling water), resulting in a specific chlorine load of 2.3 kg/day for MSF and 1 kg/day for MED for every 1,000 m<sup>3</sup>/d. The estimated total load for the Arabian Gulf is 22.2 tons of chlorine from MSF plants and 1.5 tons from MED plants per day. The map shows all sites with an installed capacity  $\geq 1,000$  m<sup>3</sup>/d and displays the chemical load for all sites with a chlorine load  $\geq 100$  kg/d. The map does not take chlorine discharges from co-located power plants into account

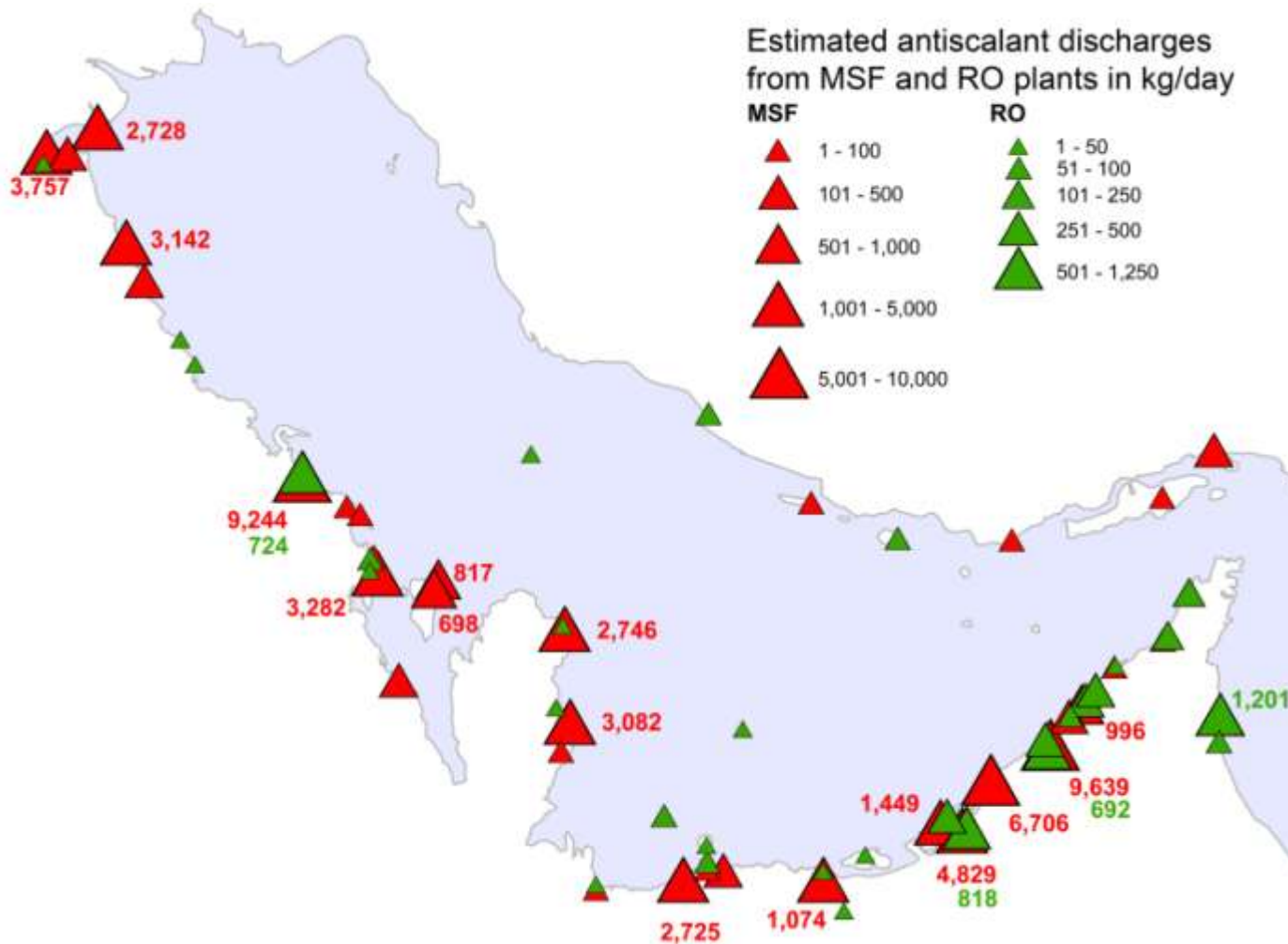


Figure 29: Antiscalant: Estimated discharge of antiscalants from MSF and RO plants in kg/day. The figures were calculated from the installed desalination capacity, assuming a product recovery rate of 10 % for MSF and 33.3 % for RO plants, and assuming an antiscalant dosage of 2 mg/l to the make-up water in the MSF plant / respectively to the feedwater in the RO plant (for the given assumptions, the specific antiscalant loads are identical for MSF and RO plants, i.e. 6 kg/day for every 1,000 m<sup>3</sup>/d installed capacity). The estimated total load for the Arabian Gulf is 59.1 tons of antiscalants from MSF plants and 5.8 tons from RO plants per day. The map shows all sites with an installed capacity ≥ 1,000 m<sup>3</sup>/d and displays the chemical load for all sites with an antiscalant load ≥ 500 kg/d

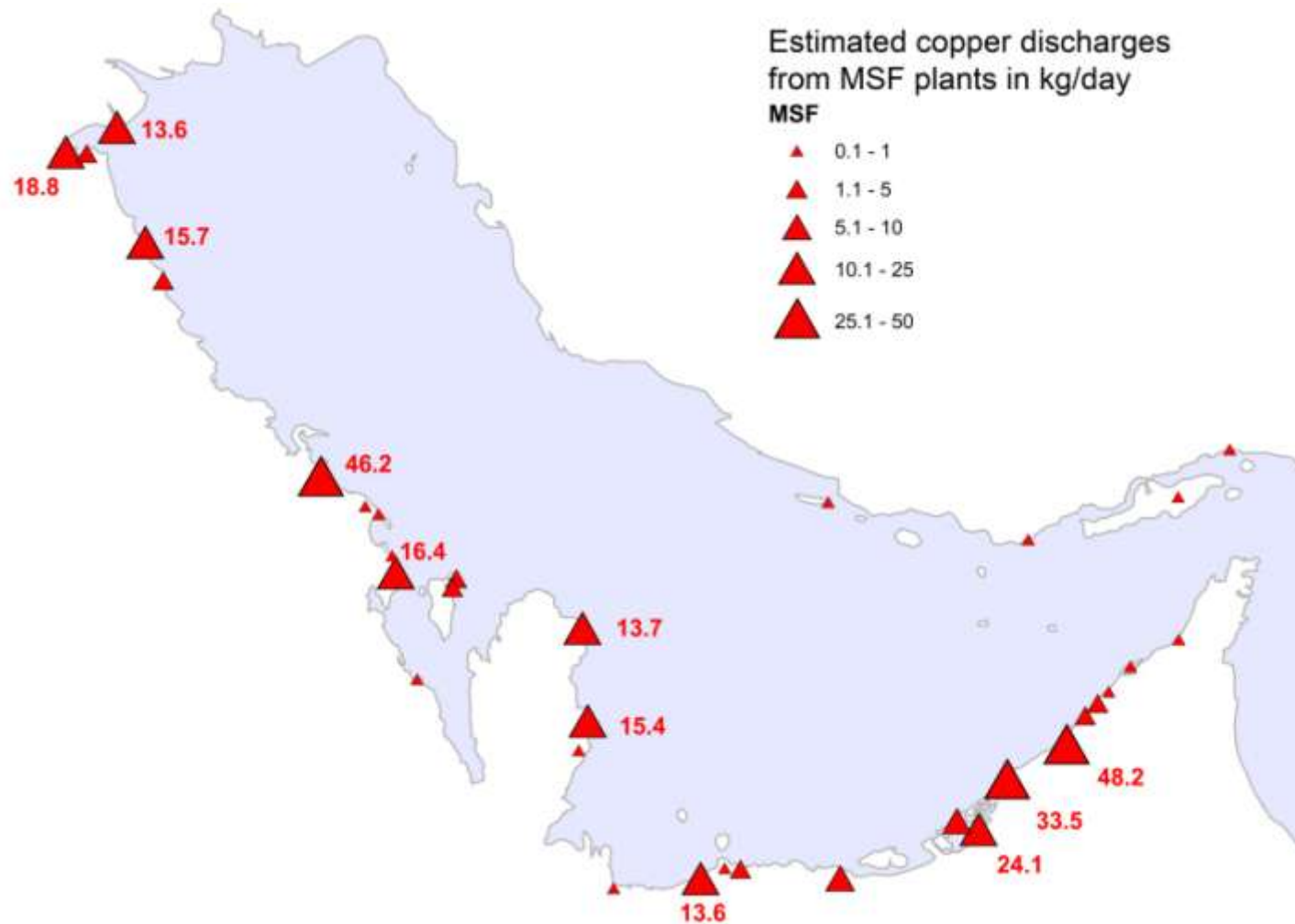


Figure 30: Copper: Estimated discharge of copper from MSF plants in kg/day. The figures were calculated from the installed desalination capacity, assuming a product recovery rate of 10 % and a residual copper level of 15  $\mu\text{g/l}$  in the concentrate of the MSF plant, resulting in a specific copper load of 0.03 kg/day for every 1,000  $\text{m}^3/\text{d}$ . The estimated total load for the Arabian Gulf is 296 kg of copper from MSF plants per day. The map shows all sites with an installed capacity  $\geq 1,000 \text{ m}^3/\text{d}$  and displays the chemical load for all sites with a copper load  $\geq 10 \text{ kg/day}$ . The map does not take copper discharges from cooling water discharges (neither from the distillation plant nor from co-located power plants) into account

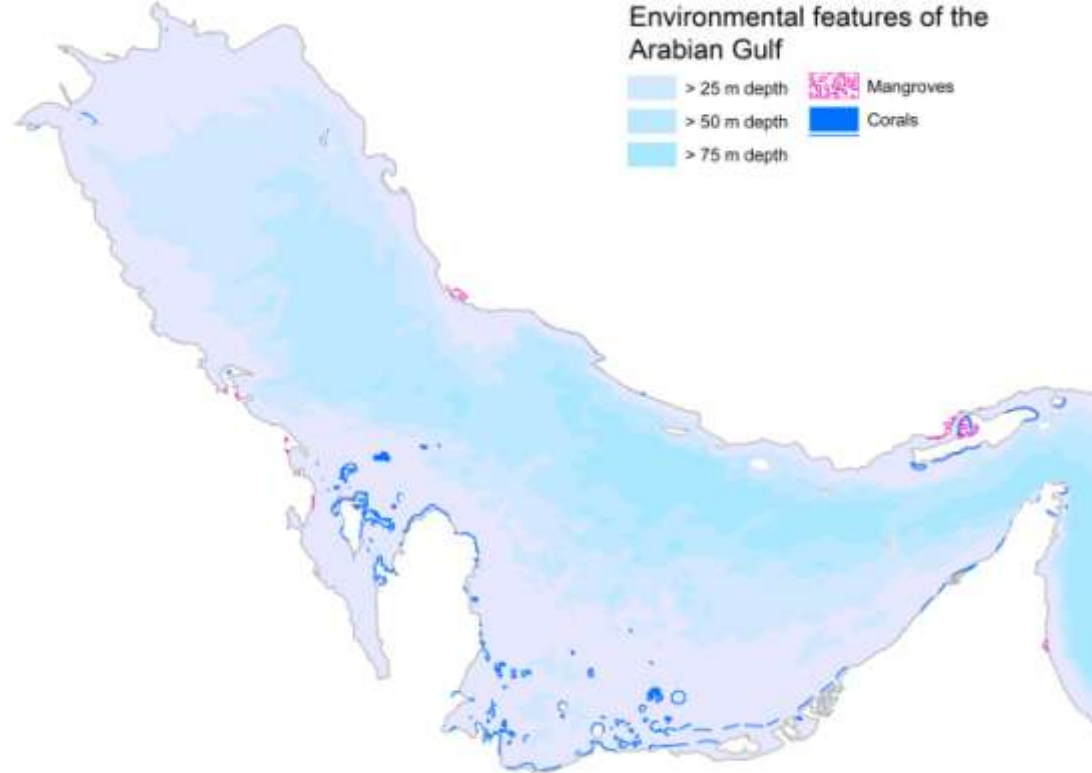


Figure 31: Ecosystems. Most of the desalination plants are located on the south-western shoreline of the Arabian Gulf which is characterized by shallow waters (< 25 m), bays fringed with coral reefs, mangroves and seagrasses. It can be estimated that the combined discharge of all MSF plants (9.9 million m<sup>3</sup>/day) amounts to a waste water flow of more than 1000 m<sup>3</sup>/s, which is the equivalent of a large river. This waste water is characterised by increased salinity and temperature and loaded with residual additives, including chlorine and antiscalants, as well as corrosion products such as copper. Daily discharge loads of these compounds from desalination plants into the Arabian Gulf are estimated to be at about 24 tons of chlorine, 65 tons of antiscalants and 0.3 tons of copper per day. Residual chlorine and chlorination by-products such as trihalomethanes, chlorophenols and chlorobenzenes are detectable near desalination plants, and chlorine pollution has been reported to affect two mud flat areas in the Bay of Kuwait, which is probably caused by the Doha power and desalination plant. Nothing is known about the environmental fate and effects of the antiscalant discharges, and signals of copper contamination in water, sediment and organisms attributed to desalination activity are also missing, possibly due to a lack of consequent monitoring. To date, no impact assessment study has been published which is based on field investigations and comprehensively investigates the single or cumulative impacts of desalination plants on the Arabian Gulf's ecosystem

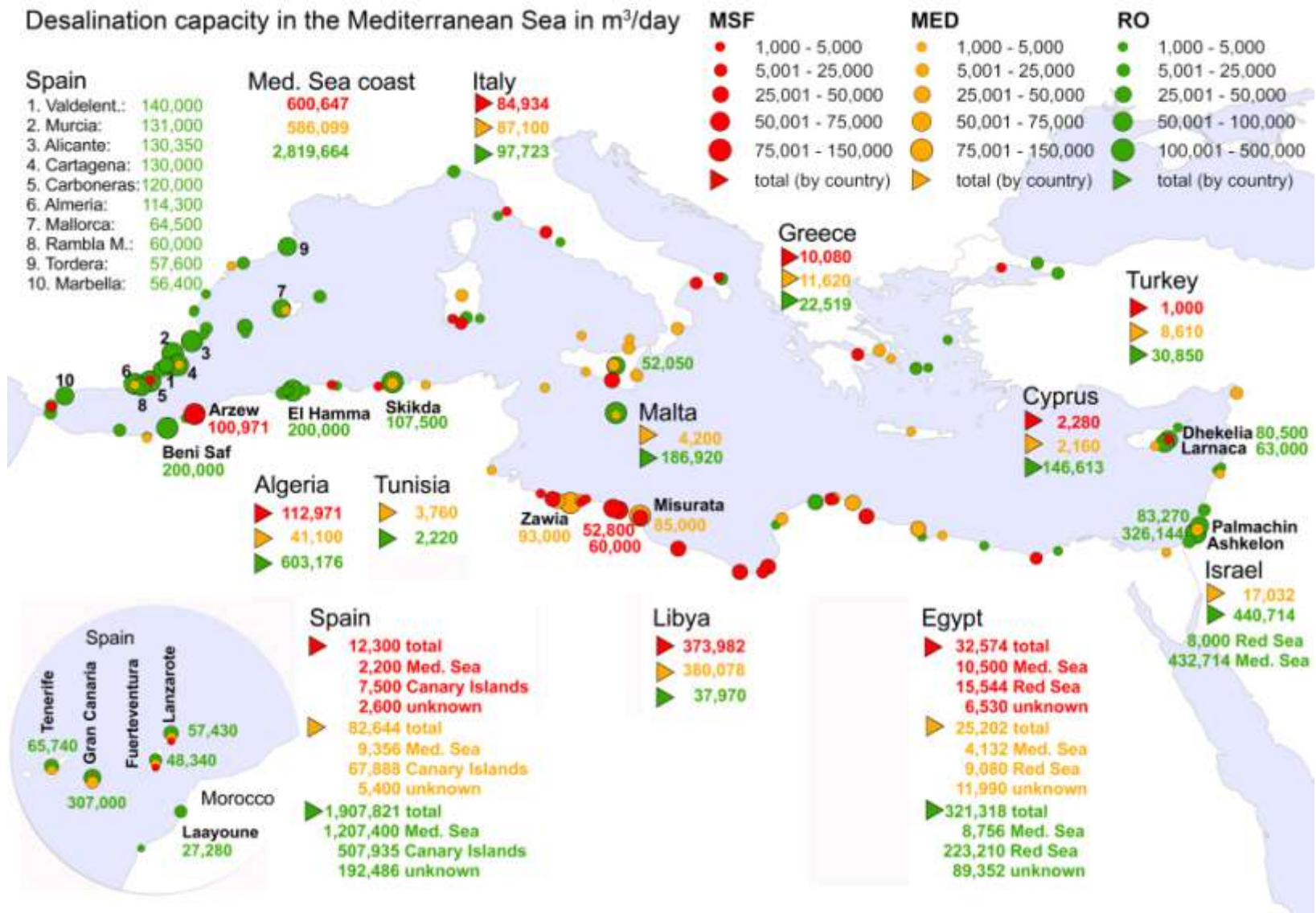


Figure 32: Capacity: Cumulative MSF, MED and RO capacities in m<sup>3</sup>/day by site location (dots) and by country (triangles). The map shows all sites with an installed capacity ≥ 1,000 m<sup>3</sup>/d and displays sites with a capacity ≥ 50,000 m<sup>3</sup>/d by name and capacity. The map was first published in Lattemann and Höpner (2003) and updated using raw data from IDA and GWI (2008)

Estimated chlorine discharges  
from MSF and MED plants  
in kg/day



Figure 33: Chlorine: Estimated discharge of chlorine from MSF and MED distillation plants in kg/day. The figures were calculated from the installed desalination capacity, assuming a product recovery rate of 10 % for MSF and 20 % for MED plants (i.e. waste water flows of 90 % and 80 %, respectively), and assuming a residual chlorine concentration of 0.25 mg/l in the combined waste water of the MSF and MED process (i.e. concentrate and cooling water), resulting in a specific chlorine load of 2.3 kg/day for MSF and 1 kg/day for MED for every 1,000 m<sup>3</sup>/d. The estimated total load for the Mediterranean is 1,356 kg of chlorine from MSF plants and 588 kg from MED plants per day. The map shows all sites with an installed capacity  $\geq 1,000$  m<sup>3</sup>/d and displays the chemical load for all sites with a chlorine load  $\geq 50$  kg/d. The map does not take chlorine discharges from co-located power plants into account

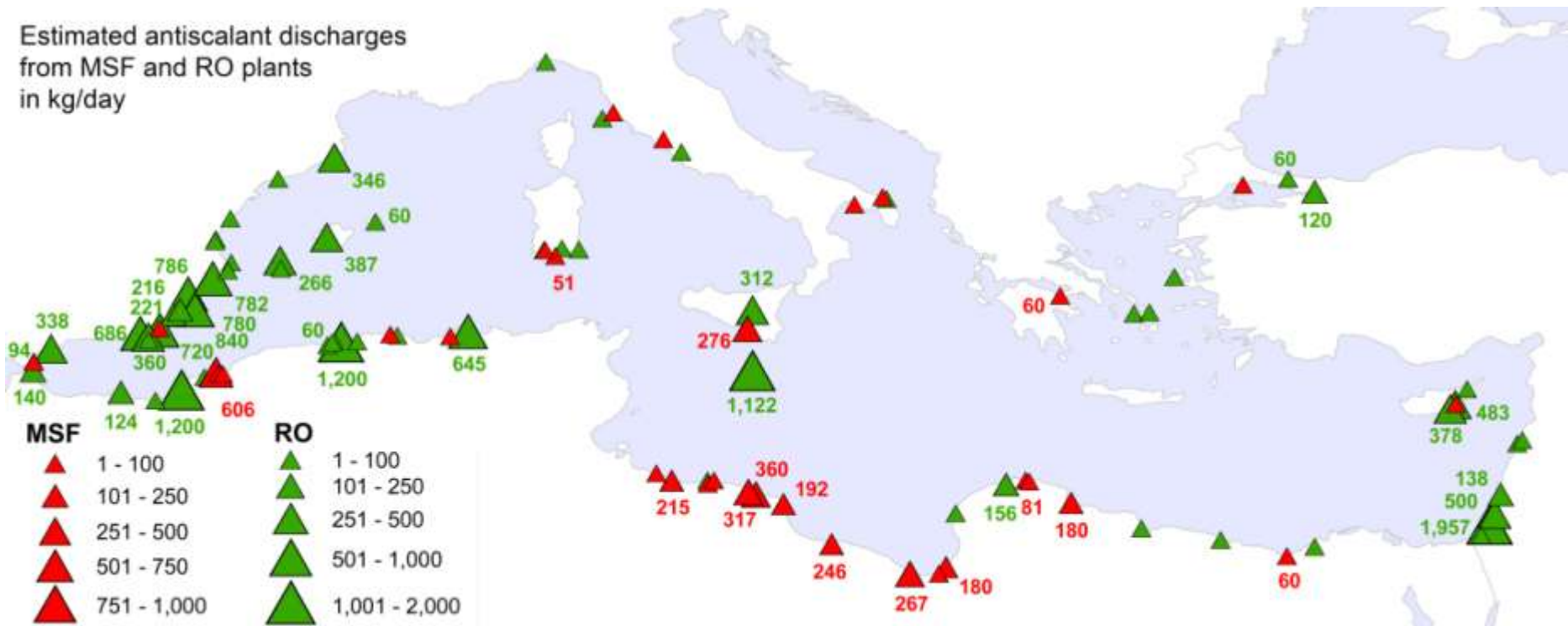


Figure 34: Antiscalant: Estimated discharge of antiscalants from MSF and RO plants in kg/day. The figures were calculated from the installed desalination capacity, assuming a product recovery rate of 10 % for MSF and 33.3 % for RO plants, and assuming an antiscalant dosage of 2 mg/l to the make-up water in the MSF plant / respectively to the feedwater in the RO plant (for the given assumptions, the specific antiscalant loads are identical for MSF and RO plants, i.e. 6 kg/day for every 1,000 m<sup>3</sup>/d installed capacity). The estimated total load for the Mediterranean is 3.6 tons of antiscalants from MSF plants and 19.4 tons from RO plants per day. The map shows all sites with an installed capacity  $\geq 1,000$  m<sup>3</sup>/d and displays the chemical load for all sites with an antiscalant load  $\geq 50$  kg/d

Estimated copper discharges  
from MSF plants  
in kg/day



Figure 35: Copper: Estimated discharge of copper from MSF plants in kg/day. The figures were calculated from the installed desalination capacity, assuming a product recovery rate of 10 % and a residual copper level of 15 µg/l in the concentrate of the MSF plant, resulting in a specific copper load of 0.03 kg/day for every 1,000 m<sup>3</sup>/d. The estimated total load for the Mediterranean is 18 kg of copper from MSF plants per day. The map shows all sites with an installed capacity ≥ 1,000 m<sup>3</sup>/d and displays the chemical load for all sites with a copper load ≥ 1 kg/day. The map does not take copper discharges from cooling water discharges (neither from the distillation plant nor from co-located power plants) into account

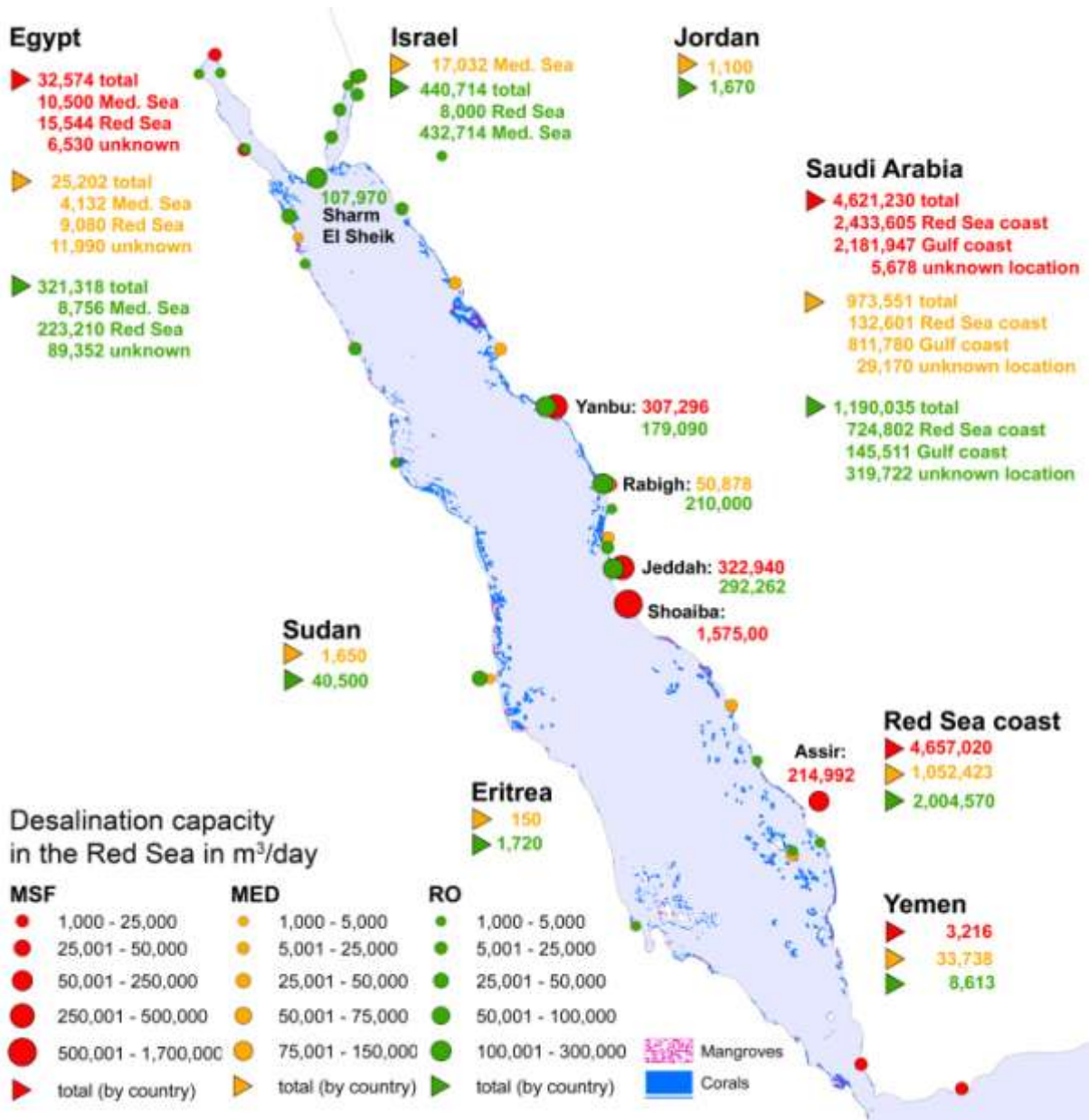


Figure 36: Capacity: Cumulative MSF, MED and RO capacities in m<sup>3</sup>/day by site location (dots) and by country (triangles). The map shows all sites with an installed capacity  $\geq 1,000$  m<sup>3</sup>/d and displays sites with a capacity  $\geq 100,000$  m<sup>3</sup>/d by name and capacity. The map was first published in Lattemann and Höpner (2003) and updated using raw data from IDA and GWI (2008)

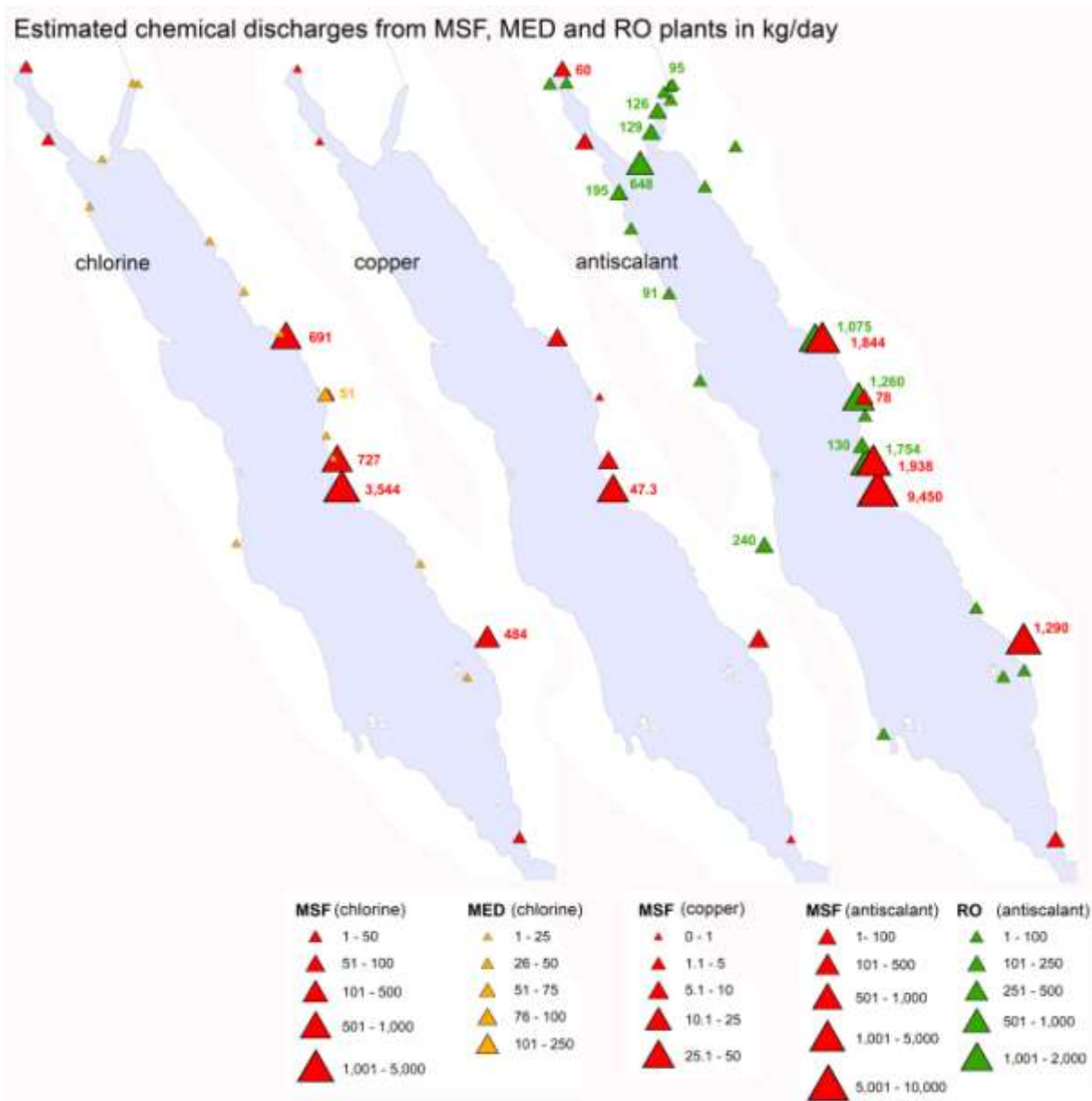


Figure 37: Chlorine: Estimated chemical discharges from MSF, MED and RO plants in kg/day. The figures were calculated from the installed desalination capacity, assuming a product recovery rate of 10 % for MSF, 20 % for MED plants and 33.3 % for RO plants. The chlorine estimate is based on a residual chlorine concentration of 0.25 mg/l in the combined waste water of the MSF and MED process (i.e. concentrate and cooling water), resulting in a specific chlorine load of 2.3 kg/day for MSF and 1 kg/day for MED for every 1,000 m<sup>3</sup>/d. The estimated total load for the Red Sea is 5.5 tons of chlorine from MSF plants and 144 kg from MED plants per day. The copper estimate is based on a residual copper level of 15 µg/l in the concentrate of the MSF plant, resulting in a specific copper load of 0.03 kg/day for every 1,000 m<sup>3</sup>/d. The estimated total load for the Red Sea is 74 kg of copper from MSF plants per day. The antiscalant estimate is based on an antiscalant dosage of 2 mg/l to the make-up water in the MSF plant / respectively to the feedwater in the RO plant (for the given assumptions, the specific antiscalant loads are identical for MSF and RO plants, i.e. 6 kg/day for every 1,000 m<sup>3</sup>/d installed capacity). The estimated total load for the Red Sea is 14.7 tons of antiscalants from MSF plants and 6 tons from RO plants per day. The maps show all sites with an installed capacity ≥ 1,000 m<sup>3</sup>/d and display the chemical load for all sites with a chlorine and antiscalant loads ≥ 50 kg/d and a copper load ≥ 10 kg/d. It does not take chlorine and copper discharges from co-located power plants into account

## 3.2. Literature review on environmental impacts

The first paper to note that the brine and chemical discharges from desalination plants may pose a risk to the marine environment probably appeared in 1979. It called for a thorough investigation of both the physical and biological components of the environment, prior to construction baseline data and on a regular basis once the plant is in operation (operation monitoring, Winters et al., 1979). However, it took until the 1990s before the scientific interest in the marine environmental concerns of desalination plants became more pronounced, as reflected in the increasing number of publications on that topic at that time, (e.g. Abdel-Jawad and Al-Tabtabaei, 1999; Ahmed et al., 2000; Altayaran and Madany, 1992; Del Bene et al., 1994; Höpner, 1999; Mannaa, 1994; Mickley, 1995; Morton et al., 1996; Shams El Din et al., 1994). In 2001, the first comprehensive review of the existing literature sources on desalination plant effluents and their potential impacts on the marine environment was carried out and the results published as a book (Lattemann and Höpner, 2003). On this basis, a data bank was developed within the MEDRC project “Assessment of the Composition of Desalination Plant Disposal Brines” (project 98-AS-026, Hodgkiess et al., 2003).

Although the number of publications discussing the *potential* for negative environmental impacts of effluents from desalination facilities has been steadily increasing over the last years, "a surprising paucity of *useful experimental data*, either from laboratory tests or from field monitoring" (NRC, 2008) still exists, as a recent report from the United States National Research Council concludes.

This research project does not have the objective to repeat what has been written about the potential environmental concerns of desalination plant effluents elsewhere, but to provide a literature critique and overview on the most relevant sources of *secondary* literature (see Appendix E). Furthermore, the results from the available monitoring and laboratory studies are summarized in order to prove an update of the data contained in the desalination discharge databank (Hodgkiess et al., 2003). Although a handful of experimental studies is available to date, the problem is that only a few of these studies have performed a *comprehensive* analysis of the effects of brine discharge on the marine environment. The majority of studies focus on a *limited number of species* over a *short* period of time with no baseline data. The studies show the wide range of approaches and methods that are used to investigate the environmental impacts of desalination plant effluents and underline the need for a more uniform assessment and monitoring approach.

A detailed description of effluent characteristics and their general impacts has been given in the above mentioned publications. Appendix E provides a list of a literature overview on the most relevant sources of *secondary* literature. It also contains a short summary for the major constituents.

A list summarizing information regarding environmental impact assessments can be found in Appendix F, with projects especially considering a strong public involvement for the permitting process. The review discusses mainly two aspects: the physical descriptions and their impacts “field and modeling studies for brine discharges”, and the ecological descriptions and their impacts, “bioassay studies: salinity tolerance and toxicity studies”.

### **3.3. Literature review of socio-economic aspects**

Public acceptance of or opposition against desalination plants depends on many factors. The importance of desalination for the development of a country and the magnitude of water scarcity play an important role for the public opinion. The general environmental awareness of the people, financial aspects of desalination projects and the social function of coastal areas are other influencing factors. Accordingly, the opinions and the approval of desalination differ around the globe. This section provides an overview over different regions and countries.

#### **3.3.1. MENA region**

The MENA region is characterised by high water scarcity and quickly growing populations in many of the countries. The production of clean and sufficient drinking water is essential and has become an industrial sector of utmost importance. All capacities are currently extended.

Tolba and Saab (2006) conducted a survey which investigated the public opinion of the Arab world towards environmental issues. Between November 2005 and March 2006, 3,876 citizens from 18 countries of the Arab League were questioned. 60 % of the respondents declared that the state of the environment had deteriorated in the past ten years and only 30 % thought it had improved.

65 % considered sea, coastal and lake pollution to be a major problem and 27 % considered it to be a minor problem. Considering all topics, sea and coastal pollution was only ranked the 8<sup>th</sup> most urgent problem on the environmental agenda as seen in Figure 38. The share of respondents who considered sea pollution a major problem was considerably higher in countries with long coasts e.g. Morocco (96 %) and Saudi Arabia (85 %). Oman and UAE (both 68 %) were in the middle field.

Drinking water was indicated as a major problem by 69 % of the respondents and as a minor problem by 17 % (Figure 38). The share of people who did not consider drinking water supply to be a major problem was considerably higher in countries with the highest water scarcity, which are all highly dependent on desalinated water (41 % in Qatar, 35 % in Oman and Kuwait, 31 % in UAE). In countries such as Iraq and Sudan where many people do not have access to sufficient water, in contrast, drinking water constitutes a major problem according to the vast majority of the respondents.

95 % of the informants agreed that their country should do more about the environment but only 68 % were willing to pay taxes for the sake of environmental protection.

The study shows that seawater pollution is considered a major environmental issue by the majority of people in Arab countries, but not one of the most urgent ones. Sensitivity towards the drinking water problem correlates with the undersupply of the population, not with the scarcity of natural water resources. Countries with the highest desalination capacities rate the drinking water problem the least critical. This indicates that seawater desalination is a well accepted technology for drinking water production in these countries. Environmental concerns, criticism or even opposition concerning desalination plants in Arab countries cannot be derived from this study.

### Level Of Importance Of Environmental Problems

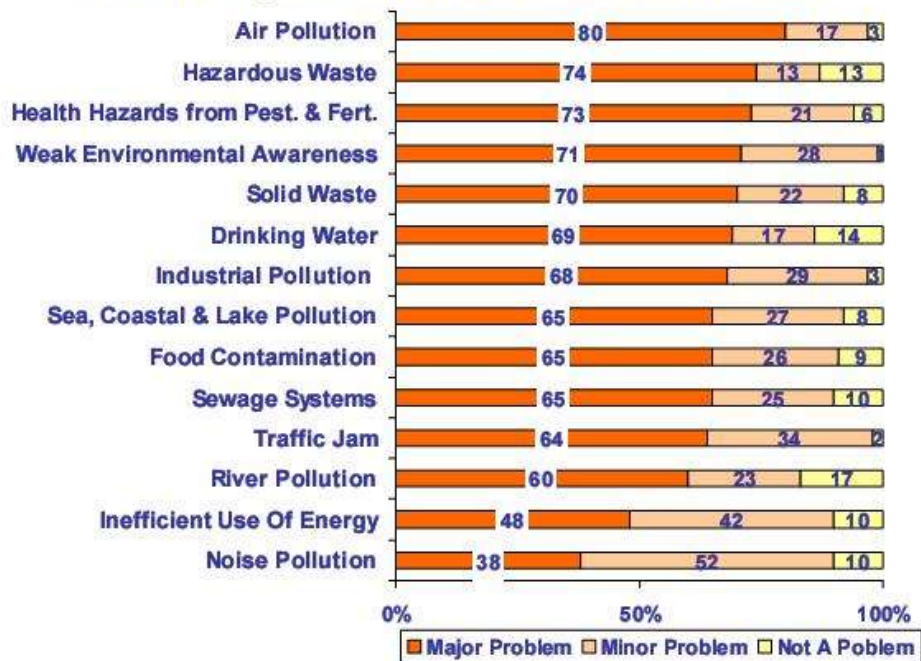


Figure 38: Assessment of environmental problems according to respondents in MENA countries (Tolba and Saab, 2006)

#### Saudi Arabia

Saudi Arabia currently possesses a total desalination capacity of 3,000,000 m<sup>3</sup>/d and an additional 6,000,000 m<sup>3</sup>/d is planned to be installed within the next 20 years (Global Water Intelligence, 2004). The Saudis pay relatively cheap rates for their water although the production and distribution costs are very high. Public concern or resistance against desalination is not reported. Instead, the highly inefficient Saudi Arabian water management in general is criticised by external observers. The WWF criticised that the country combines very low water prices with the highest production and distribution costs worldwide. Traditional water use restrictions have been abandoned and highly unproductive agricultural farms in desert areas in the interior are irrigated with ground water. Thus, desalinated water for domestic use has to be provided via pipelines over hundreds of kilometres from coastal locations. The World Bank criticised the subsidised energy prices which favour inefficient desalination technologies in the kingdom, notably thermal desalination (WWF, 2007).

#### Israel

Israel is also highly dependent on desalinated water since extensive agricultural activities and recurring droughts have accelerated the depletion and contamination of ground water resources. The world's largest RO desalination plant with a capacity of 320,000 m<sup>3</sup>/d is situated in Ashkelon.

Israelis are getting increasingly concerned about the pollution of the marine environment but the focus is much more on industrial sewage than on desalination effluents. The fears of ocean pollution are partly based on the possibility of rising water prices due to deteriorating quality of intake water for desalination plants. Specific concerns about scheduled desalination plants are mainly politically motivated, e.g. as a result of plans to build a channel between the Red Sea and the Dead Sea in order to supply more water for Jordan.

## **Oman**

Oman might be exemplary for the Arabian Gulf states when it comes to the public opinion towards desalination. A stay in the country provided the opportunity to talk to different Omanis around the capital area in 2007. When asking the Omanis, among them university students, professors and ordinary people, about their opinion on desalination and the possible adverse effects, the answers were almost unanimous. The Omanis evaluated desalination plants as essential for the country and for their own life. They could not imagine any alternative to desalination since the ground water resources were too small and unreliable. Most of the questioned people were not aware of possible adverse effects and could not imagine any impacts of desalination plants, except may be for air pollution. This might be due to a lack of knowledge about the technology. When pointed to the possible side effects, most people agreed that such effects should be avoided but that desalination would still remain indispensable. When visiting two MSF plants, the plant operators assured that they would stick to the environmental regulations which they believed to be sufficiently stringent. All in all, hardly any of the interviewed person uttered major concerns regarding desalination, but most agreed that the impacts of brine discharges should be restricted.

Dr. Abdul-Wahab from the Department of Mechanical and Industrial Engineering at the Sultan Qaboos University in Muscat investigated the environmental awareness of the Omani public and their willingness to protect the environment in 2007. 425 people in the Muscat governorate area from different educational backgrounds were questioned for the survey. The study examined three aspects (Abdul-Wahab, 2008):

- Environmental knowledge
- Environmental attitudes
- Environmental behaviour

The basic environmental knowledge of the respondents was generally low and more than half of them gave incorrect answers to basic questions like the chemical composition of the atmosphere. They were more knowledgeable about local environmental problems and international environmental problems such as climate change.

Environmental attitudes reflected the opinion on the state of the environment and the satisfaction with environmental protection by the government and were found overall to be positive. However, most respondents requested the government to do more about the environment. Only a minority thought that the individual should take more responsibility for environmental protection.

The environmental behaviour was revealed to be low. Only around 40 % were willing to change their lifestyle in order to protect the environment.

The question of seawater desalination was not included in the survey, which might reflect the low local sensibility for the problem. The results on environmental behaviour indicate that the willingness to restrict the lifestyle in order to save water resources is probably low. The reported deficiencies in environmental knowledge might explain that Omanis do not know about possible environmental impacts and thus do not have reservations towards the desalination technology. Another answer could be that the Omani desalination capacities are still too small to show any obvious detrimental effects. There are only four major plants on the long north-eastern coast which leads directly into the Arabian Sea. Pollutant accumulation and impact multiplications like in the semi-enclosed Arabian Gulf are less probable.

To conclude, all in all, no public opposition or major reservations against desalination plants based on environmental concerns were found in MENA countries. The most important reason seems to be that desalinated water is an inherent part of many peoples' lives and that many countries are highly dependent on it. Lack of knowledge about the desalination technology and its possible impacts might explain the findings. In countries like Oman, where the seawater desalination capacities are still low, the potential impacts are not visible at first glance. The public attitude might change if the environmental impacts rise to an extent which would significantly interfere with peoples' standards of living.

### **3.3.2. USA, Spain, Australia**

The traditionally high environmental awareness and the existence of alternative water sources and water saving options lead to a more controversial debate about desalination.

#### **United States of America**

In the USA the states of Texas, Florida and California suffer from the most serious water scarcities and account for the highest desalination capacities in the country. Public opinion about desalination differs.

*Texas* is primarily relying on brackish water desalination. Most seawater projects were dismissed because of the high expenses and not because of strong public opposition.

*Florida* is the state with by far the highest installed desalination capacity in the United States, but predominantly relies on brackish water desalination. The first major seawater plant of the country was built at Tampa Bay. It was designed to produce 95,000 m<sup>3</sup>/d but never reached this capacity due to filter and membrane failures. Financing problems and contractor bankruptcies led to long delays in the construction phase and prevented proper operation. In 2005 the plant eventually had to be closed for two years since the chemical pretreatment system did not meet the water quality standards of the RO membranes, but has now been retrofitted with an advanced pretreatment system that seems to produce a reliable feedwater quality. In a survey issued by the Tampa Bay Water company in 2005 only 4 % of the respondents supported a focus on desalination in order to meet the drinking water needs of the region. 47 % were not willing to pay more than 10 US-\$ per month in addition for the development of new water supplies like desalination plants. Another 20 % were not willing to pay anything at all (Tampa Bay Water, 2005). The negative experiences with seawater desalination at Tampa Bay also fuelled controversial debates at the west coast.

*California* is predicted to emerge as one of the new desalination hotspots within the next decades. 15-20 major seawater desalination plants with a total capacity of 1,700,000 m<sup>3</sup>/d are planned until 2030, covering 6 % of the state's water supply by that time (Höpner and Lattemann, 2008). In 2002, a public opinion poll of 601 Californian voters issued by the West Basin Municipal Water District found that 70 % favoured desalination as a future drinking water option. The reduced dependence on imported water, improved quality of local water supplies and increased water availability for environmental and agricultural use were given as main reasons for the approval (Miller, 2003). In 2004, the San Diego County Water Authority conducted a study about the public opinion on seawater desalination. The results for desalination were quite favourable as Figure 39 illustrates (San Diego County Water Authority, 2004).

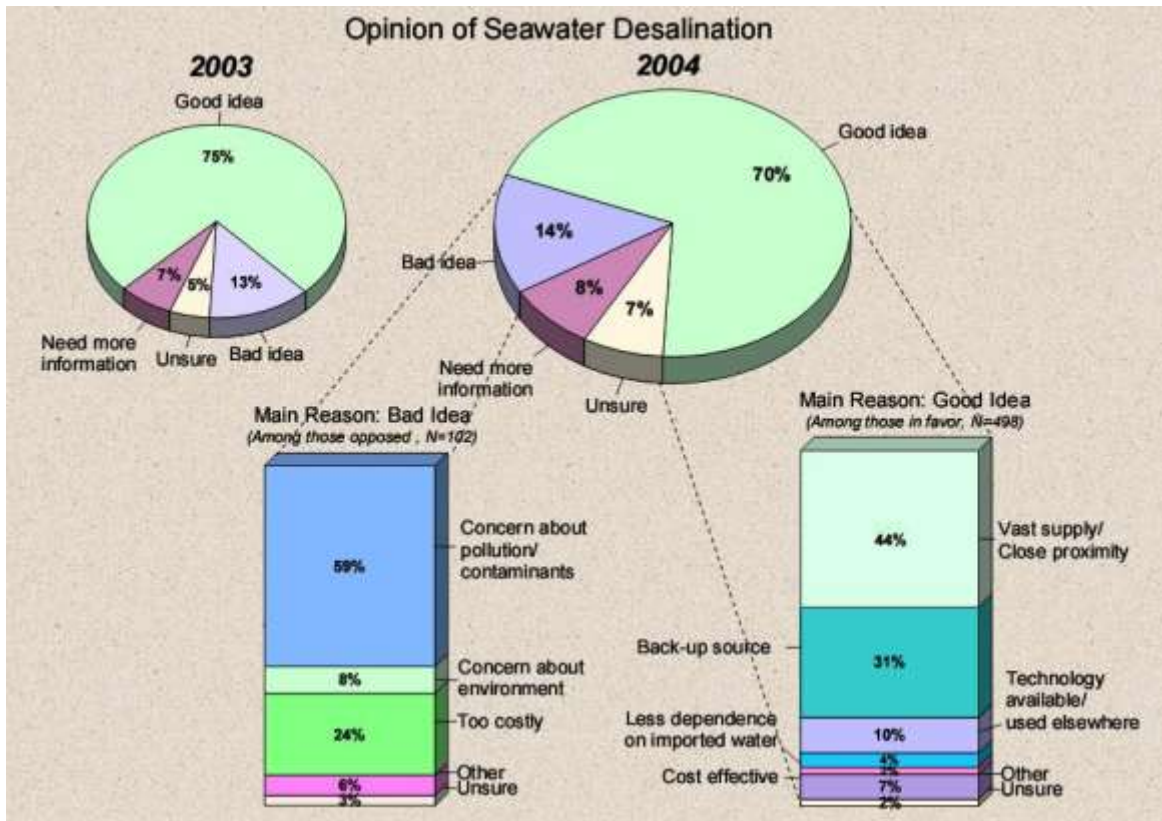


Figure 39: Results of an opinion poll on seawater desalination in San Diego County (San Diego County Water Authority, 2004)

70 % of the respondents thought that sea water desalination is generally a good idea and only 14 % explicitly disagreed with the idea. Desalination supporters primarily listed the large water supplies in close proximity and the function as a possible backup source as an advantage. Those who opposed desalination were mainly concerned about a possible contamination of the product water and secondly about the high costs. Only 8 % of the opponents had environmental concerns. When asked directly about environmental implications, 46 % believed that desalination would not be harmful to the ocean environment. Only 20 % believed that desalination could be harmful to the ocean. Most of them worried that seawater desalination alters the salinity of the ocean, has general bad impacts on the environment and disturbs the natural balance. Only 6 % listed chemicals as potential harm for the ocean life (Figure 40).

When it comes to the construction of a specific plant in the San Diego County instead of discussing desalination in general, even 75 % stated they would favour the project and only 7 % were opposed, with costs being the primary concern. However, the share of people who were 'unsure' about environmental impacts (34 %) or claimed to 'need more information' was significant and indicates that many citizens believe they do not have enough knowledge to entirely assess the risks of desalination plants or are sceptical. But altogether, the polls indicate that public concerns about seawater desalination are moderate and a large majority favours the technology.

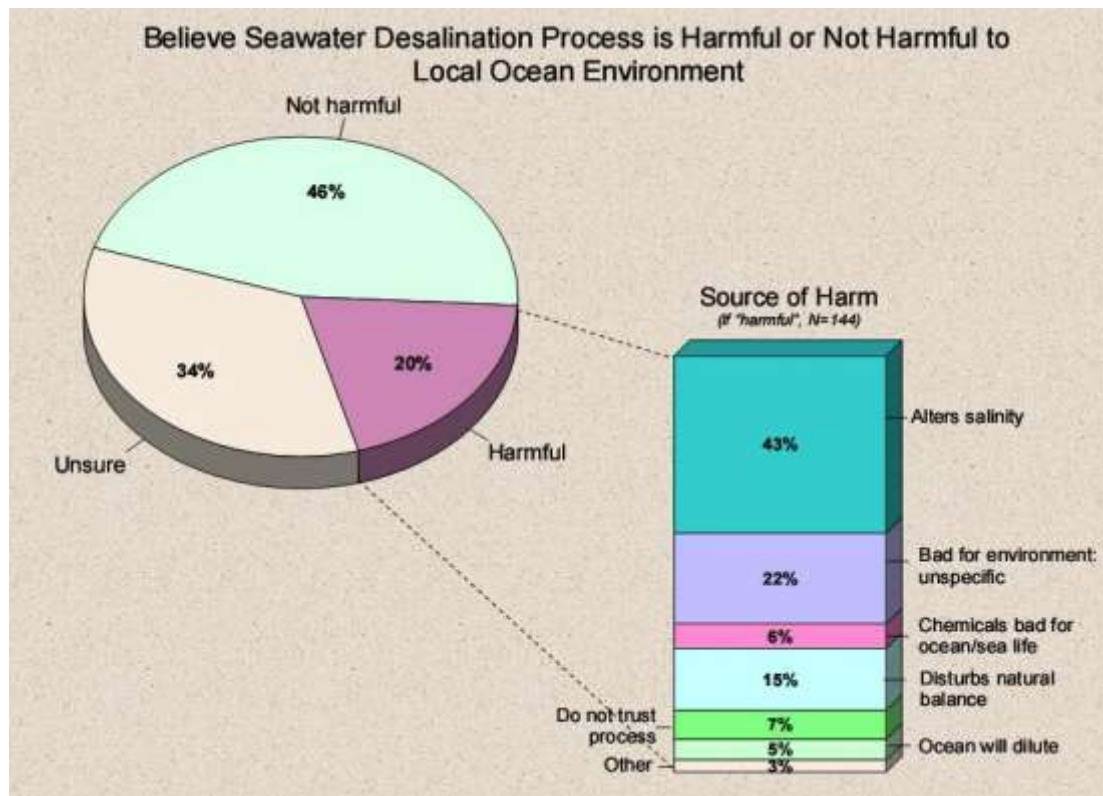


Figure 40: Environmental concerns about seawater desalination in San Diego County (San Diego County Water Authority, 2004)

However, Californian minds seem to change when it really comes to implementing specific projects. None of the large scheduled desalination projects in California easily got the necessary approvals or were started in time. Due to strong public opposition and regulatory obstacles, the construction and operation starts of many plants were delayed and some projects were completely dropped. Until now, none of the large projects have been finished.

The 189,500 m<sup>3</sup>/d RO plant in *Carlsbad* in San Diego County was scheduled to begin construction in 2005 and to be finished in 2008. Despite the high theoretical approval rates in San Diego County resulting from the presented poll, it took much longer to get adequate approval rates in the municipality as well as state level authorisations (WWF, 2007). As a result, construction will not be completed until 2010.

Even harder battles with local communities had to be fought at *Huntington Beach* where another 189,500 m<sup>3</sup>/d RO plant was to be built. The construction start was scheduled for 2004 and operation start for 2006. But when the project was announced, strong citizen movements arose, e.g. the activist group 'Residents for responsible desalination'. A clear statement and the main motivation of the group can be found at its website (RFRD, 2008): "We believe sea water desalination should not replace conservation or reclamation and reuse of water, and should not harm the ocean environment, should not damage local property values, neighbourhood residential communities, or our tourist economy, and should not diminish local public control of our vital water resources. We believe that the Poseidon proposal for Huntington Beach fails on all these points." Many letters from annoyed residents concerned about a decline in living standards caused by the plant can be found on the website. Due to the rigorous public opposition, the construction start of the Huntington Beach plant was delayed to the year 2007 and the completion is expected for 2009.

The reasons for opposition against specific desalination projects in California are diverse. But most public concerns are based on environmental and cost arguments as the following selection shows (WWF, 2007; RFRD, 2008):

- Unacceptable environmental impacts of the desalination units expected
- Cogeneration of most projected plants with coastal power stations using ‘flow through cooling intakes’ → controversial as these are likely to be harmful for the marine environment
- Urban water saving, enhanced water recycling and efficiency improvements in the agriculture sector should be preferred
- Doubts in the cost-effectiveness of desalination
- Possible taxpayer subsidies for financing the energy costs
- Projected privatisation of most plants induces losses of public ownership and control
- Fears of coastal overdevelopment
- Devaluation of the coastal area and decreasing tourist activities
- Increasing noise and air pollution

To conclude, passionate commitment for civil rights and ecological campaigns has a long tradition in the U.S. public. It seems that the high theoretical approval rates for seawater desalination are dropping when it comes to the realisation of a specific project. Even if opposition is only based on a minority of the population or some annoyed residents, the movements are obviously capable of substantially delaying major projects. The Californian experience can translate to other states if they decide to embrace large scale desalination plans. Unless the desalination industry can dispel the major cost and environmental concerns about desalination plants, it seems to be difficult for the technology to gain ground in the United States.

### **Spain**

Spain has a renowned desalination industry with customers around the world. The country disposes of the largest desalination capacity in the Western world with current capacities of more than 1.6 million m<sup>3</sup>/d. But despite its long and strong tradition, desalination is not an entirely uncontroversial topic in Spain.

The country has heavily invested in desalination to secure its water supply. Critics say that this is too costly and unnecessary and call for improvements of the bad water management instead. Spain is using more than one fifth of the desalinated water for its highly subsidised agriculture which is more than in any other country. It is more accepted in the public arena to build a desalination plant for supplying the agriculture than for supporting tourism and urban development. Despite the large supplies of desalinated water, farmers still continue to illegally access the groundwater in order to save costs. Operation start in Carboneras had to be delayed due to funding disputes with local farmers. Obviously, opposition is grounded on the high water prices, although desalinated water is already strongly subsidised by the government. On the other side, a boom of tourist estates can be noticed throughout the country which eventually also has to be supplied by costly desalination plants.

The New Water Culture Foundation, a Spanish non-profit organisation, demands more reasonable desalination policies. The foundation calls for improving the water management, slowing down the capacity extensions and conducting full environmental assessments of each desalination plant. Furthermore, desalination sites shall be restricted to industrial areas and

zero discharge plants should be taken into consideration (WWF, 2007). Zero discharge plants enable desalination without brine discharges and will be covered in detail later on.

It can be seen that the debates in Spain are concentrating on costs, environmental impacts and possible mitigation measures. It is not a debate about the usage of desalination, but about the extent of usage and the preferred fields of application.

### **Australia**

A survey among a representative number of 1000 Australians about their perception of desalination and water recycling was conducted by the University of Wollongong in 2007. When asked about their main concerns regarding desalination, high costs, environmental burden and health-related topics were mentioned. Costs and environment were the most urgent issues for the interviewees.

When asked directly about the environmental impacts of desalination, 81 % were aware of the high energy consumption of the plants. Desalination was perceived as less environmentally friendly than recycled water. A majority of 69 % believed that desalinated water is healthy, but 24 % believed it is purified sewage and 20 % agreed that it contains endocrine disruptors which could affect fertility. This reflects the ignorance about the topic.

However, the overall acceptance for desalinated water was higher than for recycled water. A majority of respondents would prefer the use of desalinated water for close body contact like bathing or drinking and chose recycled water for purposes like watering the garden or irrigation of parks (Dolnicar and Schafer, 2007; Birnbauer, 2007).

When it comes to specific projects, the differing opinions about desalination in Australia abound. The scheduled desalination plant in Sydney was controversially debated. When the plant was first proposed in 2005, the State premier himself denounced it as “bottled electricity”. The ‘Sydney Community United against Desal’, an activist group made up of scientists, engineers and environmentalists, formed to oppose the Sydney plant. They called for more water recycling and improved water management instead.

A survey revealed that almost 60 % of the Sydneysiders opposed the desalination project. Only 34 % were in favour of the plant and even half of the proponents preferred to invest in water reuse and recycling instead. Two thirds of the respondents were worried about the greenhouse gas emissions. Due to strong opposition from environmentalists, the unpopularity in the community and the discovery of additional ground water resources, the project was dropped in 2006 (Frew, 2005; Davis, 2006). It was not before 2007 that the government pushed through the project and launched the construction start of a plant with much smaller capacity than originally planned. Cannesson et al. (2009) illustrated the result of a community consultation on the question: which factor is the most important when considering the location of a desalination plant (Figure 41).

In other regions of the country like Queensland and Perth, desalination projects have been implemented without major delays and hesitation. The RO plant near Perth with a capacity of 140,000 m<sup>3</sup>/d was the first major plant to start operation and is currently the only one. The reason for the quick project implementation was that the water supply could not keep pace with the fast, uncontrolled urban development. Water management was badly organised and the time for demand side adaptations had run out. In order to quiet the ecological minds, relatively high attention was paid to environmental issues when designing the Perth plant (WWF, 2007).

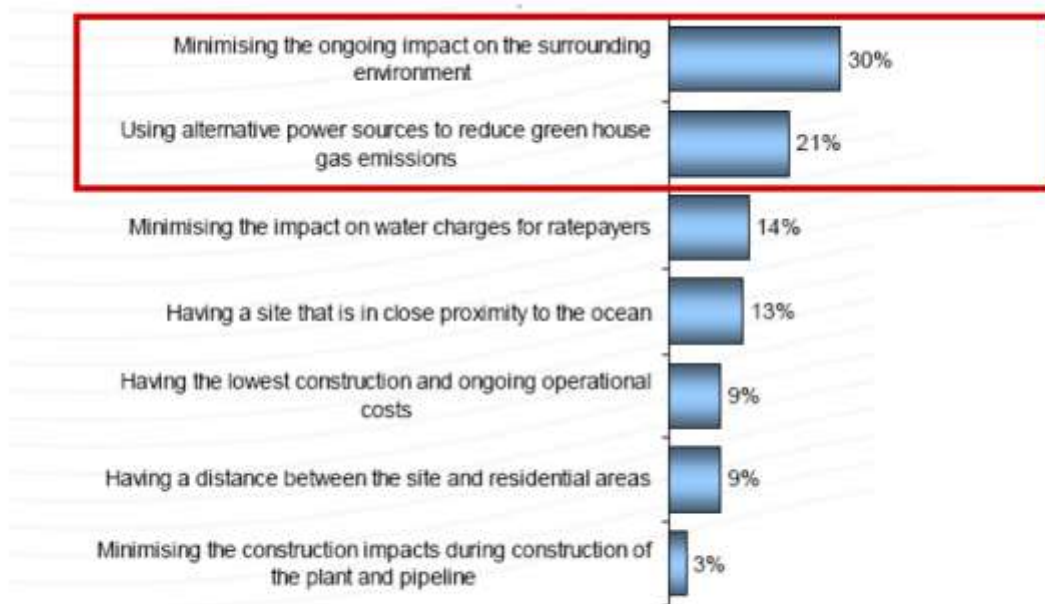


Figure 41: Result of a community consultation on the question: which factor is the most important when considering the location of a desalination plant (Reproduced from Cannesson et al., 2009)

To conclude, public opinion about seawater desalination in the USA, Spain and Australia is ambiguous. Whereas a majority of people in relevant countries generally favour desalination, the community approval rates often drop when a specific project is announced or when people are getting directly concerned. Environmental and cost concerns are most commonly raised. Certain ignorance can be detected since many people do not know what to expect from desalination. Opponents often demand to intensify the water saving efforts and to concentrate on natural water resources. Nevertheless, after significant initial opposition several major projects are on the way or already running in California and Australia. Spain is only debating about the extent of desalination application.

### 3.3.3. Socio-economic effects

Seawater desalination has obviously improved the access rates to water and triggered (possibly unsustainable) economic growth in rich MENA countries. In Western countries with moderate climatic conditions, the growth effects of desalination cannot definitely be detected and may not even be desired, like in California. The economic development on islands which have specialised in tourism can be boosted by desalination, as examples from Malta and the Canary Islands show. In each case, growth effects will be limited to coastal regions unless inefficient water transport systems are installed. Due to the high costs, desalinated water will mostly be restricted to domestic application.

Due to the high investment and energy costs, however, the social and economic benefits of desalination are not or only restrictively applicable for poorer countries, even if current water overuse and depletion generates higher economic costs.

### **3.4. Environmental standards**

An important way to control and restrict adverse environmental impacts of seawater desalination plants is to put up appropriate national laws or transnational agreements. These may regulate the brine discharge management, set up discharge limits or impose environmental standards and conditions mandatory for receiving operating permits. With respect to the worldwide desalination activities, the regulatory situation is very diverse and unclear. No common standards exist as each country has their own water regulations which are more or less publicly accessible. Most regulations are abstract and do not apply specifically to desalination plants, but to industrial effluents in general. Furthermore, international standards such as World Bank Guidelines may be used as a reference. When national regulations differ from international guidelines, the World Bank recommends applying the more stringent regulations. The following gives an overview and comparison of regional and national regulations relevant for seawater desalination effluents in order to assess the level of regulatory protection of the marine environment.

Point-source discharges are usually controlled by setting environmental standards. Most common standards are effluent standards (ES), also called emission limit values in European regulations, and ambient standards (AS), also called environmental quality standards in European regulations. There are existing different philosophies in applying either just one of these standards or combinations of them for pollution management, which is discussed as follows. ES encourage source control principles, such as effluent treatment and recycling technologies. AS require the consideration of the ambient response often associated with the concept of the “mixing zone”, an allocated impact zone in which the numerical water quality standards can be exceeded (Jirka et al., 2004a, b). Ragas et al. (1997) have reviewed the advantages and disadvantages of different control mechanisms in the permitting processes of releases into surface water.

ES are preferred from an administrative perspective because they are easy to prescribe and to monitor (end-of-pipe sampling). From an ecological perspective, however, a quality control that is based on ES alone appears illogical and limited, since it does not consider directly the quality response of the water body itself and therefore does not hold the individual discharger responsible for the water body. To illustrate that point consider a large point source on a small water body or several sources that may all individually meet the ES but would accumulatively cause an excessive pollutant loading. ES are usually set as concentration values for pollutants or minimum required treatment levels.

AS, usually set as concentration values for pollutants or pollutant groups or set as maximum loads (e.g. TMDL="total maximum daily load"-approach in the USA), that may not be exceeded in the water body itself. They have the advantage that they consider directly the physical, chemical and biological response characteristics due to the discharge. They therefore put a direct responsibility on the discharger. But a water quality practice that would be based solely on AS could lead to a situation in which a discharger would fully utilize the assimilative capacity of the water body up to the concentration values or total loads provided by the AS. Furthermore, the water quality authorities would be faced with additional burdens because of a more difficult monitoring – where in the water body and how often should be measured? – in the case of existing discharges or due to the increased need for a prediction modeling in case of new discharges.

A “combined approach” as for example described in the European Water Framework Directive, WFD (EC, 2000), combines the advantages of both of these water quality control mechanisms while largely avoiding their disadvantages. Both criterias have to be met for a discharge permit.

Concentration or load limits for ES and AS can be found in state, national, and international legislations for different substances, effluents, and receiving water characteristics. Examples for ES and AS for various pollutants are described in the following sections. The most relevant parameters for seawater desalination plant effluents are salinity, temperature, pH, dissolved oxygen, turbidity, dissolved organic matter and residual chemical pollutants such as copper, nickel, residual free chlorine and chlorinated by products. It is beyond the scope of this research project to provide an overview on emission and immission limit values for all of these parameters at a global scale. Presented below are selected standards from readily available literature sources. The list does not claim to be complete.

Environmental standards for pollutants are generally determined from laboratory ecotoxicity tests conducted on a range of sensitive aquatic plant and animal species exposing the regionally occurring species to different pollutants and pollutant concentrations under regional climate and water body conditions and natural background concentrations. However, salinity and temperature are two stressors that are naturally very variable seasonally and among and within ecosystem types, and natural biological communities are adapted to the site-specific conditions. This suggests that trigger values for these three stressors may need to be based on site-specific biological effects data (ANZECC, 2000).

The World Bank Group released new Environmental, Health and Safety (EHS) Guidelines in April 2007 which replace the previously published documents in Part III of the Pollution Prevention and Abatement Handbook from 1998 (World Bank Group, 1999). The new guidelines consist of General EHS Guidelines (World Bank Group, 2007b), containing cross-cutting information potentially applicable to all industry sectors, and specific industry sector guidelines. Projects for which no industry-specific guidelines are available should reference the guidelines of an industry sector with suitably analogous processes and effluents. For seawater desalination plants, the most relevant document is the EHS Guidelines for Water and Sanitation (World Bank Group, 2007a), which covers potable water treatment systems for water from conventional sources as well as seawater and brackish water. Furthermore, the Guideline ‘Thermal Power: Guidelines for New Plants’ from the Pollution Prevention and Abatement Handbook, which is still under review, may be consulted (World Bank Group, 1998) for thermal desalination plants due to the similarity of effluent properties.

The General EHS Guidelines (World Bank Group, 2007b) state that discharges of wastewater from *utility operations*<sup>2</sup> to surface water “should not result in contaminant concentrations in excess of local ambient water quality criteria or, in the absence of local criteria, other sources of ambient water quality”. As an example, the U.S. EPA National Recommended Water Quality Criteria (US EPA, 2006) is given, which are also cited as a reference below, in addition to the available World Bank Guidelines criteria.

---

<sup>2</sup> Utility operations include cooling towers and demineralization systems which may result in high rates of water consumption, as well as the potential release of high temperature water containing high dissolved solids, residues of biocides, residues of other cooling system anti-fouling agents, etc. This definition can be applied to discharges from desalination plants which are increased in temperature where cooling waters are used (i.e. distillation plants), which contain high contents of dissolved solids (i.e. minerals/salts), residues of biocides (i.e. chlorine, discharged by distillation plants only), and other ‘anti-fouling’ agents such as ‘anti-scalants’.

### 3.4.1. Temperature

The World Bank recommends that the temperature of heated water is reduced prior to discharge to ensure that the discharge water temperature does not result in an increase greater than 3 °C of ambient temperature at the edge of a scientifically established mixing zone, which takes into account ambient water quality, receiving water use, potential receptors and assimilative capacity among other considerations (World Bank Group, 2007b). The EHS guideline does not specify the extent of the mixing zone. For effluents from thermal power plants, the Pollution Prevention and Abatement Handbook (which is currently under review) recommends to use 100 m from the point of discharge when there are no sensitive aquatic ecosystems within this distance (World Bank Group, 1998).

According to Omani regulations on the discharge of liquid waste into the marine environment, the temperature of liquid waste at the discharge point should not exceed 10 °C over the temperature of the water surrounding the seawater intake. The discharge should not result in a temperature increase in seawater of more than 1 °C (weekly average) in a circular area of 300 m diameter around the point of discharge (Sultanate of Oman, 2005).

### 3.4.2. Salinity

Similar to thermal ‘pollution’, increased salt concentrations can be harmful and even lethal to marine life. In general, toxicity depends on the sensitivity of the species to increased salinity, the natural salinity of their habitat, and the life cycle stage.

For example, experiments on the Mediterranean seagrass *Posidonia oceanica* showed that salinities of about 45 caused about 50 % mortality in 15 days. In contrast, two seagrasses common to Western Australian waters, *Posidonia australis* and *Posidonia amphibolis*, seem to be adapted to naturally higher salinities, as the densest covers of seagrass meadows occur at salinities of 40 to 50.

This indicates that some marine species are more salinity tolerant than others. Certain macrofauna taxa, such as the echinoderms (e.g. sea urchins, starfish) which are strictly marine species, are assumed to be rather sensitive to salinity variations, especially during their young life cycle stages such as sea urchin embryos. Salinity thresholds must therefore reflect the salinity tolerance of the local marine flora and fauna, taking a range of species into account, as well as natural habitat salinity and variability. In the following, thresholds and aspired dilution rates from different desalination plants are given.

- The Western Australian guidelines for fresh and marine waters specify that the median salinity increase is to be less than 5 % from background. This corresponds to a change of 2 units in marine environments with a salinity of 40. The criteria for the concentrate discharge set by the Western Australia Environmental Protection Authority for the Perth SWRO plant require that salinity is within 1.2 units of ambient levels within 50 m of the discharge point and within 0.8 units of background levels within 1,000 m of the discharge point (Wec, 2002).
- For the Sydney SWRO project, seawater quality was assessed using relevant indicators from the Australia and New Zealand Guidelines for Fresh and Marine Water Quality (ANZECC, 2000). The near field mixing zone was established as the area within 50 to 75 m of the outlet. Modeling studies were conducted showing that salinity at around 50-75

m from the outlets is expected to be around 36, which is within approximately one unit of background seawater salinity (salinity of 34-36) (Sydney Water and Fichtner, 2005).

- Modeling of diffuser plumes for the Gold Coast SWRO project resulted in a maximum impact circle diameter of 43 m and a dilution plume impact point at 16 m from the diffusers. Based on this, the predicted near-field mixing zone is expected to be about 120 m wide and 225 m long. Allowing for error in the model calculations, it is expected that salinity at the sediment surface at the boundary of the mixing zone will not exceed 2 units above background i.e. 37.5 compared with background salinity of 35.5) under any operational scenario (GCD Alliance, 2006).
- In the U.S., EPA recommendations state that salinity variations from natural levels should not exceed 4 units from natural variation in areas permanently occupied by food and habitat forming plants when natural salinity is between 13.5 and 35 (City of Carlsbad and Poseidon Resources, 2005). This corresponds to an increase in salinity between 11 % and 39 % from background levels.
- For a SWRO plant in Okinawa, Japan, a maximum salinity of 38 in the mixing zone and a maximum increase of 1 unit where the plume reaches the seafloor was established (Okinawa Bureau for Enterprises). This corresponds to an increase in salinity of 2.6 % from background levels.
- In Abu Dhabi, a 5 % increase in salinity may not be exceeded at the edge of the mixing zone (Kastner, 2008).
- According to Omani regulations on the discharge of liquid waste into the marine environment, the salinity should not deviate from the surrounding average for more than 2 units on a daily basis in a circular area of 300 m diameter around the point of discharge (Sultanate of Oman, 2005).
- For Mediterranean seagrass *Posidonia oceanica* meadows, salinity thresholds have been recommended based on field and laboratory experiments. Salinity should not exceed a value of 38.5 in any point of a seagrass meadow for more than 25 % of the observations (on an annual basis) and should not exceed a value of 40 in any point of the meadow for more than 5% of those observations. This threshold applies to *Posidonia oceanica* of the Western Mediterranean and requires verification by further studies (Sánchez-Lizaso et al., 2008). Ambient salinities in the western Mediterranean range between 37 and 38.

### **3.4.3. Residual chemicals – effluent standards (ES)**

The World Bank Pollution Prevention and Abatement Handbook, which is under review, recommend the following maximum values for effluents from thermal power plants (World Bank Group, 1998). The effluent levels should be achieved daily without dilution.

The values may also be applied to thermal desalination plants due to similarities in effluent properties. The most relevant parameters are probably residual chlorine and copper. Other parameters such as pH and total suspended solids (TSS) and metal concentrations may be relevant depending on the feedwater composition, the desalination process and pretreatment or the selection of construction materials. A water analysis should be conducted to identify the relevant waste water constituents. In the Sultanate of Oman, the maximum values described in Table 6 apply for effluents discharged into the marine environment.

Table 5: Maximum values for *effluents* from thermal power plants (World Bank Group, 1998)

Parameter	Maximum value in mg/l (except for pH)
<b>Total residual chlorine<sup>3</sup></b>	<b>0.2</b>
<b>Copper</b>	<b>0.5</b>
Iron	1.0
Zinc	1.0
Chromium (total)	0.5
Oil and grease	10
pH	6-9
Total suspended solids (TSS)	50

Table 6: Maximum values for selected parameters for *effluent discharges* into the marine environment (Sultanate of Oman, 2005)

Parameter	Maximum value in mg/l (unless otherwise stipulated)
<b>Total chlorine</b>	<b>0.4</b>
<b>Copper</b>	<b>0.2</b>
Iron	1.5
Zinc	1.0
Chromium	0.05
Molybdenum	0.05
Nickel	0.100
Aluminum	5.0
Cadmium	0.01
Lead	0.08
Oil	15.0
Oxygen biological deficiency	20.0
Oxygen chemical deficiency	200.0
Total suspended solids (TSS)	30.0
Organic halogen	< 0.001

In Qatar, the state environmental regulator has adopted most stringent environmental standards for chlorine discharges, incrementally reducing the maximum chlorine concentration permitted in discharged cooling seawater from 0.2 to 0.05 mg/l (KEMA, 2006).

#### **3.4.4. Residual chemicals – ambient standards (AS)**

The U.S. EPA National Recommended Water Quality Criteria (US EPA, 2006) are a summary table containing recommended water quality criteria for the protection of aquatic life in fresh and marine waters for approximately 150 pollutants. They include the Criteria Maximum Concentration (CMC) and the Criterion Continuous Concentration (CCC), which are estimates of the highest concentration of a material in surface water to which an aquatic community can be exposed briefly (CMC) or indefinitely (CCC) without resulting in an unacceptable effect. The criteria are intended to be protective of the vast majority of the aquatic communities in the United States. Some of the parameters are relevant to desalination plant discharges, and may serve as an indication for regulating these discharges in other parts of the world (Table 7 below).

<sup>3</sup> "Chlorine shocking" may be preferable in certain circumstances. This involves using high chlorine levels for a few seconds rather than a continuous low-level release. The maximum value is 2 mg/l for up to 2 hours, not to be repeated more frequently than once in 24 hours, with a 24-hour average of 0.2 mg/l. (The same limits would apply to bromine and fluorine.)

Table 7: US EPA National Recommended Water Quality Criteria for selected pollutants

Parameter	CMC in µg/L	CCC in µg/L
Chlorine	13	7.5
Copper	4.8	3.1
Iron	not given	
Zinc	90	81
Chromium (VI)	1100	50
Nickel	74	8.2
Cadmium	40	8.8
Lead	210	8.1
Oil and grease	narrative statements, see (U.S. EPA, 2006)	
Dissolved Oxygen		
Total suspended solids (TSS)		
pH		6.5 – 8.5

### 3.4.5. Regulatory mixing zone regulations

The mixing processes due to discharges into water bodies occur according to well understood physical principles, and lead to a spatial and temporal configuration of the mass plume and the associated concentration distribution. To what degree do the water quality control measures, in particular its “combined approach” consisting of emission standards (ES) and ambient standards (AS), correspond to these physical facts?

The relevant values for ES and AS for various pollutants and pollutant groups have been described above for a few examples. By way of example for further analysis, Table 8 contains the values for two chemical pollutants (copper and chlorine). The ratio ES/AS is approximately 100 for copper and 27 for chlorine. The range of 5 to 1000 is typical for most chemical as well as physical parameters, such as heat (temperature). This ratio describes the impact of the pollutants on the ecosystem, since the ES is considered to protect against acute (lethal) effects on organisms, while the AS is supposed to prevent long-time chronic influences. The ratio also expresses the necessary dilution that must be attained through physical mixing or – to some extent – through biological decay and chemical transformation processes. These concentration values are useful to reduce and control water pollution, but where do these values apply? The "end-of- pipe" specification for the ES is clear (e.g. adopted from the WFD, 2000):

*"The emission standards (ES) for substances shall normally apply at the point where the emissions leave the installation, dilution being disregarded when determining them".*

Table 8: Examples for emission standards (ES) and ambient standards (AS) for two selected pollutants

Pollutant example	Emission standard ES	Ambient standard AS	ES/AS
Copper	500 µg/l (World Bank)	4.8 µg/l (US EPA)	104
Chlorine	200 µg/l (World Bank)	7.5 µg/l (US EPA)	27

Surprisingly, and quite illogical from the viewpoint of the physical features of the mixing processes, most regulations do not provide any information on the spatial application of the AS-values. Therefore, it must be expected that considerable uncertainties and highly variable interpretations or monitoring methods will occur in the practice of water authorities, regarding both the continuing approval of existing discharges as well as the permitting of new ones.

The “combined approach” that appears sensible for an integrated ecological water pollution control is in danger of being by-passed or undermined in its practical implementation.

From discussions with personnel from regional water authorities, the authors know of two extreme interpretations regarding this omission:

- 1) The AS-value shall be applied “as near as possible” to the discharge point in order to obtain a good chemical status in an area as large as possible. This highly restrictive interpretation negates the fact that the physical mixing process cannot be reduced to extremely small areas (in the limit this approaches an “end-of-pipe” demand for ES), but requires a certain space – in particular for imposed high ES/AS ratios. It undermines the balanced objectives of the “combined approach”.
- 2) The AS-value is supposed to apply “after the completion of initial mixing” or “at the beach” or “at the water surface”. Such qualitative statements have specific deficiencies that make them either unenforceable or overly generous and likely to create sacrificial areas with high concentration levels not meeting a good quality status.

Thus, the “combined approach” concept requires a regulatory mixing zone regulation that preserves the water quality objectives and accounts for the physical aspects of the mixing processes (e.g. amendment to the European Water Framework Directive (EU, 2008)). Therefore, a recommendation for future amendments of national regulations should contain the following approximate wording:

*"The ambient standards (AS) apply in the case of point sources outside and at the edge of the mixing zone. The mixing zone is a spatially restricted region around the point source whose dimensions shall be specified either according effluent characteristics in relation to water body type, use, and physical/chemical, and biological characteristics, or on an ad-hoc basis. Concentrations of one or more substances may exceed the relevant AS within the mixing zone if they do not affect the compliance of the rest of the body of surface water with those standards."*

The mixing zone defined in the above statement is a regulatory formulation with the following general attributes:

- 1) The term “mixing zone” signifies explicitly that mixing processes require a certain spatial extent within which mixing processes operate.
- 2) The term “spatially restricted” should guarantee that the mixing zone shall be minimized by the regulatory authority for the purpose of attaining the environmental quality goals.
- 3) While the mixing zone includes a portion - namely the initial one - of the actual physical mixing processes, these processes will continue beyond the mixing zone where they lead to further concentration drop-offs in the pollutant plume below the AS-values.
- 4) The definition is restricted to “point sources” since diffuse sources usually do not contain clearly distinct mixing processes.

The regulatory concept of mixing zones can also be found in the water quality regulations of other countries. As an example, the U.S. Environmental Protection Agency defines in its Water Quality Handbook “... *the concept of a mixing zone as a limited area or volume of water where initial dilution of a discharge takes place*” (US EPA, 1994). A number of supplementary restrictions further define this water quality control principle such as “... *the area or volume of an individual mixing zone ... limited to an area or volume as small as practicable that will not interfere with the designated uses or with the established community of aquatic life in the segment for which the uses are designated,*” and the mixing zone shape be “... *a simple configuration that is easy to locate in the body of water and avoids*

*impingement on biologically important areas."* Another example is the amendments to the European Water Framework Directive (EU, 2008, Article 4) defining mixing zones as *"designated zones adjacent to points of discharge. Concentrations of substances may exceed the relevant AS within such mixing zones if they do not affect the compliance of the rest of the body of surface water with those standards."*

Once the principle of a mixing zone has been adopted and defined in the national regulations, it is also necessary that national water authorities provide clear guidance for the actual specification of mixing zone dimensions. However, there are several authorities in different countries with such modern regulations, which are reluctant to undertake the additional work to implement the mixing zone concept. Their arguments are often related to the difficulty in defining mixing zones on one hand, and on the application of it on the other hand. The following paragraphs are intended to show that indeed very simple approaches exist to define mixing zone standards and to demonstrate and proof compliance.

Figure 42 shows the most common definition of regulatory mixing zones for coastal discharges. As described in the previous sections it seems advisable to constrain the regulatory mixing zone to a limited region around the outfall in which the initial mixing processes (compare with section 4) are dominant. In that fashion and assuming a proper discharge design, the AS-values can be achieved within short distances. Thus the following specification appears effective:

*"The mixing zone is a volume with vertical boundaries in the coastal water body that is limited in its horizontal extent to a distance  $D_{MZ}$  equal to  $N$  multiples of the average water depth  $H_{ave}$  at the outfall location and measured in any direction from the outfall structure."*

The mixing zone definition in the above statement is a regulatory formulation with the following general attributes:

- 1) Geometrically this specification results in a cylindrical volume with the port in its center (Figure 42a) for a single port outfall. For a multiport diffuser outfall with many ports arranged along a straight diffuser line it would be a rectangular prismatic volume with attached semicircular cylinders at the diffuser ends located along the diffuser line (Figure 42b). For diffusers with a curved diffuser line or piecewise linear sections the volume would follow the diffuser line.
- 2) It accounts for the typical scales of initial mixing processes, where the local water depth at the discharge location is a major parameter limiting those processes. Thus discharges in deep waters have larger mixing zones, because of their better mixing characteristics. Whereas shoreline discharges ( $H_{ave} = 0$ ) result in  $D_{MZ} = 0$ , thus need a high level treatment to achieve the AS directly at the discharge location. This is justified due to very small mixing of shoreline discharges, and the existence of multi-directional flows and usually more sensitive ecosystems close to shore. It also follows the philosophy to avoid shoreline discharges completely.
- 3) The multiplier  $N$  accounts for physical, chemical, and biological characteristics of the receiving waters, and/or effluent characteristics. The value  $N$  would typically be in the range of at least 1 to about 10 and set by the regulatory authority. For highly sensitive waters the minimum of 1 should be set. Common values for most coastal waters might be  $N = 2$  to 3.

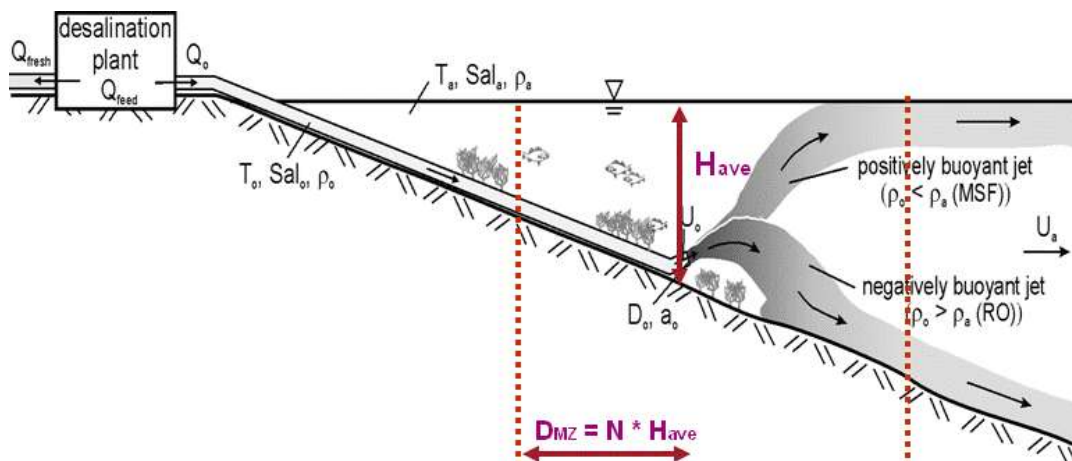
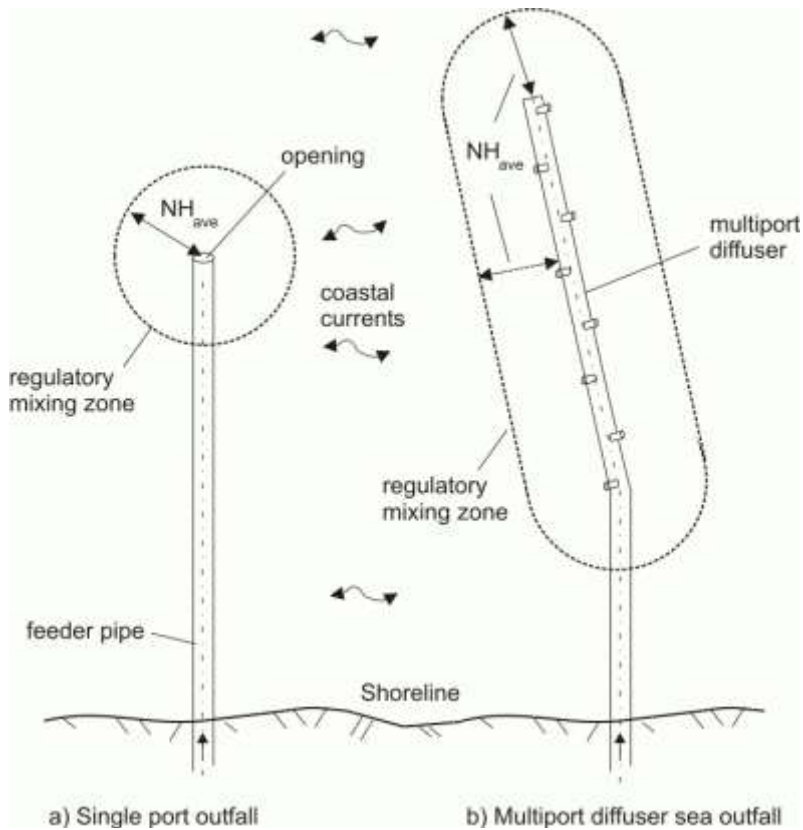


Figure 42: Example of regulatory mixing zone specification for offshore submerged coastal discharges: The horizontal extent of the mixing zone is defined by some multiple  $N$  of the average water depth  $H_{\text{ave}}$  at the sea outfall

The following statements provide some guidance on how to specify the value of  $N$ .  $N$  can be specified regarding effluent types and characteristics, as well as receiving water characteristics. Former can be done defining a value  $N$  for every discharged substance, based on factors like biodegradability, half-time decay coefficients, or the ES/AS ratio. Latter can be done by using existing water quality ecological parameters to describe the susceptibility and vulnerability on one hand, and the assimilative capacities and further existing pressures on the other hand. The lowest  $N$  value is than chosen for the mixing zone definition. Usually only one mixing zone size is defined for a specific discharge location. However, an exception is done in US regulations, where two mixing zones are defined for toxic discharges. For those cases another, much smaller toxic discharge zone is defined where toxic AS need to be met outside that toxic mixing zone.

Further approaches have been proposed in Spain (Freire, 2008) to compute the values for  $N = (D + B + V) / 3$ , with  $D =$  Depth Index,  $B =$  sediment index,  $V =$  Vulnerability index based on the sediment characteristics (hard substrates, mixed substrates and soft substrates) and ecological parameters (susceptibility, biotope protection status, biotope conservation status, and biotope sensitivity) combined to  $V = (I_s + I_{bps} + I_{bcs} + I_{bs}) / 4$  as shown in Table 9.

Table 9: Proposed indexes for defining N (reproduced from Freire, 2008)

Index		Categories	Index value
WATER DEPTH (D)		0 – 30 m	1
		30 – 60 m	2
		> 60 m	3
BOTTOM SUBSTRATE (B)		Hard substrates (rocky)	1
		Mixed substrates	2
		Soft substrates (sandy or muddy)	3
VULNERABILITY OF COASTAL WATERS TO OUTFALLS DISCHARGES (V)	Susceptibility ( $I_s$ )	High	1
		Intermediate	2
		Low	3
	Biotope protection status ( $I_{bps}$ )	High	1
		Intermediate	2
		Low	3
	Biotope conservation status ( $I_{bcs}$ )	Extirpated	1
		Severely declined	1
		Significantly declined	2
		Probability of significant decline	3
	Biotope sensitivity ( $I_{bs}$ )	High	1
		Intermediate	2
Low		3	
Not sensitive		3	
Not relevant		3	

Those values strongly depend on available data bases and could be quantified by unique values in this specific case. The combination of the the values result in a single numeric value for N. Freire (2008) also showed the applicability of that approach for three case studies applied for discharges into the Mediterranean and Atlantic coast.

In addition, specification of mixing zone dimensions can be defined in an ad-hoc manner. After prior ecological evaluations or predictions the discharger can request the authority for a mixing zone with a certain dimension with the claim that this would guarantee an integrated water quality protection. Based on its own examinations the authority can agree with that proposal or else demand further restrictions.

Mixing zone regulations should furthermore include statements like the following (modified from Freire, 2008):

*"Though AS can be exceeded within the mixing zone it is not allowed to discharge substances in concentrations, which could form objectionable deposits, floating debris, oil, scum, or which produce objectionable colour, odour, taste or turbidity, or which produce undesirable aquatic life or result in a dominance of nuisance species, or which result in acutely lethal toxic conditions to aquatic life or irreparable environmental damage including risk to ecosystem integrity and human health or which interfere with common water quality objectives. Mixing Zones of different discharges may not overlap. Mixing zones may not interfere with natural and human recognized uses, such as water supply, recreational, fishing, aquaculture, nature conservation or other water uses."*

### 3.4.6. Omani regulations on mixing zones

The Omani Ministerial Decision No. 159/2005 deals with “Promulgating the bylaws to discharge liquid waste in the marine environment”. It is the core legislation for liquid waste discharges into the sea and is based on the “Law to monitor marine pollution”, promulgated by Royal Decree No. 34/74, and the “Environment protection and pollution control law”, promulgated by Royal Decree No. 114/2001.

The ministerial decision defines liquid waste as “any liquid containing environmental pollutants discharged into the marine environment from land or sea sources”. As stated in Article 5, “no liquid waste shall be directly or indirectly discharged in the marine environment without obtaining prior license”. The license is issued by the Department of Inspection and Environment Control and depends on the following conditions. First, the plant operators must reuse or recycle the liquid waste, destroy hazardous components or mitigate impacts by environmental treatment, if this is feasible in an appropriate way (Article 7). Second, they have to provide a detailed description of the characteristics of the liquid waste (Article 8) and the waste has to conform to the discharge limits of pollutants specified in Annex 1 (Article 9). Third, they have to provide information about the discharge location, such as physical and biological characteristics of the seawater and recreational or other usages of the concerned shoreline (Article 10). The maximum concentrations for selected substances in the effluent according to Annex 1 of the regulation are summarized in Table 10.

Besides the discharge limits, a mixing zone of 300 m in diameter around the outfall is specified. Within the mixing zone, no marine life at the seabed may be destroyed. Beyond the mixing zone,

- the ambient water temperature must not be increased by more than 1 °C (weekly average).
- the average ambient salinity must not be changed by more than 2 g/l.
- the average dissolved oxygen level should not be reduced by more than 10 % .

Table 10: Omani discharge limits for selected effluent pollutants (based on Decision No. 159/2005)

<b>Pollutant</b>	<b>Max. concentrations (mg/l)</b>
<b>Temperature</b>	+ 10 °C
<b>Suspended solids</b>	30.0
<b>Total chlorine</b>	0.4
<b>Copper</b>	0.2
<b>Nickel</b>	0.1
<b>Molybdenum</b>	0.05
<b>Iron</b>	1.5

Moreover, some constructional targets are set for plants. The outfall pipes must not be installed less than one metre from the lowest tide line. The discharge pipes must be located in a place where it is impossible for the waste plume to hit corals and seaweed at the bottom. Due to the results of the Sur plant case study, the proper application of the latter regulation must be questioned.

For the selection of the discharge site and the construction of the outfall, information about wind speed and direction for one month, low and high tide currents in an area of 1 km around the outfall and the average sea depth in the same area should be included. Multiport diffuser pipes are recommended to be installed in order to improve the brine dilution.

For those violating any of these regulations, the penalties of the Environment Protection and Pollution Control Law shall be applied.

### **3.5. Summary and recommendations for mitigation measures**

The previous sections demonstrate the variety of ways to analyze and control environmental impacts from brine discharges. Furthermore they illustrate the variety and sensitivity of different ecological regions and applied technologies. From the analysed data, the following conclusions about environmental impacts of brine discharges can be drawn:

- The marine environment is affected by *physical and chemical properties* of desalination effluents (pollutants).
- *Pollutant concentrations* cause acute impacts within a local mixing zone until they are decreased to harmless or ambient levels. The acute impact zone depends on the dilution of the brine in the receiving water.
- *Pollutant loads* can cause chronic impacts and long term effects if the accumulation rate surpasses the natural decomposition rate. Chronic impacts are not necessarily restricted to a zone around the outfall but can occur in the whole water body.
- Increased salinity and temperature cause local problems. The impact of salinity is more critical for RO plants due to the higher recovery rates. Increased temperature is an environmental problem of thermal plants.
- Antifouling chemicals like chlorine are highly toxic, but are mainly an acute problem within the mixing zone of MSF plants. However, the problem with oxidizing biocides is that the acute toxicity is transferred into a chronic, often carcinogenic, toxicity of the oxidation by-products, which are usually more stable and can be dispersed over considerable distances.
- Antiscalant chemicals are non-toxic to invertebrate and fish species, but some agents are poorly degradable and might cause chronic impacts due to load accumulation. Some products have been classified as being harmful to algae.
- Coagulants are non-toxic, but may be otherwise harmful by increasing water turbidity and affecting marine life by the high discharge loads, e.g. by blanketing. Antifoaming additives are non-toxic and generally well degradable.
- Heavy metal discharge due to corrosion is a major problem in MSF plants. Copper is the only critical element in terms of discharged loads and possible impacts. It can be acutely toxic to a certain degree but mainly generates load problems through accumulation. Other heavy metals may also be toxic but are discharged at non-critical concentrations.
- The pH values prevalent during chemical cleanings are toxic if directly rejected. The chemical mix used for RO membrane cleaning can have highly toxic local effects as well as long term impacts due to poorly degradable constituents.

- The ecosystem of water bodies with high desalination activities and restricted water exchange like the Arabian Gulf or the Red Sea are particularly endangered. Large parts of the shorelines can be affected and load accumulation risks are higher. Low water depths, sensitive coastal ecosystems and significant pollutant discharges make the Arabian Gulf especially susceptible to any form of pollution.
- The complete spectrum of impacts provoked by desalination effluents is still not entirely known and tolerance or toxicity levels have not been examined for all concerned marine species. Furthermore, complex synergy and cumulative effects of different pollutants add another uncertainty factor to the real extent of environmental impacts. For instance, synergetic effects of increased temperature and residual chlorine levels have been well-documented. Thus, the results of present studies should be treated as a minimum impact.

All in all, environmental impacts of brine discharges cannot be neglected and further research is needed to validate and extend the current knowledge. Field monitoring data and laboratory toxicity tests in particular should be conducted on a broader scale. Table 11 summarises the results on marine impacts of RO and MSF plants.

Table 11: Environmental impact of RO and MSF effluents

<b>Effluent characteristic</b>	<b>Concentrations</b>	<b>Environmental impact</b>
<b>Salinity</b>	RO ( $\approx 70$ mg/l) MSF ( $< 50$ mg/l)	can be harmful; reduces vitality and biodiversity at higher values; harmless after good dilution
<b>Temperature</b>	MSF (+ 10-15 °C)	can be harmful; can have local impact on biodiversity
<b>Chlorine</b>	MSF ( $\approx 2$ mg/l)	very toxic for many organisms in the mixing zone, but rapidly degraded,
<b>THM</b>	RO MSF	carcinogenic effects; possible chronic effects, more persistent, dispersal with currents, main route of loss is through evaporation
<b>Antiscalants</b>	RO ( $\approx 2$ mg/l) MSF ( $\approx 2$ mg/l)	poor or moderate degradability + high total loads $\rightarrow$ accumulation, chronic effects, unknown side-effects
<b>Coagulants</b>	RO (1-30 mg/l)	non-toxic; increased local turbidity $\rightarrow$ may disturb photosynthesis; possible accumulation in sediments
<b>Antifoaming</b>	MSF (0.1 mg/l)	non-toxic at used concentration levels; good degradability
<b>Copper</b>	MSF (15-100 $\mu$ g/l)	low acute toxicity for most species; high danger of accumulation and long term effects; bioaccumulation
<b>Other metals (Fe, Cr, Ni, Mb)</b>	RO MSF	only traces; partly natural seawater components; no toxic or long term effects (except maybe for Ni in MSF)
<b>RO cleaning solutions</b>	Low or high pH, disinfectants, detergents, complexing agents	Highly acidic or alkaline cleaning solutions that may cause toxicity without neutralization, disinfectants highly toxic at very low concentrations; detergents moderate toxicity; complexing agents very poorly degradable
<b>MSF cleaning solutions</b>	Low pH, corrosion inhibitor	Highly acidic cleaning solutions that may cause toxicity without neutralization low toxicity; poor degradability

A classification is established for the pollutants in order to display their potential harmfulness in MSF and RO processes (Table 12). The classification considers the outlined results about toxicity, degradability, applied dosages and process relevance. The following ranking seems appropriate. Highest efforts should be undertaken to reduce or avoid the discharge of pollutants classified as ‘critical’ and ‘very critical’.

Table 12: Potential harmfulness of major pollutants in MSF and RO effluents

	<b>MSF</b>	<b>RO</b>
<b>Very critical</b>	Chlorine/Trihalomethanes	Cleaning solution, Salinity
<b>Critical</b>	Temperature, Antiscalants, Copper	Antiscalants, Coagulants
<b>Less critical</b>	Salinity, Cleaning solution, Nickel	Trihalomethanes
<b>Non-critical</b>	Antifoaming, Other metals	Temperature, Metals

Efficient and economical technologies exist to reduce the impact of brine discharges on the marine environment. Modern physical water pretreatment with Ultrafiltration membranes or sponge ball systems may reduce the need for most chemicals if the plant is well-designed. Residual antiscaling chemicals should be replaced by more biocompatible, P-free chemicals. Copper pollution may be reduced by using more corrosion resistant copper-nickel grades or titanium. The impact of high salinity and temperature is mitigated by discharging the brine via multiport diffuser outfalls. The combination of these measures removes critical pollutants from the effluent and significantly reduces the environmental impacts of brine discharges. Intermittently produced waste-waters, such as backwash water from media filters or chemical cleaning solutions, should be treated.

The environmental benefits and costs of major mitigation technologies, in comparison to conventional seawater desalination systems, are summarised in Table 13. Following the recommendations of Lamei et al. (2009) one should however not only consider direct economic costs but also potential environmental costs, such as reduced fishing, reduced tourism or other effects caused by cheaper solution. All of these mitigation measures should be considered in the planning phase. This report focuses on the receiving waters and the outfall system, thus allowing an analysis of the efficiency of the applied mitigation measures in relation to the receiving waters' quality.

Table 13: Environmental benefits and costs of major technologies in reference to conventional desalination systems

<b>Technology</b>	<b>Environmental benefit</b>	<b>Financial expenses</b>
Sub-seabed intake (RO)	SDI (Silt Density Index) < 5, no antifouling chemicals, antiscaling and coagulation chemicals reduced or eliminated, chemical cleaning intervals 4-6 times higher	Higher investment costs, lower operating costs → lower TCO (the cost overhead)
UF pretreatment (RO)	SDI < 3, no antifouling chemicals, antiscaling and coagulation chemicals reduced, chemical cleaning intervals at least 4 times higher, but often requires chemically enhanced backwashing operational optimisation might replace all chemicals	Higher investment costs, lower operating costs → slightly lower TCO
Green additives	Biocompatible, P-free, non-hazardous antiscaling chemicals	Unknown costs, no significant cost increases expected
Stainless steel components	Excellent corrosion resistance	Moderate prices, depends on grade of alloying materials
Duplex steel components	Excellent corrosion resistance	Low prices due to low alloying concentrations
Multiport diffuser and discharge design	Improved dilution performance → impact area reduced	Similar to submerged outfalls, more cost-efficient in shallow low energy waters
Cleaning of intermittent waste waters	Significantly reduces chemical discharge loads into the sea	Depends on site and project

## 4. MIXING PROCESSES OF BRINE DISCHARGES

When performing design work and predictive studies on effluent discharge problems, it is important to clearly distinguish between the physical aspects of hydrodynamic mixing processes that determine the fate and distribution of the effluent from the discharge location (this section), and the administrative formulation of mixing zone regulations (previous section 3.4.5) that intend to prevent any harmful impact of the effluent on the aquatic environment and associated uses.

Mixing processes are an interplay of ambient conditions and the outfall configuration. Different hydrodynamic processes drive and control the system. Most processes are running simultaneously, but with very clear dominance in different temporal and spatial regions, according to their predominant flow characteristics, schematized in Figure 43 for one specific situation and in Figure 44 for constant ambient conditions, but varying discharge conditions.

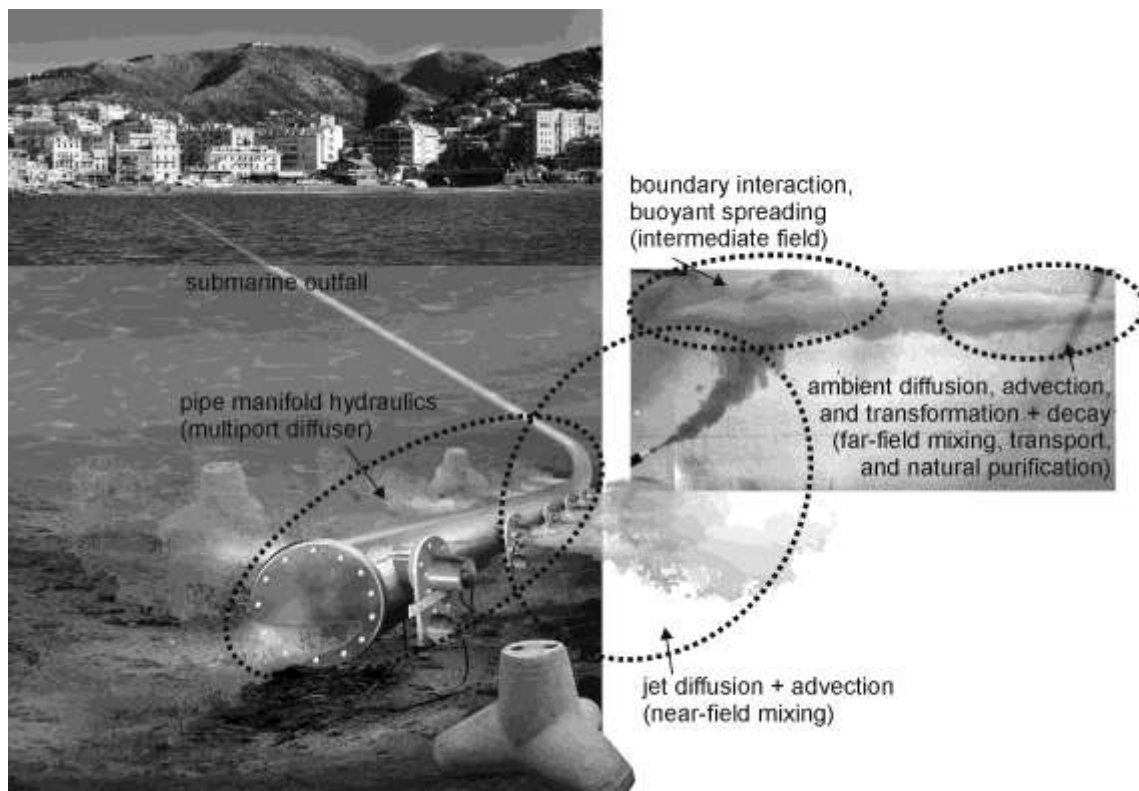


Figure 43: Schematic view of an operating multiport diffuser outfall merged with a laboratory picture of a trapped waste plume in stratified ambient (modified from Domenichini et al., 2002)

The first region is the outfall pipe system, conceptualized as an *internal hydraulic manifold*. It does not change effluent characteristics, but considerably contributes to the subsequent dispersion processes by conveying the effluent to adequate discharge locations and spatially distributing the effluent in the discharge region. The flow is driven by the pressure difference between the headworks and the receiving waters as well as the density difference between the effluent and the ambient water. Manipulations of various geometries have direct implications on the flow distribution and the pressure losses.

In the second region, the "*near-field*" (also called active dispersal region or initial mixing region), the initial jet characteristics of momentum flux, buoyancy flux, and outfall configuration (orientations and geometries) influence the effluent trajectory and degree of mixing (visualized in Figure 44). Source-induced turbulence entrains ambient fluid and

dilutes the effluent. Though ambient characteristics affect the discharge once the effluent has left the diffuser openings, (in most cases) they are still only of minor importance until any bottom, surface or terminal layer interaction occurs. This characterizes the transition to the intermediate field. Figure 44 shows how different discharge conditions (here varying only the vertical discharge angle) strongly influence the near-field flow region. The horizontal discharge almost immediately contacts the bed, causing eventual benthic impacts (top image on left side of Figure 44), whereas provides the best solution regarding shoreline impacts (top image on right side in Figure 44). The 60° discharge results in the longest trajectories, before contacting the bed or surface, thus providing the best initial dilution, but requires the largest water depths (almost impinging on the water surface in the experiment in the lower left image of Figure 44). These results show that the near-field mixing characteristics can be strongly influenced by the design.

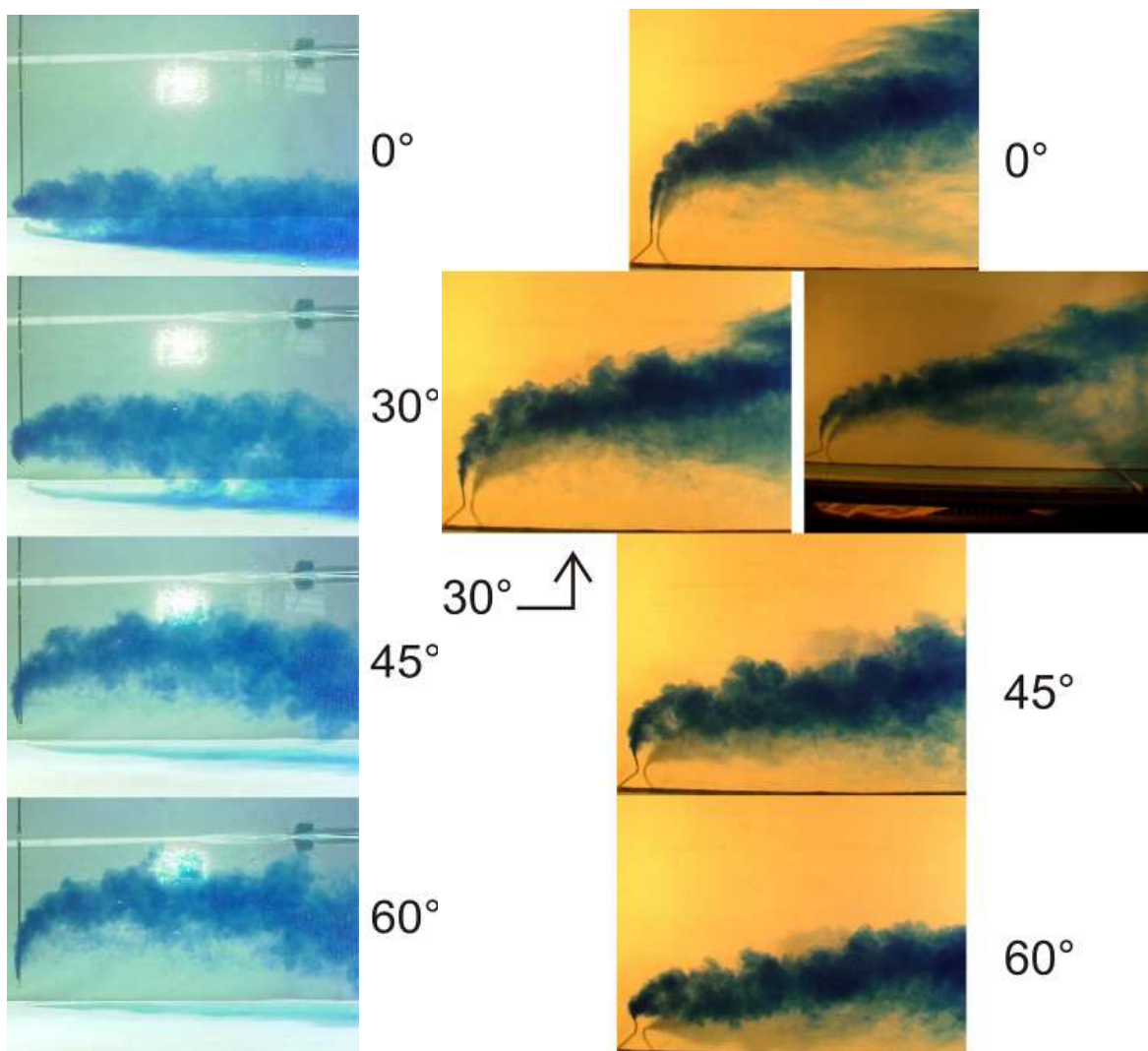


Figure 44: Laboratory studies showing a dense discharge, having a density difference scaled to a difference resulting from an RO effluent with 50% recovery. The ambient conditions are equal for all experiments with a constant flow from left to right. The ratio of the discharge velocity to the ambient velocity has been chosen according to real values  $R = 5\text{m/s} / 0.2\text{m/s} = 25$ . For the discharge conditions only the vertical discharge angle varied from 0° (horizontal discharge) to 60°. The images show the side views on the left and the top views on the right side for each discharge angle.

The “*intermediate field*” (or zone of wastefield establishment (Ridge, 2002)) is characterized by the impact of the turbulent plume with boundaries and the transition from the vertically

rising (positively buoyant effluent) or falling (negatively buoyant effluent) plume characteristics to a horizontal motion generated by the gravitational collapse of the pollutant cloud. Source characteristics become less important. Generally, a pool of initially diluted effluent water is formed either at the surface (positively buoyant effluent) or at the bed (negatively buoyant effluent) or the level of submergence under stratification conditions (shown in Figure 43 on the right side), where the diluted plume reaches a level of equal density before reaching the surface, which also may occur with negatively buoyant effluents falling in stratified environments. Vertical and horizontal boundary conditions will control trajectory and dilution in the intermediate field through buoyant spreading motions and passive diffusion due to interfacial mixing. Such buoyant spreading motions are of specific interest for negatively buoyant effluents discharged on sloped sea-beds, where density currents of high velocities may develop. Intermediate field processes have often been neglected in practical applications (i.e. model formulations), because focus has been given to either the near-field or the far-field processes and not their combination. In addition, only a few laboratory and field studies have examined these processes in more detail (Jirka and Lee, 1994; Akar and Jirka, 1995). Although these works generally confirm negligible scales of intermediate field effects for discharges into reasonable strong turbulent current fields, they clearly show their importance in either stagnant or shallow waters, where large spreading processes or instabilities occur.

After the wastefield establishment, ambient conditions will control trajectory and dilution of the turbulent plume in the “*far-field*” (also called passive dispersal region), through passive diffusion due to ambient turbulence, and passive advection by the often time-varying, non-uniform, ambient velocity field. The flow is forced by tides and large-scale currents, wind stress at the surface, pressure gradients due to free surface gradients (barotropic) or density gradients (baroclinic), and the effect of the Earth's rotation (Coriolis force). Dynamic discharge related effects are unimportant in that region. Vertical mixing in stratified water bodies is damped by buoyancy, so dilution is mainly due to horizontal mixing by turbulent eddies (Zielke and Mayerle, 1999). Concentration reductions in the far-field are related to natural dispersion but also significantly to natural biological/chemical transformation processes.

An overview of the physical processes is given in Table 14, and an example for their characteristic length and time scales for large discharges in the coastal environment in Figure 45. The combination of strong initial mixing induced by a multiport diffuser installation and adequate siting regarding high ambient mixing, transport and natural purification capacities reduces concentrations significantly. In total, the discharge plume and associated concentration distributions generated by a continuous efflux from a sea outfall can display considerable spatial detail and heterogeneities as well as strong temporal variability, especially in the far-field. This has great bearings on the application of any water quality control mechanisms.

Table 14: Overview of dominant processes for coastal submerged multiport discharges

	<b>manifold</b>	<b>near-field</b>	<b>intermediate-field</b>	<b>far-field</b>
<b>dominant forcing</b>	pressure difference	momentum and buoyancy flux	buoyancy flux and boundary resistance	tidal, baroclinic, barotropic and wind
<b>dominant advection</b>	mean pipe velocity	jet/plume induced velocity field	density current or ambient velocity	ambient velocity field
<b>dominant mixing</b>	fully mixed	strong shear induced turbulence	frontal mixing at plume borders	bed and wind shear induced turbulence
<b>temporal variance</b>	steady	quasi steady	unsteady	highly unsteady
<b>spatial variance</b>	uniform	non-uniform	non-uniform	non-uniform

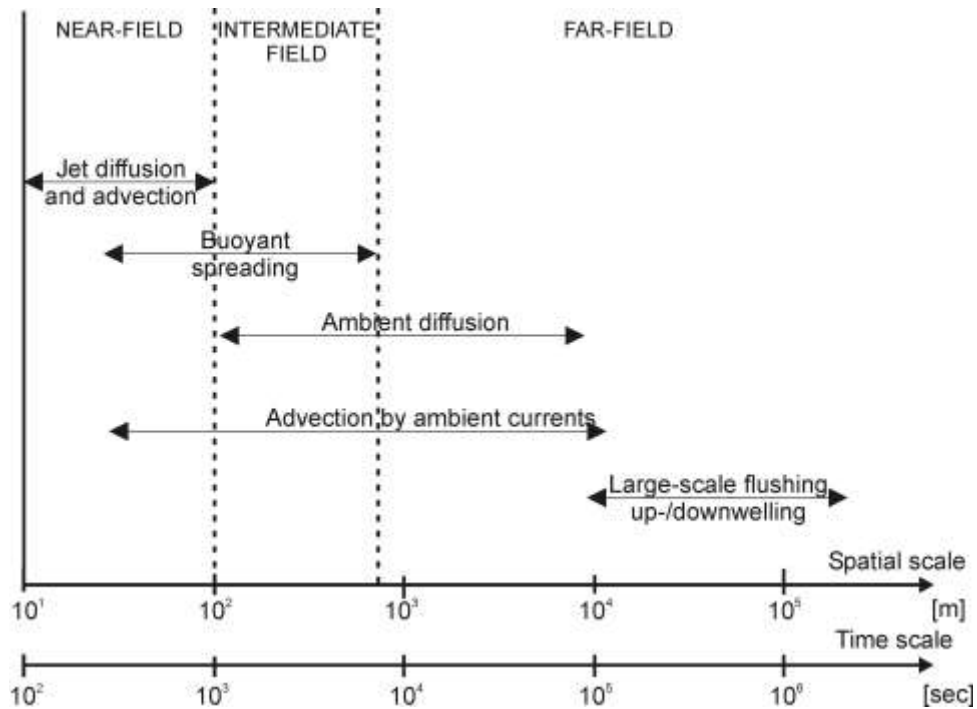


Figure 45: Typical temporal and spatial scales for transport and mixing processes related to coastal wastewater discharges (Jirka et al., 1976; Fischer et al., 1979)

## 4.1. Near-field processes

Discharge orientation, ambient currents, and densities influence the jet trajectories shown in Figure 46 for the example of single buoyant jets. Consequences are generally higher dilutions for ambient velocity-induced jet deflections and lower dilutions due to density-induced dampening of vertical motions for trapped plumes. Multiport jets are additionally influenced by the merging processes of individual jets, forming a two-dimensional jet plane with its own characteristics, as illustrated in Figure 47 and Figure 48. A general review of these processes has been given by Fischer et al. (1979), Wood et al. (1993), Roberts (1990, 1996) or Jirka and Lee (1994).

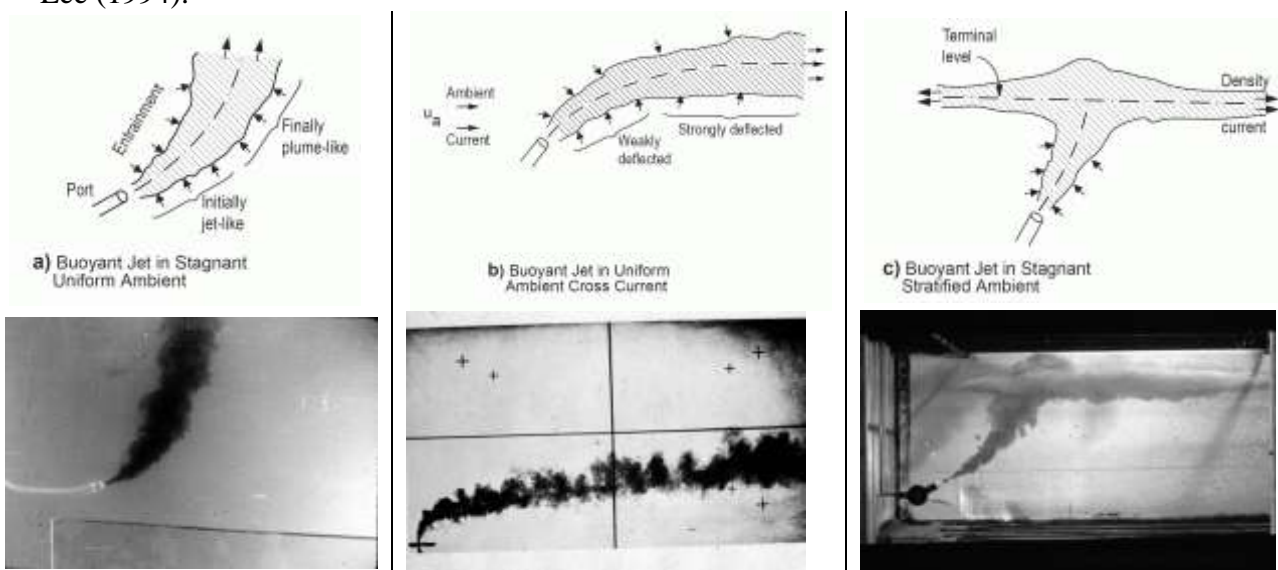


Figure 46: Schematized figures and visualizations from laboratory experiments showing different positively buoyant jet trajectories influenced by *a*) ambient density, *b*) ambient current  $u_a$ , and *c*) ambient stratification (Jirka et al., 1996; pictures from G.H. Jirka; L. Fan)

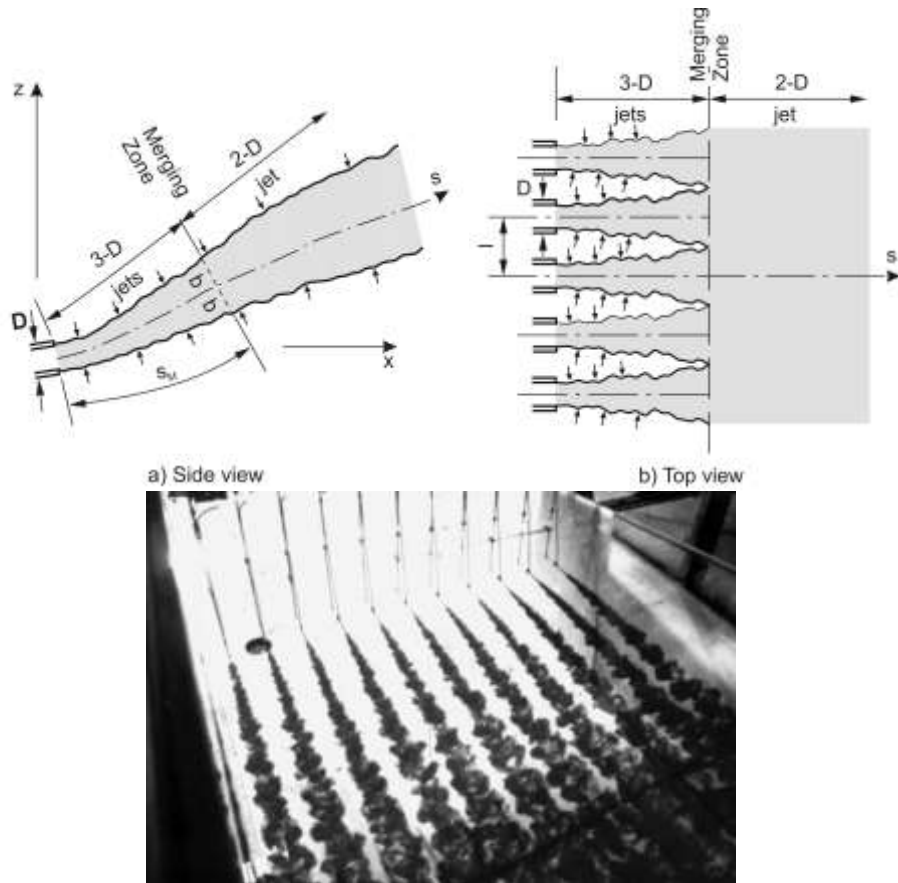


Figure 47: Schematization and visualization of laboratory experiment for merging of jets discharged unidirectional by multiport diffusers (reproduced from Jirka, 2006)

The near-field processes are dominated by the initial source fluxes and geometries:

- the initial volume flux  $Q_o = U_o A_o$ , for single port discharges, or  $q_o = Q_o/L_D$  for multiport discharges with the initial discharge velocity  $U_o$  and the individual or total pipe discharge cross-section  $A_o$  and the diffuser length  $L_D$
- the initial mass flux  $Q_{co} = U_o C_o A_o$ , or  $q_{co} = Q_{co}/L_D$  with the initial concentration  $C_o$
- the initial momentum flux  $M_o = U_o^2 A_o$ , or  $m_o = M_o/L_D$
- and the initial buoyancy flux  $J_o = U_o g_o' A_o$ , or  $j_o = J_o/L_D$  with the reduced gravity  $g' = \Delta\rho/\rho g$  and  $\Delta\rho = \rho_o - \rho_a$ , with the initial effluent density  $\rho_o$  and the ambient density  $\rho_a$ .

General ambient characteristics further dictate the trajectory:

- the average ambient flow velocity  $u_a$
- and the density stratification  $d\rho/dz$

Near-field instability is defined as the situation when discharge-induced motions considerably influence the ambient motions in the near-field region (Jirka 1982; 2006). Large recirculation zones or vertically mixed currents that laterally entrain ambient water are typical examples for an unstable near-field (Figure 49b).

"Stable discharge" conditions, usually occurring for a combination of strong buoyancy, weak momentum, and deep water, are often referred to as "deep water" conditions. "Unstable discharge" conditions, on the other hand, may be considered synonymous with "shallow water" conditions, when a multiport diffuser represents a large source of momentum with a relatively weak buoyancy effect (i.e. for thermal plumes). Technical discussions on discharge stability are presented elsewhere (Jirka, 1982; Holley and Jirka, 1986).

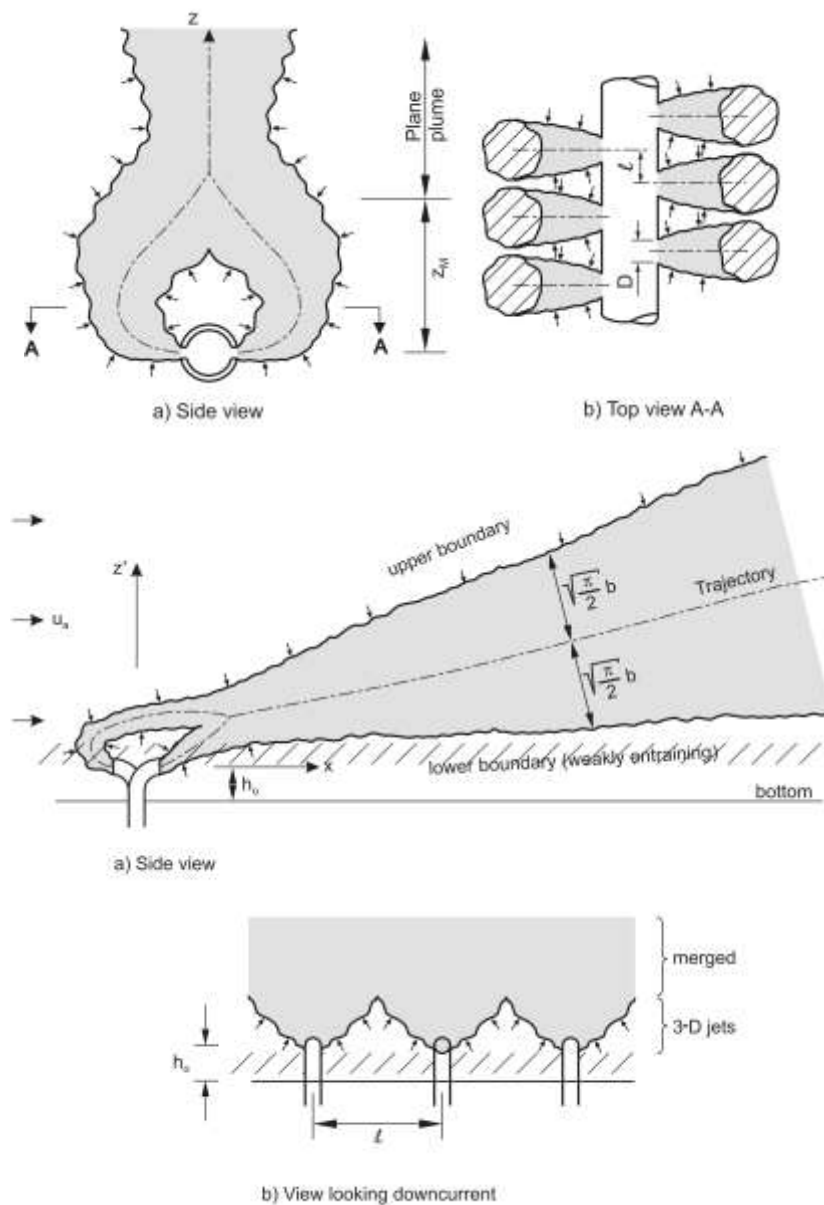


Figure 48: Schematization of merging jets discharged by a multiport diffusers with an alternating port arrangement in stagnant conditions and in crossflow (reproduced from Jirka, 2006)

## 4.2. Intermediate-field processes

The intermediate field starts at the end of the jet regime (region (1) in Figure 49a) and is classified according to two main processes: the boundary interaction, where boundaries, such as the water surface or the sea bed or other fixed boundaries as the shoreline inhibit motion (region (2) in Figure 49a), and the buoyant spreading, where the effluent field establishes horizontally or as a density current (part of region (3) in Figure 49a). Once these processes are of minor order compared to far-field transport and dispersion processes, the far-field is attained (region (4) in Figure 49). For weak ambient flows or quiescent ambient the intermediate-field may extend over distances that are substantially greater than the water depth (Jirka, 1982); however, for strong ambient motions its effects are often negligible. The effect of ambient flow velocities on intermediate field processes can be seen in Figure 50.

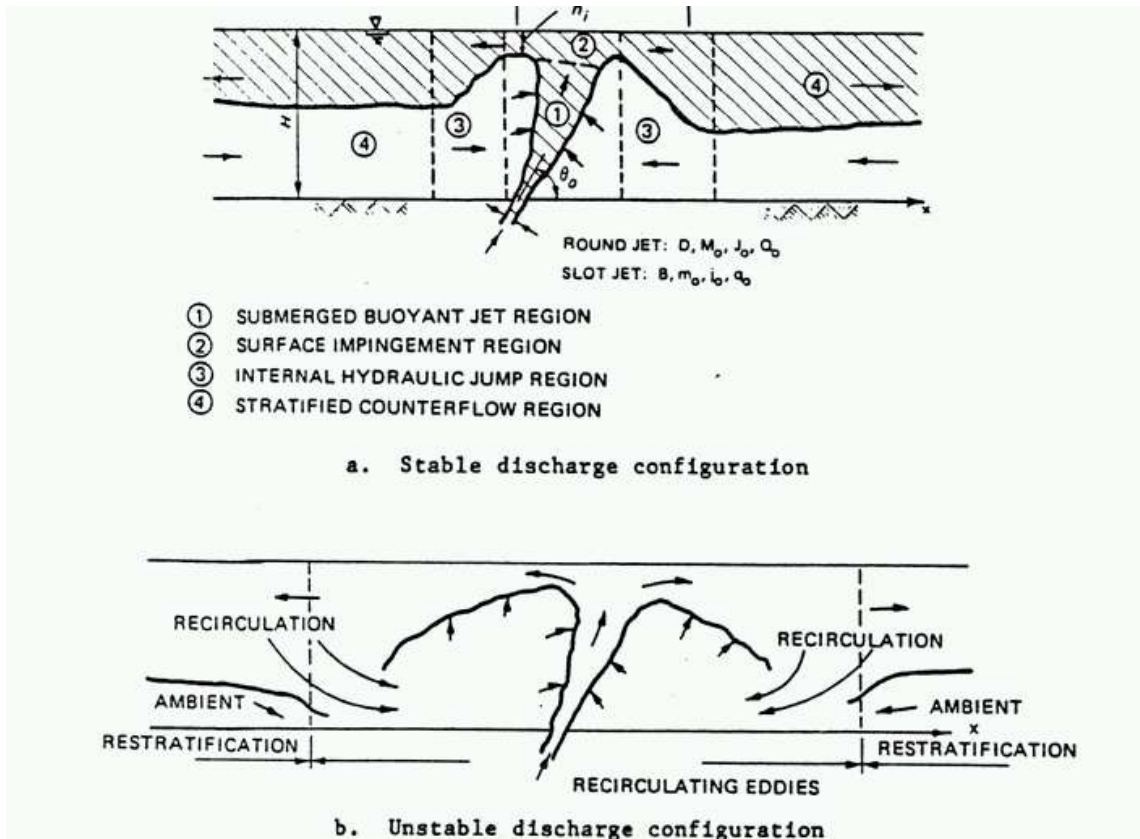


Figure 49: Submerged buoyant slot jet discharging into stagnant water of finite depth (Jirka, 1982). *a*) Deep water discharge with stable discharge configuration, *b*) shallow water discharge with unstable recirculation zone (reproduced from Jirka et al., 1996)

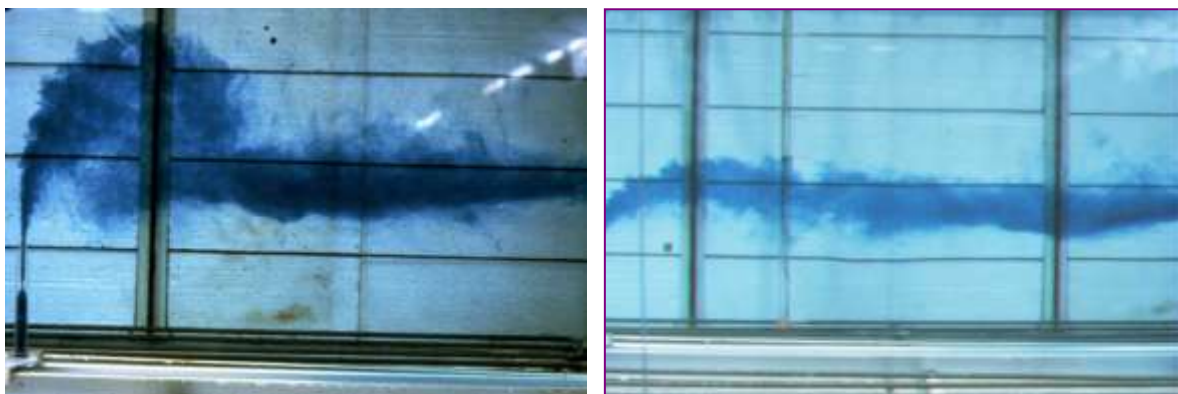


Figure 50: Laboratory experiment for a dense jet discharge into a density stratified and flowing environment. Left image: slow ambient velocity. Right image: higher ambient velocity (courtesy of G.H. Jirka, L. Fan, Keck Lab, CIT)

Boundary interactions have strong implications on discharge assessments, because the location and concentration of plumes when hitting either the surface, the bed or the shoreline are important project criteria. Boundary interaction processes are classified into interaction with horizontal boundaries (surface, bed, or pycnocline) and lateral boundaries (shoreline), as illustrated in Figure 51.

For large ambient velocities the boundary interaction can simply be conceptualized as a gradual transition of a bent-over plume to a far-field surface or bed layer flow (Figure 52a). However, boundary interaction processes become important for weak ambient currents. The almost vertically rising (Figure 46c) or falling plume (Figure 50) motions are either stopped

suddenly by surface or bed impingement or overshoot and fall down (Figure 46c) or rise back on the terminal layer for pycnocline impacts (Figure 50). Both plumes consequently experience rapid horizontal spread in all directions. Additional mixing is referred to this impact and spreading motions, where so-called upstream spreading may extend considerably (Figure 52b). Shallow conditions may furthermore lead to local recirculation (Figure 52c,d). The more complex interactions of negatively buoyant jet discharges on sloping beds and the influence of ambient velocity are illustrated in Figure 53.



Figure 51: Pictures of laboratory experiments showing boundary interactions with the surface, the bottom and the pycnocline (courtesy of G.H. Jirka, L. Fan, Keck Lab, CIT)

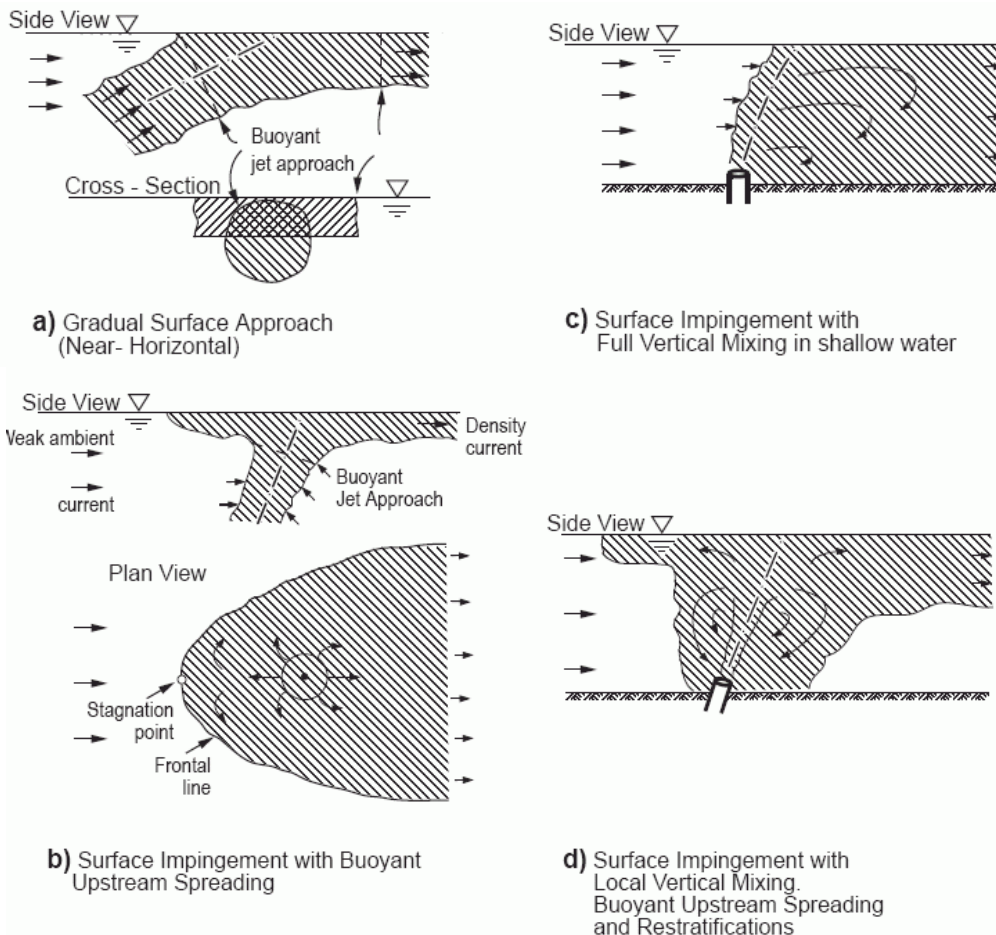


Figure 52: Examples of boundary interactions for submerged positively buoyant jets in finite depth (reproduced from Jirka et al., 1996)

The mentioned subsequent buoyant spreading processes are related to the plume collapse after boundary or pycnocline interaction. These motions are no longer jet-like and concentration distributions change according to transport motions and spreading motions. Transport motions carry the substances away from the source with ambient velocities. Spreading motions spread

the effluent field in the horizontally and/or downwards (Figure 53 for negatively buoyant and Figure 54 for positively buoyant discharges). There is a clear distinction between the far-field spreading motions by turbulent spreading and the intermediate spreading by density differences. The former is related to mixing motions, whereas the latter are density current-like motions, with rather small mixing due to entrainment at the frontal heads of the current. Thus, buoyant spreading collapses the vertical, initially thick effluent field into a thin and wide horizontal layer. The weaker the ambient currents and the stronger the stratification, the faster buoyant spreading motions are induced. This holds especially for a steady quiescent ambient (i.e. lakes or reservoirs or bays), where density differences of the discharge and the ambient cause density current spreading over large distances at the terminal layer.

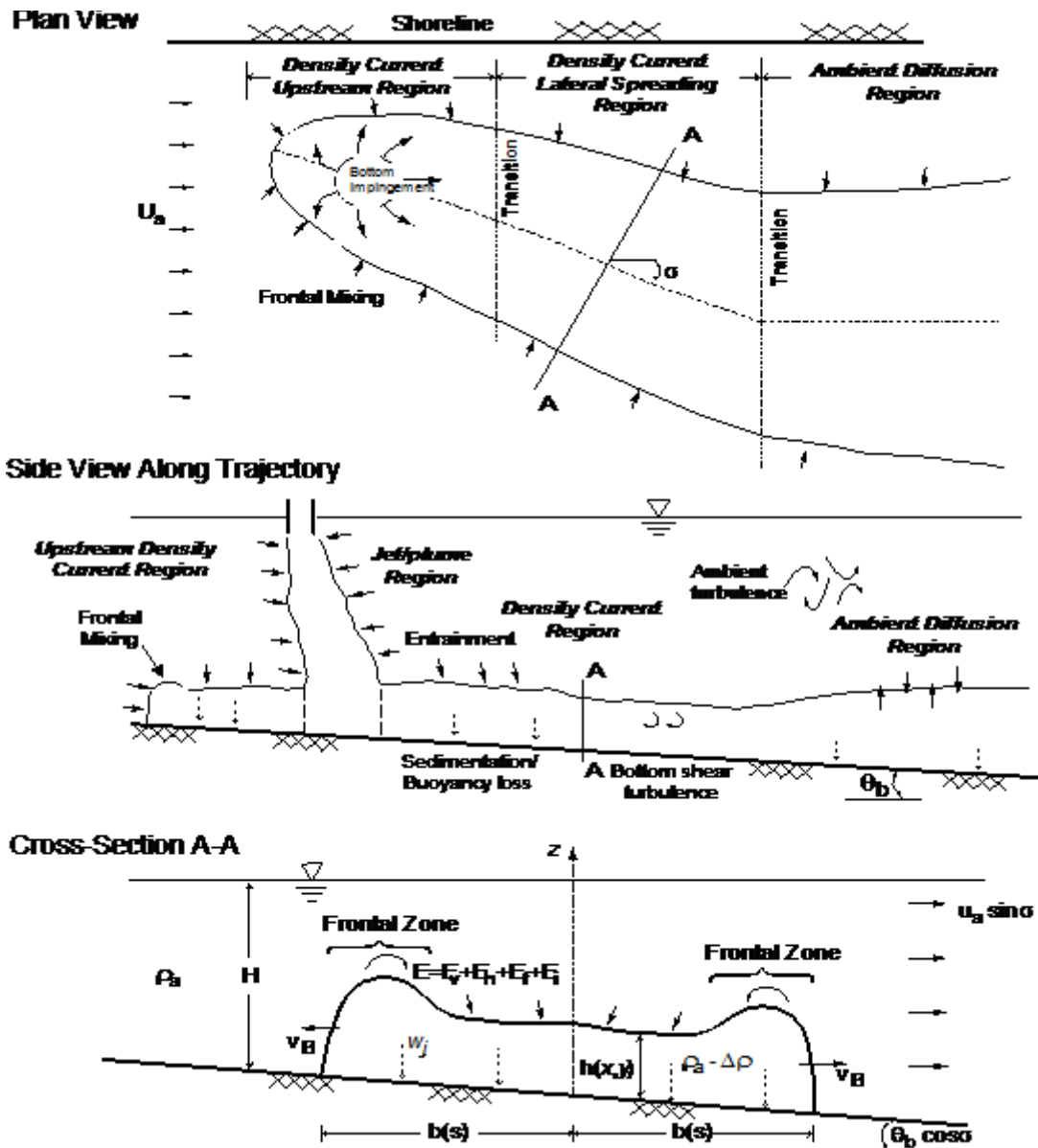


Figure 53: Submerged negatively buoyant single port discharge into a flowing unstratified receiving water on a sloping bottom (source: Doneker et al., 2004)

Consequences of large buoyant spreading processes are modified flow fields superimposed on far-field transport processes, thus influencing concentration distributions. In addition, near-field dilutions are relatively small during periods with weak ambient velocities. Both in combination cause higher risk for environmental impacts. Therefore, the stagnant ambient water case has traditionally been considered as the worst case for discharge assessments,

however, only when related to pure near-field considerations, i.e. without influence of spreading motions. Furthermore, most recently used approaches using additional far-field dispersion models either do not include any buoyant spreading process, or do have considerable deficiencies in calculating these thin near-field-diluted waste layers, spreading at either the surface, the bed or the pycnocline in unsteady environments.

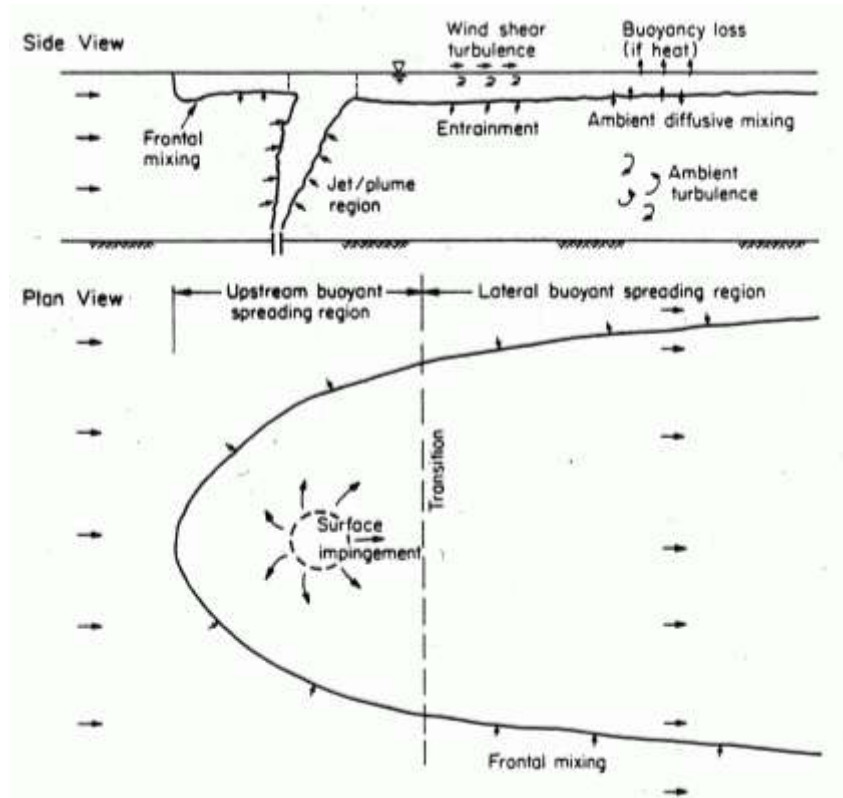


Figure 54: Buoyant spreading processes after near-field region (upstream and lateral spreading), superimposed on the transport by ambient currents (reproduced from Jirka and Akar, 1991)

Such spreading effects have been observed for desalination plant discharges in several field studies, indicating their importance for the discharge assessment. Figure 55 shows concentration maps resulting from two dense RO discharges with higher concentration on the bed spreading in offshore direction. Figure 56 shows measured velocities indicating that near-bed velocities of such density currents can be even higher than wind induced surface velocities or average current velocities.

Another type of interaction process concerns submerged jets discharging in the vicinity of the water bottom into a stagnant or flowing ambient. Two types of dynamic interaction processes can occur that lead to rapid attachment of the effluent plume to the water bottom as illustrated in Figure 57. These are wake attachments forced by the receiving water's cross flow or Coanda attachments forced by the entrainment demand of the effluent jet itself. The latter is due to low-pressure effects as the jet periphery is close to the water bottom. Jirka et al. (1996) described criteria for the prediction of boundary interactions, which are mainly based on dimensionless numbers, parameterized out of ratios of the geometrical length scales (e.g. port elevation, water depth, distance to shore) and the hydrodynamic length scales (Jirka et al., 1996).



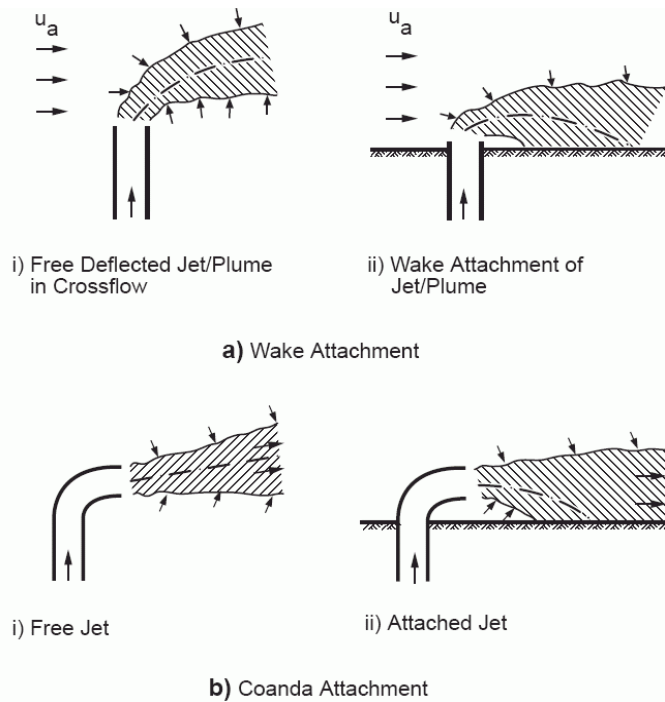


Figure 57: Examples of *a*) wake attachment and *b*) Coanda attachment conditions for jets discharging near boundaries (reproduced from Jirka et al., 1996)

### 4.3. Far-field processes

The further away from the source, the less important the discharge characteristics. The *far-field* extends from hundreds of meters to tens of kilometres. The ambient conditions are dominating the mixing processes. The established plume is transported through passive advection by a generally unsteady ambient current. Large scale motions, such as buoyant spreading processes, and passive diffusion control the slow mixing and the trajectory of the plume. Figure 58 gives an infrared image of the continuous plume produced at the water surface by a submerged cooling water discharge.

*Passive ambient diffusion* is a far-field mixing process which arises due to existing ambient turbulence. As shown in Figure 59 (right), the established plume increases in width and thickness until it interacts with boundaries (bottom or banks). The strength of passive diffusion depends mainly on ambient flow characteristics and the degree of stratification. In a stable ambient stratification, buoyancy in general strongly damps the vertical diffusive mixing processes.

Distinct from near-field motions, far-field processes do not focus on the jet, plume, or wastefield driven motions, but on the natural water body motions. Whereas background turbulence and spatial velocity field characteristics can be fully neglected in near-field approaches, they play a considerable role in the far-field region. Therefore, far-field processes are mainly related to the description of natural coastal flows. Once these processes are known, wastefield characteristics, as a result from the intermediate region, are coupled with these flows either at the surface level or trapped within density stratification, and transported and dispersed by ambient currents and ambient turbulence.



Figure 58: Surface plume in a long shore coastal current produced by a submerged sea outfall. The infrared image shows the plume produced by the cooling water discharge from a power plant at the western coast of Florida.

Brooks (1960) gives a widely used method of estimating the subsequent dilution of a wastewater field due to lateral mixing by oceanic turbulence. However, rigorous assumptions are necessary, i.e. a steady, two-dimensional, uniform flow condition without external forcing.

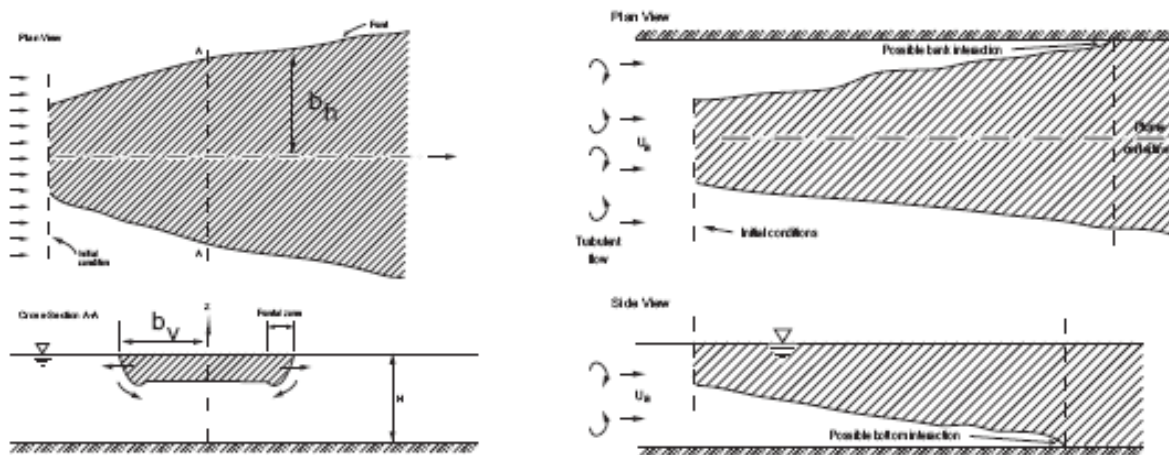


Figure 59: Left: Buoyant spreading process, right: passive ambient diffusion process (modified from: Doneker and Jirka, 2007)

Subject to the global flushing constraints, Brooks' (1960) descriptions are useful in giving a conservative estimate for the order of magnitude analysis of the subsequent dilution and elucidating the relative importance of horizontal diffusion and decay processes. It is, however, limited in the following respects, illustrated in Figure 60: a) coastal currents are unsteady, b) near-shore currents are horizontally non-uniform (e.g. vortex shedding at headlands), and c) coastal currents are vertically non-uniform (a wind-generated onshore surface current is usually accompanied by a compensatory offshore bottom current). Munro and Mollowney (1974) have shown that in shallow coastal waters vertical mixing in such a counter current system can lead to substantial additional reductions in concentration.

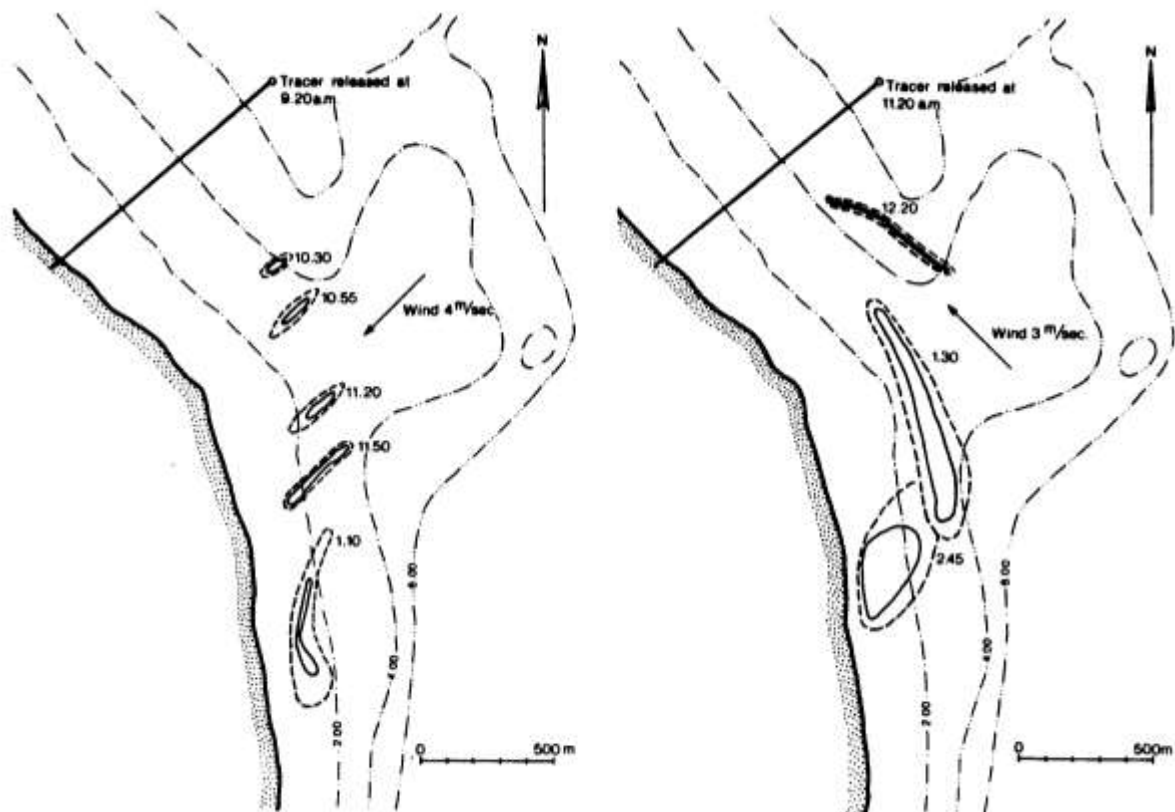


Figure 60: Example showing far-field waste plume transport and dispersion. The transport is governed by the tidal current and mixing is governed by the wind shear stress (courtesy of Torben Larsen, Denmark)

Thus, the required detail of predicting far field processes can vary considerably from case to case. It depends on i) the spatial complexity of the coastal ocean environment, ii) the availability of data, and finally, iii) the severity of the pollution problem:

Regarding *spatial complexity*: For an open coastal environment with a prevailing unidirectional current structure, consideration of simple plume near-field and intermediate-field mixing processes using typical and critical current regimes may suffice if a far field consideration is needed at all. For complex spatial conditions, such as estuaries or semi-enclosed bays flushing processes may need to be considered to ascertain the net flow-through and potential long-term accumulation of pollutants. Latter usually requires detailed simulations over large time scales (of the order of two flushing cycles, usually much larger than spring-neap tidal cycles).

Regarding *available data*, good information on current velocities and density profiles is essential for analyzing and modeling far-field transport. Estimates show that for long diffusers (e.g. 500 m), it is more important to describe where the wastefield goes rather than whether the far-field dilution is of the order of 3 or 5 (Roberts, 1979; 1980). However, for short diffusers, the far-field dilution increases to considerable values. The number of minimum simulations and minimum simulation periods needed to cover such processes should in any case cover typical characteristic length and time scales, to include large scale flow variations, critical meteorological conditions and characteristical temporal patterns. Usually simplified and low resolution large scale ocean circulation models are used to define critical periods and scales within a number of years simulations. These critical and average conditions are then studied and modeled with higher resolutions covering the minimum time scales of the order of spring-neap tide tidal cycles.

Regarding the *pollution problem*, near-field and intermediate-field process considerations suffice, if only acute impacts on the outfall zone are of interest. A simple reversal motion with built-up effects can be considered if currents are clearly oscillating with the tidal cycle. However, near-shore, water-quality impacts on the shore are related to large and unsteady plume travel times of the order of several hours, defining the necessity of an unsteady tidal flow model. Moreover, because an “old” diluted plume can return with the tidal current, the scenario for a single computation should be around 24 hours to assess the discharge performance. A whole water quality analysis in any case needs to cover minimal characteristic length and time scales, to include large scale flow variations, critical meteorological conditions and characteristic tidal patterns (i.e. spring-neap tidal cycles), thus minimum simulation periods of the order of complete spring-neap cycles are recommended.

Finally, water quality parameters demand extensive information on additional parameters, like salinity and temperature, and plume depth and geometry (to define light attenuation), to name only a few (Bleninger and Jirka, 2004). A full far-field analysis includes a general flow model coupled with a transport model. Both are described in detail in the following chapter.

Therefore, large outfall projects for coastal cities should not only include an “order of magnitude analysis”, but also a full far-field flow analysis. Generally, numerical models in combination with field-measurements provide such information. This far-field analysis may also serve to deduce the relevant parameter for near- and intermediate-field analysis, especially if predictions beyond the measured parameters are to be considered. At first sight, this recommendation appears to be rather costly; in fact, it is relatively small compared to the considerably large investments for coastal outfalls and even insignificant compared to the potential socio-economic and environmental impacts due to the inappropriate solutions.

## 5. BRINE DISCHARGE MODELS

Brine discharge systems need to be designed to minimize environmental impacts and costs while being in compliance with regulatory demands. A major principle before working on the brine discharge designs is to reduce the source concentrations and loads by proper mitigation measures within the desalination plant (e.g. reducing additive usage and dosing, improving plant efficiency, etc.) or proper intake and pre-treatment technologies.

### 5.1. Brine discharge design objectives

Once the plant design has been drafted, initial brine effluent characteristics should be computed within an order of magnitude / screening analysis. This report includes a description for a simple calculator to compute effluent characteristics in comparison with ambient conditions (see Section 0, and Bleninger et al., 2009).

The design of a discharge structure should then follow the following general principles:

#### 1. Discharge siting

- The discharge location should be chosen in less-sensitive coastal regions. *No discharge permit* should be given for discharges, which are planned in sites where direct and immediate impacts are to be expected:
  - a. in environmentally sensitive or even environmentally protected sites, such as within or nearby coral reefs, in lagoons, in enclosed bays, within or nearby mangrove regions or similar places
  - b. directly on shore or at beaches or at the shoreline
- The discharge location should be chosen in coastal regions with good transport and flushing characteristics to avoid accumulation and allow for further mixing. *No discharge permit* should be given for discharges which are planned in sites with stagnant flows or enclosed, protected bays, such as
  - a. between structures for erosion protection or wave-breakers
  - b. lagoons, or harbors
  - c. very shallow waters with low current velocities

#### 2. Discharge design

- The discharge structure should be designed to avoid any direct or immediate impact with nearby boundaries. Therefore designs should:
  - a. be oriented into the open water body and not against the bed or the water surface
  - b. not cause strong bed or surface interactions
  - c. not be concentrated at one single point
- The discharge structure should be designed to enhance effluent mixing. Therefore designs should:
  - a. allow for energetic discharges to allow for strong initial mixing
  - b. be oriented perpendicular or co-flowing to predominant ambient currents
  - c. optimally distribute the effluent within the water body

The above design objectives can be met for offshore, submerged, multiport diffusers. The offshore location provides the necessary distance to the sensitive region. Submerged discharges allow for improved mixing before interacting with boundaries, and multiport diffusers guarantee enhanced mixing. The above objectives should be considered for several siting and design alternatives to find optimal and cost-efficient solutions. An offshore, submerged, multiport diffuser is the best acceptable discharge structure. This restrictive

conclusion is generally true for RO plants. However for thermal desalination plants, in particular the case of combined power and desalination plants with (very) high effluent flows, other options need to be considered too, because thermal impacts of large flowrates are often considered less harmful than salinity or substance impacts. In such cases, the excess salinity and temperature of the effluent discharge can be small to moderate, making other discharge structures such as an open channel feasible (of course provided that its location is not in environmentally sensitive or environmentally protected sites).

In order to demonstrate compliance with ambient standards (AS) for discharge permitting, it appears that both dischargers, as well as water authorities, must increase the application of quantitative predictions of substance distributions in water bodies (water quality parameters in general, mixing processes in particular). This holds for both existing discharges (diagnosis) as well as planned future discharges (prediction).

There are several diagnostic and predictive methodologies for examining the mixing from point sources and showing compliance with AS-values:

- 1) **Field measurements or tracer tests** can be used for existing discharges in order to verify whether AS-values are indeed met. Field measurements are costly, often difficult to perform, and usually limited to certain discharge and ambient conditions. Frequently, they must be supported through mathematical model predictions: on one hand, to establish a clear linkage to the considered discharge (especially if more than one discharge exists); and on the other hand, to synthesize conditions allowing for variability in the hydrological or oceanographic conditions or in the effluent rates.
- 2) **Hydraulic model studies** replicate the mixing process at a small scale in the laboratory. They are supported by similarity laws and are quite reliable if certain conditions on minimum scales are met, as has been demonstrated in the past. But just like field tests, they are also costly to perform and inefficient for examining a range of possible ambient/discharge interaction conditions.
- 3) **Simple analytical equations or nomograms** (e.g. Rutherford, 1994; Holley and Jirka, 1986) are often satisfactory to reliably predict the mixing behavior of a pollutant plume and will be covered in Section 5.2.
- 4) **Mixing zone models** are simple versions of more general water quality models. They describe with good resolution the details of physical mixing processes (mass advection and diffusion), but are limited to relatively simple pollutant kinetics by assuming either conservative substances or linear decay kinetics. This is acceptable for most applications, since residence times in the spatial limited mixing zones (see previously mentioned specifications) are typically short so that chemical or biological mass transformations are usually unimportant. The application of the mixing zone model CORMIX will be covered for brine discharge applications in Section 5.5.2.
- 5) **General flow, transport and water quality models** may be required in more complex situations. In simple water bodies, such as rivers, coastal regions or estuaries with well defined uni-directional current regimes or with simple reversals and moderate pollutant loadings, the use of mixing zone models alone may be sufficient to arrive at, or to evaluate, a design of a point source discharge that meets regulations. However, in coastal regions with multiple current regimes (inertial, tidal, wind- or buoyancy-driven) and in rivers and coastal regions with large pollutant loadings, especially where several sources

may interact and additional diffuse sources may exist, and where complex boundary conditions exist, mixing zone models must be supplemented by larger-scale (far-field) flow, transport and water quality models. Flow models hereby provide the required physical background flow situation, such as current and density profiles in the whole domain. Transport models are then applied to mix and transport the substances through that flow domain using proper turbulent mixing coefficients. Finally, a water quality model is applied to predict substance concentrations over greater distances in the water body for different pollutants, but also for nutrients and other bio-chemical parameters with due consideration of mass transformation and exchange processes. Such models however do not have the high spatial resolution that is required to predict mixing processes and the compliance with AS-values in a limited mixing zone. The application of the flow, transport, and water quality model Delft3D coupled with the mixing zone model CORMIX will be covered in Section 5.5.5.

It is important to remember that mixing processes of brine discharges have widely varying length and time scales (Figure 61). Since it is not possible to simulate them with one overall model, separate models are used in the near-field and far-field and then linked together. Existing "jet models" cover the near-field region, before boundary interactions take place. Regulatory mixing zones, such as the ones defined in section 3.4.5 are usually larger than the jet regions, thus require further model applications. As shown later, the CORMIX model is the only modeling suite containing a jet model coupled to intermediate field models, being able to predict outfall performance under different limiting conditions. The far-field models instead are not necessarily required for showing compliance with outfall related mixing zones, but more for water body related general effects of the outfall on the coastal ecosystem.

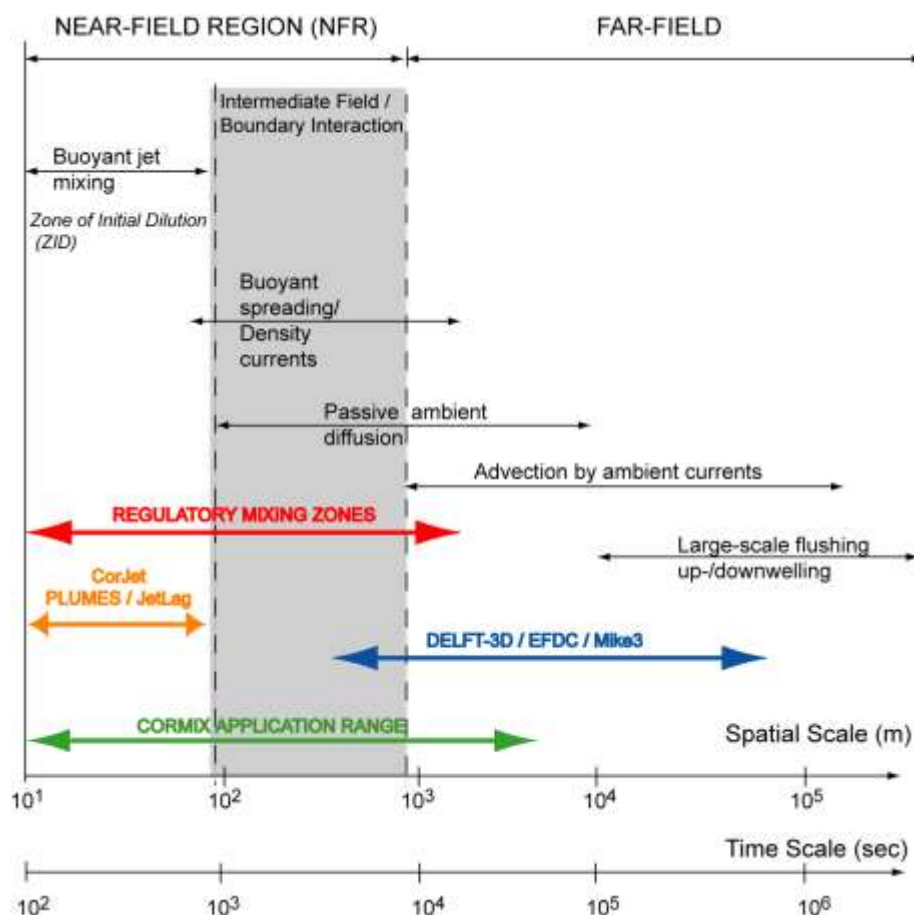


Figure 61: Typical temporal and spatial scales for transport and mixing processes related to coastal wastewater discharges and model capabilities (Jirka et al., 1976; Fischer et al., 1979)

## 5.2. Screening equations - nomograms

Once the plant design has been drafted, initial brine effluent characteristics should be computed within an order of magnitude / screening analysis, and flow classification. Those studies follow a very strong generalization and schematization, thus only allow computing the orders of magnitude of concentrations and geometries. In addition, however, the definition and computation of these basic parameters allows proceeding with a flow classification distinguishing between different flow types, expected plume trajectories and geometries, as well as expected boundary interactions. Thus, one should not underestimate the value of such investigations during the planning phase and as a starting point for more detailed environmental impact studies and process modelling.

The screening calculators are all based on simplified but validated scientific theories. They are coded in Excel spreadsheets and illustrated with nomograms. The spreadsheet is named the discharge calculator and includes a density calculator, and both of them are described in the following sections. The spreadsheets can be downloaded under [www.brinedis.net.ms](http://www.brinedis.net.ms).

### 5.2.1. Density and viscosity calculator

The most important brine property from the hydrodynamic viewpoint is the density and the density difference to the receiving waters, because density differences strongly influence the mixing and dispersion processes. The density of seawater, brine or freshwater itself is a function of salinity, temperature and pressure. The pressure influence is neglected in the following definitions, assuming applications only under normal atmospheric pressures and not within industrial facilities. The calculator is programmed in a MS Excel spreadsheet and available for download under [www.brinedis.net.ms](http://www.brinedis.net.ms).

The density calculator is based on El-Dessouky and Ettouny (2002) and is valid for salinities between 0 to 160 ppt and temperatures between 10 to 100 °C at pressures of  $p = 1$  atm. The density correlation is given by:

$$\rho = (A_1F_1 + A_2F_2 + A_3F_3 + A_4F_4) \cdot 10^3 \quad [\text{kg/m}^3]$$

where  $F_1 = 0.5$ ;  $G_1 = 0.5$ ;  $A_1 = 4.032219G_1 + 0.115313G_2 + 3.26 \cdot 10^{-4}G_3$ ;  $F_2 = A$ ;  $G_2 = B$ ;  $A_2 = -0.108199G_1 + 1.571 \cdot 10^{-3}G_2 - 4.23 \cdot 10^{-4}G_3$ ;  $F_3 = 2A^2 - 1$ ;  $G_3 = 2B^2 - 1$   $A_3 = -0.012247G_1 + 1.74 \cdot 10^{-3}G_2 - 9.0 \cdot 10^{-6}G_3$ ;  $F_4 = 4A^3 - 3A$ ;  $A_4 = 6.92 \cdot 10^{-4}G_1 - 8.7 \cdot 10^{-5}G_2 - 5.3 \cdot 10^{-5}G_3$ ;  $A = (2T - 200)/160$ ;  $B = (2Sal - 150)/150$  with  $T$  in °C and  $Sal$  in ppt.

The dynamic viscosity correlation of sea water is given by:

$$\mu = \mu_W \cdot \mu_R \cdot 10^{-3} \quad [\text{kg/(ms)}]$$

$$\nu = \mu / \rho \quad [\text{m}^2/\text{s}]$$

where  $\ln(\mu_W) = -3.79418 + 604.129/(139.18 + T)$ ;  $\mu_R = 1 + A \cdot Sal + B \cdot Sal^2$  ;  
 $A = 1.474 \cdot 10^{-3} + 1.5 \cdot 10^{-5} T - 3.927 \cdot 10^{-8} T^2$

Figure 62 shows a screenshot of the density calculator, which requires the input of temperature and salinity to compute the density using the above described equations. Figure 64 shows a nomogram for defining either the density or the viscosity for a given salinity and temperature. Thus, no PC is needed for first estimates.

There are different formulas for density calculation given in literature (eg. UNESCO Technical Papers) and online (eg. [www.csgnetwork.com/h2odenscalc](http://www.csgnetwork.com/h2odenscalc), [www.phys.ocean.dal.ca/~kelley/seawater/density.html](http://www.phys.ocean.dal.ca/~kelley/seawater/density.html)). Since UNESCO uses different equations for different ranges of salinities and temperatures, the equation of El-Dessouky and

Ettouny (2002) has been chosen, covering a major range of salinities and temperatures with only one equation and considering seawater desalination processes as the main application.

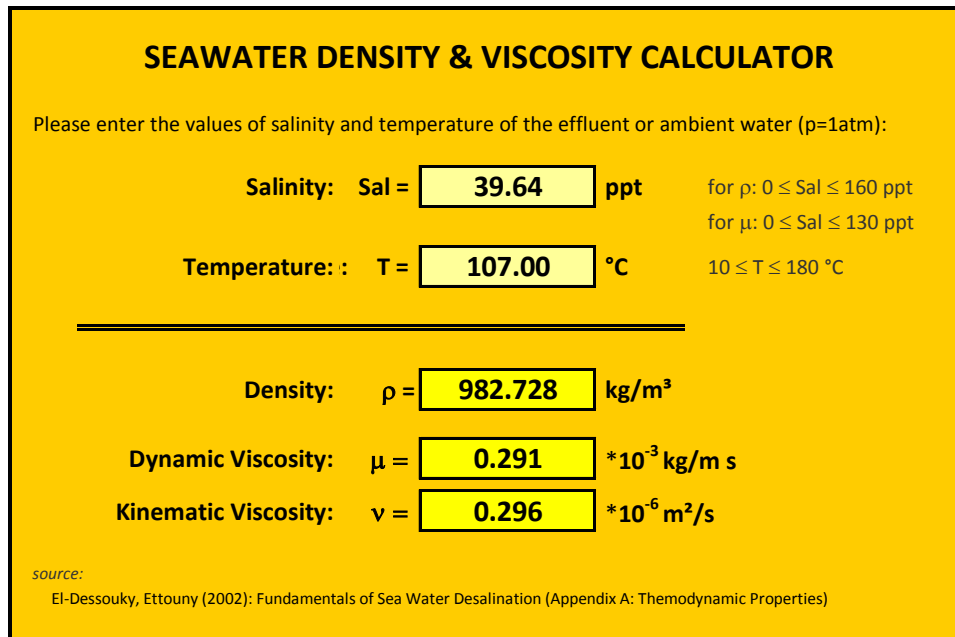


Figure 62: Screenshot of density calculator (download under: [www.brinedis.net.ms](http://www.brinedis.net.ms))

However, the available equations are giving different results. A comparison with two other calculating possibilities is shown in Figure 63. The calculations are based on:

A. the SW Density & Viscosity Calculator ( $Sal = 0-160$  ppt,  $T = 10-180$  °C,  $p = 1$  atm)

B. the UNESCO equations

-  $Sal = 0 - 42$  ppt,  $T = -2 - 40$  °C,  $p = 1$  atm, following UNESCO (1981)

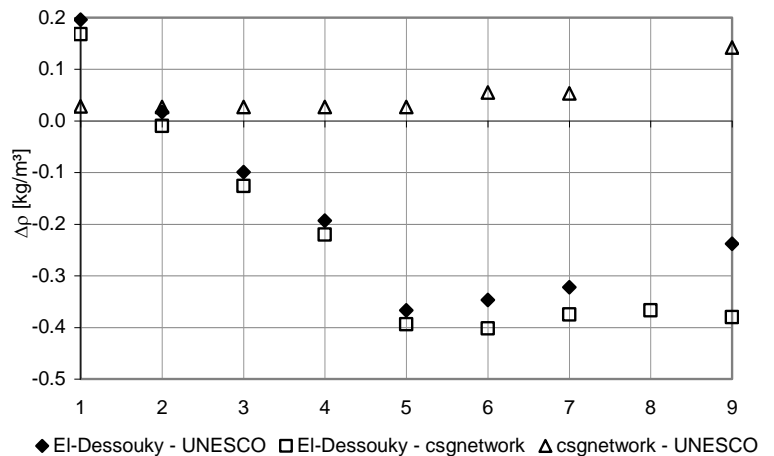
-  $Sal = 42 - 50$  ppt,  $T = 10 - 35$  °C,  $p = 1$  atm, following UNESCO (1991)

C. the “Water Density Calculator” (<http://www.csgnetwork.com/h2odenscalc.html>)

No formula is not specified and no restrictions are made.

The values are always computed for the water surface ( $p = 1$  atm), since density depends on pressure. The UNESCO equation of state consider the water depth ( $p = 0$  to 1000 bar) for salinities in the range of 0 to 42 ppt and temperatures in the range of -2 to 40°C.

	Sal (ppt)	T (°C)	$\rho$ [kg/m³]		
			A	B	C
1	0	20	998.402	998.206	998.234
2	10	20	1005.810	1005.793	1005.820
3	20	20	1013.263	1013.362	1013.389
4	30	20	1020.761	1020.954	1020.981
5	42	30	1026.621	1026.988	1027.015
6	45	30	1028.874	1029.221	1029.276
7	45	35	1027.053	1027.375	1027.428
8	45	36	1026.672	-	1027.039
9	50	35	1030.800	1031.038	1031.180



A: SW Density & Viscosity Calculator (El-Dessouky/Ettouny)

B: UNESCO equations

C: water density calculator (csgnetwork.com)

Figure 63: Differences in density calculation between different calculators for varying salinities and temperatures.

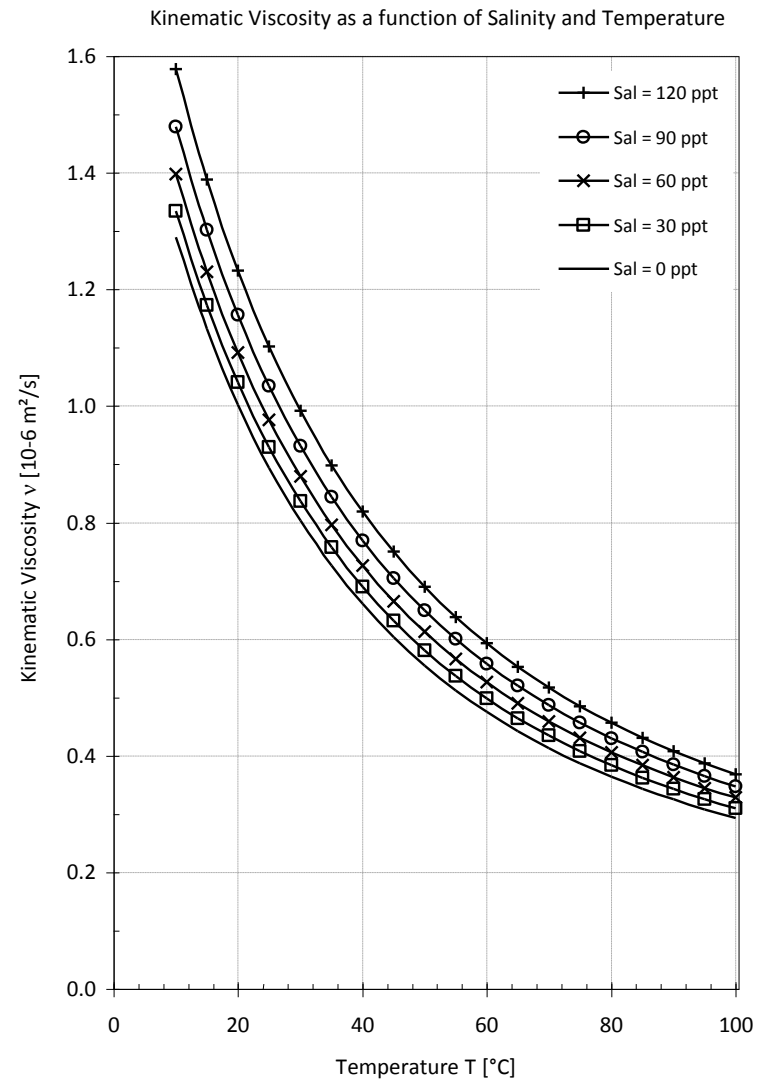
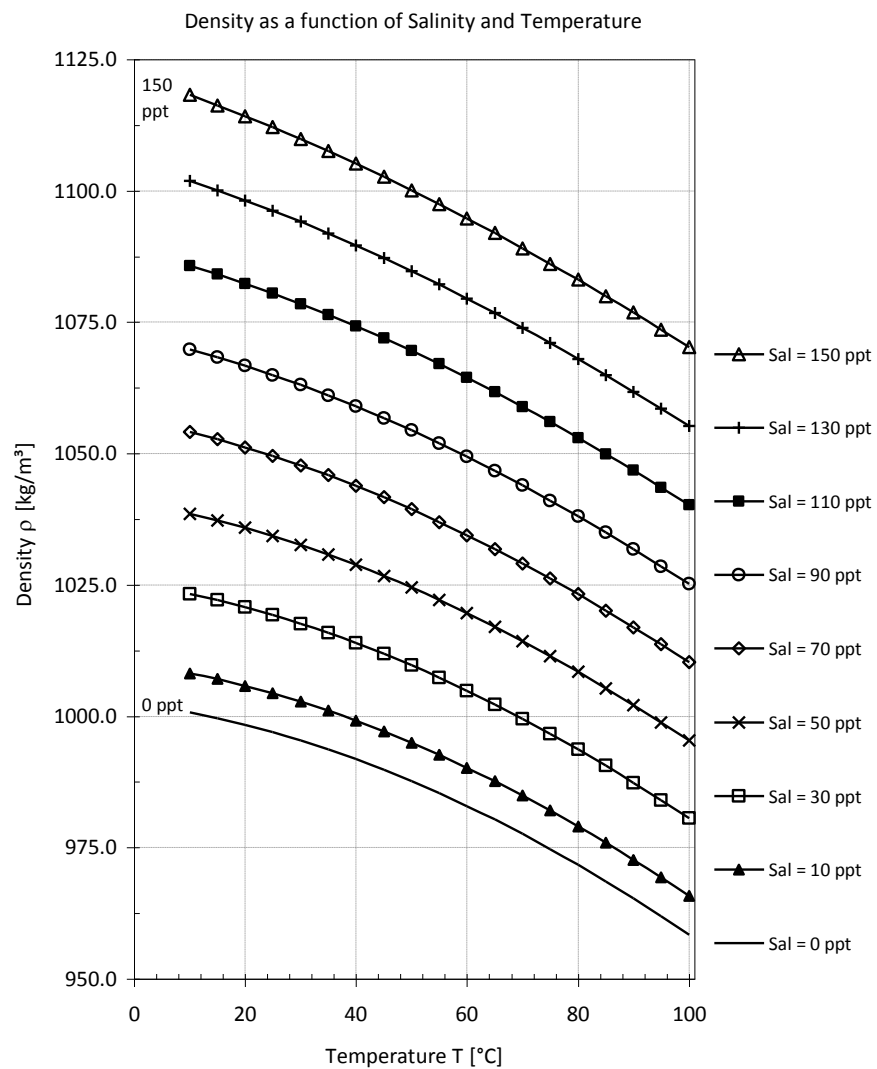


Figure 64: Nomogram for defining the effluent or seawater density and viscosity for different salinities and temperatures using the relationship from El-Dessouky and Ettouny (2002)

The comparison in Figure 63 show clear differences of the order of 0.3-0.4 kg/m<sup>3</sup> especially for higher salinities. For most applications these differences, which are of the relative order of per thousands can be neglected. However, for all applications dependent on density differences, those small variations may cause significantly different results. This is especially true for environmental hydrodynamic mixing and transport processes, which are very sensitive to density differences. Further investigations will be necessary on one hand to further examine the reason for the inaccuracies in the mentioned equations. On the other hand, sensitivity analysis is recommended to account for the variation and the formulation inaccuracies in those terms. And in any case measurements should be done at planned locations and existing effluents.

### **5.2.2. Discharge calculator**

The discharge calculator computes the effluent and general ambient properties at the discharge point. The results are used to interpret the discharge situation. Two calculators have been developed. One is for dense discharges and is called the RO-discharge-calculator, which also includes an estimation of the near-field / initial dilution in the near-field for very simplified conditions. The other for thermal discharges, called MSF-discharge-calculator which includes an estimator for the initial dilution. The calculators are programmed in a MS Excel spreadsheet and available for download under [www.brinedis.net.ms](http://www.brinedis.net.ms).

Figure 65 and Figure 66 show the first table of the discharge calculators to define the final effluent characteristics. Yellow boxes indicate where user-input is necessary. The other boxes are computed and updated automatically.

#### **Ambient characteristics**

First the user needs to define the ambient temperature and salinity, which is the average coastal water temperature and salinity at the intake location. Thus, temperature and/or salinity variations and their effect on the discharge characteristics can easily be investigated by trying different temperature and/or salinity values and comparing their effects. The calculator then automatically computes and updates the related density and viscosity in the boxes below, using the embedded density calculator.

#### **Drinking water (permeate) characteristics**

The desired permeate flow has to be defined, as well as the recovery rate, defined as the total permeate flow divided by the total intake flow. For thermal desalination plants the recovery rate is related only to flow without considering the cooling water (which will be added later), so just to the desalination process. The calculator then automatically computes the necessary intake flowrate and the brine flowrate using mass-balance equations.

#### **Concentrate characteristics**

The calculator only needs the input of the concentrate temperature (usually only slightly above the intake water temperature for RO and around 10°C above ambient for MSF) to compute the concentrate characteristics. The calculator then computes the concentrate salinity and density automatically. Furthermore, the calculator allows to define an additional substance concentration (one for RO, three for MSF) to consider additive (flocculants, anti-scalants, chlorine) usage and dosage and studying the effect of different concentration values on the final effluent characteristics.

#### **Blended effluents**

The calculator allows the input of up to one (RO) or two (MSF) different additional effluents, which are merged at the discharge point. This is to allow the consideration of effluents from

the desalination plant blended with other effluents like treated wastewater or cooling waters from the process itself or a cogenerating power plant. Those effluents have to be specified by giving the flowrate, temperature and salinity, and if applicable, additive substance concentrations related to the substances considered for the concentrate.

### Results - Final effluent characteristics

Results are the final effluent flowrate, the effluent temperature and salinity, and the resulting density and viscosity and substance concentrations. In addition the calculator computes the buoyant acceleration defined as  $g_o' = g (\rho_o - \rho_a)/\rho_o$  with  $g$  = earth acceleration,  $\rho_o$  = effluent density at discharge point,  $\rho_a$  = ambient density. The buoyant acceleration is a measure for density induced motions. The effluent is positively buoyant for positive  $g_o'$  and negatively buoyant (sinking down) for negative  $g_o'$ . In case of MSF, the final plant characteristics as the feedwater flowrate, the recovery rate (whole plant), and the temperature difference between the effluent and ambient water are computed.

Flowrates & Effluent Characteristics		annotations:
<b>- ambient characteristics</b>		
ambient temperature	$T_a =$ <input type="text" value="20.00"/> °C	$T = 10$ to $180$ °C
ambient salinity	$Sal_a =$ <input type="text" value="33.00"/> ppt	$Sal = 0$ to $160$ ppt (ppt = g/kg)
ambient density	$\rho_a =$ <input type="text" value="1023.02"/> kg/m <sup>3</sup>	allowed ranges for viscosity calculation:
ambient kin. viscosity	$\nu_a =$ <input type="text" value="1.05E-06"/> m <sup>2</sup> /s	$Sal = 0$ to $130$ ppt, $T = 10$ to $180$ °C (following El-Dessouky, Ettouny (2002))
<b>- drinking water (permeate)</b>		
flowrate	$Q_{drink} =$ <input type="text" value="6.00"/> m <sup>3</sup> /s	recovery rate:
recovery rate	$r =$ <input type="text" value="50"/> %	percentage of intake water converted into permeate;
intake flowrate	$Q_{in} =$ <input type="text" value="12.00"/> m <sup>3</sup> /s	plant characteristic; following Lattemann: $r = 40$ - $65$ %
<b>- brine characteristics (effluent from desalination process)</b>		
plant effluent flowrate	$Q_{desal} =$ <input type="text" value="6.00"/> m <sup>3</sup> /s	ambient or $1$ °C above with $Sal_{drink} = 0$ ppt  e.g. coagulants, anti-scalants, ....
temperature	$T_{desal} =$ <input type="text" value="20.00"/> °C	
salinity	$Sal_{desal} =$ <input type="text" value="66.00"/> ppt	
density	$\rho_{desal} =$ <input type="text" value="1048.12"/> kg/m <sup>3</sup>	
substance concentration	$c_{desal} =$ <input type="text" value="20.00"/> ppm	
<b>- blended effluent - external -</b> (e.g. waste water or others)		
flowrate	$Q_{effl,ex} =$ <input type="text" value="5.00"/> m <sup>3</sup> /s	$Sal = 0$ to $160$ ppt, $T = 10$ to $180$ °C
temperature	$T_{effl,ex} =$ <input type="text" value="20.00"/> °C	
salinity	$Sal_{effl,ex} =$ <input type="text" value="8.00"/> ppt	
density	$\rho_{effl,ex} =$ <input type="text" value="1004.33"/> kg/m <sup>3</sup>	
<b>Final effluent characteristics:</b>		
flowrate	$Q_o =$ <input type="text" value="11.00"/> m <sup>3</sup> /s	mean average mean average
effluent temperature	$T_o =$ <input type="text" value="20.00"/> °C	
effluent salinity	$Sal_o =$ <input type="text" value="39.64"/> ppt	$g_o' = g * ( \rho_a - \rho_o )/\rho_a$ $g_o' < 0$ : negatively buoyant, $g_o' > 0$ : positively buoyant
effluent density	$\rho_o =$ <input type="text" value="1028.03"/> kg/m <sup>3</sup>	
buoyant acceleration	$g_o' =$ <input type="text" value="-0.04804"/> m/s <sup>2</sup>	allowed ranges for viscosity calculation: $Sal = 0$ to $130$ ppt, $T = 10$ to $180$ °C (following El-Dessouky, Ettouny (2002))
-> negatively buoyant, ok!		
kin. viscosity	$\nu_o =$ <input type="text" value="1.06E-06"/> m <sup>2</sup> /s	
substance concentration	$c_o =$ <input type="text" value="10.91"/> ppm	

Figure 65: First table of the RO-discharge-calculator to compute the final effluent characteristics

## Flowrates & Effluent Characteristics

### - ambient characteristics (= intake water)

ambient temperature	$T_a =$	20.00	°C
ambient salinity	$Sal_a =$	33.00	ppt
ambient density	$\rho_a =$	1023.02	kg/m <sup>3</sup>
ambient kin. viscosity	$\nu_a =$	1.05E-06	m <sup>2</sup> /s

### - drinking water (permeate)

flowrate	$Q_{drink} =$	5.00	m <sup>3</sup> /s
recovery rate	$r_{dist} =$	33	%
distillation intake flowrate	$Q_{in} =$	15.15	m <sup>3</sup> /s

### - brine characteristics (effluent from desalination process)

brine flowrate	$Q_{brine} =$	10.15	m <sup>3</sup> /s
temperature	$T_{brine} =$	90.00	°C
salinity	$Sal_{brine} =$	49.25	ppt
density	$\rho_{brine} =$	1001.58	kg/m <sup>3</sup>
substance concentration 1	$C_{brine1} =$	20.00	ppm
substance concentration 2	$C_{brine2} =$	25.00	ppm
substance concentration 3	$C_{brine3} =$	30.00	ppm

### - blended effluent 1 - internal - (i.e. cooling water)

flowrate	$Q_{int} =$	35.35	m <sup>3</sup> /s
temperature	$T_{int} =$	20.00	°C
salinity	$Sal_{int} =$	33.00	ppt
density	$\rho_{int} =$	1023.02	kg/m <sup>3</sup>
substance concentration 1	$C_{int1} =$	0.00	ppm
substance concentration 2	$C_{int2} =$	0.00	ppm
substance concentration 3	$C_{int3} =$	0.00	ppm

### - blended effluent 2 - external - (e.g. waste water or others)

flowrate	$Q_{ex} =$	0.00	m <sup>3</sup> /s
temperature	$T_{ex} =$	20.00	°C
salinity	$Sal_{ex} =$	0.00	ppt
density	$\rho_{ex} =$	998.40	kg/m <sup>3</sup>
substance concentration 1	$C_{ex1} =$	0.00	ppm
substance concentration 2	$C_{ex2} =$	0.00	ppm
substance concentration 3	$C_{ex3} =$	0.00	ppm

### Plant characteristics:

feedwater flowrate	$Q_{feed} =$	50.51	m <sup>3</sup> /s
rejected effluent	$Q_{plant} =$	45.51	m <sup>3</sup> /s
recovery rate (desal. plant)	$r =$	9.9	%
effluent temperature	$T_{plant} =$	35.62	°C
temp. difference to ambient	$\Delta T =$	15.62	°C

### Final effluent characteristics:

flowrate	$Q_o =$	45.51	m <sup>3</sup> /s
effluent temperature	$T_o =$	35.62	°C
effluent salinity	$Sal_o =$	36.63	ppt
effluent density	$\rho_o =$	1020.57	kg/m <sup>3</sup>
buoyant acceleration	$g_o' =$	0.02351	m/s <sup>2</sup>
kin. viscosity	$\nu_o =$	7.56E-07	m <sup>2</sup> /s
substance concentration 1	$C_{o,1} =$	4.46	ppm
substance concentration 2	$C_{o,2} =$	5.58	ppm
substance concentration 3	$C_{o,3} =$	6.69	ppm

-> positively buoyant, ok!

### annotations:

$T = 10$  to  $180^\circ\text{C}$  (see density calculator)

$Sal = 0$  to  $160$  ppt (ppt = g/kg)

allowed ranges for viscosity calculation:

$Sal = 0$  to  $130$  ppt,  $T = 10$  to  $180^\circ\text{C}$  (El-Dessouky, Ettouny (2002))

recovery rate:

percentage of distillation feedwater converted into distillate;

without cooling water, only for distillation!!

following Lattemann (2006):  $r_{dist} = 30$ - $35$  %

$T = 10$  to  $180^\circ\text{C}$  (following Lattemann:  $90$ - $115^\circ\text{C}$ )

with  $Sal_{drink} = 0$  ppt (following Lattemann: up to  $50$  ppt)

e.g. chlorine

e.g. anti-scalants

...

2 to 3 times the intake water flowrate

ambient temperature (allowed range:  $T = 10$  -  $180^\circ\text{C}$ )

ambient salinity (allowed range:  $Sal = 0$  to  $160$  ppt)

e.g. chlorine (same substance as  $C_{brine1}$ )

e.g. anti-scalants (same substance as  $C_{brine2}$ )

... (same substance as  $C_{brine3}$ )

$T = 10$  to  $180^\circ\text{C}$

$Sal = 0$  to  $160$  ppt

e.g. chlorine (same substance as  $C_{brine1}$ )

e.g. anti-scalants (same substance as  $C_{brine2}$ )

... (same substance as  $C_{brine3}$ )

intake water for distillation & cooling

following Lattemann (2006):  $r = 10$ - $13$  %

following Lattemann (2006):  $5$ - $15^\circ\text{C}$  above ambient

mean average

mean average

$g_o' = g * (|\rho_a - \rho_o|) / \rho_a$

$g_o' > 0$ : positively buoyant,  $g_o' < 0$ : negatively buoyant

Figure 66: First table of the MSF-discharge-calculator to compute the final effluent characteristics

### 5.2.3. Length scale analysis and flow classification

Characteristical discharge parameters are computed in the second table of the discharge calculators to analyze and interpret a specific discharge condition. Furthermore, the RO-calculator already includes design considerations regarding the discharge geometry and allows computing a first set of design alternatives. The procedure is hereby based on the methodology proposed by Jirka (2008).

The computation of characteristical discharge parameters does hereby not aim for computing dilutions or concentration profile distributions, but to distinguish between different flow regimes, namely a flow classification. The so-called length scale analysis allows distinguishing, for example, between dominating jet flow regions, thus classifying the flow itself and different flow regions, as illustrated in Figure 67. Herefore the initial source properties are used in a dimensional analysis to define characteristic length scales. The initial source fluxes have been mentioned earlier, but are repeated here for convenience:

- the initial volume flux  $Q_o = U_o A_o$ , for single port discharges, or  $q_o = Q_o/L_D$  for multiport discharges with the initial discharge velocity  $U_o$  and the individual or total pipe discharge cross-section  $A_o$  and the diffuser length  $L_D$
- the initial mass flux  $Q_{co} = U_o C_o A_o$ , or  $q_{co} = Q_{co}/L_D$  with the initial concentration  $C_o$
- the initial momentum flux  $M_o = U_o^2 A_o$ , or  $m_o = M_o/L_D$
- and the initial buoyancy flux  $J_o = U_o g_o' A_o$ , or  $j_o = J_o/L_D$  with the reduced gravity  $g' = \Delta\rho/\rho g$  and  $\Delta\rho = \rho_o - \rho_a$ , with the initial effluent density  $\rho_o$  and the ambient density  $\rho_a$ .

A consistent length scale based categorization of the different jet regimes in the presence of crossflow and/or stratification is summarized in Fischer et al. (1979) and modified for plane jets from multiport diffusers by Jirka and Akar (1991) resulting in the following length scales, which provide order of magnitude estimates of transitional locations.

Jet/plume transition length scale:

the distance at which transition from jet to plume takes place (compare with Figure 67)

$$L_M = \frac{M_o^{3/4}}{J_o^{1/2}} \quad \text{or} \quad l_M = \frac{m_o}{j_o^{2/3}} \quad \text{for multiport diffuser}$$

Jet-to-crossflow length scale:

the distance beyond which the jet is strongly deflected by the crossflow

$$L_m = \frac{M_o^{1/2}}{u_a} \quad \text{or} \quad l_m = \frac{m_o}{u_a} \quad \text{for multiport diffuser}$$

Plume-to-crossflow length scale:

the distance beyond which the plume is strongly deflected by the crossflow

$$L_b = \frac{J_o}{u_a^3}$$

Jet-to-stratification length scale:

the distance beyond which the jet is strongly affected by the stratification

$$L_m^\epsilon = \frac{M_o^{1/4}}{\epsilon^{1/2}} \quad \text{or} \quad l_m^\epsilon = \frac{m_o^{1/3}}{\epsilon^{1/3}}, \quad \text{where } \epsilon = -(g/\rho a)(d\rho_a/dz) = \text{ambient buoyancy gradient.}$$

Plume-to-stratification length scale:

the distance beyond which the plume is strongly affected by the stratification

$$L_b^\epsilon = \frac{J_o^{1/4}}{\epsilon^{3/8}} \quad \text{or} \quad l_b^\epsilon = \frac{j_o^{1/3}}{\epsilon^{1/2}}$$

Tidal currents are characterized by flows which reverse direction. During the reversal period, or the so-called slack tide, the ambient water may be momentarily stagnant. When the slack tide is approached, meaning  $u_a = 0$ , the steady state length scale  $L_m$  becomes unbounded and thus an unsatisfactory measure for the jet behavior (Nash, 1995). A relationship between the

ambient acceleration  $|du_a/dt|$  and the discharge momentum flux  $M_o$  gives a measure for describing the unsteady trajectory leading to following scales:

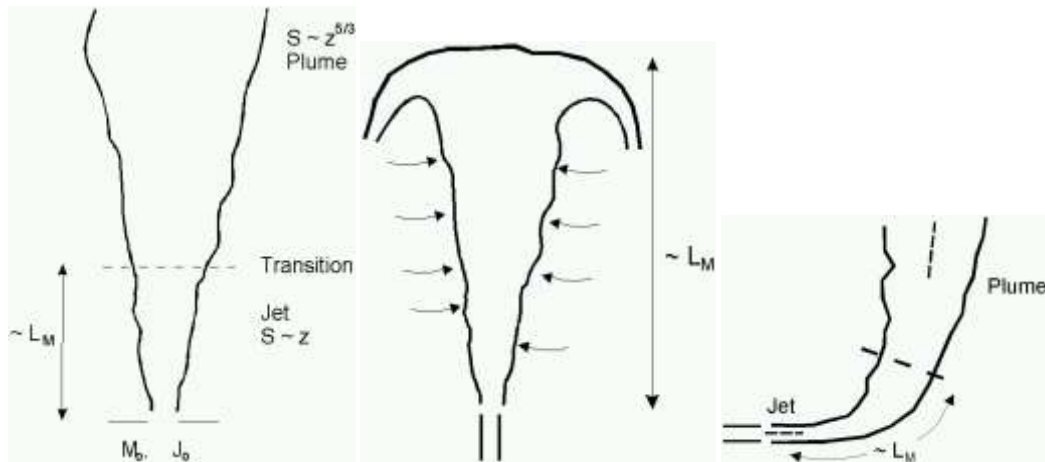


Figure 67: Jet to plume transition length scale  $L_M$  for a single jet allows distinguishing between a jet like or plume like single jet behavior (reproduced from Jirka et al, 1996)

Jet-to-unsteady crossflow length scale, a measure of the distance of the forward propagation into the ambient flow of a discharge during the reversal episode.

$$L_u = \left( \frac{M_o}{|du_a/dt|} \right)^{1/2} \quad \text{or} \quad l_u = \left( \frac{m_o}{|du_a/dt|} \right)^{1/2}$$

Jet-to-unsteady crossflow time scale, a measure of the duration over which an effluent may be considered as discharging into stagnant water while the velocity field is reversing.

$$T_u = \left( \frac{M_o}{|du_a/dt|^{1/4}} \right)^{1/6} \quad \text{or} \quad t_u = \left( \frac{m_o}{|du_a/dt|^3} \right)^{1/4}$$

Jirka et al. (1981) showed that buoyant jet deflection is primarily influenced by discharge momentum and not by buoyancy, thus scales for the interaction of the buoyancy flux  $J_o$  and  $du_a/dt$  are not considered to be dominant.

### Computed discharge characteristics

The calculators compute the initial individual mass fluxes  $M_o$ , and  $J_o$ , as well as the length scale  $L_M$  for single port discharges. Multiport diffuser analysis is considered only in the CORMIX modeling system. For example a resulting  $L_M = 20\text{m}$  indicates that the jet-like behavior will dominate in a region of the order of 20m before density induced motions will dominate further mixing (compare with Figure 67).

For further computation of discharge characteristics the RO discharge calculator requires the definition of an average offshore bed slope, a discharge angle for the submerged discharge pipe(s) and the number of openings. The MSF discharge calculator requires only the definition of the number of submerged openings applied. It is recommended that the user starts with one port and increases the number to achieve required characteristics. The calculator then automatically computes the port diameter of the discharge pipe, assuming an energetic discharge (with  $U_o = 4\text{-}6\text{ m/s}$ ). It then computes the densimetric Froude Number

$$F_o = U_o / \sqrt{|g'_o| D}$$

and the Reynolds number

$$\text{Re} = \frac{U_o D}{\nu},$$

both measures to characterize the mixing characteristics of the discharging jet, where high Froude and Reynolds numbers indicate good mixing conditions. The calculator includes recommendations for typical design values ( $F > 10$ ,  $Re \gg 4000$ ), thus allowing to easily find proper configurations and fast analysis. A screenshot of the second table of the calculators is given in Figure 68 and Figure 69.

## Discharge Characteristics RO

### - ambient characteristics

ambient density	$\rho_a =$	<input type="text" value="1023.02"/>	kg/m <sup>3</sup>
buoyant acceleration	$g'_o =$	<input type="text" value="-0.04804"/>	m/s <sup>2</sup>
offshore slope	$\theta_B =$	<input type="text" value="10"/>	°

### - effluent characteristics

flowrate	$Q_o =$	<input type="text" value="11.00"/>	m <sup>3</sup> /s
discharge density	$\rho_o =$	<input type="text" value="1028.03"/>	kg/m <sup>3</sup>
kin. viscosity	$\nu_o =$	<input type="text" value="1.06E-06"/>	m <sup>2</sup> /s

### - discharge characteristics

Choose a discharge angle (recommended: 45°):

discharge angle	$\theta_o =$	<input type="text" value="45"/>	°
discharge angle as recommended!			
port discharge velocity	$U_o =$	<input type="text" value="5.00"/>	m/s
number of openings	$n =$	<input type="text" value="3"/>	
port diameter	$D =$	<input type="text" value="0.97"/>	m
dens. Froude Number	$Fr_o =$	<input type="text" value="23.21"/>	
Reynolds Number	$Re_o =$	<input type="text" value="4.58E+06"/>	

Checking of characteristic properties:

Diameter  $D$ : in required range, ok!  
 Froude Number  $Fr_o$ : in recommended range, perfect!  
 Reynolds Number  $Re_o$ : in required range, ok!

Choose an appropriate port diameter (DN according to ISO standard):

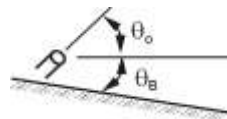
port diameter	$D =$	<input type="text" value="1.00"/>	m
---------------	-------	-----------------------------------	---

### Final discharge characteristics:

port diameter	$D =$	<input type="text" value="1.00"/>	m
number of openings	$n =$	<input type="text" value="3"/>	
discharge angle	$\theta_o =$	<input type="text" value="45"/>	°
flowrate (individual)	$Q_{o,ind.} =$	<input type="text" value="3.67"/>	m <sup>3</sup> /s
port discharge velocity	$U_o =$	<input type="text" value="4.67"/>	m/s
dens. Froude Number	$Fr_o =$	<input type="text" value="21.30"/>	
Reynolds Number	$Re_o =$	<input type="text" value="4.42E+06"/>	
buoyancy flux	$J_o =$	<input type="text" value="-0.176"/>	m <sup>4</sup> /s <sup>3</sup>
momentum flux	$M_o =$	<input type="text" value="17.12"/>	m <sup>4</sup> /s <sup>2</sup>
discharge length scale	$L_Q =$	<input type="text" value="0.89"/>	m
momentum length scale	$L_M =$	<input type="text" value="20.05"/>	m

annotations:

$[0^\circ \leq \theta_B \leq 30^\circ]$  only integer!



$[0^\circ \leq \theta_o \leq 90^\circ]$  only integer!

recommended:  $U_o = 4-6$  m/s  
 start with one opening!

$$Fr_o = U_o / (g'_o * D)^{1/2} = Q_o / (D^2 \rho / 4) / (g'_o * D)^{1/2}$$

$$Re_o = U_o * D / \nu_o$$

required:

$0.1 \leq D \leq 1.0$   
 $Fr_o \geq 10$ , recommended:  $Fr_o = 20-25$   
 $Re_o > 4000$

$$J_o = g'_o * Q_o \quad (<0: \text{negatively buoyant})$$

$$M_o = U_o * Q_o$$

$$L_Q = (D^2 * \pi / 4)^{1/2} = Q_o / M_o^{1/2}$$

$$L_M = M_o^{3/4} / J_o^{1/2}$$

Figure 68: Table 2 of the RO-discharge-calculator to compute characteristic discharge parameters

## Discharge Characteristics MSF

### - ambient characteristics

ambient density	$\rho_o =$	<input type="text" value="1023.02"/>	kg/m <sup>3</sup>
buoyant acceleration	$g'_o =$	<input type="text" value="0.02351"/>	m/s <sup>2</sup>

### - effluent characteristics

flowrate	$Q_o =$	<input type="text" value="45.51"/>	m <sup>3</sup> /s
discharge density	$\rho_o =$	<input type="text" value="1020.57"/>	kg/m <sup>3</sup>
kin. viscosity	$\nu_o =$	<input type="text" value="7.56E-07"/>	m <sup>2</sup> /s

### - discharge characteristics

port discharge velocity	$U_o =$	<input type="text" value="5.00"/>	m/s
number of openings	$n =$	<input type="text" value="10"/>	
port diameter	$D =$	<input type="text" value="1.08"/>	m

dens. Froude Number	$Fr_o =$	<input type="text" value="31.43"/>	
Reynolds Number	$Re_o =$	<input type="text" value="7.12E+06"/>	

annotations:

recommended:  $U_o = 4-6$  m/s

start with one opening!

$$Fr_o = U_o / (|g'_o| * D)^{1/2} = Q_o / (D^2 \pi / 4) / (|g'_o| * D)^{1/2}$$

$$Re_o = U_o * D / \nu_o$$

Checking of characteristic properties:

Diameter  $D$ : **out of range, please add openings!**

Froude Number  $Fr_o$ : **in required range, ok!**

Reynolds Number  $Re_o$ : **in required range, ok!**

required:

$$0.1 \leq D \leq 1.0$$

$$Fr_o \geq 10, \text{ recommended: } Fr_o = 20-25$$

$$Re_o > 4000$$

Choose an appropriate port diameter (DN according to ISO standard):

port diameter	$D =$	<input type="text" value="1.10"/>	m
---------------	-------	-----------------------------------	---

### Final discharge characteristics:

port diameter	$D =$	<input type="text" value="1.10"/>	m
number of openings	$n =$	<input type="text" value="10"/>	
flowrate (individual)	$Q_{o,ind.} =$	<input type="text" value="4.55"/>	m <sup>3</sup> /s
port discharge velocity	$U_o =$	<input type="text" value="4.79"/>	m/s
dens. Froude Number	$Fr_o =$	<input type="text" value="29.78"/>	
Reynolds Number	$Re_o =$	<input type="text" value="6.96E+06"/>	
buoyancy flux	$J_o =$	<input type="text" value="0.107"/>	m <sup>4</sup> /s <sup>3</sup>
momentum flux	$M_o =$	<input type="text" value="21.79"/>	m <sup>4</sup> /s <sup>2</sup>
discharge length scale	$L_Q =$	<input type="text" value="0.97"/>	m
momentum length scale	$L_M =$	<input type="text" value="30.83"/>	m

$$J_o = g'_o * Q_o \quad (> 0: \text{ positively buoyant})$$

$$M_o = U_o * Q_o$$

$$L_Q = (D^2 * \pi / 4)^{1/2} = Q_o / M_o^{1/2}$$

$$L_M = M_o^{3/4} / J_o^{1/2}$$

Figure 69: Table 2 of the MSF-discharge-calculator to compute characteristic discharge parameters

A complete flow classification system based on the above length scale definitions have been established by Jirka and Akar (1991) and Jirka and Doneker (1991), and briefly illustrated in Figure 70 to Figure 72. This classification system alone allows the definition of resulting flow classes without even starting a numerical computation. The near-field mixing model CORMIX (presented in detail in Section 5.3.1) is, in fact, a collection of several models for several sub-processes. These models are invoked through a length-scale based classification scheme that first predicts the discharge flow behavior (so-called flow classes) and then consecutively links (couples) the appropriate zone models (so-called modules) to provide near-field predictions. Also the near-field far-field coupling algorithm is initiated by a flow classification algorithm to provide appropriate coupling times and geometries.

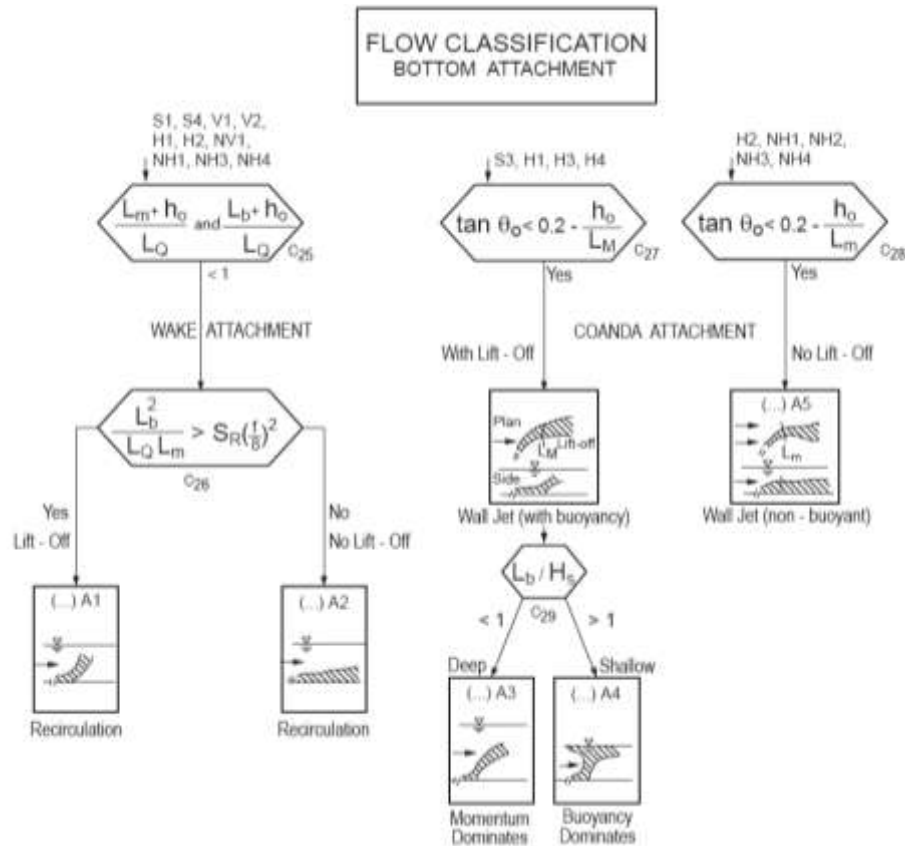


Figure 70: CORMIX flow classification tree for bottom attachment (reproduced from Jirka et al., 1996)

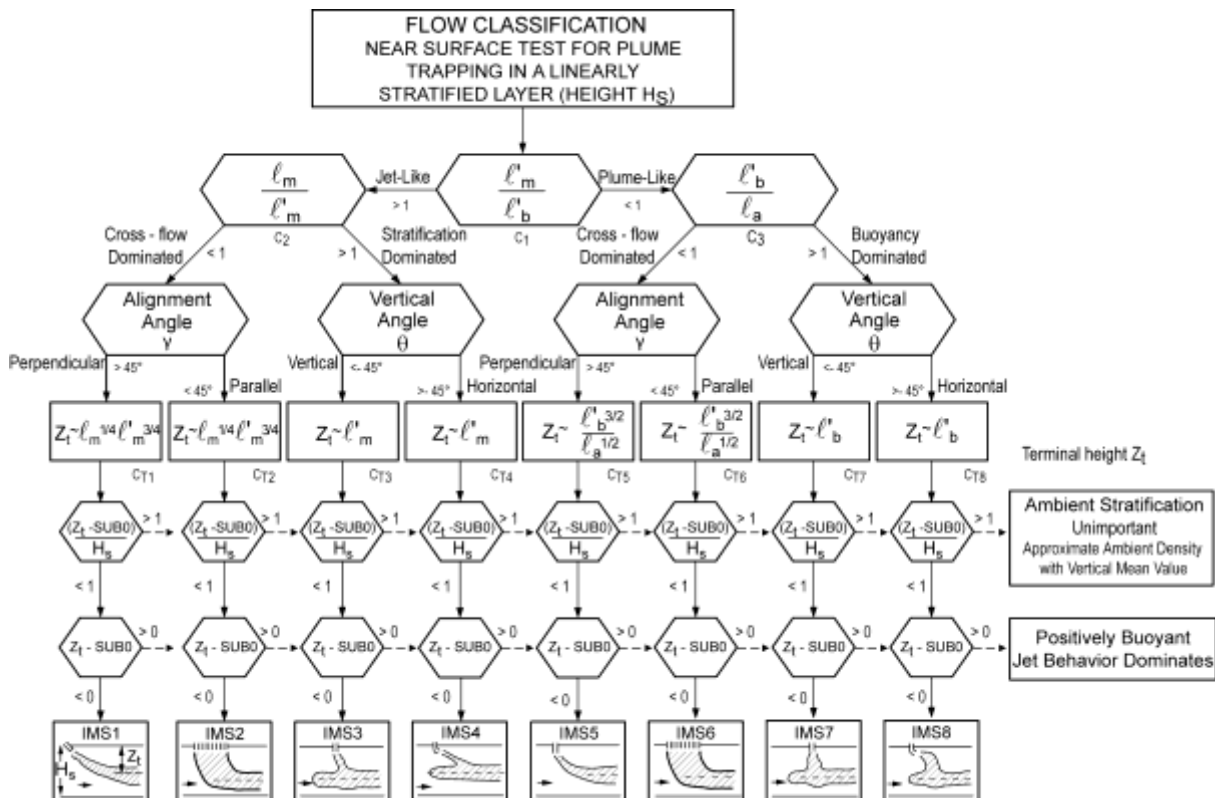


Figure 71: CORMIX flow classification tree for a near-surface negatively buoyant multiport discharge into stratified ambient water (reproduced from Jirka et al., 1996)

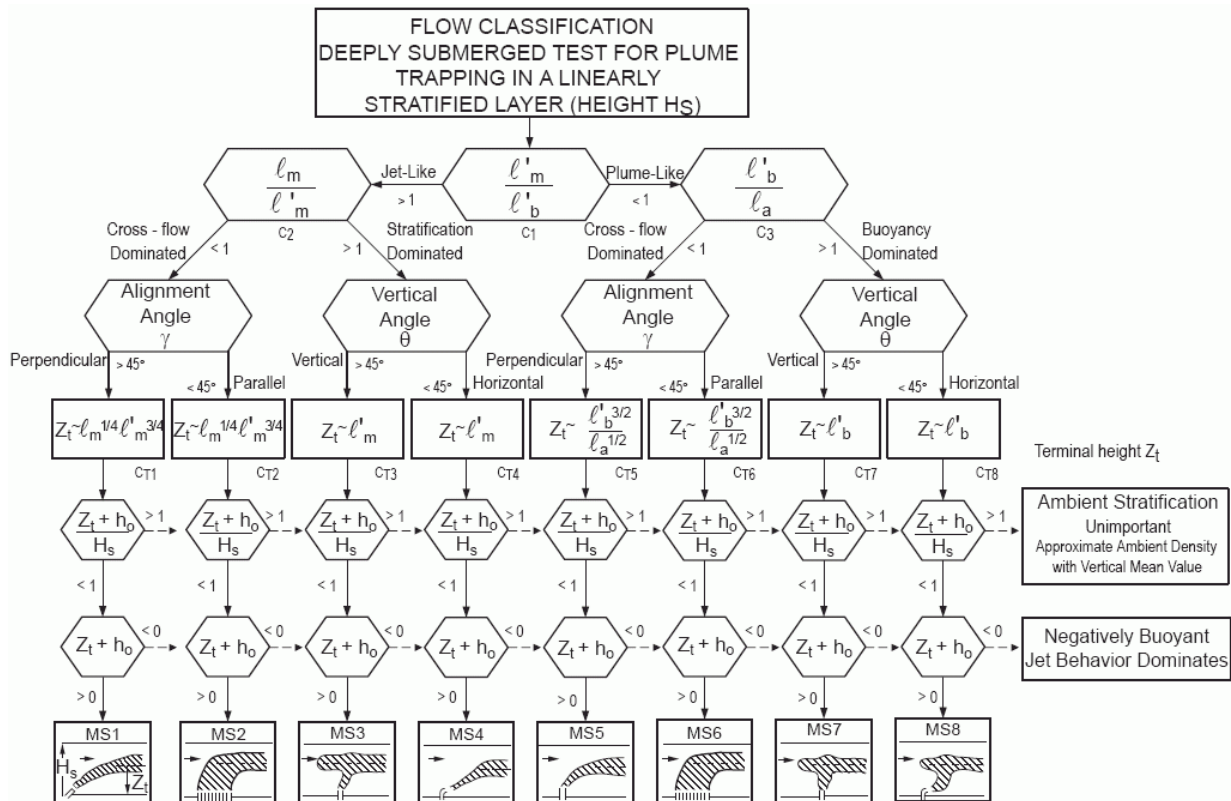


Figure 72: Flow classification tree within CORMIX, for a buoyant multiport discharge in stratified ambient waters (reproduced from Jirka et al., 1996)

### 5.2.4. Nomograms and screening equations (RO)

Another advantage of characteristic length scale analysis is the normalization of different configurations and conditions, which is the base for nomograms. Whereas velocities and concentrations can successfully be normalized by their initial values, results for measured trajectories which are historically normalized by the individual jet diameter showed large scatter (Figure 73, left for single buoyant jets). Numerous different solutions have hereby been obtained for different initial densimetric Froude numbers. The parameter combination based on the flux definitions instead resulted in the correct scaling (Figure 73, right) using the momentum length scale  $L_M = M_o^{3/4} / J_o^{1/2}$  (Jirka, 2004). Such diagrams can be used to predict and estimate the trajectory location.

The RO-discharge-calculator already includes first results for such nomograms. The procedure is hereby based on Jirka (2008). For simplicity, the most conservative case of stagnant ambient flow (no ambient velocity) is considered here. Figure 74 defines general parameters in a schematic side view of a negatively buoyant jet discharging into a receiving water body with a local ambient water depth  $H_{a0}$  and a sloping bottom with inclination angle  $\theta_B$ . The port geometry is given by its diameter  $D$ , its height above bottom  $h_o$ , and its inclination angle  $\theta_o$  above the horizontal, pointing offshore. The receiving water is unstratified with a constant density  $\rho_a$  and stagnant. The jet has a discharge velocity  $U_o$  and density  $\rho_o > \rho_a$ . The turbulent jet that results from this high velocity discharge first rises to a maximum level (upper plume boundary  $Z_{max}$ , centerline elevation  $z_{max}$ , both at a distance from the discharge  $x_{max}$  and a centerline dilution  $S_{max}$ ) and then falls downward under the influence of the negative buoyancy until it impinges on the sloping bottom (at  $x_i$  with dilution  $S_i$ ). Impingement is a complex three-dimensional process, with forward, lateral, and partially reverse spreading, until a density current is formed that propagates downslope.

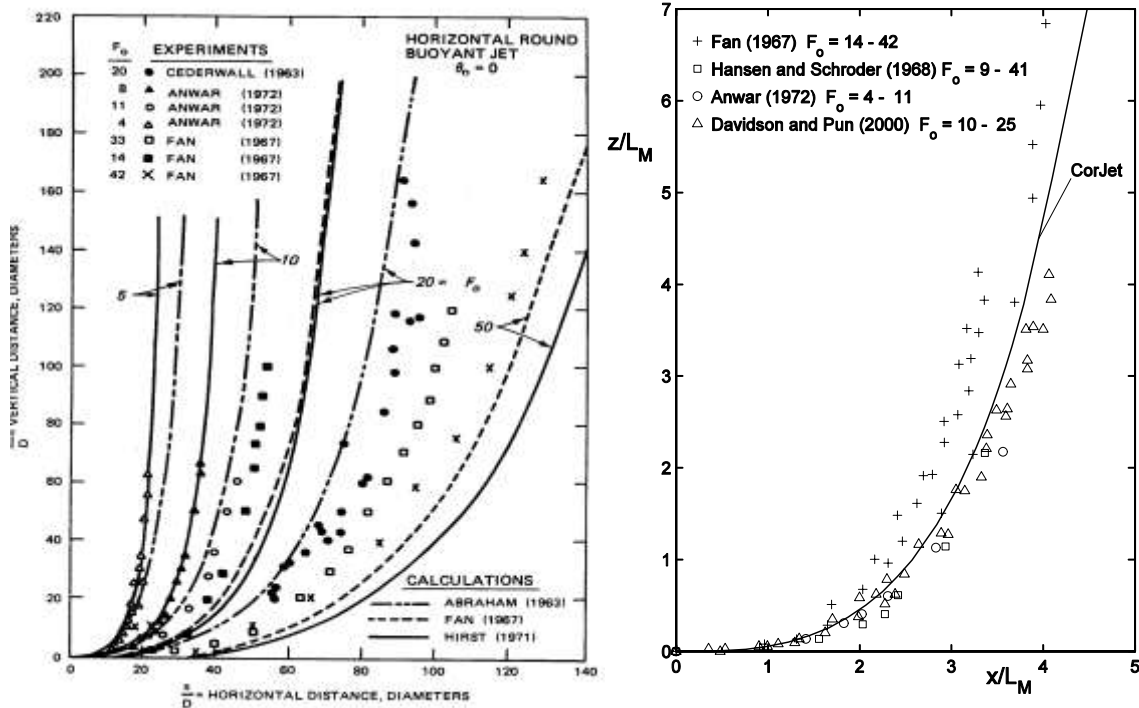


Figure 73: 3-dimensional horizontal buoyant jet trajectories for a single port discharge in stagnant ambient. Comparison between predictions and experimental data. *Left*: normalized with port diameter. *Right*: normalized with momentum length scale  $L_M$  (reproduced from Jirka, 2006)

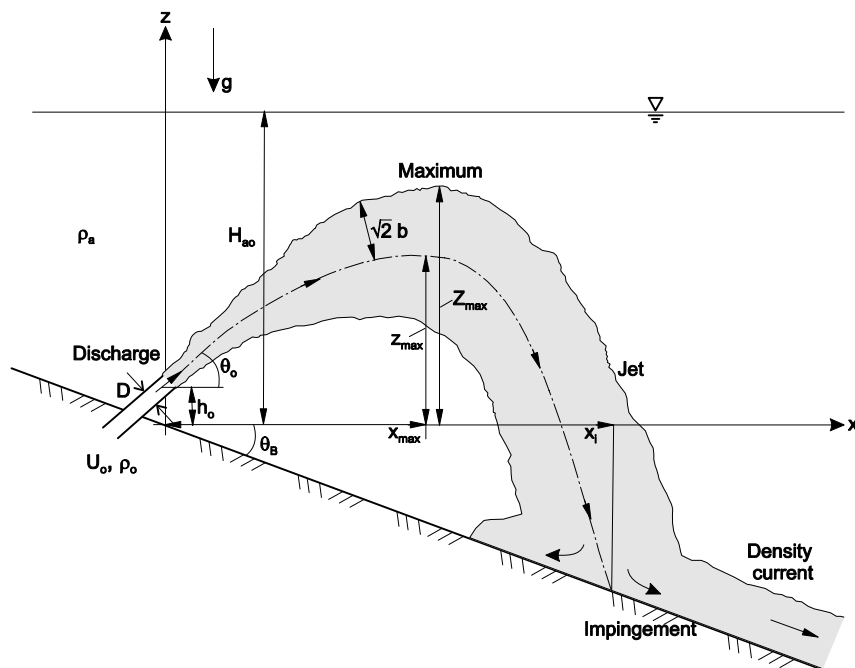


Figure 74: Schematic side view of negatively buoyant jet discharging into stagnant ambient with sloping bottom (Jirka, 2008)

The geometric and mixing characteristics of the turbulent buoyant jet can be determined by two length scales, the discharge length scale  $L_Q$  and the momentum (jet/plume transition) length scale  $L_M$ . A related non-dimensional parameter is the jet densimetric Froude number  $F_o$  that is simply proportional to the length scale ratio,  $L_M/L_Q = (\pi/4)^{-1/4} F_o$ . Thus, for high Froude number discharges,  $F_o \gg 1$ ,  $L_Q$  ceases to be a dynamically important parameter, as is well

known for many other jet configurations (Jirka, 2004). Detailed studies by Zhang and Baddour (1998) for a vertical negatively buoyant jet have shown that the dilution at the maximum level becomes independent of Froude number when  $F_o \geq 10$ . For smaller Froude numbers, the initial dilution becomes lower. A high Froude number discharge,  $F_o > 10$ , is assumed in the following so that  $L_M$  is the unique length scale for displaying jet properties.

Jirka (2008) applied the jet integral model CorJet (see Section 5.3.1) in a preliminary parametric study of submerged negatively buoyant jets discharging over a flat or sloping bottom and covering the entire range of angles from  $0^\circ$  to  $90^\circ$  above the horizontal and compared the results with experimental data from literature. Resulting inconsistencies are generally larger among different experimental studies than the disagreement with the numerical model (Jirka, 2008) because of deficiencies in the experimental set-up (e.g. flat bottom with possible recirculation effects after impingement; limited tank sizes) and in the measurement techniques (e.g. ambiguities in visual determinations; incomplete suction sampling in view of jet fluctuations). Considering other validation cases (trajectories and dilutions) for negatively buoyant jets with or without crossflow that have been reported in Jirka (2008), it is therefore concluded that CorJet can be used as a screening tool for negatively buoyant jet discharge configurations covering a wider range of possible site conditions (Bleninger, 2007). However, CorJet, being a "jet model" is a strict near-field model and does not include any boundary interaction processes. The presented trajectories in Figure 75 therefore pass beyond the "virtual" bed slopes, because the model does not consider, not even know about these boundaries. Only more sophisticated mixing models like CORMIX, include the impingement dynamics and further intermediate field flows. The CorJet model has therefore been listed as screening tool in this report.

Figure 75 shows the normalized centerline trajectories,  $z/L_M$  versus  $x/L_M$ , and their intersections with the possible bottom slopes. The discharge angle range  $\theta_o$  from  $30^\circ$  to  $45^\circ$  provides the largest offshore impingement location,  $x_i/L_M$ . The locations and elevations of the maximum rise level are given in Figure 77a, the dilutions at the maximum rise level,  $S_m/F_o$ , in Figure 77b. CorJet predicts an optimal value of  $45^\circ$ , but a wide flat plateau between  $30^\circ$  and  $60^\circ$ . What is important from the viewpoint of environmental impacts is the dilution at the impingement point (e.g. for exposure of benthic organisms). Figure 76 gives the predicted bulk dilution  $\bar{S}_i/F_o$  as a useful measure for that impact. For a flat bottom (and with zero discharge height), the maximum dilution is attained in the range  $\theta_o$  from  $60^\circ$  to  $75^\circ$ ; for moderate slopes ( $10^\circ$  to  $20^\circ$ ), the maximum is found at about  $45^\circ$  to  $60^\circ$ ; while for strong slopes ( $30^\circ$ ), this shifts to a discharge angle between  $30^\circ$  to  $45^\circ$ . Rather flat plateau values apply in all of these cases. Note that increasing discharge heights  $h_o$  have a qualitatively similar effect as increasing offshore slopes.

These results, together with several other siting factors, lead to the conclusion that the discharge angle range of  $30^\circ$  to  $45^\circ$  appears preferable for negatively buoyant jet discharges located in a near-shore environment. This is for the following reasons:

- (1) It produces the highest dilutions at the point of maximum rise (Figure 77b).
- (2) It provides high dilutions at the impingement point (Figure 76), especially if a sufficient offshore slope is given, or equivalently, if the discharge port is raised above the bottom.
- (3) It locates the jet impingement region further offshore (Figure 75) and, because of the flatter impingement angle, provides more offshore momentum for the ensuing bottom density current.
- (4) It provides considerably flatter trajectories (Figure 75), thus allowing the discharge to be located nearer the shore in shallower water.

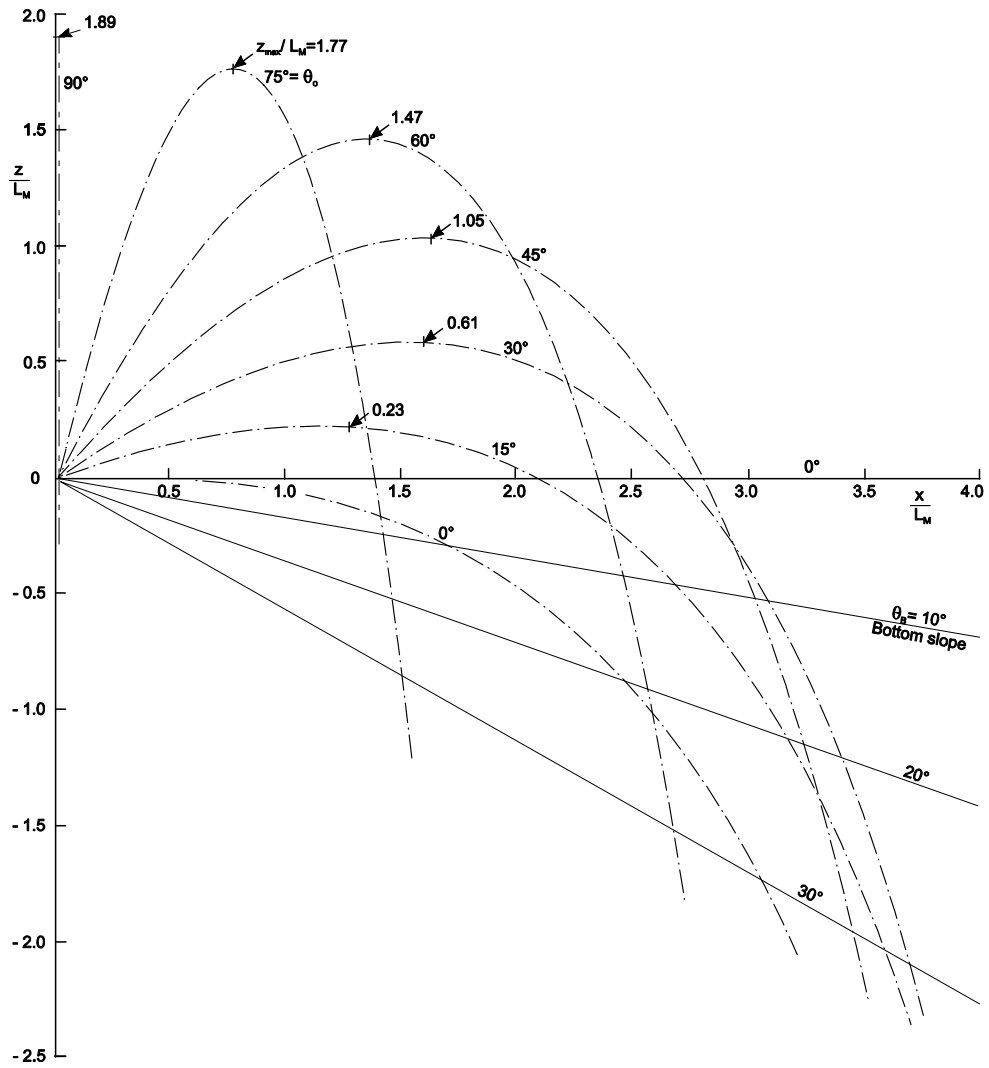


Figure 75: Jet trajectories. Negatively buoyant jet behavior for a complete range of discharge angles  $0^\circ \leq \theta_0 \leq 90^\circ$  and with variable offshore slopes  $\theta_B$  from  $0^\circ$  to  $30^\circ$ . A zero discharge height,  $h_0 = 0$ , is assumed.

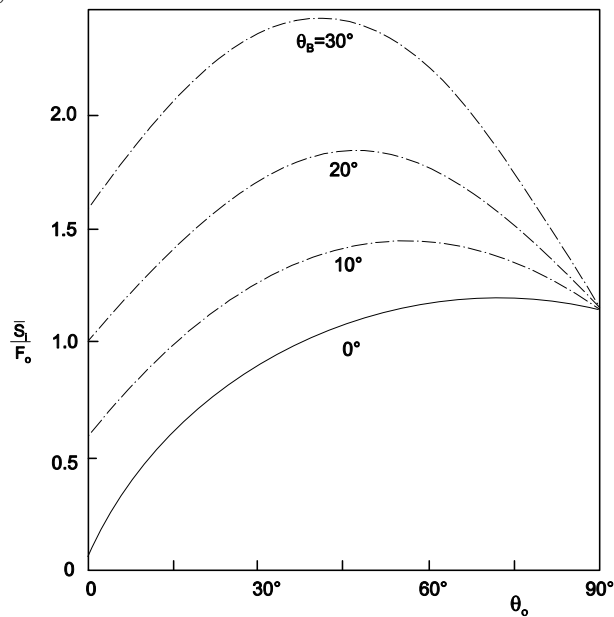


Figure 76: Bulk dilutions  $S_i$  at impingement point as a function of discharge angle  $\theta_0$ . Negatively buoyant jet behavior for complete range of discharge angles  $0^\circ \leq \theta_0 \leq 90^\circ$  and with variable offshore slopes  $\theta_B$  from  $0^\circ$  to  $30^\circ$ . A zero discharge height,  $h_0 = 0$ , is assumed.

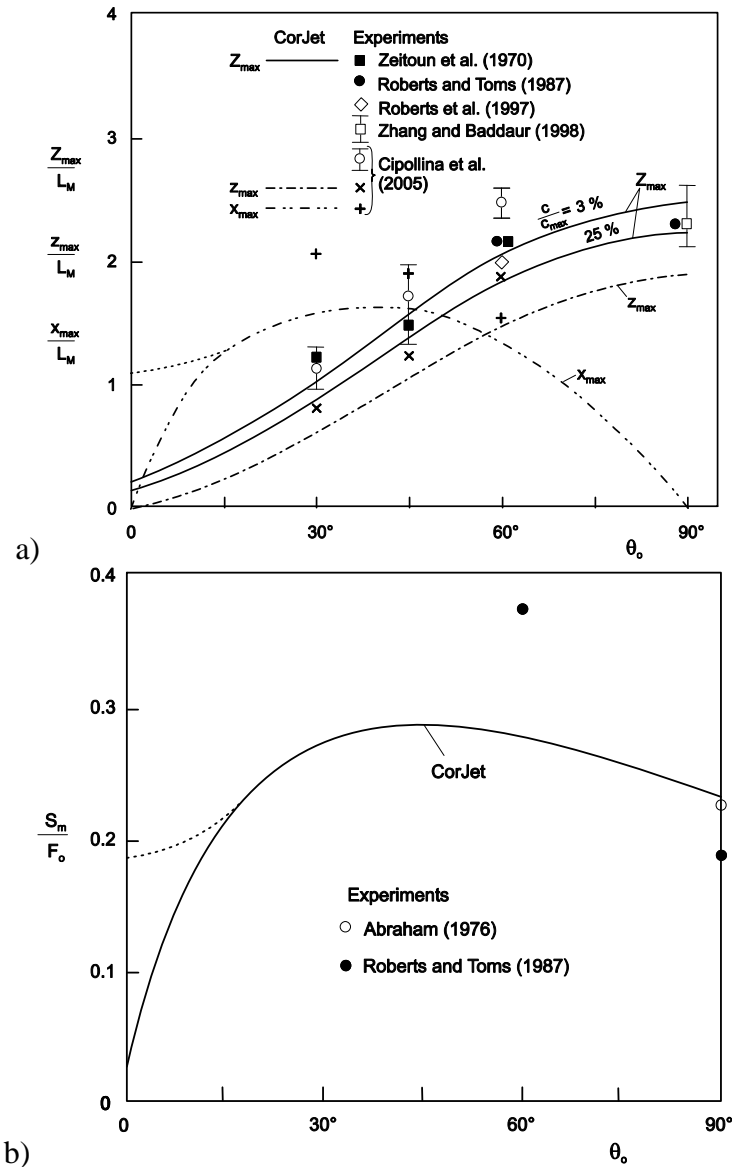


Figure 77: Jet properties at maximum level of rise. Comparison of CorJet model with experimental data. (a) Geometric properties, (b) Minimum centerline dilution, both as a function of discharge angle  $\theta_0$ .

The following initial design procedure is recommended for a discharge with given plant flow rate  $Q_0$  and discharge density  $\rho_0$  (hence, given  $g'_0$  and  $J_0$ ) located on an offshore slope with angle  $\theta_B$ :

- 1) Choose a sufficiently high Froude number design,  $F_0 \geq 10$  (Note that higher values imply larger pumping head losses). With  $U_0 = Q_0/(D^2\pi/4)$  the required port diameter is computed as  $D = \left[ (4/\pi)Q_0 / (F_0 |g'_0|^{1/2}) \right]^{2/5}$  as well as the values of  $M_0$  and  $L_M$ .
- 2) Choose a discharge angle  $\theta_0 = 45^\circ$  for weaker bottom slopes ( $\theta_B \leq 15^\circ$ ) or  $\theta_0 = 30^\circ$  for stronger slopes. (See step 5 for consideration of port height.)
- 3) Evaluate jet geometry using Figure 75.
- 4) Select the offshore location for the discharge in terms of a local water depth  $H_{a0}$  that guarantees that the upper jet boundary  $Z_{max} \leq 0.75 H_{a0}$ , in order to prevent dynamic surface interference.
- 5) Choose a port height  $h_0 = 0.5$  to  $1.0$ m. (In a second iteration, the effect of the port height can be considered as an added slope angle in steps 3 and 4).

6) Evaluate the concentration of key effluent parameters at the impingement point using Figure 75 and compare with applicable environmental criteria or regulations. If the dilution effect is insufficient, design iteration is necessary.

The above procedure has also been coded into the RO-discharge-calculator spreadsheet to allow for fast screening calculations. The calculator automatically computes the jet centerline position at the maximum level of rise ( $x_{max}$ ,  $z_{max}$ ) and at the impingement point ( $x_i$ ,  $z_i$ ) which is used to determine the outfall location (required water depth H and distance from shoreline x). Furthermore, the minimum centerline dilution  $S_m$  at  $z_{max}$ , the bulk dilution  $S_i$  at impingement point and the substance concentrations  $C_i$  at these two points are calculated (Figure 78).

Jet Properties		annotations:
<b>- discharge &amp; ambient characteristics</b>		
discharge angle	$\theta_o = 45^\circ$	
port height	$h_o = 0.00$ m	$h_o = 0$ m or $h_o = 0.5-1.0$ m
port at seabed		
offshore slope	$\theta_B = 10^\circ$	
imaginary offshore slope	$\theta_B^* = 10^\circ$	due to port height, not yet implemented
momentum length scale	$L_M = 22.88$ m	
dens. Froude Number	$Fr_o = 20.26$	
<b>- geometric jet properties</b> (for discharge angles that are not a multiple of 15°: linear interpolation!)		
	$Z_{max}/L_M$ (3%) = 1.576	(taken from Fig. 2(a)) $(c/c_{max} = 3\%)$
	$Z_{max}/L_M$ (25%) = 1.385	
	$z_{max}/L_M = 1.057$	(taken from Fig. 4(a)) $(c/c_{max} = 25\%)$
	$x_{max}/L_M = 1.606$	
	$z_i/L_M = -0.536$	!port height not considered!
	$x_i/L_M = 3.038$	
upper jet boundary	$Z_{max}$ (3%) = 36.07 m	
	$Z_{max}$ (25%) = 31.70 m	
maximum jet centerline position	$z_{max} = 24.18$ m	
	$x_{max} = 36.74$ m	
jet centerline position at the impingement point	$z_i = -12.26$ m	
	$x_i = 69.50$ m	
offshore location	$x \geq 1344.28$ m	
local water depth	$H_{oo} \geq 23.77$ m	$H_{oo} \geq 0.75Z_{max}$ (25%)
<b>Choose an appropriate outfall location:</b>		
offshore location	$x = 1350.0$ m	in required range,
local water depth	$H_{oo} = 23.88$ m	offshore location ok!
<b>- dilutions &amp; concentration</b> (for bottom slopes that are not a multiple of 10°: linear interpolation!)		
minimum centerline dilution at $z_{max}$	$S_m/Fr_o = 0.29$	Fig. 2(b)
	$S_m = 5.8$	
bulk dilution at impingement point	$S_i/Fr_o = 1.42$	Fig. 4(b)
	$S_i = 28.8$	
substance concentration at the centerline of		
max. level of rise ( $z_{max}$ )	$c_m = 1.88$ ppm	$S = c_o/c_c \rightarrow c_c = c_o/S$
impingement point ( $z_i$ )	$c_i = 0.38$ ppm	

Figure 78: Table 3 of the RO-discharge-calculator to analyze jet discharge characteristics and dilution values

Note that the calculation of the imaginary offshore slope and the consideration of the port height for the calculation of the new  $x_i$  position is not (yet) implemented. A higher port position causes slightly higher  $z_i$  values if bottom slope  $> 0^\circ$  and increasing  $x_i$  values for decreasing slopes  $\theta_B$  and decreasing discharge angles  $\theta_o$  as shown in Figure 79. For first estimates this displacement is negligible, it does not significantly influence the plume behavior and properties.

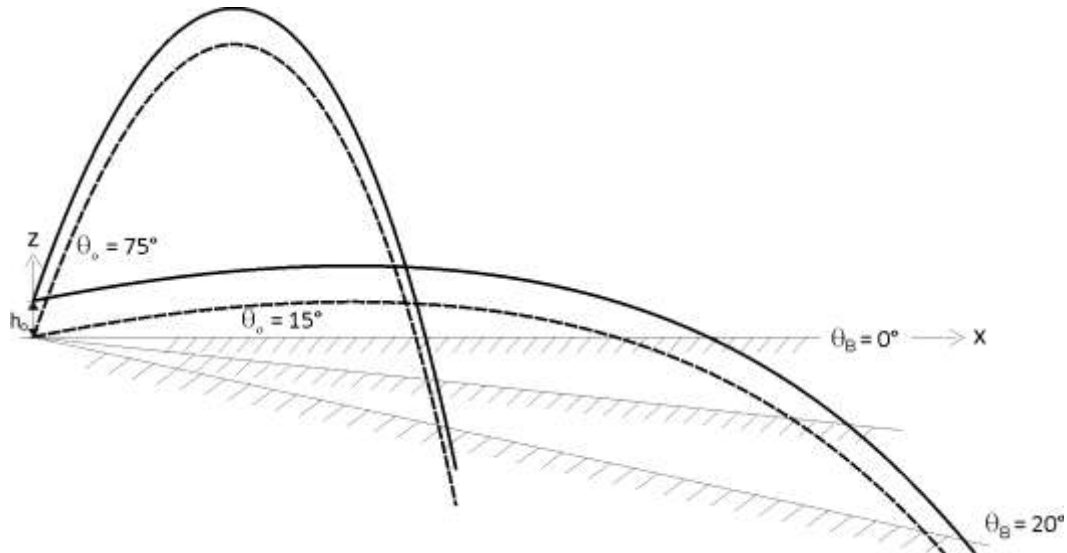


Figure 79: Displacement of impingement point due to increasing port height

The above procedure and illustrations apply to a discharge into stationary, non-flowing and constant uniform density ambient conditions that typically are the most limiting for dilution. However, CorJet, being a "jet model" is a strict near-field model and does not include any boundary interaction processes. The presented trajectories (e.g. Figure 75) therefore pass beyond the "virtual" bed, because the model does not consider, not even know about these boundaries. For further studies, beyond the screening process CorJet can be used embedded within the CORMIX expert system that allows for the prediction of not only the negatively or positively buoyant jet phase, but also of other mixing processes, such as the formation of the bottom density currents, boundary interactions, and transitions to far-field mixing, and include the impingement dynamics and further intermediate field flows. In addition there exist further near-field models within CORMIX which are special versions of CorJet for brine discharges from desalination plants (Del Bene et al., 1994), or for sediment currents (Doneker et al., 2004), that includes the dynamics of the downward propagating density current.

Given the paucity of reliable experimental data (notably dilution measurements) for the entire negatively buoyant jet including sloping bottom interaction, the above recommendations are considered preliminary. To further corroborate them, a vigorous program of experimental studies using modern field-resolving techniques, such as LIF and PIV, supported by detailed CFD modeling, is called for in several laboratories. This appears crucial in view of ongoing design and siting activities for numerous new desalination plants all around the globe.

### 5.2.5. Empirical dilution equations (MSF)

The previous analysis of jet trajectories for RO discharges has still not been done for thermal discharges. This is mainly because of the complexities of plant complexes of thermal desalination plants and blended cooling water effluents, but also due to much larger flow rates, which considerably influence the coastal hydrodynamics in the near-field region.

Therefore only a few principles and scaling methods are described for MSF discharges as follows. However, these are only valid for positively buoyant discharges. Major contributions are from Brooks (1960; 1980; 1984; 1988) and Brooks and Koh (1965). Comprehensive reviews are given in Fischer et al. (1979), Wood et al. (1993) and Jirka and Lee (1994). Detailed discussion on buoyant jets were presented by Jirka (1979; 1994), Roberts (1980; 1986), Roberts et al. (1989a,b,c), Lee and Jirka (1981) and Lee and Neville-Jones (1987). The resulting equations are all based on the near-field assumption and trying to calculate the minimum jet centerline dilution  $S_c = c_o/c_c$  at the end of the near-field, i.e. after surface contact or at the terminal layer for trapped plumes. As stated previously, they do not consider the dynamics of boundary interactions or further intermediate field flows.

Larger flow rates usually require multiport diffuser installations. The individual jet discharges through each port of such a diffuser merge after a certain distance and create a 2D line plume, which further rises to the surface and then impinges with the surface and spreads horizontally. One of the key equations is the equation for a line plume in a stagnant unstratified ocean (Rouse et al., 1952):

$$S_c = 0.38 \frac{j_o^{1/3} H}{q_o}$$

For a given flow  $Q_o$ , the unit discharge  $q_o$  and unit buoyancy flux  $j$  are inversely proportional to the diffuser length  $L_D$ , and the above equation suggests that a higher dilution is obtained by increasing the length of the diffuser. For a line plume, the minimum dilution can be multiplied by a factor of  $2^{1/2}$  to give the average dilution.

It has been demonstrated both theoretically and experimentally (Fischer et al., 1979) that maximum mixing can be achieved with closely spaced ports that allow some interference of adjacent jets. In relatively shallow coastal waters of typical depth 5 – 15 m, however, it is often the case that, given practical considerations (e.g. in order to maintain a minimum jet velocity and minimum diameter), multiport diffusers are designed to maximize interference of adjacent plumes. In such cases, the required spacing is about  $H/3$ .

In case of a linearly stratified ambient with a density gradient  $d\rho_a/dz$  the maximum height of rise  $z_{max}$  to the terminal level and corresponding dilution  $S_c$  are given by

$$z_{max} = 2.84 j_o^{1/3} \left( -\frac{g d\rho_a}{\rho_a dz} \right)^{-1/2} = 2.84 \ell_b'$$

$$S_c = 0.31 \frac{j_o^{1/3} z_{max}}{q_o}$$

In a linearly stratified ambient, the spreading layer is found to occupy about 40 – 50 % of the rise height. For computing bulk dilutions, one must allow for the thickness of the wastewater field. Simple models to account for blocking in the presence of an ambient current can be found in Fischer et al. (1979).

Roberts (1979; 1980) studied the mixing of a line source of buoyancy in an ambient current, and found that the shape of the flow field and the dilution are determined by the ambient Froude number  $F_o = u_a^3/j_o$ .  $F_o$  measures the ratio of the ambient current velocity to the buoyancy-induced velocity. For  $F < 0.1$ , the minimum surface dilution  $S_m$  is little affected by the current and is given by:

$$S_m = 0.27 \frac{j_o^{1/3} H}{q_o}$$

The smaller dilution coefficient reflects the effect of blocking of the surface layer. For higher crossflow,  $F > 0.1$ , however, the entrainment is dominated by the crossflow, and the alignment angle  $\gamma$  between the diffuser line and the current direction is important. Higher

dilution results for a perpendicular alignment,  $\gamma = 90^\circ$ , in which the maximum amount of flow is intercepted while the parallel alignment,  $\gamma = 0^\circ$ , gives the lowest dilution. For  $F \approx 100$ , the perpendicular alignment results in a dilution

$$S_m = 0.6 \frac{u_a H}{q_o}$$

that is proportional to volumetric mixing between ambient (velocity  $u_a$ ) and discharge flow, but with a reduced coefficient 0.6. For parallel alignment, the dilution is lower by a factor of about four. Experiments by Mendez-Diaz and Jirka (1996) have examined the different plume trajectories for various crossflow strengths.

The simple dilution equations given in the foregoing are useful for initial design screening of alternatives. They are limited to simplified ambient conditions. For final design evaluations and for more general and complex ambient oceanographic conditions, models like CORMIX that are more comprehensive must be employed.

## 5.3. Near-field models

The previously mentioned screening equations are useful for order of magnitude analysis, but are not applicable for the final design and analysis of discharge systems. Prediction models are needed, which include the effect of ambient currents, ambient density variations (i.e. stratified water bodies), and boundary interactions, as well as different discharge configurations, including multiport diffuser designs, and surface discharges.

There are only two near-field models capable to model brine discharges, including dense discharges with negatively buoyant plumes. These are CORMIX and VisJet.

### 5.3.1. CORMIX system

The CORMIX system (Doneker and Jirka, 1990; Jirka and Akar, 1991; Jirka et al., 1996) addresses the full range of discharge geometries and ambient conditions, and predicts flow configurations ranging from internally trapped plumes, buoyant plumes in uniform density layers with or without shallow water instabilities, and sinking (negatively-buoyant) plumes. Boundary interaction, upstream intrusion, buoyant spreading, and passive diffusion in the far field are also considered. A flow classification system based on hydrodynamic criteria using length scale analysis and empirical knowledge from laboratory and field experiments provides a rigorous and robust expert knowledge base that distinguishes among the many hydrodynamic flow patterns that may occur. For every flow class, CORMIX assembles and executes a sequence of appropriate hydrodynamic simulation modules. The modules are based on buoyant jet similarity theory, buoyant jet integral models, ambient diffusion theory, stratified flow theory, and simple dimensional analysis. The basic tenet of the simulation methodology is to arrange a sequence of relatively simple simulation modules which, when executed together, predict the trajectory and dilution characteristics of a complex flow.

Additional features are contemporary 3D plume and diffuser visualizations, a comprehensive documentation and help system, GIS linkage, a benchmarking analysis and validation database, a far-field locator post-processor, sensitivity analysis, and a batch running mode and time-series, all fully linked within the expert-system interface. CORMIX results include design recommendations, flow class descriptions and reporting oriented on discharge zone analysis.

At the heart of CORMIX is the integral jet model CorJet developed by Jirka (2004; 2006). The model formulation includes the significant three-dimensional effects that arise from the complex geometric details that distinguish actual diffuser installations in the water environment. Local three-dimensional effects deal with the merging process to form the plane buoyant jet. A simple flux-preserving merging transition that considers geometric contact between adjacent individual jets is found to be sufficiently accurate for simple port arrangements with 2D plume like orientation. For complex port arrangements with opposing or rosette-like orientation, the highly complicated merging process is not considered in detail and a buoyancy flux-preserving equivalent slot jet assumption is made for the zone of flow establishment. A variable drag force formulation is introduced to provide an accurate representation of the merging and jet bending process under crossflow conditions. Finally, proximity effects due to the presence of a horizontal bottom boundary near the level of the efflux are included in CorJet. These are related to a “leakage factor” that measures the combined effect of port height and spacing in allowing the ambient flow to pass through the diffuser line in order to provide sufficient entrainment flow for the mixing downstream from the diffuser. Multiport diffuser discharges with small leakage factors are thus predicted to have reduced plume rise trajectories in the crossflow. The model has been validated intensively and the range of applicability of the integral model has been carefully evaluated where a number of spatial limitations have been proposed beyond which the integral model necessarily becomes invalid. Whenever horizontal or lateral boundaries exist in the flow domain, e.g. the free surface or bottom of a water body, complex flow interactions may occur. Such resulting phenomena as jet impingement, attachment, internal hydraulic jumps, instabilities and recirculation are of course beyond the predictive powers of a simple integral model. In these instances, additional techniques for flow classification and prediction must be used, and are embedded in the CORMIX expert system structure.

### **5.3.1.1 BRINEDIS RELATED CORMIX DEVELOPMENTS**

At the time of this report generation, the current supported version of CORMIX that is available for download, distribution and licensing is CORMIX v6.0. It includes the software related outcomes of the BrineDis project as alpha-versions.

MixZon Inc is a BrineDis project partner and the sole source for sales, and support of CORMIX. Dr. Robert L Doneker is the primary contact for CORMIX technical support at MixZon Inc (info@mixzon.com). Information on CORMIX downloads, availability, licensing, sales and support is available at <http://www.mixzon.com>. Additional CORMIX resources, information on applications, references, and validation are available at <http://www.cormix.info>.

The following additions, updates, code modifications and improvements were made by MixZon to the CORMIX software within the BrineDis project (compare with Table 15):

1. Enhanced CORMIX capability to handle dense discharge/brine discharge cases. This includes modifying the CORMIX UI to allow for data entry relevant to a brine discharge study. The rule base was modified to handle dense brine discharge cases with the addition on several image flow classes ex: IV1, IV2 etc. to simulate near-surface discharge configurations. In addition the new FORTRAN hydrodynamics module DHydro has been integrated to simulate such cases.

2. The post-processing capabilities of the visualization tools like CorVue and CorSpy have been enhanced to handle brine discharge cases, including visualizations of DHydro and CORMIX1 and CORMIX2.
3. Designed, implemented and added CorTime for CORMIX time series data simulation. CorTime is a tool designed, implemented and added to CORMIX which allows for the automated calculation of time series data for ambient and discharge conditions. Using CorTime, one can perform time series analysis due to time varying ambient conditions or discharge characteristics (e.g. varying ambient velocity, current direction, effluent flow rate for each time step). CorTime is an automated tool for linkage of CORMIX to set boundary conditions in far-field coastal circulation models.

CorTime is a research tool developed to support the requirements of the BrineDis project. While the tool has been successfully implemented and used in the project, additional development and testing is necessary before widespread distribution. As part of CorTime development, several in-built data validation routines within CORMIX had to be overridden. Because the built-in data validations can be circumvented in CorTime, it is not appropriate for general release to the public at this time for routine commercial application. As a result, CorTime is currently available under the research version of CORMIX – CORMIX v6.0-GTR.

Work is in progress to develop a complete validated end user interface, data management and graphing tools to CorTime. It is planned to incorporate CorTime into the commercial release of CORMIX with further improvements, development and testing in the near future, and financially covered by MixZon.

4. Support for a universal coordinate system to CORMIX has been added. CORMIX output will now include plume centreline trajectory in Lat/Long coordinates. This is part of the coupling interface with far-field models improving the data handling between the different coordinate systems applied in different models.
5. The capability to post process CORMIX output files into the NetCDF file format has been added. NetCDF (network Common Data Form) is a set of software libraries and machine-independent data formats that support the creation, access, and sharing of array-oriented scientific data. The NetCDF file format will allow CORMIX prediction files to be more easily integrated into a wide variety of far-field models circulation models.
6. The density and discharge calculators have been made available as features within CORMIX and as direct link to the project web pages.

As part of the BrineDis Project, a 50% discount for commercial licensing is available until February 2012 on CORMIX commercial licensing from MENA countries. Commercial licensing of CORMIX is available to the following MENA countries: Algeria, Bahrain, Cyprus, Djibouti, Egypt, Iraq, Israel, Jordan, Kuwait, Lebanon, Morocco, Oman, Palestinian territories, Qatar, Saudi Arabia, Syria, Tunisia, Turkey, United Arab Emirates, and Yemen. To obtain the 50% discount, mention the BrineDis project when requesting pricing information.

Table 15: Feature comparison table amongst different CORMIX 6.0 versions is as follows:

Features	CORMIX Versions					
	v6.0E	v6.0G	v6.0GT	v6.0GTS	v6.0GTD	v6.0GTR*
	FREE RELEASE	GENERAL RELEASE	ADVANCED TOOLS	ADVANCED TOOLS SEDIMENT	ADVANCED TOOLS DESIGN	RESEARCH TOOLS RELEASE
CORSUPPORT CORMIX TECHNICAL SUPPORT <sup>†</sup>		✓	✓	✓	✓	✓
Print/Save		✓	✓	✓	✓	✓
CORDATA - LEGACY DATA IMPORT TOOL		✓	✓	✓	✓	✓
CORHELP ONLINE USER GUIDE	✓	✓	✓	✓	✓	✓
CORMIX USER MANUAL (PDF)	✓	✓	✓	✓	✓	✓
CORSPY 3D/2D OUTFALL GRAPHICS	✓		✓	✓	✓	✓
CORVUE 3D/2D MIXING ZONE GRAPHICS	✓		✓	✓	✓	✓
CORSENS SENSITIVITY ANALYSIS TOOL	✓		✓	✓	✓	✓
CORMIX1 SINGLE PORT DISCHARGES	✓	✓	✓	✓	✓	✓
CORMIX2 MULTIPORT DIFFUSERS	✓	✓	✓	✓	✓	✓
CORMIX3 SURFACE DISCHARGES	✓	✓	✓	✓	✓	✓
CORJET 3D JET INTEGRAL MODEL	✓	✓	✓	✓	✓	✓
FFL FAR-FIELD PLUME ANALYSIS	✓	✓	✓	✓	✓	✓
CORGIS BASINS/ARCVIEW TOOL	✓	✓	✓	✓	✓	✓
BRINE DISCHARGE MODELING	✓	✓	✓	✓	✓	✓
SEDIMENT DISCHARGE MODELING	✓			✓	✓	✓
CORHYD - INTERNAL DIFFUSER HYDRAULICS	✓				✓	✓
CORUCS - COORDINATE SYSTEM CONVERTER	✓				✓	✓
CORDOCS TECHNICAL DOCUMENTATION		✓	✓	✓	✓	✓
CORVAL - CASE VALIDATION SERVICE <sup>†</sup>		✓	✓	✓	✓	✓
CorBatch - Batch Processing Utility						✓
CORTIME - TIME SERIES/FAR-FIELD MODEL LINK						✓

\* GTR version for research and development use. [CONTACT US](#) for availability/licensing.

<sup>†</sup>Subscription Fee required in addition to current software licensing. [CONTACT US](#) for more details.

### **5.3.2. VisJet**

VisJet (Lee and Cheung, 1990) is a general predictive, flow visualization tool to portray the evolution and interaction of multiple buoyant jets discharged at different angles to the ambient tidal current. VisJet can be used to study the impact of either a single or a group of inclined buoyant jets in three-dimensional space.

Special features are computer graphics techniques to trace the path and mixing characteristics of a group of arbitrarily inclined jets in three-dimensional space, in a uniform or density-stratified crossflow.

The Lagrangian buoyant jet model JetLag (Lee and Cheung, 1990) is part of the model VisJet and predicts the mixing of buoyant jets with three-dimensional trajectories. The model, strictly speaking, does not solve the usual Eulerian governing differential equations of fluid motion and mass transport. Instead, the model simulates the key physical processes expressed by the governing equations. The unknown jet trajectory is viewed as a series of non-interfering “plume-elements” which increase in mass as a result of shear-induced entrainment (due to the jet discharge) and vortex-entrainment (due to the crossflow), while rising by buoyant acceleration. The model tracks the evolution of the average properties of a plume element at each step by conservation of horizontal and vertical momentum, conservation of mass accounting for entrainment, and conservation of tracer mass/heat. The vortex entrainment is determined by a heuristic Projected-Area Entrainment (PAE) hypothesis for buoyant jets with 2D trajectories, while pressure drag is ignored. Predictions of the model have compared well with basic laboratory experimental data; the model also correctly predicts the asymptotic behavior of pure jets and plumes, and advected line puffs and thermals.

The model has been validated for discharges with relatively small flowrates, such as wastewater discharges and brine discharges, and does not include a physical, dynamic interaction with boundaries. It is therefore limited to strictly near-field applications and jet regimes.

### **5.3.3. Model comparison and model choice**

Near-field jet models assume unlimited and steady ambient conditions. This assumption holds until the plume reaches boundaries, such as the water surface or the sea bed, or the shallowness of a water body prevents the development of a stable jet regime. Comparing usability, range of application, physical process simulation, and modeling, philosophical differences are identified:

- CorJet and JetLag give results on trajectories, centerline dilution, flow, and entrainment characteristics
- CorJet applies for arbitrary, i.e. non-uniform, multi-directional velocity profiles, which are not covered in JetLag
- CorJet deals with significant three-dimensional effects regarding the merging process to form the plane buoyant jet and / or the bending process under crossflow. It allows defining merging positions and characteristics. VisJet instead neglects this effects and uses superposition principles
- CorJet includes proximity effects due to the presence of a horizontal bottom boundary near the level of the efflux; JetLag does not consider those

- The application of CorJet within CORMIX includes clear statements of spatial limitations beyond which the integral model necessarily becomes invalid. JetLag lacks such clear statements

Both jet models, CorJet, and JetLag are embedded in major mixing zone models, but CORMIX, however, is the only package which includes boundary interactions and is capable to also predict concentration distributions for cases which cannot be considered as unlimited and steady. Desalination brine discharges are commonly installed in shallow waters and either have strong interactions with the lower boundary (e.g. negatively buoyant RO discharges) or strongly influence the near-field motions (e.g. large flow discharges resulting from MSF plants).

Thus, major differences in the model systems are regarding model extensions beyond the buoyant jet model. There are a number of other mixing processes that occur in the near-field of the discharge depending on a given situation, such as boundary / surface interaction, internal hydraulic jumps and unstable mixing, stratified exchange flow, and buoyant spreading processes. The CORMIX model is, in fact, a collection of zone models for all these sub-processes. These models are invoked through a length-scale based classification scheme that first predict the discharge flow behavior (so-called flow classes) and then consecutively links (couples) the appropriate zone models (so-called modules) to provide a prediction. VisJet does not address the effects of vertical or horizontal boundaries on mixing or on discharge stability. It simply assumes the ambient water body is infinite.

Both jet models have been validated with a wide range of fundamental laboratory data sources. The amount of comprehensive and reliable field data for actually operating diffusers that can be used for model validation is still limited at present. The field survey of Carvalho et al. (2002) for the Ipanema outfall in Rio de Janeiro has provided a highly satisfactory validation for CORMIX regarding the near-field predictions and additionally as regarding its predictive ability and accuracy, not only for the immediate near-field, but also for the transition to the far-field in the form of buoyant spreading of the internally or surface-trapped plume (see Jirka and Doneker, 2003). Other models are clearly limited in that regard (compare with Figure 80).

VisJet and CORMIX are both commercial models. No open source models exist which cover similar flow regimes. There are simple jet models available as freeware, but they only resolve strictly near-field processes for single port discharges, and do not provide the required validation through peer-reviewed literature. The CORMIX system includes a high-level quality assurance, professional support and detailed documentation (Jirka et al., 1996), help system and bug fixing. VisJet is at the beginning in that regard.

In summary, situations where VisJet can be applied would typically be deep ocean outfalls (e.g. sewage outfalls) and if only near-field mixing is of interest and there is no possibility of dynamic bottom attachments and surface interaction is unimportant. However, if discharge zone information after the near-field is desired, then the possibility of a density current in the far-field must be considered.

The CORMIX model system has been chosen for this study, because of its additional capabilities and the expert system approach allowing especially for design optimization and regulatory discharge zone analysis. An overview of the decision matrix is shown in Figure 81.

This choice is confirmed by other studies comparing models. For example, Ragas (2000) provides a comparison of different mixing zone models. The mixing zone model CORMIX (Doneker and Jirka, 1991; Jirka et al., 1996), in particular, is characterized by its wide applicability to many water body types (rivers, lakes, estuaries, coastal waters) and has been successfully used for water quality management under different regulatory frameworks.

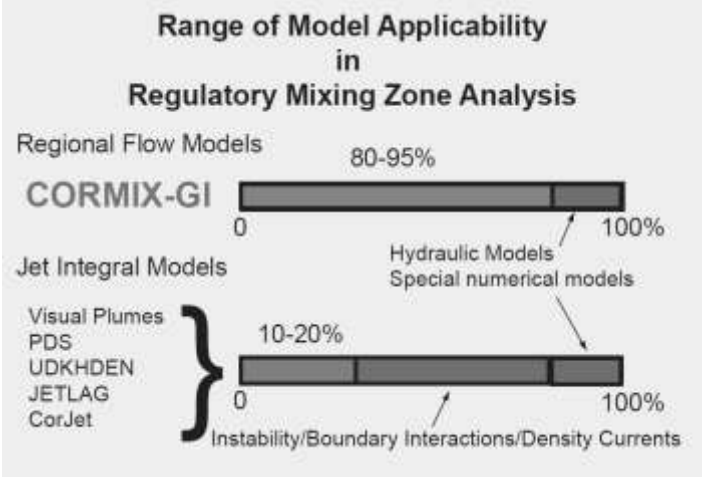


Figure 80: Comparison of jet and mixing models

**Hydrodynamic Models for Mixing Zone Analysis**

■ Denotes CORMIX problem domain

Near Field Region Models	Far-field Region Models
<p>A) General Case</p> <ul style="list-style-type: none"> <li>- high/low momentum flux</li> <li>- high/low buoyancy flux</li> <li>- arbitrary discharge alignment geometry</li> <li>- deep/shallow conditions (stable &amp; unstable)</li> <li>- arbitrary ambient stratification</li> <li>- boundary interaction/dynamic attachments</li> </ul> <p>Applicable Models:</p> <p><b>CORMIX - Mixing Zone Model Expert System</b></p>	<p>A) General Case</p> <ul style="list-style-type: none"> <li>- complex coastal topography &amp; bathymetry</li> <li>- complex current structure (tidal, wind driven)</li> <li>- arbitrary ambient stratification</li> </ul> <p>Applicable 3D Circulation and Transport Models:</p> <p><b>Delft3D (hydrostatic)</b>  <b>Mike3 (non-hydrostatic)</b>  <b>POM/ECOM (hydrostatic)</b>  <b>Telemac3 (hydrostatic)</b></p>
<p>B) Restricted Case</p> <ul style="list-style-type: none"> <li>- combination of weak momentum &amp; high buoyancy flux</li> <li>- deep conditions (stable)</li> <li>- typical for coastal sewage discharge</li> </ul> <p>Applicable Models:</p> <p><b>CorJet - (included in CORMIX)</b>  <b>JetLag / PLUMES</b></p>	<p>B) Restricted Case</p> <ul style="list-style-type: none"> <li>- open coastal areas</li> <li>- simple current patterns</li> <li>- rivers</li> </ul> <p>Applicable Models:</p> <p><b>CORMIX</b></p> <ul style="list-style-type: none"> <li>- Tidal Data Option</li> <li>- Far Field Locator (FFL post-processor)</li> </ul>

Figure 81: Schematic illustration of the range of model applicability in regulatory discharge zone analysis (source: [www.cormix.info](http://www.cormix.info))

## 5.4. Far-field models

The quality of a discharge assessment strongly depends on a good knowledge of the receiving waters. In contrast to the near-field assessment, a far-field analysis needs much more detail on ambient currents and turbulence than the time, depth, and spatial averaged values used for the near-field. This holds especially for the description of stratified coastal waters.

Deep-sea oceanography and coastal oceanography hereby offer process descriptions and modeling tools that help to understand the main features of the current scheme in an ocean region (Davies et al., 1997a,b). However, most of these models are set up for large domains (order of hundreds of kilometers), where near coastal features are not as important, thus not resolved in detail. However, discharge modeling in particular needs to know about near coastal flow features for domains of the order of tens of kilometers, with high resolution in the outfall region. Furthermore, most oceanographic models are depth averaged (Davies et al., 1997a), which is sufficient for large-scale flows, but not for discharge assessments.

Wind-shear effects on stratified waters, non-uniform velocity profiles, and baroclinic processes require a three dimensional flow representation (Signell et al., 2000). This is even more relevant considering the limitations of field measurements, especially regarding the surface layer. Fully three dimensional models without the hydrostatic assumption are still under development (DVWK, 1999), with one exception being the MIKE3 modeling system from the Danish Hydraulics Institute. On the other hand, there are fully 3D models available, which are generally used in mechanical engineering, but not for coastal currents (Fluent, CFX, etc.). Their deficiencies are related to the free surface, the complexity for grid generation and the appropriate calculation of the dispersion coefficient, which is often directly related to the turbulence model used (Law et al., 2002). Generally, they can only be used for limited regions and several restricting limitations (rectangular geometries, rigid lid surface). However, unless strong vertical motions occur (due to strong bed slopes or breaking of internal or surface waves), a 3D hydrostatic model captures all important processes.

There are more than 20 circulation models in use today. Most are used for oceanographic studies (ocean models), whereas only a few are applied for more resolved coastal circulation studies (coastal models) (Tetra Tech, 2000). With a few exceptions, these are all finite difference models. Most cited models are MIKE3 (from the Danish Hydraulics Institute), POM (Princeton Ocean Model - Princeton University), ECOM-si (modified version of POM used at Hydroqual), Delft3D (from Delft Hydraulics), Telemac 3D (from EDF, Electricité de France, and Wallingford), SisBAHIA (University of Rio de Janeiro, COPPE, 2000).

Coastal circulation problems generally demand time-varying velocity information all over the problem domain. The Eulerian flow description is used. The heat (temperature) and salinity conservation equations have to be solved in parallel with the equations of motion since these parameters are linked to the water density by an equation of state.

A drawback of Eulerian models is the requirement of a substantial amount of input data, in terms of detailed topographical information, and temporal and spatial varying ambient data at the open boundary conditions (such as current speeds, temperature and salinity distributions). This data is generally not available and has to be provided from either a larger scale model, where the problem domain is nested in, or by field measurements. A combination would be optimal.

Nonetheless, although these models promise to solve the majority of problems related to waste discharges, a few problems are still not solved in that regard. There is, for example, the problem of Huntington Beach (USGS, 2004), where complex modeling efforts in combination with extensive field-studies have been undertaken to verify hypotheses regarding the bacterial pollution at Huntington Beach. Whether it is internal waves together with wind induced flow transport that may cause bacteria pollution or if these are caused by other sources, it was not solved in that case. The results at least indicate that outfall contributions are not the most significant. The main open question in pollutant transport modeling is whether trapped waste plumes may reach the beaches or sensitive ecological areas at certain conditions due to upwelling, internal waves, or other processes.

### **5.4.1. Model choice**

The Delft3D model suite has been chosen for this project, although the other major models for coastal applications (MIKE3, POM/ECOM, Telemac 3D) are also acceptable. Moreover, the linked modelling approach can easily be modified for other far-field models too and is not strictly limited to Delft3D. Major reasons for the choice have been its widespread applications in the field of pollutant discharge assessments and its capabilities focussed on coastal applications and applications for desalination plant intake and outfall studies (e.g. Friocourt et al., 2009).

### **5.4.2. Delft3D**

Delft Hydraulics (2001) has developed a fully integrated computer software package for a multidisciplinary approach and 3D computations for coastal, river and estuarine areas. It carries out simulations of flows, sediment transports, waves, water quality, morphological developments (bottom changes) and ecology. The Delft3D package is composed of several modules, grouped around a mutual interface, while being capable to interact with one another. Delft3D-FLOW is one of these modules.

Delft3D-FLOW is a multi-dimensional (2D or 3D) hydrodynamic (and transport) simulation program which calculates non-steady flow and transport phenomena that result from tidal and meteorological forcing on a curvilinear, boundary fitted grid. In 3D simulations, the vertical grid is defined following the sigma co-ordinate approach.

#### **Physical processes**

The numerical hydrodynamic modeling system Delft3D-FLOW solves the unsteady shallow water equations in two (depth-averaged) or three dimensions. The system of equations consists of the horizontal equations of motion, the continuity equation and the transport equations for conservative constituents. The equations are formulated in orthogonal curvilinear co-ordinates or in spherical co-ordinates on the globe. In Delft3D-FLOW, models with a rectangular grid (Cartesian frame of reference) are considered as a simplified form of a curvilinear grid. In curvilinear co-ordinates, the free surface level and bathymetry are related to a flat horizontal plane of reference, whereas in spherical co-ordinates the reference plane follows the Earth's curvature. It includes: tidal forcing, Coriolis force, density driven flows (pressure gradients terms in the momentum equations), advection-diffusion solver included to compute density gradients with an optional facility to treat very sharp gradients in the vertical, space and time varying wind and atmospheric pressure, advanced turbulence models to account for the vertical turbulent viscosity and diffusivity based on the eddy viscosity concept, where four options are provided: k-, k-L, algebraic and constant model, time varying sources and sinks (e.g. river discharges), simulation of the thermal discharge, effluent

discharge and the intake of cooling water at any location and any depth, drogue tracks, robust simulation of drying and flooding of inter-tidal flats.

**Assumptions** (Delft Hydraulics, 2001)

In Delft3D-FLOW, the 2D (depth-averaged) or 3D non-linear shallow water equations are solved. These equations are derived from the three dimensional Navier Stokes equations for incompressible free surface flow. The following assumptions and approximations are applied:

- Hydrostatic assumption, thus, vertical accelerations are assumed to be small compared to the gravitational acceleration and are therefore not taken into account.
- The effect of variable density is only taken into account in the horizontal pressure gradient term (Boussinesq approximation).
- In the stand alone version of Delft3D-FLOW the bed is assumed to be fixed. For a dynamic coupling between morphological changes and flow, the Delft3D-MOR module should be used.
- At the bottom, a slip boundary condition is assumed.
- The formulation for the enhanced bed shear stress due to the combination of waves and currents is based on a 2D flow field, generated from the velocity near the bed using a logarithmic approximation.
- The equations of Delft3D-FLOW are capable of resolving the turbulent scales (large eddy simulation), but the hydrodynamic grids are usually too coarse to resolve the fluctuations. Therefore, the basic equations are Reynolds-averaged introducing so-called Reynolds stresses. These stresses are related to the Reynolds-averaged flow quantities by a turbulence closure model.
- In Delft3D-FLOW, the 3D turbulent eddies are bounded by the water depth. Their contribution to the vertical exchange of horizontal momentum and mass is modeled through a vertical eddy viscosity and eddy diffusivity coefficient (eddy viscosity concept). The coefficients are assumed to be proportional to a velocity scale and a length scale. The coefficients may be specified (constant) or computed by means of an algebraic, k-L or k-turbulence model.
- In agreement with the aspect ratio for shallow water flow, the production of turbulence is based on the vertical (and not the horizontal) gradients of the horizontal flow.
- The boundary conditions for the turbulent kinetic energy and energy dissipation at the free surface and bottom assume a logarithmic law of the wall.
- The eddy viscosity is anisotropic. The horizontal eddy viscosity and diffusivity coefficients should combine both the effect of the 3D turbulent eddies and the horizontal motions that cannot be resolved by the horizontal grid. The horizontal eddy viscosity is generally much larger than the vertical eddy viscosity.
- For large scale flow simulations, the tangential shear stress at lateral closed boundaries can be neglected (free slip). In the case of small scale flow, partial slip is applied along closed boundaries.
- For large scale flow simulations, the horizontal viscosity terms are reduced to a biharmonic operator along co-ordinate lines. In the case of small scale flow the complete Reynold's stress tensor is computed. The shear stress at the side walls is calculated using a logarithmic law of the wall.
- Delft3D-FLOW solves the so-called long wave equation. The pressure is hydrostatic and the model is not capable of resolving the scales of short waves. Therefore, the basic equations are averaged in analogy with turbulence introducing so-called radiation stresses. These stresses are related to the wave quantities of Delft3D-WAVE by a closure model.

- Without specification of a temperature model for the heat exchange through the free surface is zero. The heat loss through the bottom is always zero.
- If the total heat flux through the water surface is computed using a temperature excess model, the exchange coefficient is a function of temperature and wind speed and is determined according to Sweers. The natural background temperature is assumed to be constant in space and may vary in time. In the other heat flux formulations, the fluxes due to solar radiation, atmospheric and back radiation, convection and heat loss due to evaporation are modeled separately.

### **Coupling to other modules**

The hydrodynamic conditions (velocities, water elevations, density, salinity, vertical eddy viscosity and eddy vertical diffusivity) calculated in the Delft3D-FLOW module are used as input to the other modules of Delft3D, which are:

- Delft3D-WAQ: far-field water quality.
- Delft3D-SED: cohesive and non-cohesive sediment transport.
- Delft3D-ECO: ecological modeling .
- Delft3D-PART: mid-field water quality and particle tracking.
- Delft3D-WAVE: short wave propagation.
- Delft3D-MOR: morphodynamic simulations.

In addition to the Delft3D-FLOW module, the Delft3D-WAQ module allows concentrating the calculation of mixing and transport processes on temporal and spatial scales, which can be considerably different from the hydrodynamic scales. The advection diffusion equation is solved for the substances of interest only on that spatially limited grid within the time-scales of interest using the hydrodynamic conditions from the results of Delft3D-FLOW. An advantage compared to Delft3D-FLOW only are better temporal resolutions regarding dispersion processes and less numerical diffusion. Moreover, Delft3D-WAQ includes numerous formulations for substance decay and transformation, which will be discussed in the following section.

The Lagrangian transport model Delft3D-PART is independent of a grid, thus allowing water quality processes to be described in a detailed spatial pattern, resolving sub-grid concentration distributions. Delft3D-PART is best suited for studies over the mid-field range (200 m-15 km) of instantaneous or continuous releases. It calculates advection and diffusion processes using the Lagrangian approach and the hydrodynamic quantities resulting from Delft3D-FLOW. In addition, reaction or decay processes can be simulated using different particle attributes (density, surface area, and ages). Various realistic features (e.g. the return of previously diluted sewage over the outfall and different source conditions), substance accumulation in particular can be readily simulated by superposition methods.

### **Utilities**

Delft3D-FLOW offers various options for the co-ordinate system (rectilinear, curvilinear or spherical). For using Delft3D-FLOW the following utilities are important:

- Delft-RGFGRID: for generating curvilinear grids.
- Delft-QUICKIN: for preparing and manipulating grid oriented data, such as bathymetry or initial conditions for water levels, salinity or concentrations of constituents.
- Delft-TRIANA: for performing off-line tidal analysis of time series generated by Delft3D-FLOW.

- GETIJSYS: for performing tidal analysis on time series of measured water levels or velocities.
- Delft-GPP: for visualization and animation of simulation results.

## 5.5. Linked brine discharge modeling

The near-field and far-field models have usually been applied separately without considering either the far-field effects in detail (pure near-field modeling) or neglecting near-field processes (pure far-field modeling). However, it has been shown (Bleninger, 2006) that separate modeling is not optimal for design and siting considerations. Therefore, a simple coupling interface has been developed in this project which expands on an existing approach for waste water discharges, linking the near-field model CORMIX with the far-field model Delft3D (Bleninger, 2006).

Though the coupling algorithm is described for the specific models CORMIX and Delft3D, it is adaptable to other programs with similar capabilities with only few modifications. The required input files and transformations are generated by the use of routines. The pre- and post-processing routines and the model linking routines are coded within the commercial software MatLab<sup>®</sup> Version 7.4 R2007a from the company MathWorks<sup>®</sup>. The so-called m-files are ASCII files, thus they may simply be recorded for other languages as well if MatLab<sup>®</sup> is not available. The routines are described for multiport diffuser (CORMIX 2 module) and single port discharges (CORMIX 1 module). Slightly modified, they can also be adapted for surface discharges (CORMIX 3 module).

In addition, macros are created for the completion of the generated input files. They are coded within the text editor UltraEdit<sup>®</sup>. The coupling algorithm is usually run in the following sequence:

- 1) *Pre-processing*: preparation of field measurements as time series input for the near-field model
- 2) *CorTime*: time series near-field modeling with CORMIX based on measured data
- 3) *Post-processing*: analysis and presentation of the results of CorTime
- 4) *Model linking*: preparation of near-field results as time series input for the far-field model
- 5) Delft3D-FLOW: hydrodynamic modeling based on measured field data and the output data of the near-field model

Details of each step are described as follows. A more detailed description can be found in Niepelt (2007).

### 5.5.1. Coupling step 1: Pre-processing

CorTime is the time series analysis tool of CORMIX developed and implemented for this project. For a mixing zone analysis with CorTime two files are required: a CORMIX input file (\*.cmx) and a CorTime time series input file (*CorTimeInput.txt*) (CorTime, 2008). The CORMIX input file contains all conditions and configurations of the ambient, the effluent and the discharge. This is the same input file which is required for a single CORMIX simulation (explained in detail in the CORMIX user manual). The CorTime file *CorTimeInput.txt* includes the variation of the input data (e.g. ambient velocity, current direction, effluent flow rate) for each time step.

### CorTime input file (CorTime, 2008)

CorTime requires a certain structure of the input document *CorTimeInput.txt* as shown in Table 16. This structure is always the same, meaning it is independent of the chosen module (CMX1, CMX2, CMX3). *CorTimeInput.txt* starts with a header consisting of six lines which has to be included in the given design. It contains information about the CorTime version, the time series input file name, the total number of time steps and the order of the parameters. Note that the time steps entry has to be adjusted to the current case.

From the seventh line, the time series input data are listed column by column in the order given in Table 16. Each column is separated by a tab '\t' and each row is separated by a new line '\n'. Depending on the used model or on the ambient density, some parameters do not apply or are unavailable, and so '-' is used for indication.

There are several possibilities to define the input parameters in CORMIX. For example, the velocity can be defined through a velocity or through a flow rate. However, the time series analysis with CorTime requires a determinate specification. Therefore, the following assumptions are applied to *CorTimeInput.txt*:

- All values are specified in SI units
- Ambient velocity will always be specified as 'steady velocity' (not 'flow rate' or 'unsteady')
- Effluent velocity will always be specified as 'effluent flow rate' (not 'velocity')
- Both the ambient and the effluent density will always be specified as 'density' (not 'temp.')
- CMX1: Port specification will always be 'port diameter' (not 'port area')
- CMX3: Discharge outlet will always be specified as 'channel' (not 'pipe')

Table 16: Structure of the CorTime input document *CorTimeInput.txt*, parameter definitions

```

CorTime v5.0
File Name: CorTimeInput.txt
TOTSTEP: <total # of time steps>
TIME HA HD UA UorS RHOAM SType RHOAS RHOAB HINT DROHJ Q0 C0 RHO0 ...
0 13 12.5 0.42 U 1023.4 - - - - - 0.45 100 1046.7 ...
300 14.7 12.7 0.485 U 1023.5 - - - - - 0.46 100 1046.7 ...
600 14.6 12.6 0.486 S - A 1023.1 1023.5 - - 0.52 100 1046.7 ...
...

```

where:

column	parameter	definition	indication for:
1	TIME	time [s] or time step [-]	all steps
2	HA	average depth $H_a$ [m]	all steps
3	HD	discharge depth $H_D$ [m]	all steps
4	UA	ambient steady velocity $U_a$ [m/s]	all steps
5	UorS	<u>u</u> niform or <u>s</u> tratified density distribution	all steps
6	RHOAM	average density $\rho_{a,m}$ [kg/m <sup>3</sup> ]	if U: all steps, else '-'
7	SType	type of stratification (A, B, C)	if S: all steps, else '-'
8	RHOAS	surface density $\rho_{a,s}$ [kg/m <sup>3</sup> ]	if S (A,B,C): all steps, else '-'
9	RHOAB	bottom density $\rho_{a,b}$ [kg/m <sup>3</sup> ]	if S (A,B,C): all steps, else '-'
10	HINT	pycnocline heigth $h_{int}$ [m]	if S (B,C): all steps, else '-'
11	DROHJ	density jump $\Delta\rho_j$ [kg/m <sup>3</sup> ]	if S (C): all steps, else '-'
12	Q0	effluent flow rate $Q_o$ [m <sup>3</sup> /s]	all steps
13	C0	effluent concentration $C_o$ [mg/l]	all steps
14	RHO0	effluent density $\rho_o$ [kg/=m <sup>3</sup> ]	all steps
15	GAMMA	alignment angle $\gamma$ [fl]	CMX2: all steps, else '-'
16	SIGMA	horizontal angle $\sigma$ [fl]	CMX1/3: all steps, else '-'
17	D0	port diameter $D_o$ [m]	CMX1/2: all steps (if specified), else '-'
18	B0	channel width $B_o$ [m]	CMX3: all steps (if specified), else '-'
19	H0	channel height $H_o$ [m]	CMX3: all steps (if specified), else '-'

## Pre-processing routines

### *make CorTimeInput.m*

The MatLab<sup>®</sup> m-file named *make CorTimeInput.m* was developed for the generation of *CorTimeInput.txt*. This routine converts input data (ambient and discharge conditions) of a defined range of time steps into the necessary parameters.

The input data can either be obtained by intensive field measurements at the outfall location over long time periods or as latter is seldom available, by running far-field model simulations for the baseline situation. These far-field model simulations allow characterizing the prevailing and extreme ambient conditions. The further steps are therefore usually only done for typical and extreme spring-neap cycles and not the whole year. The MatLab routine thus allows to read different data formats.

The basis for the generation of *CorTimeInput.txt* are ASCII files (from field measurement equipments) or NetCFD or dat-files (from model simulations) containing information of the variable ambient conditions and/or varying effluent characteristics considering the same period and the same time steps. The routines CorField (field data) and Cor3D (for model data) allow to reformat those files to accelerate the further pre-processing. The resulting input files include information about the ambient current magnitude and direction (*current.txt*), the ambient water depth (*averageddepth.txt*), density profiles (*density.txt*), and the effluent discharge (*effluentflow.txt*). If further information is available, e.g. effluent concentration variations, they can simply be implemented as a new file. The values are listed line by line for each time step like in *CorTimeInput.txt*. The first column always contains the time step and the following columns comprise of the respective parameter values. For constant values no input file is necessary, but the constant value is provided within Matlab-routine. In addition, the declaration of the considered angle  $\alpha$  of the diffuser position (CMX2) or respectively of the port centerline (CMX1) is required.  $\alpha$  is the port centerline / diffuser orientation angle measured clockwise from the north to the port centerline / diffuser axis. CMX1:  $\alpha = 0^\circ$  to  $360^\circ$ , CMX2:  $\alpha = 0^\circ$  to  $180^\circ$ .

Using these input files, the CorTime input parameters are determined and then transformed into vectors. The generation of a vector itself is simple but the calculation of the parameters can be complex due to different coordinate systems and parameter resolutions. In case of the constant input data (e.g.  $C_o$ ,  $\rho_o$ ) or of parameters that are not available or do not apply (e.g.  $\sigma$  for CMX2) the fixed value or the icon '-' is written in each row of the vector. For the variable parameters, the file input has to be converted first. If one value per time step is specified, the data are only transported to the vector of the concerning parameter as in the case of *effluentflow.txt* for  $Q_o$  or *averageddepth.txt* for  $H_a$ . If several values are given for one time step, the (mean) parameter has to be calculated as in the case of the ambient current parameters  $U_a$ ,  $\gamma$ , and  $\sigma$  (*current.txt*) and the ambient density parameters  $\rho_{a,m}$ ,  $\rho_{a,s}$ ,  $\rho_{a,b}$  (*density.txt*). Considering the definitions of CORMIX, these parameters are computed for every time step as follows.

### **Ambient current parameters**

Measurements or simulations of the velocity magnitude  $Vel$  and the current direction  $\Phi$  are given at, for example, six points over the depth (Figure 82).  $\Phi$  is measured from the north. The values are positive ( $0^\circ$  to  $180^\circ$ ) when measured clockwise to the south, and negative ( $0^\circ$  to  $180^\circ$ ) when measured counterclockwise. The six velocity vectors are decomposed in the x- and y-coordinates and then averaged over depth. The depth averaged velocity  $U_a$  and the depth averaged current direction  $\phi$  is calculated by the mean values  $x_{mean}$  and  $y_{mean}$  as shown in Figure 83.

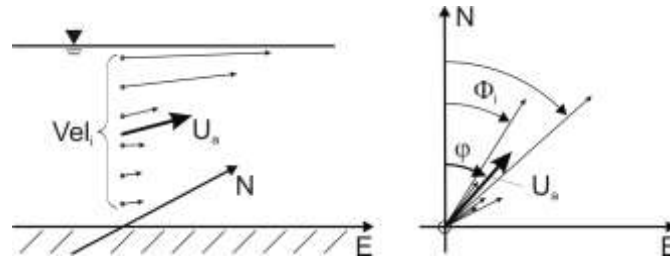


Figure 82: Depth averaged ambient velocity  $U_a$  and its direction  $\phi$  measured clockwise from the north, calculated from measured velocities  $Vel_i$  and directions  $\Phi_i$

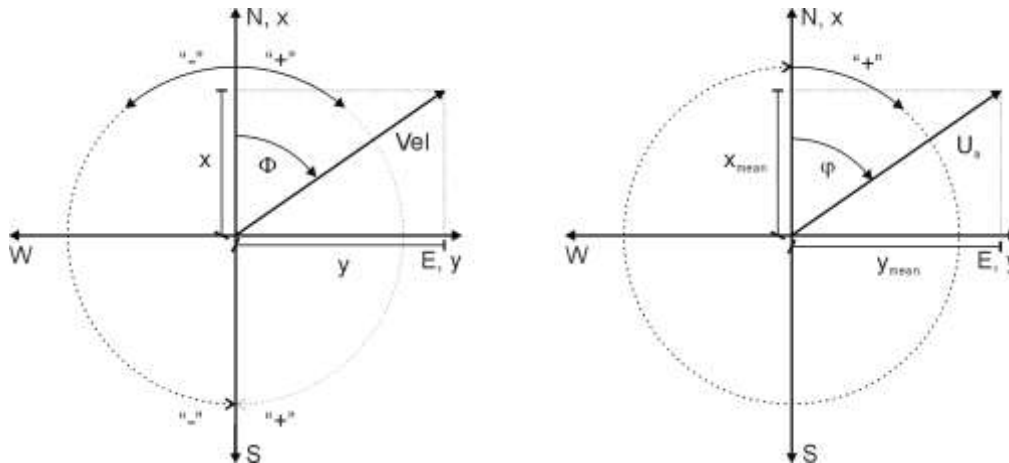


Figure 83: Determination of the magnitude of the depth averaged ambient velocity  $U_a$  and its direction  $\phi$  measured clockwise from the north (field data: velocity  $Vel$ , direction  $\Phi$ )

*Definition  $\phi$*

$\phi$  is the depth averaged ambient current direction angle measured clockwise from the north.  $\phi = 0^\circ$  to  $360^\circ$  (illustrated in Fig. 3.2).

The coordinate system used within CORMIX refers to the current direction. This means that the x-coordinate is always oriented in the direction of  $U_a$ . The current direction is described relative to the port centerline through  $\sigma$  (CMX1) or relative to the diffuser axis through  $\gamma$  (CMX2) as shown in Figure 84.

*Definition  $\sigma$*

$\sigma$  is the port horizontal angle defined as the angle measured counterclockwise from the ambient current direction (x-axis) to the plan projection of the port centerline.  $\sigma$  may range between  $0^\circ$  and  $360^\circ$ , excluding the range of  $135^\circ$  to  $225^\circ$ .

*Definition  $\gamma$*

$\gamma$  is the diffuser alignment angle defined as the angle from the ambient current direction (x-axis) to the diffuser axis, measured counterclockwise.  $\gamma = 0^\circ$  to  $180^\circ$ .

The 'real' direction of the ambient flow is specified by  $\sigma$  within CORMIX. For CMX2,  $\sigma$  will be recalculated in direct relation to changes in  $\gamma$  for each time step. It is not necessary to enter  $\sigma$  values for varying time steps. In fact, these values will simply be ignored. Both  $\gamma$  and  $\sigma$  are functions of the current direction so they will have the same amount of response to any change in ambient current direction. Considering these definitions, the current direction  $\phi$  is

converted into  $\sigma$  or  $\gamma$  depending on the chosen model. The transformation into  $\sigma$  is illustrated in Figure 85. The global current direction angles  $\phi$  are required for the analysis of the results and for the retransformation in global coordinates which are considered for the far-field modeling. Thus, the generated vector  $\phi$  is also stored in a text file called *Angle.txt*.

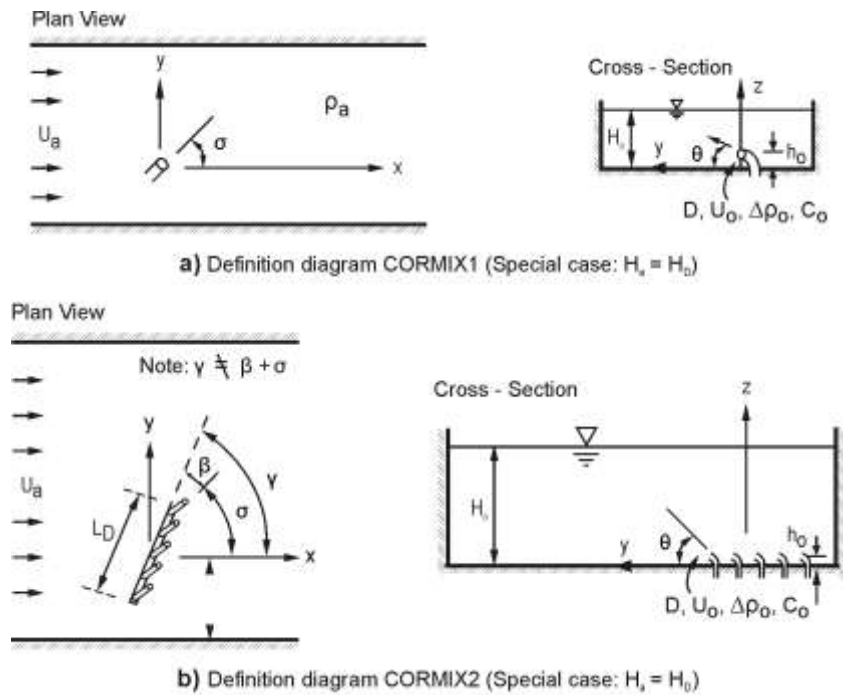


Figure 84: Discharge geometry: a) submerged single port (CORMIX1), b) multiport diffuser (CORMIX2) (modified from: Doneker and Jirka, 2007)

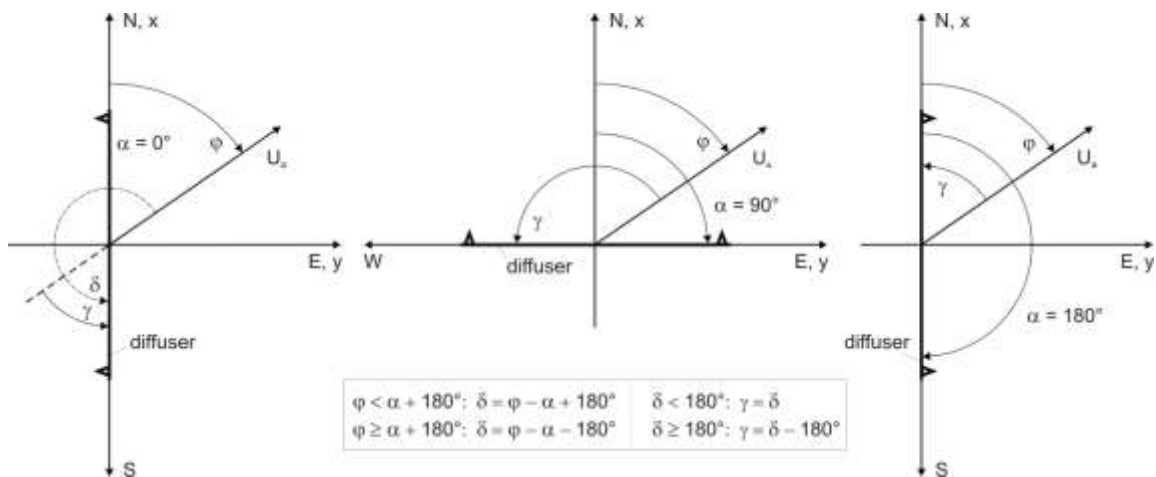


Figure 85: Definition of the alignment angle  $\gamma$ , examples for three orientation angles:  $\alpha = 0^\circ, 90^\circ, 180^\circ$  ( $\delta$  serves as auxiliary variable)

### Ambient density parameters

The ambient density can be considered as uniform or non-uniform. CORMIX requires a density difference of at least  $\Delta\rho = \rho_{a,s} - \rho_{a,b} > 0.1 \text{ kg/m}^3$  for stratified profiles. For uniform conditions, the average ambient density  $\rho_{a,m}$  is specified. For non-uniform conditions, CORMIX offers three profile types for the density distribution. They are specified by the surface density  $\rho_{a,s}$ , the bottom density  $\rho_{a,b}$ , and in the case of two layers by the density jump  $h_{int}$  and  $\Delta\rho_j$  as shown in Figure 86.

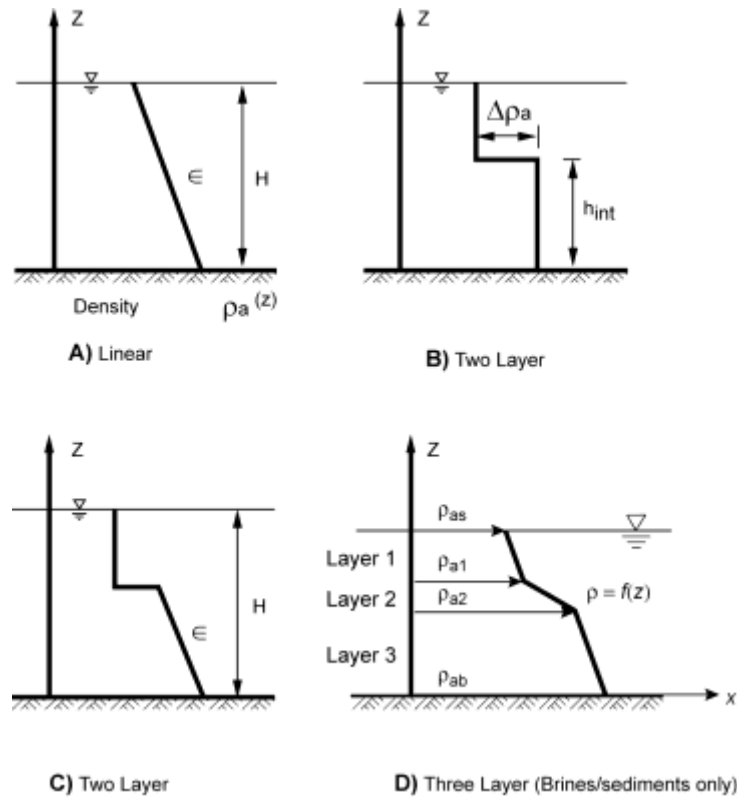


Figure 86: Different approximations for representing the ambient density stratification within CORMIX (source: Doneker and Jirka, 2007)

Within the routine *make\_CorTimeInput.m*, the determination of a uniform or a linear stratified (A) density profile is implemented. The future development and implementation of an algorithm for the calculation of the two layer profiles (B, C) is recommended. Figure 87 schematically shows the determination of  $\rho_{a,m}$ ,  $\rho_{a,s}$  and  $\rho_{a,b}$  for a constant or variable water level as executed in this routine. Measurements of the ambient density  $\rho_a$  are given at six fixed points. In the case of  $\Delta\rho < 0.1 \text{ kg/m}^3$  a uniform density is assumed and  $\rho_{a,m}$  is formed by the mean of the six values. In the case of  $\Delta\rho \geq 0.1 \text{ kg/m}^3$  meaning stratified the measurement at the bottom applies to  $\rho_{a,b}$ , the value for  $\rho_{a,s}$  is determined by linear interpolation.

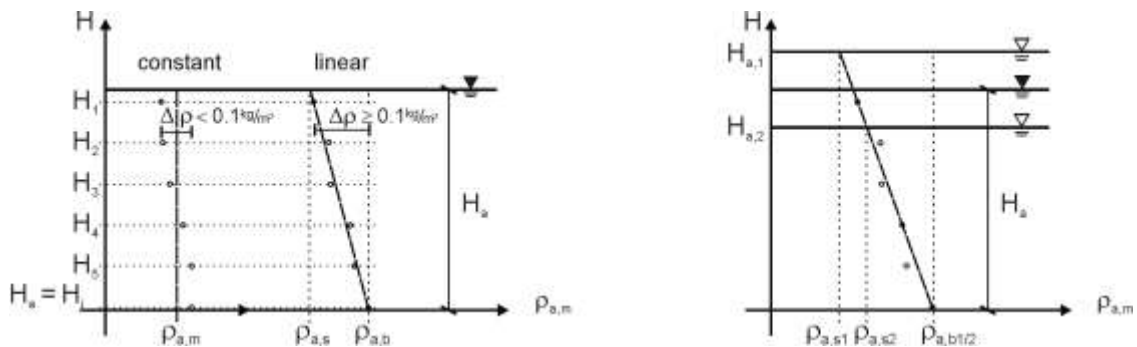


Figure 87: Approximations for ambient density distribution: uniform (defined by  $\rho_{a,m}$ ) or linear stratified (defined by  $\rho_{a,s}$  and  $\rho_{a,b}$ ). Left: constant water level, right: variable water level

MatLab<sup>®</sup> cannot handle letters and requires numbers as cell inputs. Therefore the density specifications 'U' for uniform, 'S' for stratified, and 'A' for linear density profile are replaced by numbers. They will be retransformed afterwards by running the macro *replace-l'&paste\_header.mac*.

As the final step of *make CorTimeInput.m*, the subroutine *plot\_matrix\_IN.m* is called, which optionally can be commented out.



*Plot\_matrix\_IN.m* plots graphs directly out of the matrix IN and the vector  $\phi$  which are saved in the workspace of MatLab<sup>®</sup> after running *make CorTimeInput.m*. The following plots are created:

- The first figure given as an example in Figure 88 shows all ambient and discharge conditions over time, all units in SI:  $Q_o$ ,  $C_o$ ,  $U_a$ ,  $H_a$ , and  $\rho_{a,m}$  indicating  $\rho_{a,b}$  and  $\rho_{a,s}$  if stratified.
- The second figure shown as an example in Figure 89 plots  $\phi$  and  $U_a$  as vectors on a circular grid ( $0^\circ = \text{north}$ ,  $90^\circ = \text{east}$ ) indicating the diffuser axis respectively the port centerline.
- Depending on the chosen model, the third figure plots the angle  $\sigma$  or the angle  $\gamma$  on a circular grid illustrated in Figure 89.
- The last figure represents a histogram of the relative frequency and cumulative distribution of  $\phi$  and of  $\gamma$  (Figure 90) or respectively of  $\sigma$ .

These plots represent a selection of display options. They can simply be expanded or modified.

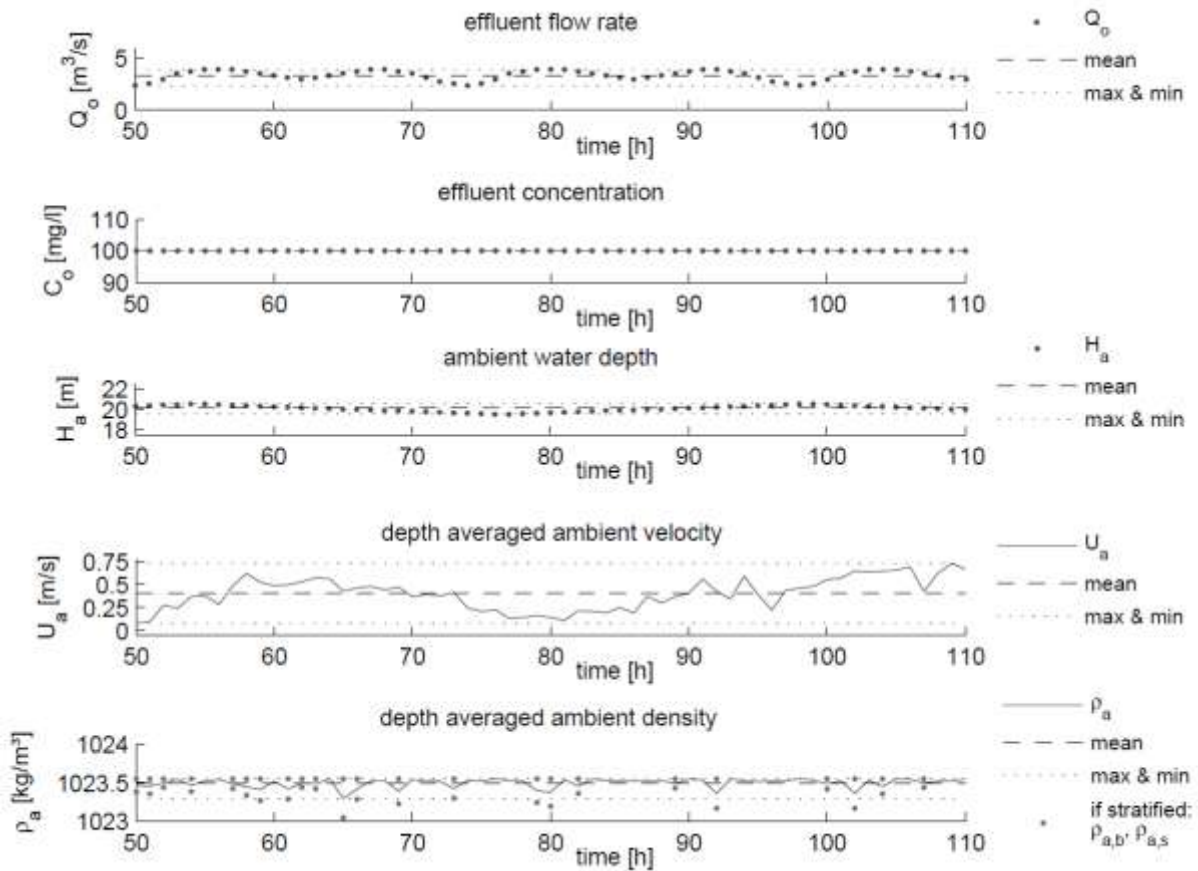


Figure 88: Example plot for CorTime input parameters  $Q_o$ ,  $C_o$ ,  $U_a$ ,  $H_a$ , and  $\rho_{a,m}$  indicating  $\rho_{a,b}$  and  $\rho_{a,s}$  if stratified

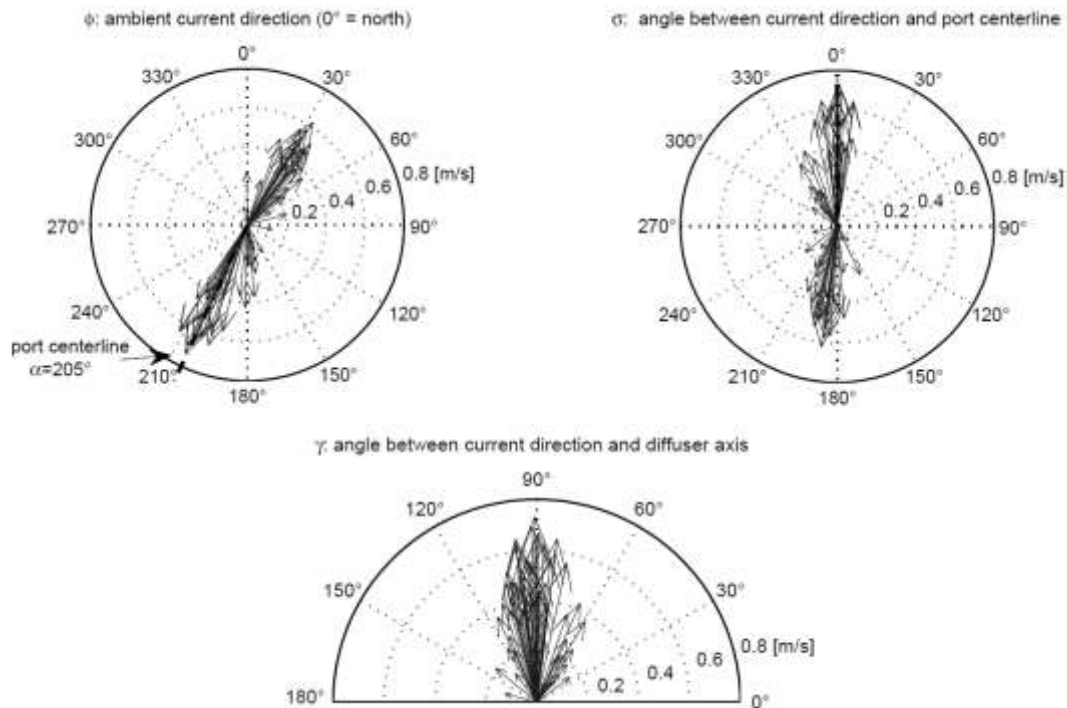


Figure 89: Example plots for current direction parameters  $\phi$ ,  $\sigma$  and  $\gamma$  plotted on a circular grid

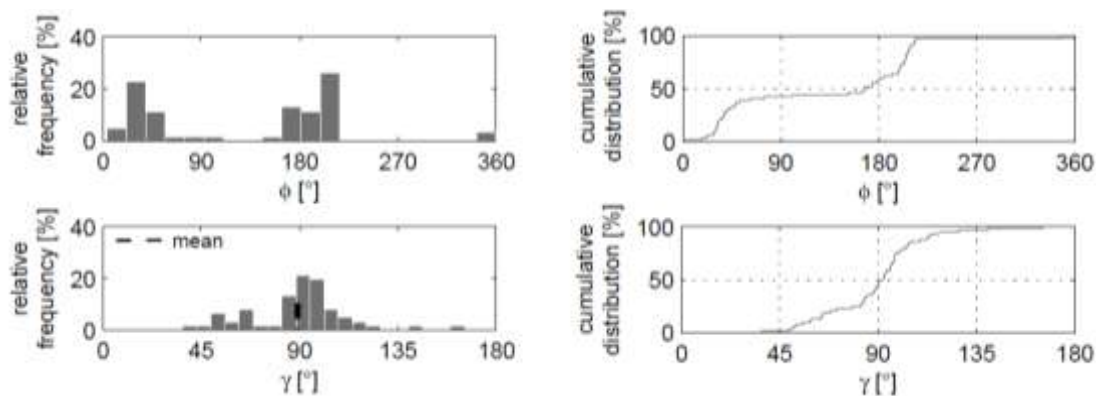
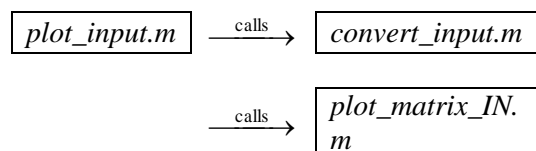


Figure 90: Example plot: Statistical analysis (relative frequency and cumulative distribution) of the ambient current direction  $\phi$  and the diffuser alignment angle  $\gamma$

### *plot\_input.m*

It is also possible to plot the input data subsequently out of the final document (after running the macro) by the use of the routine *plot\_input.m*.



The subroutine *convert\_input.m* is called first which converts the transformed file *CorTimeInput.txt* back into the matrix IN. Excluding the header, the cells with no input value marked by '-' are renamed '-1' and the density distribution definitions 'U', 'S' and 'A' are converted back into numbers. Calling *plot\_matrix\_IN.m*, the graphs are plotted as described above. Therefore, the text file *Angle.txt* is loaded since the required current direction angles  $\phi$  are no longer in the memory of MatLab®.



- Wind speed and Manning's  $n$ /Darcy-Weisbach  $f$  (*Ambient* tab)
- All discharge configurations except for  $\sigma$ ,  $\gamma$ ,  $D_o$ ,  $B_o$  and  $H_o$  (*Discharge* tab)
  - $\sigma$  is picked from input data only for CMX
  - $\gamma$  is picked from input data only for CMX2
  - $B_o$  and  $H_o$  are picked from input data only for CMX3
- All entries of the *Mixing Zone* tab

CorTime runs through the following sequence:

- 1) Open CORMIX 5.0GTR and load \*.cmx.
- 2) Click on the 'Validate&Run' button to ensure that *fn.cmx* runs successfully.
- 3) Preferably all 'Output Options' under the *Output* tab are set to "None".
- 4) In the *Post-Processing/Advanced* menu option choose the sub-menu option *CorTime* and select the appropriate time series input file *CorTimeInput.txt*. By loading this file the simulation begins immediately.
- 5) All time steps will be run thru by CorTime. CorTime will parse input for each step, load the GUI with each step value, validate and run. Three different output reports are created for each step with naming convention \*\_time-step<TIME>.cmx/.prd/.ses saved in the same folder as the input documents.
- 6) Wait for the simulation to execute and dismiss any validation warning windows.
- 7) At the end of running all steps, a CorTime Status Report will be created and saved as *CorTime-Status Report.txt* in the same folder as the input documents.

The output reports generated for every single time step mentioned in CorTime step 5 are a separate CORMIX input file (\*.cmx), a *Prediction File* (\*.prd) and a *Session Report* (\*.ses). These reports are not special CorTime features as they are created for a single CORMIX simulation as well. The *Prediction File* lists all simulation input data and the predicted plume properties. It gives details of the simulation flow modules executed for the given flow classification. The *Session Report* summarizes all discharge input data and global plume features including compliance with mixing zone regulations.

If a simulation has failed it is possible to vary time series input for this step and/or to review the data loaded in this step by loading the respective CORMIX file \*\_time step<TSTEP>.cmx. The mixing zone processes and the plume behavior can be displayed using the interactive 3-D visualization tool CorVue.

After the last time step, the output document *CorTime-Status Report.txt* is created, listing all plume characteristics at the end of the near-field region (NFR) and of a specified regulatory mixing zone (RMZ) for each time step indicating which steps were run successfully and which did not, as shown below in Table 19.

*CorTime-Status Report.txt* has a similar layout to *CorTimeInput.txt* shown in extracts in Table 19. Starting in the 11th line, the time series output data are listed column by column in the given order independent of the chosen model. The second, third and fourth columns give a report of which time steps were simulated successfully and which were not. From the fifth to the 12th column the plume characteristics at the end of the near-field region (NFR) are listed, and from the 14th to the 20th column those of the regulatory mixing zone (RMZ).

Note that the value for the plume width  $B_H$  is defined as the half plume width. The definition of the plume thickness  $B_V$  depends on the cross-sectional distribution and the centerline location of the plume as shown in Figure 92.

Table 19: Structure of CorTime output document *CorTime-Status Report.txt*, parameter definitions

```

CorTime v1.0 CorTime Series Processing Status Report

This File gives you a report of which time steps were successfully simulated and which were not.
Please review the Time step for which the simulation DID not complete, by checking
the Time Series Input file and the CORMIX case (*.cmx) file created for that step.

Key: Y => Successfully Created; N => Failed to Created.

T-  CMX  PRD  SES  NFRX  NFRY  NFRZ  NFRS  NFRC  NFRBV  NFRBH  NFRCT  RMZX  RMZY  ...
STEP
0   YES  YES  YES  7.50  0.00  13.50  202.55  0.01230  13.50  6.75  14.99  500  0.00  ...
1   YES  YES  YES  7.50  0.26  12.70  217.16  0.01110  12.70  6.88  12.93  500  0.26  ...
2   YES  NO   -   -     -     -     -     -     -     -     -     -     -     -
...
    
```

where:

column	parameter	definition
1	T-STEP	time step
2	CMX	'CORMIX File' saved?: YES/NO
3	PRD	'Prediction File' saved?: YES/NO
4	SES	'Session Report' saved?: YES/NO
5	NFRX	x-coordinate of NFR [m]
6	NFRY	y-coordinate of NFR [m]
7	NFRZ	z-coordinate of NFR [m]
8	NFRS	centerline dilution $S_C$ at NFR end [-]
9	NFRC	centerline concentration $C_C$ at NFR end [kg/m <sup>3</sup> ]
10	NFRBV	plume thickness $B_V$ at NFR end [m]
11	NFRBH	lateral plume width $B_H$ at NFR end [m]
12	NFRCT	cumulative time to NFR end [s]
13	RMZX	x-coordinate of RMZ [m]
14	RMZY	y-coordinate of RMZ [m]
15	RMZZ	z-coordinate of RMZ [m]
16	RMZS	centerline dilution $S_C$ at RMZ [-]
17	RMZC	centerline concentration $C_C$ at RMZ [kg/m <sup>3</sup> ]
18	RMZBV	plume thickness $B_V$ at RMZ [m]
19	RMZBH	lateral plume width $B_H$ at RMZ [m]
20	RMZCT	cumulative time to RMZ [s]

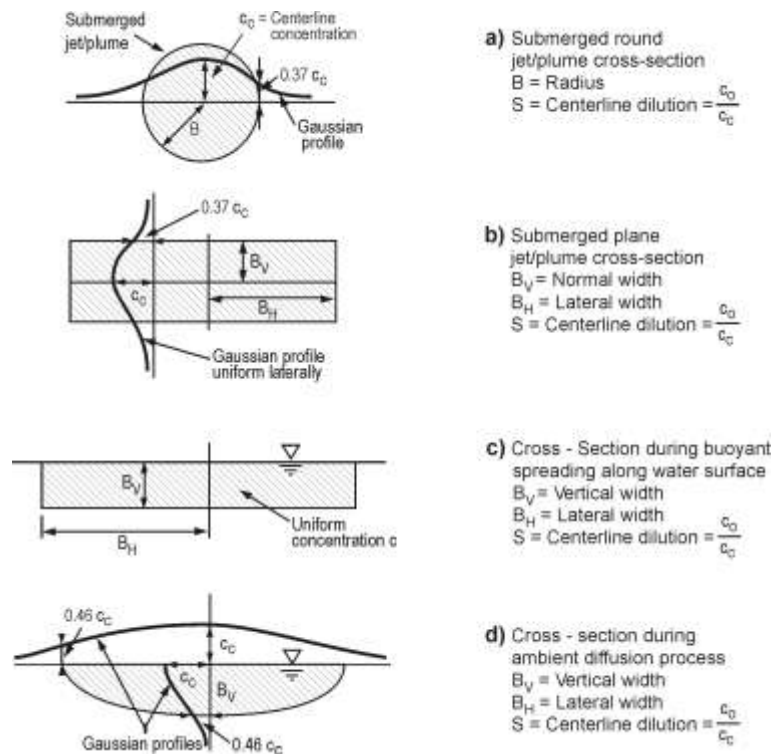


Figure 92: Cross-sectional distributions of CORMIX predicted jet/plume sections (source: CORMIX user manual (Doneker and Jirka, 2007))

### 5.5.3. Coupling step 3: Post-processing

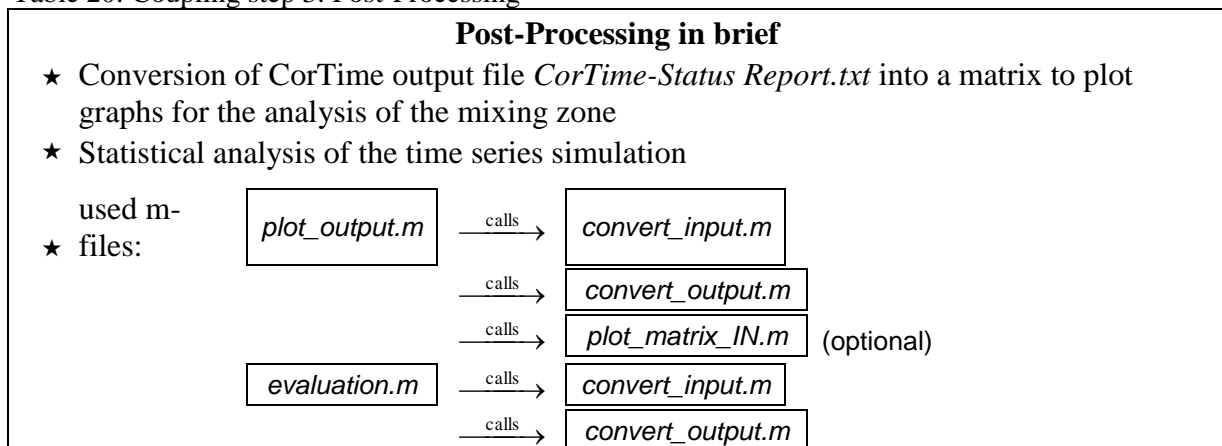
The predicted mixing zone processes and the plume behavior of every single time step can be analyzed within CORMIX by means of the *Session Report*, the *Prediction File*, the visualization tool CorVue or further output features.

For the time series analysis, the m-files *plot output.m* and *evaluation.m* were developed. Both call the two subroutines *convert input.m* and *convert output.m*. These subroutines transform the CorTime files *CorTimeInput.txt* into the matrix IN and *CorTime-Status Report.txt* into the matrix OUT in order to be read and evaluated by MatLab®.

#### *plot output.m*

*plot output.m* provides the graphical presentation of the results. Prior to plotting graphs out of the converted matrices IN and OUT, some parameters need to be calculated. According to the definitions, the plume width *pw* and the plume thickness *pt* are determined. By the use of the global current direction  $\acute{A}$ , the predicted endpoints of the NFR and of the RMZ are retransformed into global Cartesian coordinates. Therefore, the file *Angle.txt* is loaded containing  $\phi$  of all time steps. Optionally, the input parameter can be displayed calling the subroutine *plot\_matrix\_IN.m*.

Table 20: Coupling step 3: Post-Processing



The following output plots are implemented:

- The first figure shown as an example in Figure 93 represents the dilution, the plume thickness and the plume elevation at the end of the near-field as a function of time.
- The second figure given as an example in Figure 94 illustrates the distribution of the NFR and the RMZ by a scatter plot. The calculated position of the endpoints of these regions are shown indicating the range of the respective concentration. The diffuser axis, respectively, the port centerline is inserted.
- The third figure plots the statistical analysis of the predictions at the end of the near-field as relative frequency and cumulative distribution of the following parameters: near-field distance, plume elevation, plume thickness, plume width and cumulative travel time (Figure 95)
- The fourth figure plots the statistical analysis as relative frequency and cumulative distribution of the following parameters: concentration and dilution at the end of the NFR and the RMZ.

Those plots can simply be expanded or modified especially with regard to the analysis of the results at the RMZ.

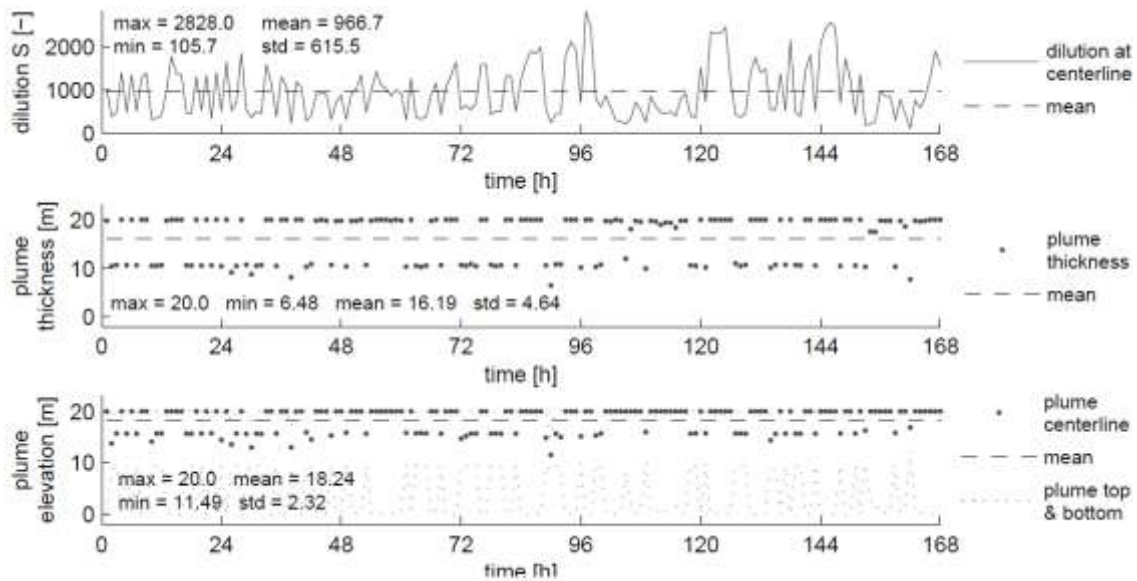


Figure 93: Example plot for CorTime output parameters: dilution, plume thickness, and plume elevation at the end of the near-field

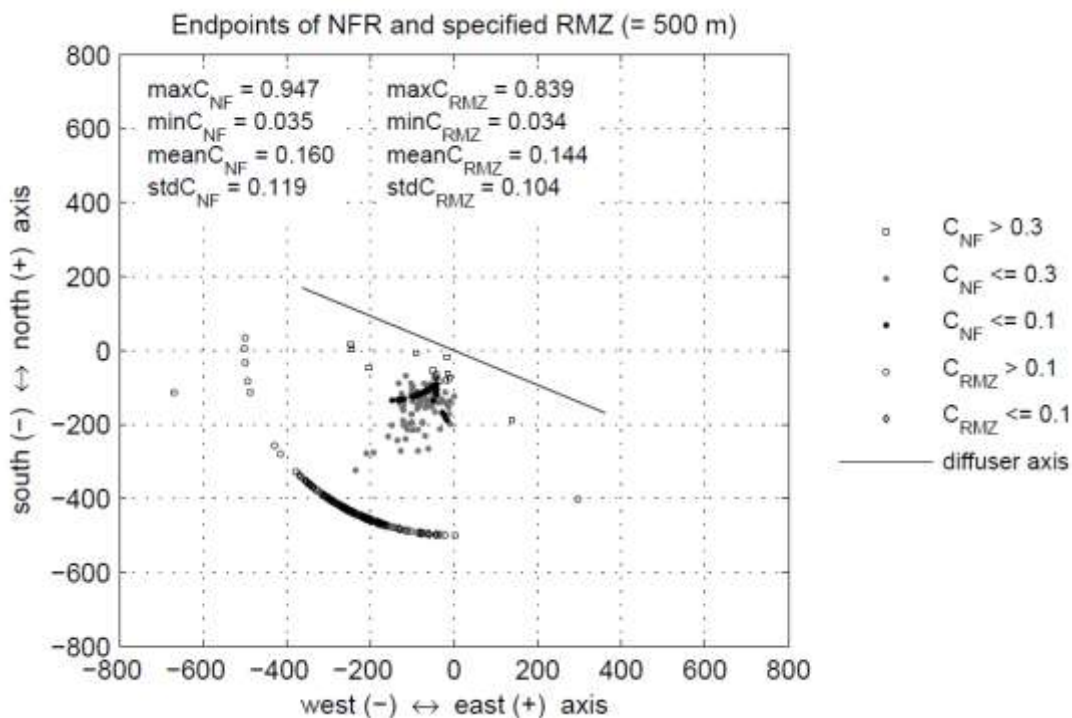


Figure 94: Example scatter plot: endpoints of the near-field and the RMZ indicating the corresponding concentration range

### ***evaluation.m***

*evaluation.m* provides the statistical analysis of the time series simulation. The maximum value, the minimum value, the mean value, and the standard deviation are calculated for every plume parameter given in *CorTime-Status Report.txt* or rather given in the matrix OUT. Assembled in a vector, the values can be saved as a table in a text file. Note that the plume width *pw* and the plume thickness *pt* are determined beforehand considering the definitions of CORMIX. By the use of a loop, it is possible to evaluate several times the series simulations in one go. The results are compiled in a matrix and saved in a single table.

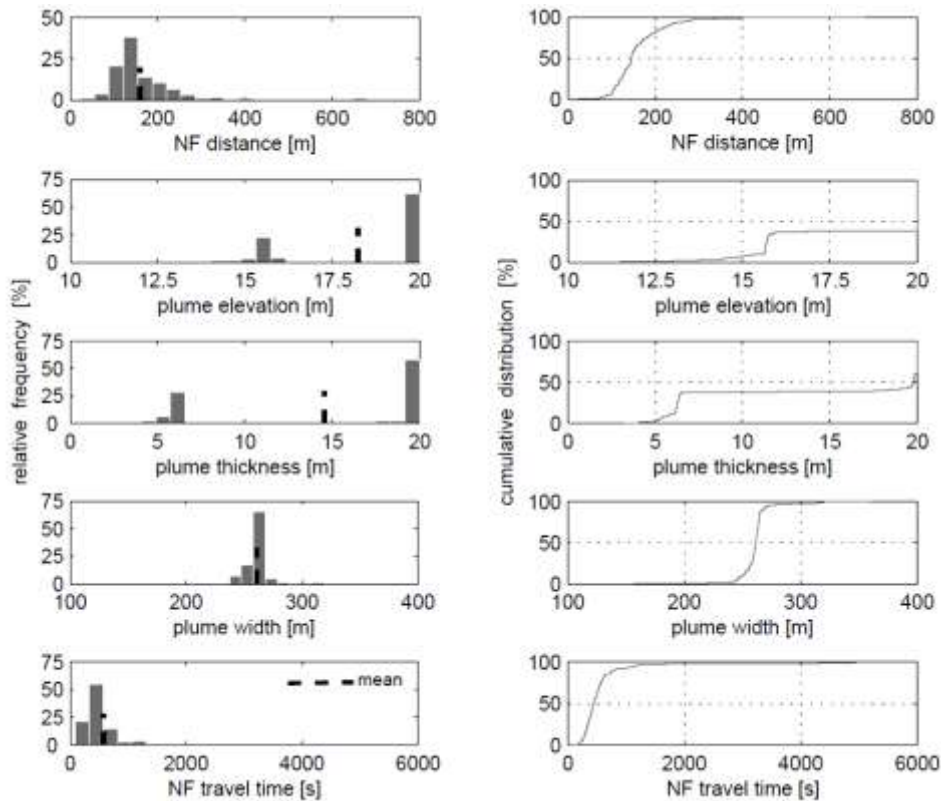


Figure 95: Example plot: Statistical analysis (relative frequency and cumulative distribution) for CorTime output parameters: NF distance, plume elevation, plume thickness, plume width, cumulative NF travel time

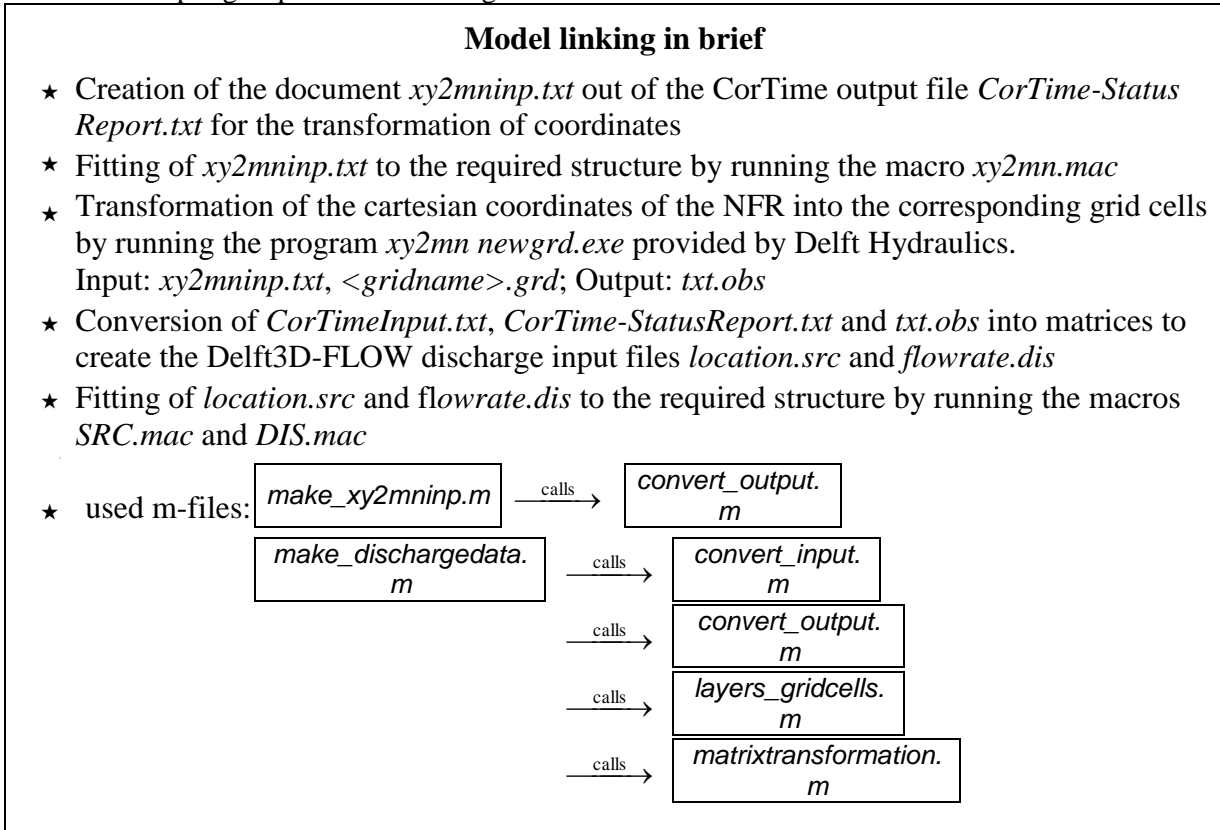
#### 5.5.4. Coupling step 4: Model linking

The main step of the model coupling is the transformation of the output data of the near-field model into input data for the far-field model. In Delft3D-Part the particle tracking model, mass fluxes can be added associated to the particle characteristics. The substance mass will then be transported and mixed with the previously calculated flow field. This coupling however does not consider any dynamics caused by the discharge (i.e. density spreading or similar). If such processes are relevant the coupling needs to be conducted within the flow simulation module Delft3D-FLOW, which will be described as follows.

In Delft3D-FLOW waste-water outfalls are considered as localized discharges of water and dissolved substances. The source is added at the center of a grid cell and then immediately distributed over the entire cell volume. The discharge locations and the respective flow rates can be read from so-called attribute files.

The application of coupling implies that in the far-field model the discharge is located at the predicted endpoints of the near-field. Figure 96 shows the transformation of the location of the end of the near-field (NFRX, NFRY), the plume width  $pw$ , and the plume thickness  $pt$  calculated in CORMIX into the corresponding grid cells of Delft3D. If the plume expands over more than one grid cell (M, N, K), the flow rate  $Q_o$  has to be apportioned in  $i$  parts ( $i$  = number of cells) while  $Q_o = \sum Q_i$  to follow mass conservation.  $Q_i$  depends on the cell size. The concentration  $C$ , the salinity  $Sal$ , and the temperature  $T$  remain the same since they are properties of  $Q$ :  $C_i = C_o$ ,  $Sal_i = Sal_o$ ,  $T_i = T_o$ .

Table 21: Coupling step 4: Model linking



Several routines were developed to transform the coordinates of the predicted plume location into the corresponding grid cells and then to generate the required input files such as the source location file and the discharge flow rate file.

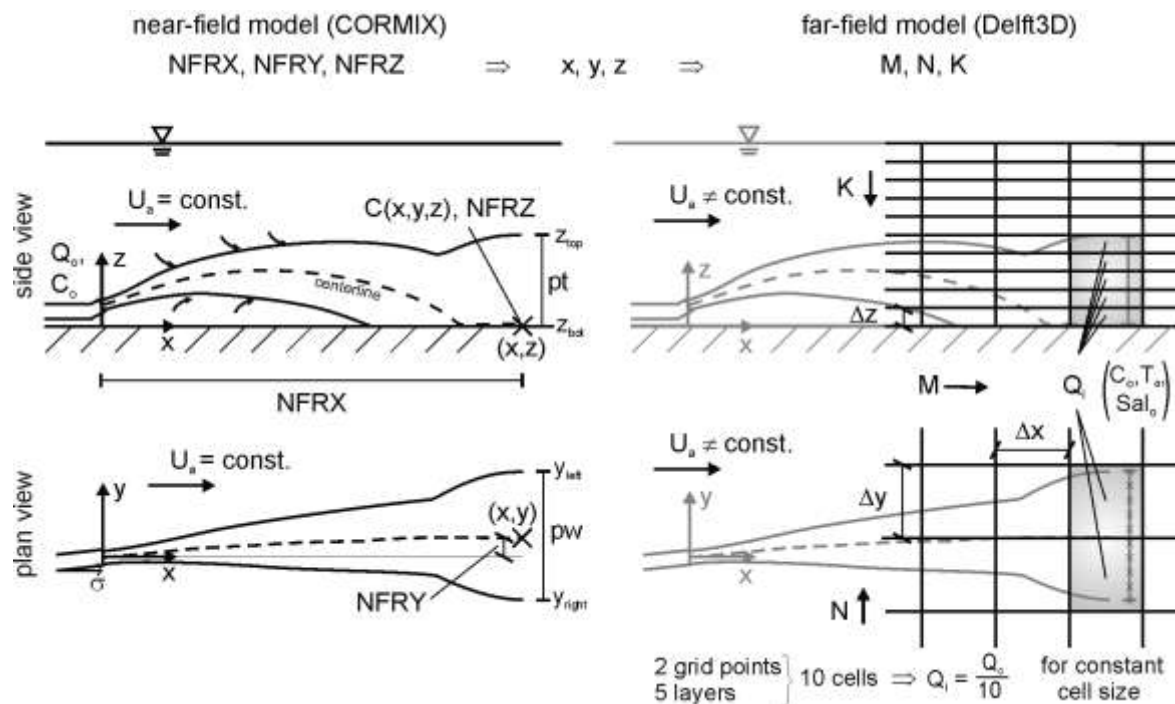


Figure 96 Transformation of CORMIX plume coordinates (NFRX, NFRY, NFRZ) into corresponding grid cells (M, N, K) of Delft3D via global coordinates (x, y, z). Division of the flow rate  $Q_o$  in  $i$  parts ( $i =$  number of cells):  $Q_o = \sum Q_i$ ,  $Q_i$  depends on the cell size. Concentration  $C$ , salinity  $Sal$ , temperature  $T$  remain the same since they are properties of  $Q$ :  $C_i = C_o$ ,  $Sal_i = Sal_o$ ,  $T_i = T_o$

### Source location file (*\*.src*)

The input file for the source location is referred to as *location.src*. It lists all discharge locations identified by the name of the location, the type of interpolation, and its grid coordinates (M, N, K).

The interpolation of time dependent discharge input can be specified as either:

- linear, indicated by Y (intermediate values are determined by linear interpolation), or
- block, indicated by N (the last value is repeated until the next value is defined).

If the effluent is discharged at one point in the vertical, the layer number K has to be specified. If the discharged flow is to be distributed uniformly over the water depth, then the layer number K is set to zero (K = 0).

Restrictions:

- The discharge name has 20 characters. (If the name has less letters it must be filled with blanks).
- Items in a record must be separated by one or more blanks.
- The number of discharges is limited to 250.

Considering these restrictions, the location file is recorded as follows.

OUTFALL-1	Y	45	31	3
OUTFALL-2	Y	45	31	4
OUTFALL-3	Y	46	30	0

Table 20: Structure of the location input document *location.src* listing the name of the location, the type of interpolation (Y: linear, N: block), and its grid coordinates (M, N, K)

### Discharge flow rate file (*\*.dis*)

The flow rate file referred to as *flowrate.dis* contains the discharge rate and its properties (concentration, salinity, temperature) as a function of time for each discharge location. The time dependent data are defined at time breakpoints and their intermediate values are determined by either linear or block wise interpolation as explained above (the same type as in *location.src* has to be applied). Several discharge type specifications are provided, e.g. 'Normal' or 'Momentum'. This routine only considers the discharge of the type 'Normal' where the discharge rate is released without taking specific aspects into account.

The input data is given in two related blocks for every single discharge location:

- 1) A header block containing a number of compulsory and optional keywords with their values.
- 2) A data block containing the time dependent data.

Restrictions:

- The parameters of the data block must be given in the following mandatory sequence: time, discharge flux, salinity, temperature, constituents. (If any property parameter is not specified, it is deleted from this sequence.)
- Input items in the data records must be separated by one or more blanks.
- The format of keywords and keyword-values in the header are fixed.
- All keywords have a length of 20 characters.
- Header records must start in position one.
- Header in each block must be ended with the keyword 'records in table' accompanied by its appropriate value.
- Times must be a multiple of the integration time step; times will be checked.

- The order of the blocks must be consistent with the sequence of discharge locations.
- The maximum record length in the file is 132.

Considering these restrictions the flow rate input file is formed as shown in Table 22.

```

table-name      'Discharge: 1'
contents        'regular'
location        'OUTFALL-1'
time function   'non-equidistant'
reference-time  20070101
time-unit       'minutes'
interpolation   'linear'
parameter       'time' unit '[min]'
parameter       'flux/discharge rate' unit '[m³/s]'
parameter       'salinity' unit '[ppt]'
parameter       'outfall-effluent' unit '[kg/m³]'
records in table 3
  0.0    7.0  66.9  100.0
  60.0   0    0    0
 1440.0  7.0  66.9  100.0

```

Table 22: Structure of the flow rate input document *flowrate.dis* of Delft3D-FLOW. The header block lists a number of compulsory and optional keywords with their values, the data block contains the time dependent input data (here: time,  $Q$ ;  $Sal$ ;  $C$ )

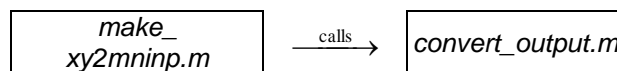
### Model linking routines

The generation of *location.src* and *flowrate.dis* is divided into two steps provided by one m-file each. In the first step, the transformation of the horizontal coordinates is accomplished. In the second step, the two files are created as stated above considering the vertical distribution and the allocation of the flow rate. The routines are described for the endpoints of the NFR. With a few modifications they can be adapted for the RMZ.

### Transformation of coordinates

#### *make\_xy2mninp.m*

The m-file *make\_xy2mninp.m* provides the transformation of the local coordinates of the horizontal plume distribution of CORMIX into the global geographic coordinate system used in Delft3D.



The basis for the calculation is the output file *CorTime-Status Report.txt* which is converted into the matrix OUT by calling the subroutine *convert\_output.m* and the ambient current direction vector  $\phi$  which is generated by loading *Angle.txt*.

The conversion is achieved using the three coordinate systems demonstrated in Figure 97.

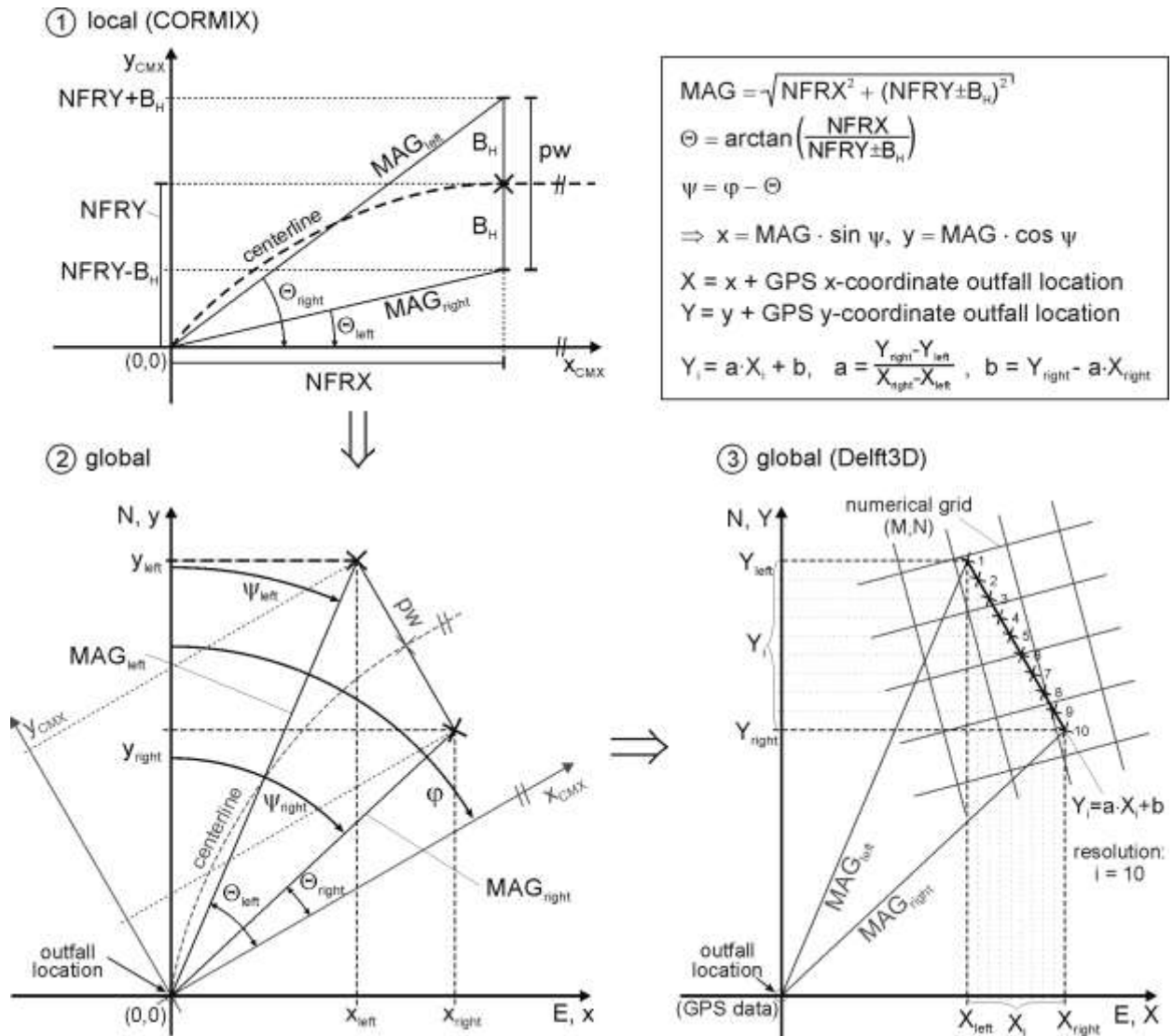


Figure 97: Transformation of coordinates of the plume at the end of the near-field:

Conversion of the CORMIX output data ( $NFRX$ ,  $NFRY \pm B_H$ ) [①] into global coordinates ( $x_{left/right}$ ,  $y_{left/right}$ ) via rotation of the coordinate system [②]. Adding the GPS data of the outfall location leads to the geographical coordinates ( $X_{left/right}$ ,  $Y_{left/right}$ ). Resolution of the plume width in ten points determines in which cells ( $M$ ,  $N$ ) of the numerical grid the plume is located [③].

### Coordinate system 1

CORMIX uses a local coordinate system shown at the top left of Figure 97 which refers to the ambient current direction. This means that the  $x$ -axis is always in the direction of  $U_a$ . At the end of the NFR, the ambient current direction defines the trajectory of the plume; thus, both lines are parallel. The horizontal location of the plume centerline at the end of the NFR is given by  $NFRX$  and  $NFRY$ . The coordinates of the boundary points of the plume are defined by addition/subtraction of the half plume width  $B_H$  ( $NFRX$ ,  $NFRY \pm B_H$ ). The distance  $MAG$  (magnitude) between the boundary points and the origin is computed using the Pythagorean theorem.  $\Theta$  is the angle between the  $x_{CMX}$ -axis and  $MAG$ .

### Coordinate system 2

The local coordinate system is pasted into the global coordinate system of which the  $y$ -axis is in direction of the north (lower left chart in Figure 97). Both have the same origin coordinates  $(0, 0)$ . The  $x_{CMX}$ -axis is rotated by  $\phi$  from the north.  $\psi$  is the angle between the north and  $MAG$

calculated from  $\psi = \phi - \Theta$ . By the use of  $\psi$  and *MAG* the global coordinates of the plume boundary points ( $x_{left/right}$ ,  $y_{left/right}$ ) are determined.

### Coordinate system 3

The outfall location in Delft3D is defined by GPS coordinates. Adding these values to  $x_{left/right}$  and  $y_{left/right}$  results in the geographic coordinates of the plume boundary  $X_{left/right}$  and  $Y_{left/right}$ . The grid points (M, N) of the numerical grid of Delft3D are defined by GPS coordinates as well. To determine over which cells the plume is extended, the plume width is split into nine equal parts resulting in ten points ( $X_i$ ,  $Y_i$ ,  $i = 10$ ) illustrated in the lower right chart of Figure 97. These ten locations are determined for every single time step. If only the endpoints were considered, the cells in between might be neglected if the plume spans more than two cells. The required resolution depends on the cell size and can be adjusted.

The conversion of the GPS coordinates ( $X_i$ ,  $Y_i$ ) into the corresponding grid cells ( $M_i$ ,  $N_i$ ) is accomplished via the program *xy2mn\_newgrd.exe* provided by Delft Hydraulics. This program requires the grid file called *<gridname>.grd* containing the coordinates of the grid cells and a text file of a determinate structure listing the coordinates of all points which should be transformed. The generation of this latter document is implemented in *make\_xy2mninp.m*.

The name of this file is defined as *xy2mninp*, but the extension (3 characters) is not fixed. Since this document is a text file the extension *\*.txt* was chosen within this description resulting in *xy2mninp.txt*.

The required input data are the Cartesian coordinates ( $X_i$ ,  $Y_i$ ) and the name of every location. Since several points are determined for each time step, the name *timestep.point(i)* (e.g. 1.01) was chosen. The parameters are listed column by column ( $X_i$ ,  $Y_i$ , *timestep.point(i)*) and row by row for each location of every time step.

*	X,Y coordinate	station names	CURRENT	locations	1.01	45	31
*	X-OBS	Y-OBS	Location		1.02	45	31
	135419.0	405521.3	1.01		1.02	46	32
	135493.7	405526.5	1.02		...	...	...
	135568.4	405531.7	1.03				
	...	...	...				

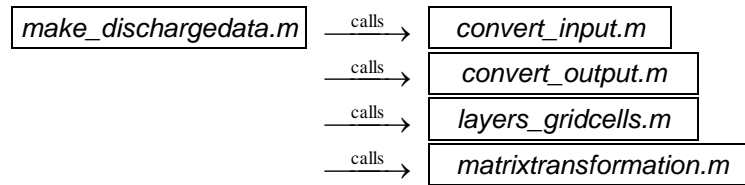
Table 23: *Left*: Structure of the input document *xy2mninp.txt* for conversion of Cartesian coordinates into corresponding grid points by using the program *xy2mn\_newgrd.exe* provided by Delft Hydraulics. *Right*: Structure of the generated file *txt.obs* listing the locations identified by its names and its grid cells (M, N)

The prescribed structure of *xy2mninp.txt* is completed by running the macro called *xy2mn.mac*. A header consisting of three rows is pasted and two blanks are inserted in front of each row leading to the layout shown on the left in Table 23. By importing *xy2mninp.txt* and the grid file *<gridname>.grd* into the program *xy2mn\_newgrd.exe* the data are transformed automatically. They are saved in the same folder listed in a text file as displayed on the right of Table 23 with the name *<extension>.obs*, in this case *txt.obs*.

## Generation of discharge input files

### *make\_dischargedata.m*

The routine *make\_dischargedata.m* provides the generation of the required input files *location.src* and *flowrate.dis*.



The calculations are based on *CorTimeInput.txt* and *CorTime-Status Report.txt* which are converted into the matrix IN and OUT by calling the subroutines *convert\_input.m* and *convert\_output.m*. Furthermore, the generated file *txt.obs* is loaded. The determined grid parameters of the horizontal discharge location are transferred into a matrix called MN.

**\* Creation of *location.src***

The plume distribution over the horizontal and the correlating grid cells have been determined. The corresponding distribution over depth meaning which layers K are involved will be calculated in the following.

Firstly, the locations of the plume top  $z_{top}$  and the plume bottom  $z_{bot}$  are determined via the plume thickness  $pt$  and the centerline position considering the CORMIX definitions. Then the subroutine *layers\_gridcells.m* is called to determine in which layers the plume is situated for every single time step.

According to Delft3D-FLOW, the so-called  $\sigma$ -grid is applied in the vertical direction where the layer thickness varies with the depth and the number of active layers is constant. The thickness of a layer is defined as a percentage of the (time varying) water depth. An arbitrary number of layers  $K_{max}$  can be chosen as long as the total sum of the layers is 100%.  $K = 1$  corresponds to the surface layer (Delft3D-FLOW, 2005).

Considering these instructions, several numbers of layers (5, 8, 10 and 13) with a different percental layer thickness are offered within this routine.

The thickness of each layer  $lt$  is calculated depending on the water depth applied in CORMIX. Via the position of the plume top  $z_{top}$  and the plume bottom  $z_{bot}$  the affected layers are determined. Therefore, the values of  $lt$  are added from the bottom layer to the surface layer since  $z_{top}$  and  $z_{bot}$  are measured from the sea bed ( $z = 0$ ). If the plume is distributed over all layers,  $K_{top}$  and  $K_{bot}$  are set to zero. The following example illustrates this calculation for five uniform layers and  $H_A = 10$  m:

layer	%	$lt$ [m]	$lt_{sum}$ [m]	
1	20	2	10	$z_{top} = 7.5\text{m} \Rightarrow K_{top} = 2$
2	20	2	8	$z_{bot} = 3.2\text{m} \Rightarrow K_{bot} = 4$
3	20	2	6	
4	20	2	4	$\Rightarrow$ The plume is located in layer $K = 2$ to 4
5	20	2	2	

Ten values ( $M_i, N_i$ ) are defined for each time step as explained above. The calculated layers  $K_{top}$  and  $K_{bot}$  are assigned to each of those ten points saved in a matrix named CELL. Afterwards the range of layers  $K_{top}$  to  $K_{bot}$  is itemized as follows:

CELL:	$\Rightarrow$	CELL <sub>new</sub> :
(M N $K_{top}$ $K_{bot}$ )		(M N K)
45 31 2 4		45 31 2
46 32 0 0		45 31 3
		45 31 4
		46 32 0

The layers are not itemized if the plume is distributed over depth.  $K = 0$  is considered as a single discharge location. Consequently, all affected locations of every single time step are known.

The required input file, however, lists all discharge locations which participate once or several times at any time of the total time series. This means that every participating cell is listed once independent of the time steps. The new matrix is sorted line by line in ascending order. Rows with the same entry, meaning the same locations, are eliminated except for one so that each location occurs only once.

Back in the main routine *make\_dischargedata.m* a name and the interpolation type are added according to the required order. As already mentioned, MatLab<sup>®</sup> cannot handle literals as cell input. Therefore, the line number is chosen as the name of the location and the interpolation type icons (Y or N) are replaced by numbers. The compiled discharge locations are saved in the text file *location.src*.

**\* Creation of *flowrate.dis***

The times when a location participates have to be specified. The corresponding flow rates  $Q$  and, if considered, the effluent properties salinity  $Sal$ , temperature  $T$  and / or constituent concentrations  $C$  have to be assigned.

To generate the data block of *flowrate.dis* the discharges are considered in the sequence of the time steps first. The matrix CELL which was generated in the subroutine *layers\_gridcells.m* is taken as a basis. The corresponding values of time  $t$ ,  $Q$ ,  $Sal$ ,  $T$  and / or  $C$  are attached to this matrix. The time  $t$  has to be entered in with the dimension of minutes. If the time given in the matrix IN is defined as 'steps' it has to be converted to the correlative time in minutes (e.g. for hourly time steps: 0, 1, 2, ...  $\rightarrow$  0, 60, 120, ...). The salinity, the temperature, and the concentration remain constant since they are properties of  $Q$ :  $Sal_i = Sal_o$ ,  $T_i = T_o$ ,  $C_i = C_o$ . Hence, all ten points of one time step receive the initial value of these parameters.  $C_o$  is transferred from the matrix IN. The specification of  $Sal_o$  and  $T_o$  of each step has to be adjusted in the routine.

Following mass conservation, the flow rate  $Q_o$  (read from the matrix IN) has to be distributed over all locations that are affected at one time step. The matrix CELL considers only the horizontal resolution  $i = 10$ . Therefore,  $Q_o$  is divided into ten parts  $Q_i$  ( $Q_o = \Sigma Q_i$ ).

Three types of horizontal discharge distribution are offered within this routine: a uniform distribution ( $Q_i = const$ ) and two non-uniform distribution types which should approach the Gaussian profile of the plume cross-section. Depending on the chosen distribution type, the values of  $Q_i$  are calculated for each time step and added accordingly to the matrix CELL.

Additionally, the vertical plume distribution has to be considered. Therefore, the range of layers  $K_{top}$  to  $K_{bot}$  is itemized as for the location file. At the same time, the amount of  $Q$  depending on the layer thickness is determined while the values of  $t$ ,  $Sal$ ,  $T$  and  $C$  remain the same. Considering a uniform layer thickness, the matrix is itemized as follows:

(M N $K_{top}$ $K_{bot}$ $t$ Q Sal T C)	$\Rightarrow$	(M N K $t$ Q Sal T C)
45 31 2 4 0 7.0 66.9 27 100		45 31 <b>2</b> 0 <b>2.33</b> 66.9 27 100
46 32 0 0 60 7.0 66.9 27 100		45 31 <b>3</b> 0 <b>2.33</b> 66.9 27 100
		45 31 <b>4</b> 0 <b>2.33</b> 66.9 27 100
		46 32 <b>0</b> 60 <b>7.0</b> 66.9 27 100

The new compilation is sorted in the same order of outfall location as given in *location.src*. Due to the horizontal resolution, it is possible that an outfall location is affected more than once at the same time  $t$ . In this case, the property parameters have the same values. Only the value of  $Q$  varies if a non-uniform distribution was chosen. The rows with the same entries neglecting  $Q$  are eliminated except for one by adding the values of  $Q$ . As a result, at every time a step is listed once at most per location. This matrix called DIS consists of the data blocks of each discharge location in the same order as *location.src*.

Regarding one data block, it is possible that only a few time steps are specified for this location. The aim is that the effluent is discharged in this cell at these specific times. However, Delft3D interpolates between consecutive time steps. That implies that between the specified times, the effluent is continuously discharged. That leads to wrong flow rates if several time steps lie in between these specified times.

To avoid this error, the data blocks are modified. The modification is implemented in the subroutine *matrixtransformation.m*. If the specified time steps are not directly consecutive, rows are inserted for the previous and / or the following time steps as follows ( $\Delta t = t_{i+1} - t_i = 60$ ):

(M N K t Q Sal T C)	⇒	(M N K t Q Sal T C)
45 31 4 60 2.33 66.9 27 100		0 0 0 <b>0</b> 0 0 0 0
45 31 4 120 2.33 66.9 27 100		45 31 4 60 2.33 66.9 27 100
45 31 4 540 3.5 66.9 27 100		45 31 4 120 2.33 66.9 27 100
		0 0 0 <b>180</b> 0 0 0 0
		0 0 0 <b>480</b> 0 0 0 0
		45 31 4 540 2.33 66.9 27 100
		0 0 0 <b>600</b> 0 0 0 0

The flow rate is set to zero to obtain no discharge in between the specified times. The other parameters are set to zero as well except for the time  $t$ . Finally, the grid parameters (M, N, K) are deleted from the matrix DIS which is then saved as text file *flowrate.dis*.

The conversion into the final layout of the input files is accomplished by macros. The macro *SRC.mac* was written for *location.src* to retransform the numbers into the interpolation icons. Furthermore, the discharge name is extended to the required 20 characters. A name (e.g. outfall-) is inserted in front of the existing number and the remaining characters are filled with blanks.

The macro *DIS.mac* pastes the header block above the first row of *flowrate.dis*. The parameter keywords have to be adjusted to the considered parameters. Via copy and paste, the header must be added manually to each discharge data block (always above time step "0"). In addition to the keyword-values of the table-name, the location and the records in table have to be adjusted to each case.

The optimization of the latter macro or (if possible) the implementation of the final adjustments into the routine is recommended to optimize and speed up the process.

### 5.5.5. Coupling step 5: Delft3D-FLOW

To execute a flow simulation (also called scenario) with Delft3D-FLOW, various kinds of information are required. These include the extent of the model area, location of boundaries and its conditions, the bathymetry, geometrical details of the area such as breakwaters, structures, discharges and the definition of which and where results of the simulation need to

be stored. Finally, a numerical grid needs to be defined on which all location-related parameters are being defined.

The far-field transport and water quality model has also to be thoroughly set-up, be calibrated / verified on base of field data at various locations and is supposed to correctly reproduce the flow conditions everywhere in the model area and in particular at the discharge site. Moreover, such models can readily generate any tidal condition in the past or future by simply inputting the date in the tidal constituents describing its boundary conditions. It can therefore be more suitable to derive the required CORMIX flow input data from the far-field model at the location of the discharge point(s). This does not only improve the consistency among the coupling steps, it also makes it possible to create accurate flow input data representing the selected full spring-neap cycle.

Table 24: Coupling step 5: Delft3D-FLOW

<b>Delft3D-FLOW in brief</b>
★ Input: <i>Master Definition Flow</i> file (MDF-file) including all necessary attribute files and further required information
★ Output: Four types of result files: a history file, a map file, a drogue file, and a communication file

Following the user manual Delft3D-FLOW (2005), the basic steps that precede a simulation are summarized as:

- Selection of the extent of the area to be modelled.
- Definition of location and extent of open boundaries and the type of boundary conditions to be prescribed, i.e. water level, velocities or discharges.
- Definition of the land boundary.
- Generation of a numerical grid.
- Generation of the bathymetry defined on the numerical grid.
- Definition of many different grid related quantities, such as open boundaries, monitoring points, discharge locations, release points of drogues.
- Definition of the time frame of the scenario, i.e. start and stop time and various time functions such as the open boundary conditions, wind speed and direction, discharges, and salinity concentrations or other substances transported by the flow.

The data are stored in separate so-called attribute files such as the flow rate file *flowrate.dis*. These files are produced by the use of external programs or other Delft3D tools (e.g. the grid generator program Delft3D RGFGRID), manually online and/or in the Delft3D-FLOW input processor (Figure 98).

The main input file for the hydrodynamic simulation program is the so-called *Master Definition Flow file* (MDF-file, *<filename>.mdf*). In the MDF-file, the necessary attribute files and further information (e.g. output options) are defined. Only a reference is made to these files instead of including all data. Therefore, the attribute files and the MDF-file are to be stored in the same folder. Consequently, the generated attribute files *flowrate.dis* and *location.src* have to be saved in the same working directory as the corresponding MDF-file. The first three characters of the filename are used as a run-id and are used in the names of the output files to ensure the link between an MDF-file and the output files.

Delft3D-FLOW usually runs through the following sequence (for a detailed description see Delft3D-FLOW user manual (2005)):

- Start the FLOW input processor of Delft3D and load the selected MDF-file (FLOW GUI shown in Figure 98).
- All data saved in the attribute files are loaded automatically into the GUI.
- The input parameters can be modified in the corresponding data groups (listed on the left in the GUI). In this case the data have to be saved anew.
- Specify which computational results will be stored, then save the MDF-file.
- After verifying the MDF-file execute the computation.
- After the simulation the specified result files are stored in the same folder as the MDF-file.

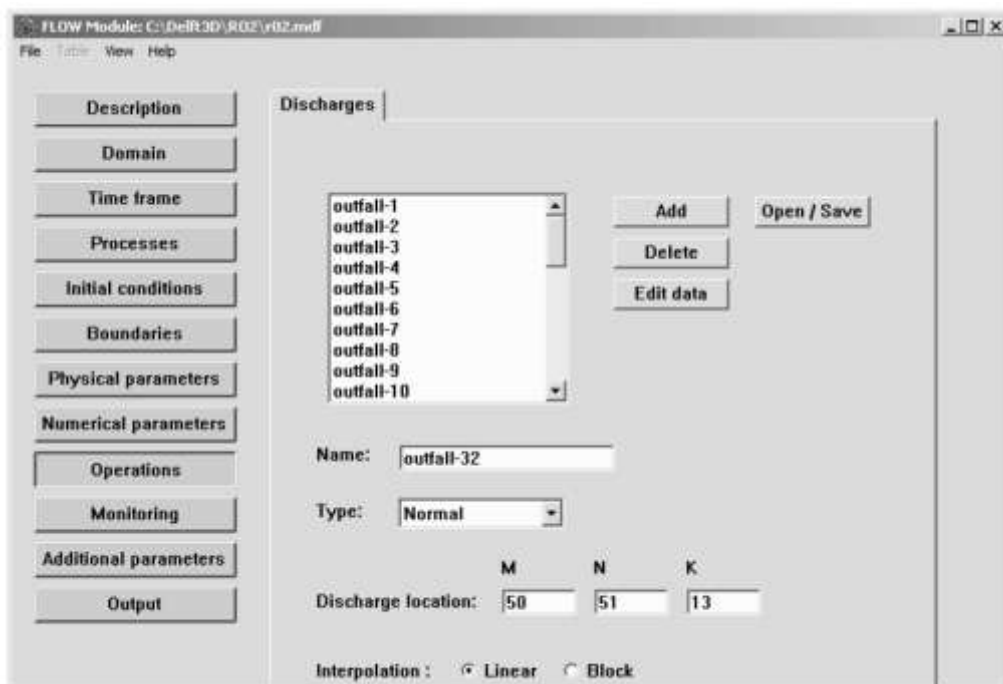


Figure 98: The GUI of the FLOW input processor of Delft3D with active data group 'Discharge'

The results of a flow simulation are stored in four types of output files:

- History file (saved as *trih- $\langle runid \rangle$ .dat*).
- Map file (saved as *trim- $\langle runid \rangle$ .dat*).
- Drogue file (saved as *trid- $\langle runid \rangle$ .dat*).
- Communication file (saved as *com- $\langle runid \rangle$ .dat*).

The *history file* contains all quantities as a function of time in the specified monitoring points and / or cross-sections. The *map file* contains results of all quantities in all grid points at a user-specified time interval. The *drogue file* contains the  $(x, y)$ -position of all drogues at each computational time step in the time interval between release and recovery time. The *communication file* includes all data which are required for other modules of Delft3D such as the hydrodynamic results for a water quality simulation. The results of all quantities in all grid points are stored.

The results can be visualized by the use of the post-processing tool Delft3D QUICKPLOT. On loading the result files into the visualization module, a large variety of graphs can be displayed. Since this program has been developed using MatLab<sup>®</sup>, the graphs can be saved in the figure file format of MatLab<sup>®</sup> for further analysis.

## **6. CASE STUDIES**

Three case studies have been chosen. The discharge calculators and modeling tools have been tested for the two Barka Plants in Oman, using RO and MSF technologies, thus covering both applications. The third case study, demonstrating the coupling of CORMIX and Delft3D-FLOW is described for a theoretical but nonetheless realistic situation in Section 6.2.

### **6.1. Case studies for discharge calculator and CORMIX modeling analysis**

The case studies will be introduced by an overview of seawater desalination in Oman (Section 6.1.1) following detailed information of the Barka plants including a report on the marine environment based on the field survey conducted in the vicinity of the intake and outfall systems in November 2004 by Dr. Sabah Abdul-Wahab, Sultan Qaboos University (Abdul-Wahab, 2007; Abdul-Wahab and Jupp, 2009) and in January 2007 by the Omani environmental consulting company, HMR Environmental and Engineering Consultants (HMR, 2007).

#### **6.1.1. Overview of seawater desalination in Oman**

The Sultanate of Oman is situated at the south-east of the Arabian Peninsula at the entrance to the Arabian Gulf (Figure 99), and its coastline stretches 1700 km along the Gulf of Oman in the north to the Arabian Sea in the south. The climate of the Sultanate is typically described as a tropical hyper-arid, with two distinct seasons: winter and summer. Hot weather with high humidity is experienced in the coastal areas during the summer months. The winter period extends from late November to April, during which light rains at irregular intervals occur. However, the annual mean rainfall is 117 mm for the whole country (Kwarteng et al., 2009). The mean temperature in northern Oman varies between 32 °C to 48 °C from May to September, and between 26 °C to 36 °C from October to April. The mean wind speeds range between 3 and 7 knots, with high wind speeds encountered during the summer months. Most of the population of Oman lives in the north-eastern coastal areas and in the capital area of Muscat.

Oman has been using desalinated water since 1976 when the Al-Ghubrah power generation and seawater desalination plant was first commissioned in Muscat (Figure 1 and Figure 100). To meet continuously growing water demand due to population growth and economic development and reduce the reliance on groundwater resources, by 1999 Al-Ghubrah plant had seven MSF desalination units installed. The first desalination unit installed had a capacity of 22,750 m<sup>3</sup>/d, and the other six MSF units each have a capacity of 27,000 m<sup>3</sup>/d. Desalinated water usage in Oman is expected to increase further in the future, due to new industrial and tourism-related developments.

To secure the production of desalinated water (in conjunction with electricity) to meet the further growing demands in Oman, and to meet the requirement for new desalination capacity to be built, owned and operated by local and foreign investors, the government of the Sultanate of Oman established in 2003 the Oman Power and Water Procurement company (OPWP). Subsequently in 2009, OPWP issued a report on the outlook covering the period from 2008 to 2015 on the demands for desalinated water in Oman, and the power generation and water desalination resources required to meet those demands (Table 25). It stated that the

total demand for the desalinated water is expected to increase from 102 million cubic meters in 2008 to 234 million by 2015, an average annual increase of 13 % per year. OPWP has forecasted also that by 2015 the peak demand for water will reach 723,000 m<sup>3</sup>/d, and thus at least 143,000 m<sup>3</sup>/d of additional water desalination capacity is needed. The peak demand is calculated as the average daily demand during the peak month of the year, and the overall planning philosophy used by OPWP is to match the installed desalination capacity with the peak demand and to rely on storage capacity and groundwater resources to cover contingencies.



Figure 99: Location and installed capacities of major seawater desalination plants in Oman (Munk, 2008)



Figure 100: Al-Ghubrah power generation and seawater desalination plant (file photo: HMR Consultants)

Table 25: Projected water demands in Oman

(in thousand m <sup>3</sup> per day)	2008	2009	2010	2011	2012	2013	2014	2015
<b>Peak demand for water</b>	<b>476</b>	<b>602</b>	<b>638</b>	<b>651</b>	<b>664</b>	<b>682</b>	<b>703</b>	<b>723</b>
Al-Ghubrah (MSF) plant	182	182	182	182	182	138	138	138
Barka I (MSF) plant	91	91	91	91	91	91	91	91
Barka II (RO) plant		120	120	120	120	120	120	120
Sohar (MSF) plant	150	150	150	150	150	150	150	150
Sur (RO) plant	12	12	12	12	12	12	12	12
New Sur (RO) plant		68	68	68	68	68	68	68
<b>Total desalination capacity</b>	<b>435</b>	<b>623</b>	<b>623</b>	<b>623</b>	<b>623</b>	<b>579</b>	<b>579</b>	<b>579</b>

The desalinated water in the capital Muscat is supplied by Al-Ghubrah and Barka plants (Figure 99). The Barka power generation and seawater desalination plant is located 65 km north-west of Muscat. It was the first plant in Oman to be built, operated in 2003 and owned by the private sector, AES Barka. The Barka I plant has three MSF desalination units installed, each with a capacity of 30,400 m<sup>3</sup>/d. Due to proximity to demand, availability of land and infrastructure, both Al-Ghubrah and Barka are the preferred locations for additional power generation and desalination capacity. The current independent water and power project, Barka II plant, is located adjacent to the existing Barka I plant. The Barka II power generation and seawater desalination plant has commenced its operation in November 2009, and is owned by the private sector, SMN Barka. The addition of the Barka II plant with a capacity of 120,000 m<sup>3</sup>/d produced through RO technology will bring the total desalination capacities for Muscat to 393,000 m<sup>3</sup>/d.

Sohar power generation and seawater desalination plant was the second plant to be built, operated in 2007 and owned by the private sector Sohar Power company to supply drinking water in the Batinah northern region, due to the economic growth of the Sohar industrial port area. It has four MSF desalination units installed, each with a capacity of 37,500 m<sup>3</sup>/d. The port of Sohar is situated 240 km northwest of Muscat just outside the Strait of Hormuz.

In 2009, the new RO seawater desalination plant at Sur brought an additional desalination capacity of 68,000 m<sup>3</sup>/d to satisfy the increasing demand of water in the Sharqiyah regions, on the north east front of Oman. Sur is an ancient port and trading town situated at the northern part of the Sharqiyah coast 300 km from Muscat. The new Sur independent water project is located alongside the existing RO plant commissioned in 1993 with a capacity of 12,000 m<sup>3</sup>/d. Neither of the RO desalination plants at Sur are co-generation plants. Besides the later mentioned Barka plants data has been available also for environmental impact studies of the Sur plant. The data has been acquired (personally, Munk (2008)) from Dr. Michel Claereboudt (Sultan Qaboos University), who investigated the marine impacts of the Sur plant on behalf of HMR Environmental and Engineering Consultants. The brine reject was discharged via an open sea pipe of about 20 cm in diameter next to the shoreline. As the RO desalination plant at Sur is not a co-generation plant, and assuming a recovery rate of 40-50 %, at least 500 m<sup>3</sup>/h of brine is discharged with a salinity of twice that of the ambient seawater. The plume of the discharged brine was visible as a shimmer on the water surface and covered an area of about 100 m<sup>2</sup>. At the bottom of the sea, in vicinity of the outfall, a large coral reef was situated. Several ten meters after the outfall - the distance needed for the dense RO plume to sink to the sea bottom - the corals started to become seriously damaged or were already dead. A clear transition zone between dead and still healthy corals became visible, as can be seen in Figure 101. The pictures also display the high turbidity of the water in the impact area. The dead coral zone extended over an area of several hundred meters in

length and width. According to Dr. Claereboudt, corals are highly sensitive to salinity changes.



Figure 101: Impact of the RO plant near Sur effluent on a nearby coral reef: Transition to the impact zone (left) and close-up view of dead corals within the impact zone (right) (courtesy of Michel Claereboudt)

From 2012 onward, without additional new desalination plants, the reduction in desalination capacity due to the retirement of two of the seven MSF units at Al-Ghubrah plant will result in shortfalls of between 103,000 to 144,000 m<sup>3</sup>/d from 2013 to 2015. In order to meet the future water demands, OPWP has identified a need for a new power and water desalination plant (possibly, Barka III) with a capacity of 55,000 m<sup>3</sup>/d to be built and operated by a private sector by 2012. OPWP has also proposed a new scheme to upgrade Al-Ghubrah plant by splitting the existing plant into two parts. The existing plant will be called Al-Ghubrah East, and the new independent water and power project Al-Ghubrah West with a total desalination capacity of 136,000 m<sup>3</sup>/d will be built and operated by a private sector by 2013.

The modern and recently operated Barka plants in Oman have been chosen for the case studies in the project. The plants are situated on the coastal plain along the Batinah coast near to the Gulf of Oman. The Batinah region is one of the most populated areas in Oman. The site has been designated as one of the preferred locations for the construction of up to four power generation and seawater desalination plants (i.e. Barka I to IV) to meet the growing demand for energy and water in Oman's capital area of Muscat.

### **6.1.2. Characteristics of Barka desalination plants**

Barka, which is situated on the coastal plain along the Batinah coast, is one of the chosen sites for the construction of up to four proposed power generation and seawater desalination plants (i.e. Barka I to IV). The Barka plants site is located near the Muscat-Sohar highway, about 6 km east of Barka town. The surface land features can be described as flat with a sandy strip parallel to the coastline, with coastal dunes and belts of scrubs and trees approximately 300 m inland. Ground surface elevations vary typically from 1.5 to 5 m above mean sea level, and the coastal zone is covered by finer sediments (i.e. sand and silt). The coastline is relatively flat with a slope not exceeding 1:100.

The nearest residence areas are located approximately 2 km south of the plants site, and the community uses the beach along the plants site for recreation. The beachfront area north of the site (approximately 50 m from the plants site) is active and open. The beach is used by fishermen for fishing and related activities (Figure 102), such as boat landing and loading of fishes into the transport vehicles.



Figure 102: Boat landing by fishermen at Barka beach (file photo: HMR Consultants)

There are no other major industries in the area, and several other features of significance situated near the Barka plants site include the jetty for the Royal Palace at Bait Al Baraka, which is situated approximately 11 km east of the site, and the Daymaniyat Island Nature Reserve, which is situated approximately 16 km offshore from the site. About 20 km west of the site is the promontory of Ra's Sawadi with a collection of seven islands. Several inter-tidal inlets are also found on either side of the site including Khwar Al Ayn, Khwar Muraysi, and Khwar Suwadi. (Khwar is the Arabic term describing an inter-tidal coastal lagoon.)

The Barka I plant (Figure 103) has the capacity of 427 MW generation of electricity based on combined cycle gas turbine technology using once through seawater cooling, and the desalination is based on multi-stage flash evaporation. It consists of the power facility, the desalination facility and the (common facility) seawater intake and outfall systems. The power facility has two gas turbine units, two heat recovery system generator units (boilers), and one steam turbine generator. The power plant is fuelled by natural gas, and the steam turbine is also providing energy for evaporating the seawater to produce potable water. The plant is installed with three identical MSF desalination units, the chemical dosing system, the acid cleaning system, and the re-mineralization plant.



Figure 103: AES Barka I power generation and seawater desalination plant (file photo: HMR Consultants)

As from 2009, adjacent to Barka I plant, the Barka II power generation and RO seawater desalination plant is constructed, powered by natural gas and generating a capacity of 685 MW of electricity. Both plants will be using and sharing the same existing seawater intake and outfall systems.

### 6.1.3. Barka intake and outfall system

There are two sets of existing intake and outfall pipelines (Figure 104). The Barka I and II plants share only one set of intake and outfall pipelines, which will be described as follows. The maximum capacity of the seawater intake systems is 126500 m<sup>3</sup>/h: currently, the Barka I plant uses up to a maximum flow rate of 67500 m<sup>3</sup>/h, and thus the remaining flow rate of 59000 m<sup>3</sup>/h could be used for cooling purposes in the Barka II plant. The cooling water from the power generation Barka I and Barka II plants are mixed with reject brine (and other effluents) from Barka I (MSF) and Barka II (RO) plants and are discharged into the sea through the existing outfall pipelines. The outfall system is designed for a maximum discharge flow rate of 122100 m<sup>3</sup>/h: currently, the brine discharge from Barka I plant is up to a maximum flow rate of 61500 m<sup>3</sup>/h, and thus the remaining up to a maximum flow rate of 60600 m<sup>3</sup>/h of discharges can be used for the Barka II plant.

The seawater intake system consists of four parallel pipes of 1.2 km in length and a diameter of 2.2 m. The pipes are spaced 2 m apart, buried under the seabed (not visible on the surface). The intake structure opens at 1.5 m above the seabed at a water depth of 10 m. Each intake is equipped with a riser and velocity cap designed to convert vertical to horizontal water flow (Figure 105).

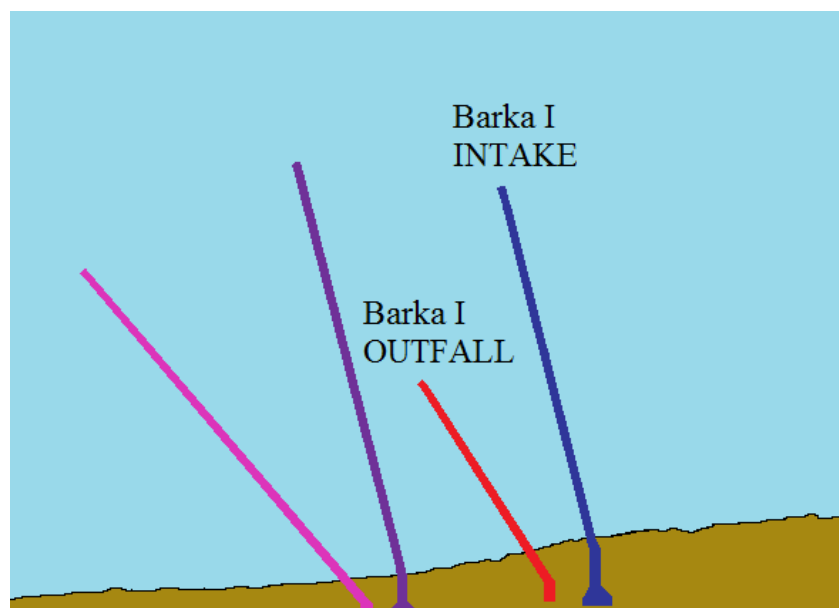


Figure 104: The intake and outfall systems of Barka I plant. Barka II will share the intake and outfall structures with Barka I. The other structures are for future installations (modified HMR, 2007)

Onshore, the seawater intake structure is equipped with the screening and pumping systems. The screening system consists of three sets of bar and travelling band screens to remove any debris that may be sucked in through the pipelines. The intake seawater is chlorinated by dosing with sodium hypochlorite solution at a maximum dosage of 0.2 ppm in the intake risers and into the inlet bar screens to prevent any algae growth in the seawater circulating system. The pumping system has two condenser cooling water pumps and two auxiliary

cooling water pumps for the power facility, and four main seawater pumps for the desalination facility (Figure 106).

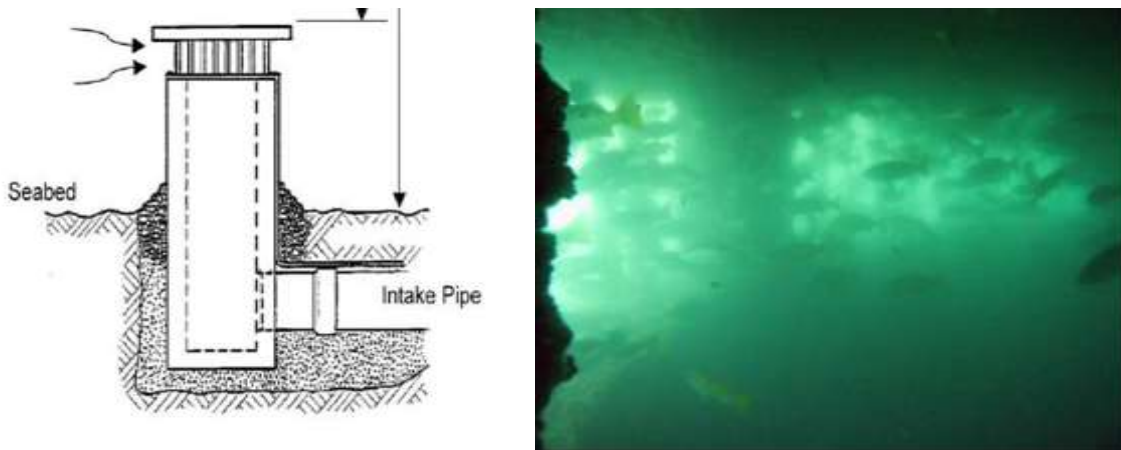


Figure 105: Velocity cap intake terminal (left) and fish community inside the velocity cap (right) (file photo: HMR Consultants)

The flowrates for Barka I plant are given in Table 26, where a flow rate of 200 m<sup>3</sup>/h is needed for spraying the travelling band screen, and another at 200 m<sup>3</sup>/h for the chlorine tank. A flow rate of 31665 m<sup>3</sup>/h is used for the three MSF units, where 69.5 % of the seawater is used for cooling water discharge. Antifoam (ethylene / propylene oxide co-polymer) at a dosage of 0.5 ppm is added to the remainder make-up water at a flow rate of 9660 m<sup>3</sup>/h. Antiscalant (hydrolyzed polymaleic anhydride) with a dosage of 1.6 ppm is also added to the brine recirculation at a flow rate of 12873 m<sup>3</sup>/h. The discharge characteristics of the MSF unit is given in Table 27. No measured data of the the Barka II plant has been available, thus project data has been used as mentioned later.

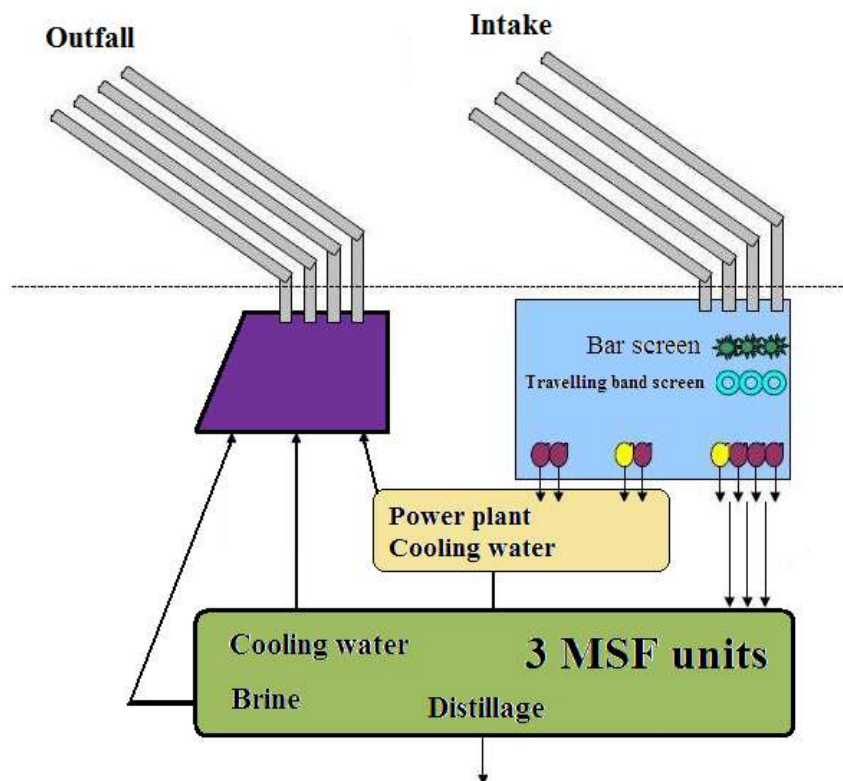


Figure 106: The intake and outfall system of Barka I plant (modified Abdul-Wahab and Jupp, 2009)

Table 26: Quantities of seawater intake and outfall discharge during normal plant operation

Barka I (MSF) plant	Seawater intake ( m <sup>3</sup> /h)	Outfall discharge (m <sup>3</sup> /h)
Desalination plant	37650	33789
Power plant	29450	27650
<b>Total</b>	<b>67100</b>	<b>61439</b>

Table 27: Barka I plant water characteristics during normal plant operation

Barka I (MSF) plant	Flow rate ( m <sup>3</sup> /h )	Temperature (°C)	Salinity (ppt)
Seawater intake	67500	24	36
Brine (blow down)	5799	42.11	66.6
Desalination plant's cooling water	22005	24.2	36
Power plant's cooling water	<b>27650</b>	<b>32</b>	<b>36</b>
Outfall discharge	61437	37	40.8

The outfall facilities are designed to discharge the combined brine reject from the desalination plants and the once through condenser cooling water system from the power plants.

To avoid the circulation of concentrated brine discharges to the intake system, the sea outfall discharge point is constructed at a distance of 800 m from the intake point. The outfall system consists of four parallel pipes oriented at 62 degrees to the coastline, each with a diameter of 2.5 m, buried at 5 m below the seabed (not visible on the surface) and spaced equally at 4.8 m apart. Each pipe has a 62.4 m long multiport diffuser, consisting of nine ports spaced equally at 7.5 m apart, to enhance the dilution rates of the brine plume with a maximum temperature of 8 °C higher than the intake seawater temperature. The multiport diffusers are arranged as illustrated in in (Figure 107), each pair diverging at an angle of 30 degrees on either side of the outfall pipelines. The two internal pipes of length 653 m have its end at 9 m below the mean sea level, while the other two shorter external pipes of length 582 m end at 8.4 m below the mean sea level. The ports of each diffuser are oriented in an alternating way each with an angle of 20 degrees to the diffuser pipe. The port diameter is 0.7 m and located at 1 m above the seabed. The ports are oriented furthermore with an angle of 10 degrees upwards against the horizontal.

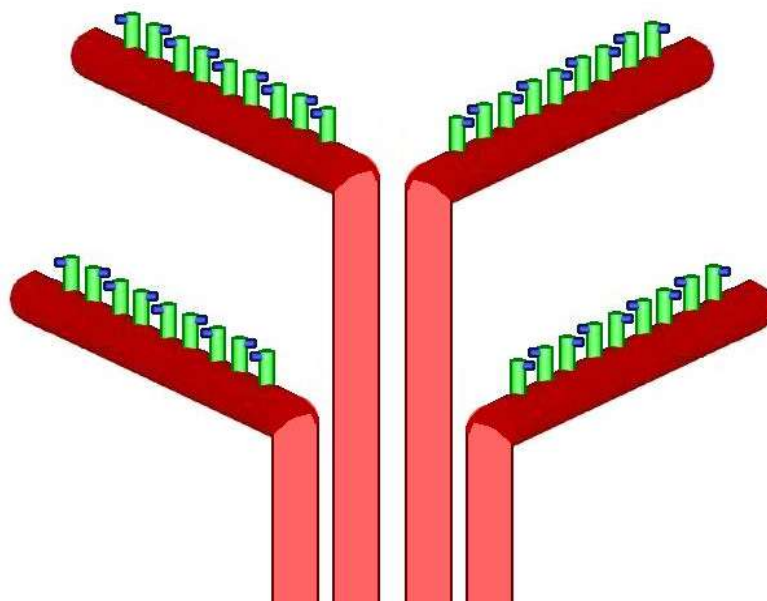


Figure 107: Multiport diffusers at the end of the outfall pipes

#### 6.1.4. Marine environment at Barka plants location

The marine environment within the region can be divided into three zones: inter-tidal zone, sub-tidal and island environments. The inter-tidal zone is typically uniform at the foreshore near the Barka plants site, and the near-shore benthic marine environment around Barka is predominantly sand. Because of the lack of a stable substrate for corals and other benthic organisms to attach to, there are very few hard bottom communities in the area. This lack of near-shore habitat has given rise to the practice of building artificial reefs by the Barka fishing community. The nearby Daymaniyat Island is an archipelago of nine islands, and these islands provide a protected habitat for a diverse population of birds, marine and terrestrial fauna. The deeper water rocky reef communities of Daymaniyat and Ra's Sawadi are the only areas in the region with good coral development. The bathymetry is shown in Figure 108.

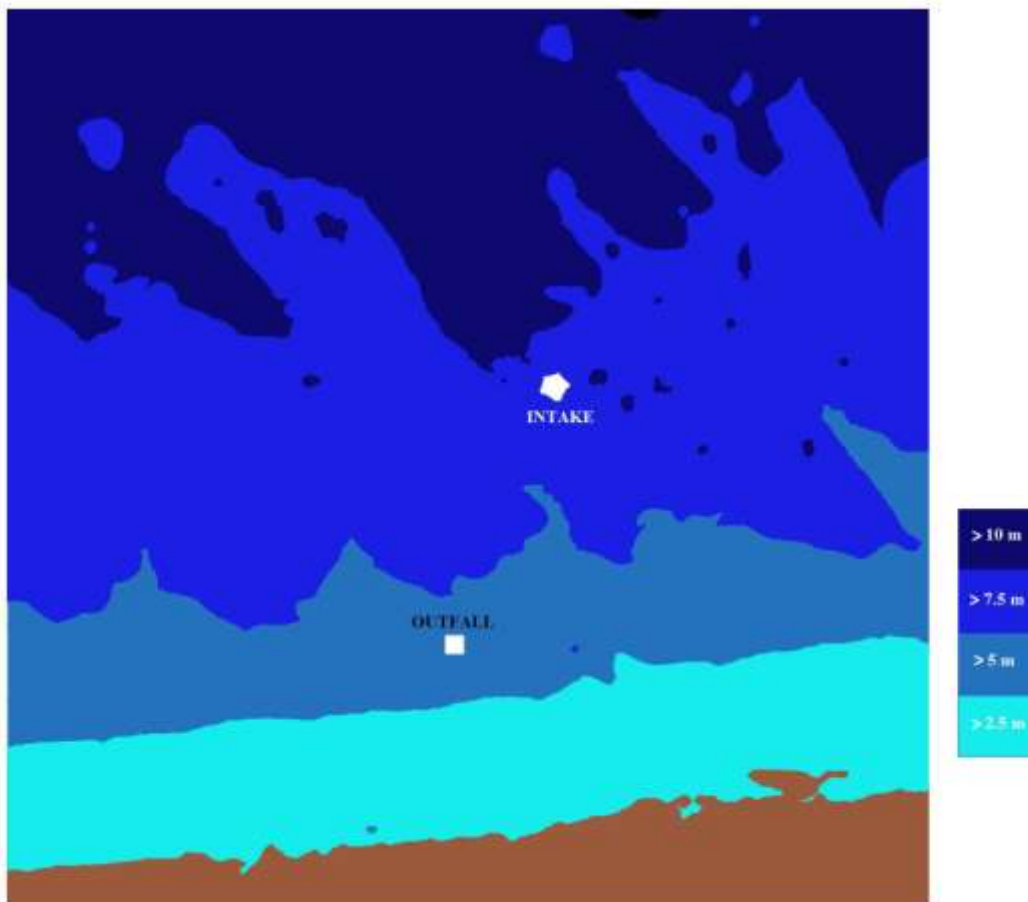


Figure 108: Bathymetry contour of the Barka plants location site (modified Wallingford, 2001)

Long stretches of the Batinah coast have unstable sand substrates resulting in high turbidity and poor underwater light penetration, making it unsuitable for coral growth. The coastline, however, is characterized by mangrove forests, and the mangrove root system traps and binds sediments. Khwar Suwadi, approximately 20 km to the west of the plants site, has been planted with a mangrove nursery to assist in stabilizing the inter-tidal area.

A field survey in the vicinity of the intake and outfall systems was conducted in January 2007 on behalf of the HMR Environmental and Engineering Consultants to determine the marine environmental quality and to assess the impacts of Barka I plant operations (Figure 109). A series of dives and two-minute swims were undertaken to provide a general understanding of the habitat around the outfall pipelines, which were constructed buried at the seabed and have a series of inspection valves at 100 m intervals. These valves are surrounded by rocks, which

provide stability but also serve as an artificial habitat for marine life. In addition to the inspection valves, there are also large filters at the ends of intake pipelines and diffusers at the ends of outfall pipelines.

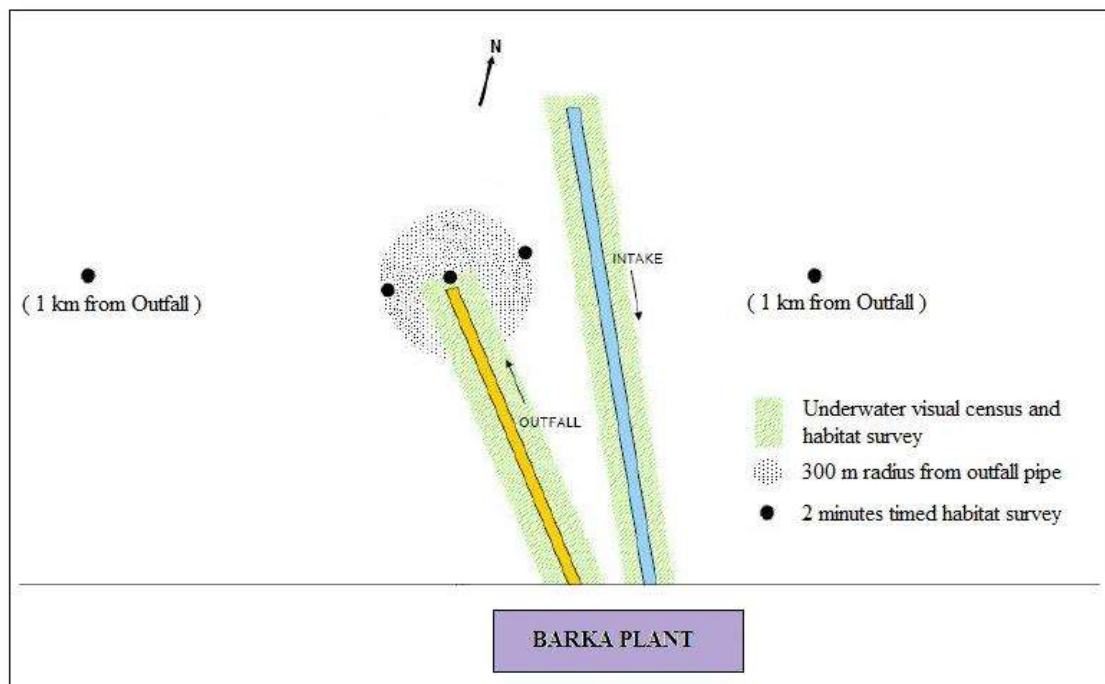


Figure 109: Location of field survey by the HMR Consultants (HMR, 2007)

Very little habitat was found away from the existing pipelines. The rock piles around the inspection valves provide a significant source of habitat and barnacles were the dominant benthic macrofauna (Figure 110a). Although hard corals were not found, there was nevertheless an abundance of other benthic macrofauna such as hydroids, sponges, tunicates, sea urchins, anemones and tube worms. There was also a particularly high density of reef scallop found within the rock piles (Figure 110b).

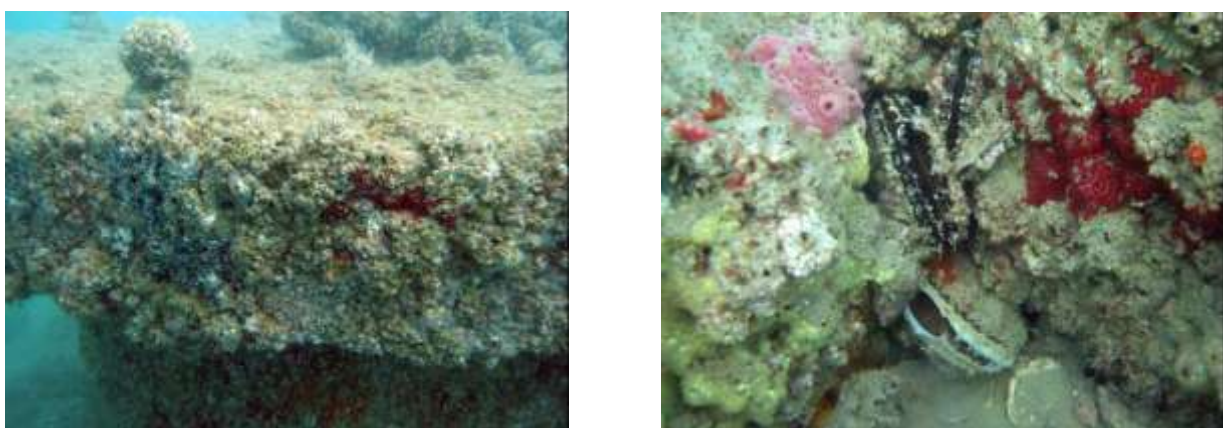


Figure 110: (a) Barnacles found at an inspection valve (left). (b) Reef scallops found on the rock piles around an inspection valve (right) (file photo: HMR Consultants)

There was a healthy fish community associated with the rock piles (Figure 111). The highest densities of fish were found at the four intakes (Figure 105). The size of the intake terminals is large enough to provide a significant habitat for shelter, somewhat similar to a ledge or cave in a natural system.



Figure 111: Fish community found on the rock piles stabilising an inspection valve (file photo: HMR Consultants)

The benthic assemblage along the outfall pipelines was found to be similar to that on the intake pipelines. However, the most obvious manifestation of a discharge effect was seen with the distribution of the reef scallops along the pipeline. No scallops were seen around the outfall diffusers, but there were some found at the inspection valves 100 m away from the discharge point; at the inspection valve 200 m away, scallop densities were observed to be similar to those seen along the intake pipelines. The actual diffusers were relatively unfouled with only a light covering of barnacles and other benthic fouling organisms (Figure 112).

Fishes were found actively swimming around the outfall diffusers (Figure 113), where they would have been immersed in higher salinity and warmer water, and displayed no signs of distress.



Figure 112: Outfall diffuser for discharge of brine (file photo: HMR Consultants)



Figure 113: Fish community around the outfall diffuser (file photo: HMR Consultants)

This study concluded that no evidence of deleterious effects was observed as a result of the existing intake pipelines. On the other hand, the intake pipelines and inspection valves were observed to be of positive influence on the local marine community by forming artificial habitats. The use of velocity cap intake terminal design was found to be a minimally obtrusive method of extracting water. The horizontal flow rates observed at these terminals were minimal, and did not create impacts for the resident fish assemblage.

Conclusions regarding the outfall impacts noted that biological effects from Barka I plant were observed (using the density of reef scallops). However, these effects were found to be localized and unnoticeable outside a 100-200 m radius around the outfall diffusers. The outfall risers were found to be effective in dispersing the hypersaline discharge from the plant, which in turn indicates that there are no significant impacts due to Barka I operations since 2003.

Another study investigated the impacts of the desalination plant on sediment characteristics. Sediments are considered to be 'sinks' for pollutants and heavy metals in sediment are of concern because of the long-term problems caused by the bioaccumulation of metals by marine organisms. Bottom sediment samples were collected by Dr. Sabah Abdul-Wahab in November 2004 to examine the concentrations of heavy metals in subtidal sediments in the vicinity of Barka I plant (Figure 114). The results were reported in Abdul-Wahab and Jupp (2009), who concluded that the sediments were not heavily polluted by heavy metals. The concentrations of Cu, Zn, Pb and Cd in sediments appear to be derived from the plant discharges of corrosion products, and the concentrations of the other metals (Cr, Fe, Ni, V) appear to have a geochemical source, i.e. presumably due to their likely common origin from mantle ophiolites rock found nearby. Note also that Vanadium is an oil-related metal present mainly in organometallic form in crude oil and has been considered as a marker for petroleum hydrocarbon contamination from illegal discharging from tankers passing the northern Gulf of Oman coast.

The distribution surface seawater temperature and salinity is given in Figure 115. As expected, the distribution shows a similar pattern following the predominant coastal current directions carrying away the thermal brine plume from the outfall.

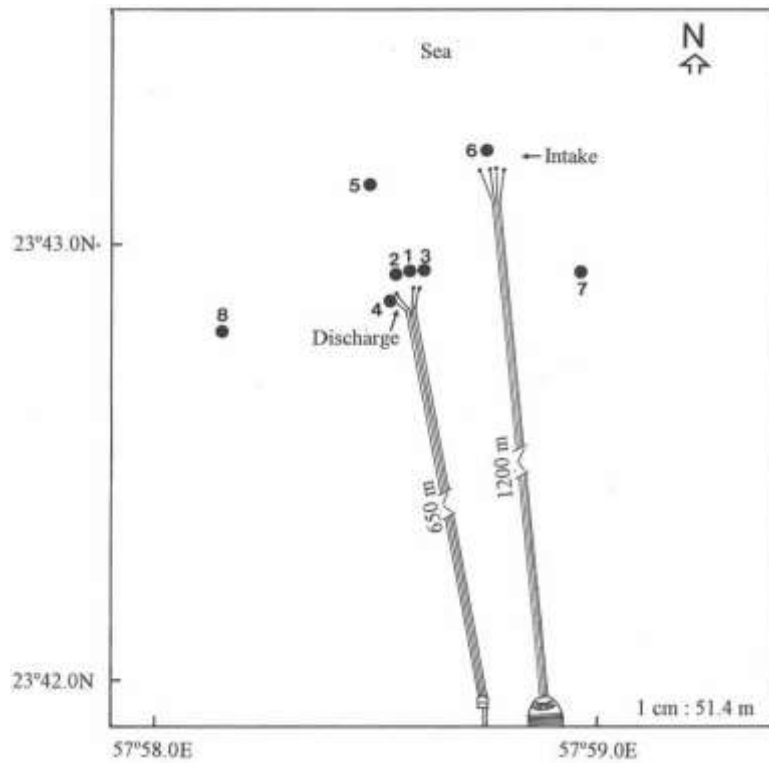


Figure 114: Sediment sampling stations in the vicinity of Barka I plant (Abdul-Wahab and Jupp, 2009)

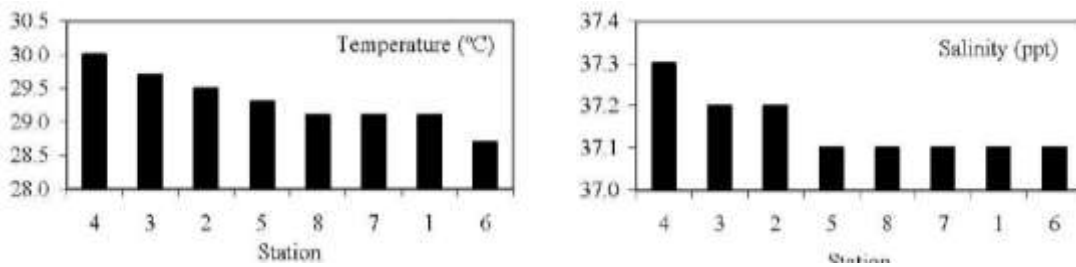


Figure 115: Distribution of temperature and salinity in surface seawater around the Barka I plant (modified Abdul-Wahab and Jupp, 2009)

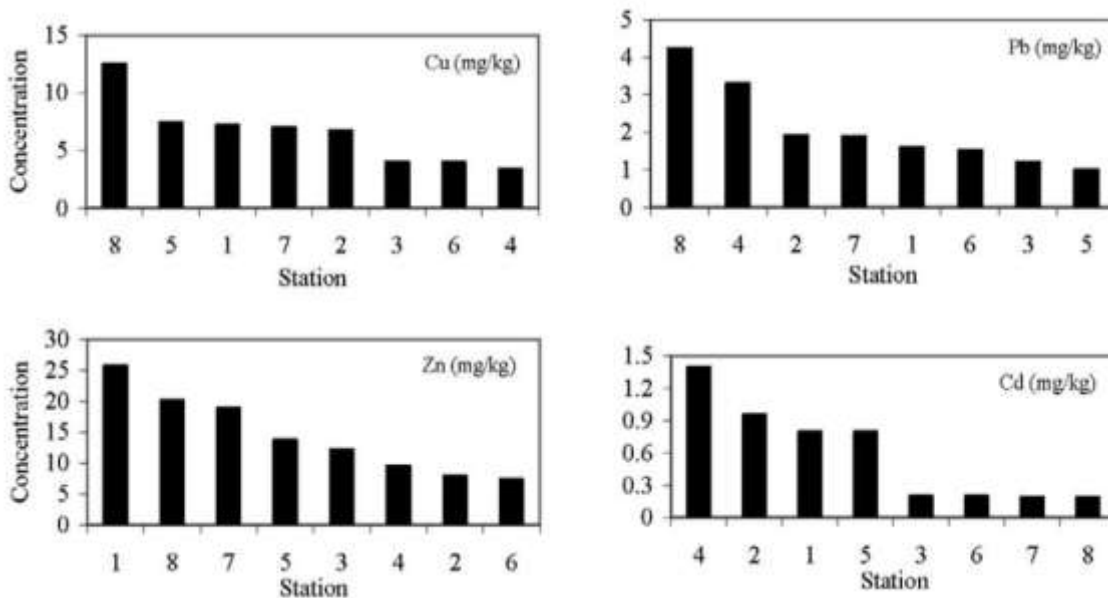


Figure 116: Distribution of heavy metals in sediment associated with the outfall discharges from Barka I plant (modified Abdul-Wahab and Jupp, 2009).

Figure 116 show the bar graphs of the heavy metal sampled concentrations of Cu, Zn, Pb and Cd in relation to possible sources from the outfall discharge. Slightly higher concentrations were observed at distances from the outfall. Due the predominant westerly coastal currents, it is possible to assume that the discharge plume carries Cu and Zn further out as dissolved metals and they fall into the sediment after being adsorbed onto suspended solids. Abdul-Wahab and Jupp (2009) also concluded that it is likely that Cu and Zn come from corrosion in pipelines or other corrosion products, but it is less clear as to where Pb and Cd may come from.

The maximum heavy metals concentrations found in the bottom sediments are given in Table 28, and were compared with the UK Ministry of Agriculture, Fisheries and Food (MAFF) action levels, the US Environmental Protection Agency (EPA) threshold levels and the trigger values quoted in the Australian Water Quality Guidelines for Fresh and Marine Waters (ANZECC). The final column shown in Table 28 indicates if any of the environmental quality standards (EQS) mentioned was met or not. Only Ni and Cr are above the guidelines but these are expected as the coastal sediment along the northern Gulf of Oman originates from weathered Cr-rich ophiolite rocks (Abdul-Wahab and Jupp, 2009).

Table 28: Comparison between sample concentrations collected from Barka I plant (Abdul-Wahab and Jupp, 2009)

Heavy metal (mg/kg)	Barka maximum levels	MAFF action levels	EPA threshold levels	ANZECC trigger values	EQS met?
Cadmium (Cd)	1.4	2	31	1.5	Yes
Copper (Cu)	12.5	40	136	65	Yes
Chromium (Cr)	56.8	100	25	80	No (EPA)
Iron (Fe)	3547	-	-	-	-
Nickel (Ni)	187	100	132	21	No
Lead (Pb)	4.2	40	132	50	Yes
Vanadium (V)	10	-	-	-	-
Zinc (Zn)	25.8	200	760	200	Yes

### 6.1.5. Oceanographic field data at Barka plant location

To assist the design of the proposed seawater intake and outfall system for the Barka I plant, a field exploration and marine survey were conducted on behalf of the HR Wallingford during February-March 2001 (Wallingford, 2001). These measurements and data collected before the plant offshore work commences include bathymetric, water elevation, wind speed and direction, current meter, and current, temperature and salinity profiles during a single spring tide (24 February) and neap tide (3 March) at five specified locations.

The regional bathymetry of the Barka coastline is available from the admiralty charts Oman 3505 (scale 1:350,000) and Oman 3523 (scale 1:100,000) supplied by the National Hydrographic Office, Oman. The gradient is about 1:140 up to 10 m depth and about 1:220 between the 10 m and 30 m depth. Near the plant site, the water depth reaches 5 m at about 700 m offshore and 10 m at about 2000 m offshore. The slope remains relatively constant along the coastline near the plant site.

Based on the bathymetric survey, defined by a 2000 m by 2000 m box extending approximately 0.5 km to the east and 1.5 km to the west of the plant site, undertaken for the Barka I plant (Wallingford, 2001), no notable seabed features in the area have been found. The site specific bathymetry data generated is shown in Figure 108.

Relatively little is known about the finer scale oceanography of the northern coast of Oman where dynamics are more likely to be driven at a local rather than regional scale. The continental shelf is narrow, and shallow water effects are generally insignificant. Therefore, the nature of tide in Oman is best treated as being diurnal in nature. Along the coast of Oman, the tide has a large daily inequality with a spring-tide range of 2.6 m or more. According to the Oman Maritime Book 2009 (National Hydrographic Office, 2008), the tidal characteristics at Wudam, the nearest tidal station to the plant site, are shown in Figure 117.

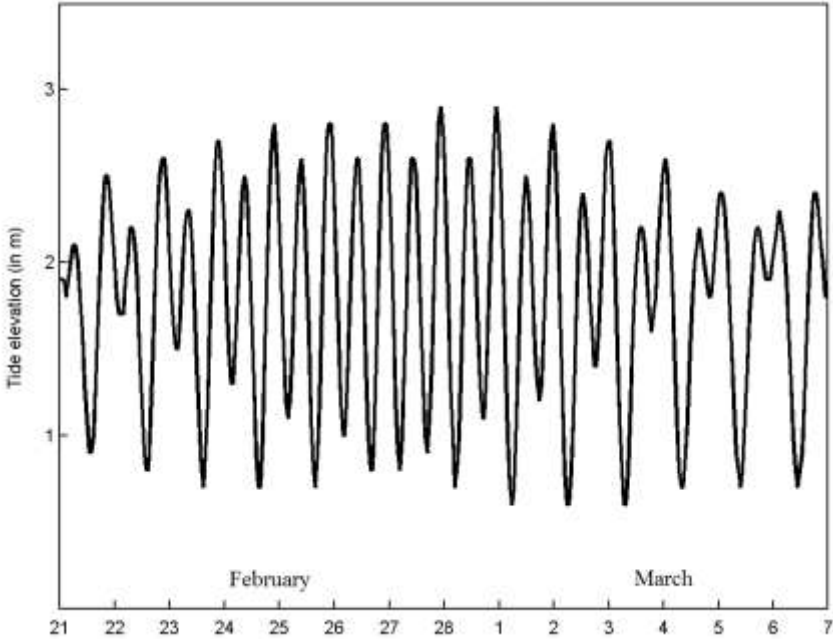


Figure 117: Tidal characteristics at Wudam station (plotted from the National Hydrographic Office, 2008) relative to the lowest astronomical tide.

Based on the field measurements undertaken for the Barka I plant (Wallingford, 2001), the autonomous tidal gauge data generated is shown in Figure 118.

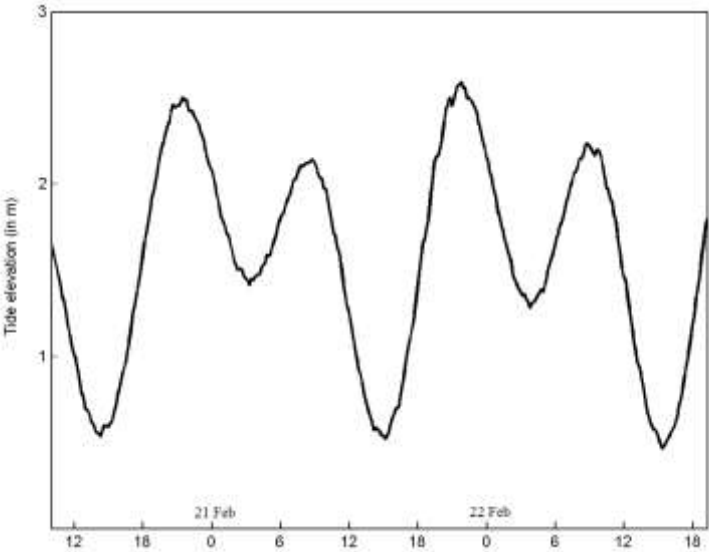


Figure 118: Water elevation measured by a tide gauge at Barka I (plotted from Wallingford, 2001) The nearest meteorological station to the plant site is located at the Muscat International Airport (formerly Seeb), which is 30 km to the east. The data for the year 2002 recorded for Seeb by the Directorate of Meteorology are presented in Table 29 and Figure 119.

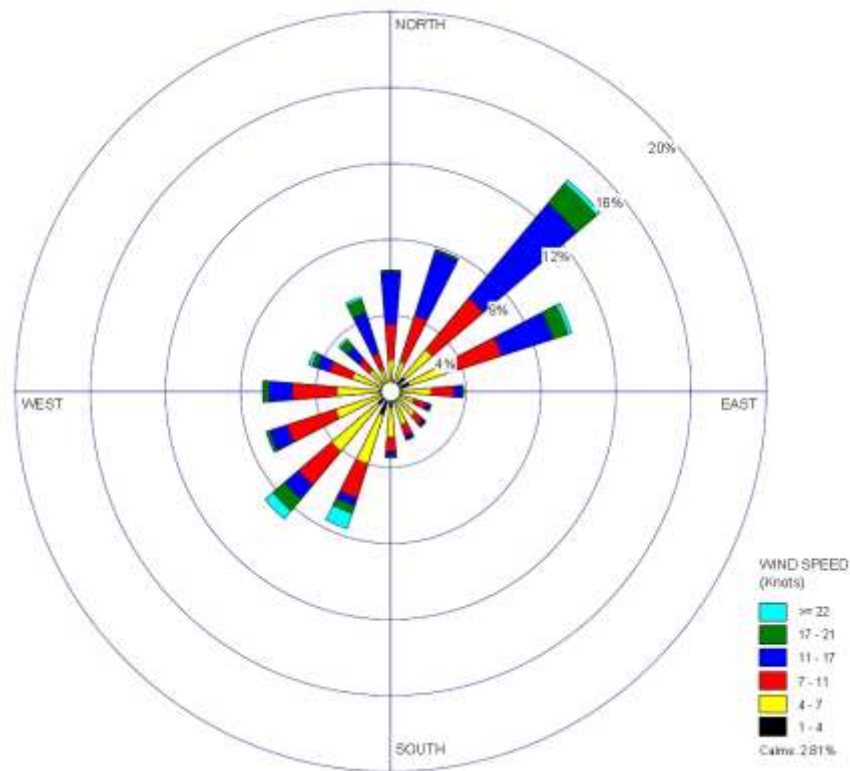


Figure 119: Statistical analysis of wind directions and speed for the year 2002 (HMR, 2007)

The meteorological data shows that mean air temperatures range from 21.3 °C in February to 35 °C in May-June, and the extreme recorded temperatures range between 11.7 °C to 47.8 °C. The mean wind speeds range between 2.16 to 3.34 m/s, with high wind speeds encountered during the summer months. The predominant wind direction is from northeast during June-September and from southwest during November-January.

Table 29: Meteorological data for Seeb for the year 2002 (HMR, 2007)

Month	Air temperature (°C)			Relative humidity (%)			Wind speed (m/s)	Dominant wind direction (degrees)
	Mean	Max	Min	Mean	Max	Min	Mean	Mean
January	21.4	30.1	12.5	55	95	21	2.68	210
February	21.3	29.3	11.7	61	97	26	2.52	210
March	25.3	35.4	16.6	57	97	6	2.57	360
April	29.5	42.7	20.8	43	94	8	2.98	330
May	35.0	47.8	25.7	36	94	4	3.34	210
June	35.0	47.5	28.4	50	95	8	3.03	60
July	33.6	47.5	27.2	64	97	7	2.98	60
August	30.7	43.9	25.3	75	96	11	2.83	60
September	29.6	42.2	23.8	77	99	16	2.47	60
October	29.5	40.5	21.3	62	95	9	2.26	30
November	25.4	35.3	19.0	66	94	22	2.16	210
December	22.4	32.4	13.2	62	92	21	2.26	210

Based on the autonomous meteorological readings undertaken for the Barka I plant (Wallingford, 2001), the data generated is shown in Figure 120.

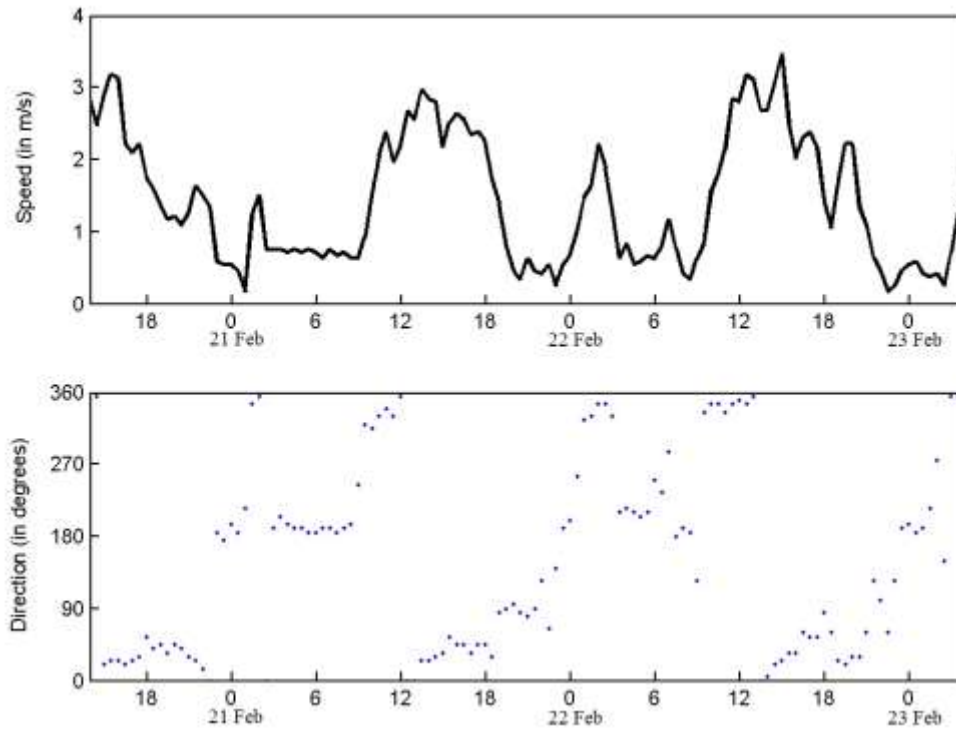


Figure 120: Wind speed (top) and direction (bottom) measured at the Barka plant I (plotted from Wallingford, 2001)

The general flow in the ocean currents in the Gulf of Oman is in anticlockwise direction. The currents originate from the coast of Iran and flow toward the Arabian Gulf, and then reverses to the Arabian Sea along the coast of Oman (Figure 121). That is, along the northern coast of Oman, the coastal current moves southeastward from the Gulf of Oman towards Muscat. The predominant coastal current flows at the Barka plants site are from the west, and the strong horizontal and mainly westerly currents with maxima at spring tides are of up to 0.22 m/s.

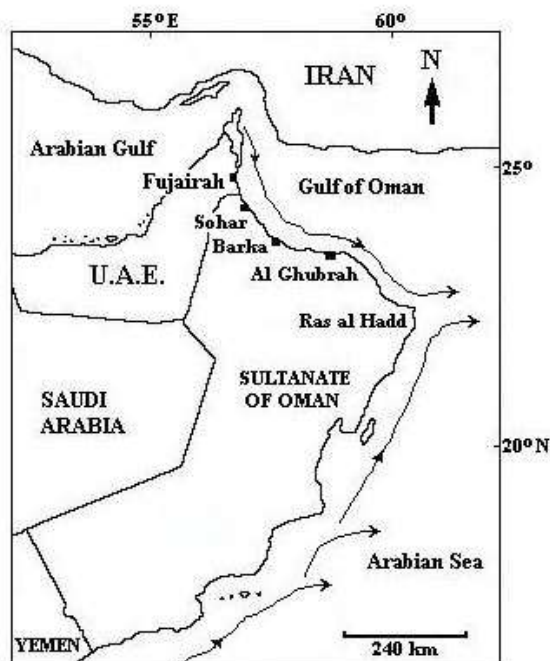


Figure 121: Coastal currents along the coast of Oman (Purnama and Barwani, 2006)

Based on the autonomous current meter readings (Wallingford, 2001), the data generated at the proposed location for the Barka I outfall is shown in Figure 122. The current speed appears to be weak and variable in magnitude. The direction is rather stable.

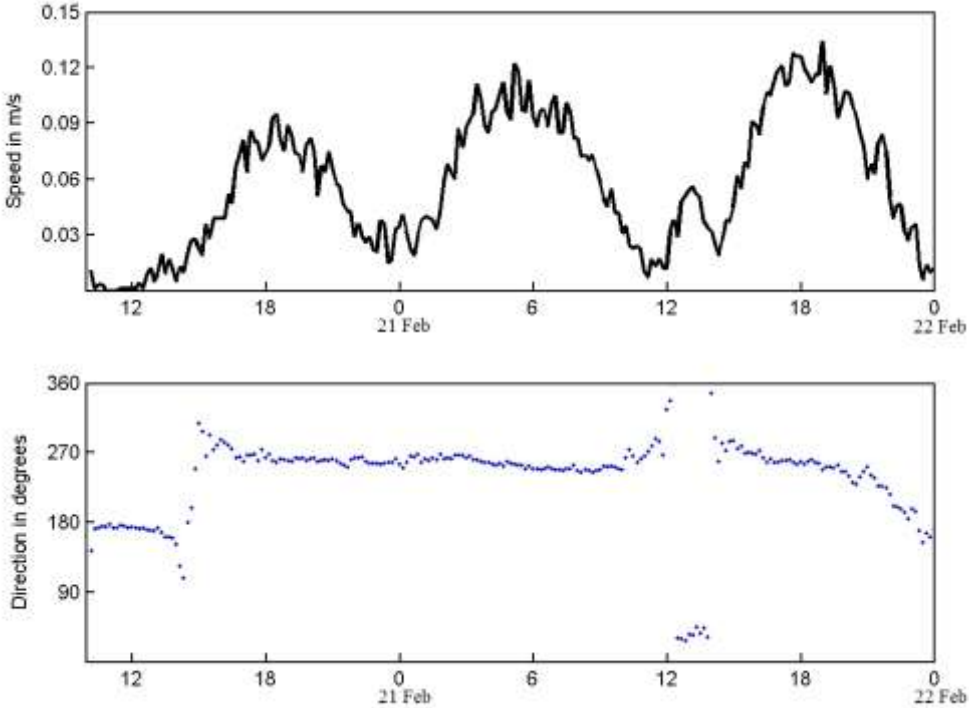


Figure 122: Current speed (top) and direction (bottom) measured at the proposed location of the Barka plant I outfall (plotted from Wallingford, 2001)

Direct reading of the current, temperature and salinity measurements were taken throughout the water column at one hourly interval over a period of 12 hours at both the spring tide (24 February) and neap tide (3 March) at five specified locations. The mean current, temperature and salinity profiles for the spring and neap tides at the proposed location for the Barka I outfall site are shown in Figure 123. The subsequent data for temperature and salinity following the Barka I plant operation are shown in Table 30.

Table 30: The surface seawater data collected annually at the Barka I plant

Date	Salinity (ppt)		Temperature ( °C )	
	Outfall	Intake	Outfall	Intake
8 June 2003	38.9	37.3	37	30.2
9 June 2003	39.1	37.5	34.7	30
6 April 2004	40.8	38.4	33.5	27.5
6 April 2004	40.7	38.3	34	27.5
3 April 2006	39.9	38.0	34	27.5
3 April 2006	40.2	38.4	33	27
18 April 2007	40.6	38.3	34	29
25 April 2007	38.6	36.3	33	28

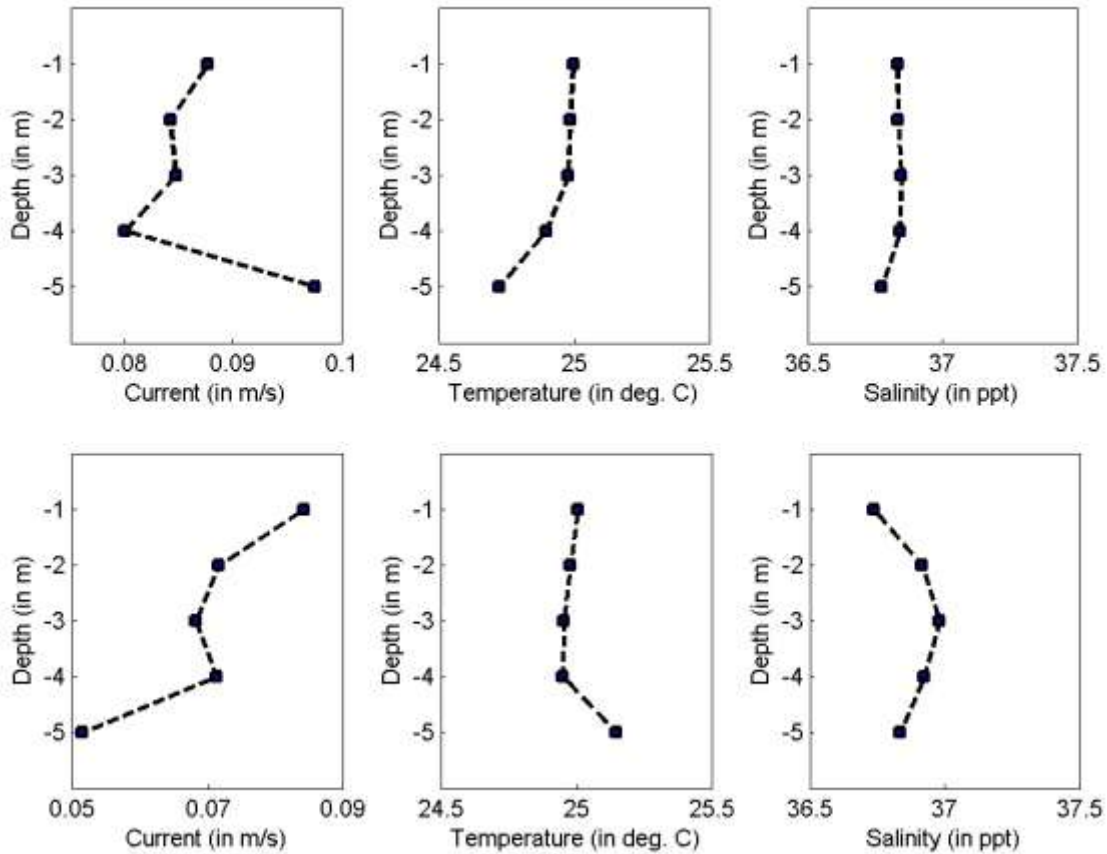


Figure 123: Spring (top row) and neap (bottom row) tides mean values of current, temperature and salinity measured at the proposed location of the Barka plant I outfall (plotted from Wallingford, 2001)

### 6.1.6. Application of discharge calculator for Barka plants

The scenarios used for modelling purposes are the effluent discharges from the Barka I (MSF) plant to represent a positively buoyant plume, and the effluent discharges from the Barka II (RO) plant to represent a negatively buoyant plume. The applications of the discharge calculator for both scenarios are given and similarly the CORMIX simulations for both scenarios in the following section.

Although both Barka I and Barka II plants use and share the same seawater intake and outfall systems, the intake seawater will be used only for cooling purposes in the Barka II plant. New intake pipelines will be constructed for Barka II (RO) plant, roughly in between the existing two intakes sites (Figure 104). The pipe will be of 1.6 m diameter and the flow rate required for Barka II plant will be of 15500 m<sup>3</sup>/h.

The first sheet of the discharge calculator for the Barka I (MSF) plant (Figure 124) computes the outfall discharges plume as positively buoyant. The second sheet of the discharge calculator for the Barka I (MSF) plant (Figure 125) suggests the Barka I plant to use a multiport diffuser with 9 ports with diameter of 0.7 m.

## Flowrates & Effluent Characteristics

### - ambient characteristics (= intake water)

ambient temperature	$T_o =$	24.00	°C
ambient salinity	$Sal_o =$	36.00	ppt
ambient density	$\rho_o =$	1024.09	kg/m <sup>3</sup>
ambient kin. viscosity	$\nu_o =$	9.59E-07	m <sup>2</sup> /s

### - drinking water (permeate)

flowrate	$Q_{drink} =$	1.07	m <sup>3</sup> /s
recovery rate	$r_{dist} =$	40	%
distillation intake flowrate	$Q_{in} =$	2.68	m <sup>3</sup> /s

### - brine characteristics (effluent from desalination process)

brine flowrate	$Q_{brine} =$	1.61	m <sup>3</sup> /s
temperature	$T_{brine} =$	42.00	°C
salinity	$Sal_{brine} =$	59.85	ppt
density	$\rho_{brine} =$	1035.37	kg/m <sup>3</sup>
substance concentration 1	$C_{brine1} =$	0.20	ppm
substance concentration 2	$C_{brine2} =$	1.60	ppm
substance concentration 3	$C_{brine3} =$	0.50	ppm

### - blended effluent 1 - internal - (i.e. cooling water)

flowrate	$Q_{int} =$	6.26	m <sup>3</sup> /s
temperature	$T_{int} =$	24.00	°C
salinity	$Sal_{int} =$	36.00	ppt
density	$\rho_{int} =$	1024.09	kg/m <sup>3</sup>
substance concentration 1	$C_{int1} =$	0.20	ppm
substance concentration 2	$C_{int2} =$	0.00	ppm
substance concentration 3	$C_{int3} =$	0.00	ppm

### - blended effluent 2 - external - (e.g. waste water or others)

flowrate	$Q_{ex} =$	7.68	m <sup>3</sup> /s
temperature	$T_{ex} =$	32.00	°C
salinity	$Sal_{ex} =$	36.00	ppt
density	$\rho_{ex} =$	1021.43	kg/m <sup>3</sup>
substance concentration 1	$C_{ex1} =$	0.20	ppm
substance concentration 2	$C_{ex2} =$	1.60	ppm
substance concentration 3	$C_{ex3} =$	0.50	ppm

### Plant characteristics:

feedwater flowrate	$Q_{feed} =$	8.95	m <sup>3</sup> /s
rejected effluent	$Q_{plant} =$	7.88	m <sup>3</sup> /s
recovery rate (desal. plant)	$r =$	12.0	%
effluent temperature	$T_{plant} =$	27.69	°C
temp. difference to ambient	$\Delta T =$	3.69	°C

### Final effluent characteristics:

flowrate	$Q_o =$	15.56	m <sup>3</sup> /s
effluent temperature	$T_o =$	29.82	°C
effluent salinity	$Sal_o =$	38.47	ppt
effluent density	$\rho_o =$	1024.04	kg/m <sup>3</sup>
buoyant acceleration	$g_o' =$	0.00046	m/s <sup>2</sup>
kin. viscosity	$\nu_o =$	8.51E-07	m <sup>2</sup> /s
substance concentration 1	$c_{o,1} =$	0.20	ppm
substance concentration 2	$c_{o,2} =$	0.96	ppm
substance concentration 3	$c_{o,3} =$	0.30	ppm

### annotations:

$T = 10$  to  $180^\circ\text{C}$  (see density calculator)

$Sal = 0$  to  $160$  ppt (ppt = g/kg)

allowed ranges for viscosity calculation:

$Sal = 0$  to  $130$  ppt,  $T = 10$  to  $180^\circ\text{C}$  (El-Dessouky, Ettouney (2002))

recovery rate:

percentage of distillation feedwater converted into distillate;

without cooling water, only for distillation!!

following Lattemann (2006):  $r_{dist} = 30-35\%$

$T = 10$  to  $180^\circ\text{C}$  (following Lattemann:  $90-115^\circ\text{C}$ )

with  $Sal_{drink} = 0$  ppt (following Lattemann: up to  $50$  ppt)

e.g. chlorine

e.g. anti-scalants

...

2 to 3 times the intake water flowrate

ambient temperature (allowed range:  $T = 10 - 180^\circ\text{C}$ )

ambient salinity (allowed range:  $Sal = 0$  to  $160$  ppt)

e.g. chlorine (same substance as  $C_{brine1}$ )

e.g. anti-scalants (same substance as  $C_{brine2}$ )

... (same substance as  $C_{brine3}$ )

$T = 10$  to  $180^\circ\text{C}$

$Sal = 0$  to  $160$  ppt.

e.g. chlorine (same substance as  $C_{brine1}$ )

e.g. anti-scalants (same substance as  $C_{brine2}$ )

... (same substance as  $C_{brine3}$ )

intake water for distillation & cooling

following Lattemann (2006):  $r = 10-13\%$

following Lattemann (2006):  $5-15^\circ\text{C}$  above ambient

mean average

mean average

$g_o' = g \cdot (|\rho_o - \rho_s|) / \rho_o$

$g_o' > 0$ : positively buoyant,  $g_o' < 0$ : negatively buoyant

Figure 124: The first sheet of the discharge calculator for the Barka I (MSF) plant

## Discharge Characteristics

### - ambient characteristics

ambient density	$\rho_o =$	<input type="text" value="1024.09"/>	kg/m <sup>3</sup>
buoyant acceleration	$g'_o =$	<input type="text" value="0.00046"/>	m/s <sup>2</sup>

### - effluent characteristics

flowrate	$Q_o =$	<input type="text" value="15.56"/>	m <sup>3</sup> /s
discharge density	$\rho_o =$	<input type="text" value="1024.04"/>	kg/m <sup>3</sup>
kin. viscosity	$\nu_o =$	<input type="text" value="8.51E-07"/>	m <sup>2</sup> /s

### - discharge characteristics

port discharge velocity	$U_o =$	<input type="text" value="5.00"/>	m/s
number of openings	$n =$	<input type="text" value="9"/>	
port diameter	$D =$	<input type="text" value="0.66"/>	m

dens. Froude Number	$Fr_o =$	<input type="text" value="287.30"/>	
Reynolds Number	$Re_o =$	<input type="text" value="3.90E+06"/>	

annotations:

recommended:  $U_o = 4-6$  m/s

start with one opening!

$$Fr_o = U_o / (|g'_o| * D)^{1/2} = Q_o / (D^2 \rho / 4)^{1/2} / (|g'_o| * D)^{1/2}$$

$$Re_o = U_o * D / \nu_o$$

Checking of characteristic properties:

Diameter  $D$ : in required range, ok!

Froude Number  $Fr_o$ : huge value, please check openings!

Reynolds Number  $Re_o$ : in required range, ok!

required:

$0.1 \leq D \leq 1.0$

$Fr_o \geq 10$ , recommended:  $Fr_o = 20-25$

$Re_o > 4000$

Choose an appropriate port diameter (DN according to ISO standard):

port diameter	$D =$	<input type="text" value="0.70"/>	m
---------------	-------	-----------------------------------	---

### Final discharge characteristics:

port diameter	$D =$	<input type="text" value="0.70"/>	m
number of openings	$n =$	<input type="text" value="9"/>	
flowrate (individual)	$Q_{o,ind.} =$	<input type="text" value="1.73"/>	m <sup>3</sup> /s
port discharge velocity	$U_o =$	<input type="text" value="4.49"/>	m/s
dens. Froude Number	$Fr_o =$	<input type="text" value="251.25"/>	
Reynolds Number	$Re_o =$	<input type="text" value="3.70E+06"/>	
buoyancy flux	$J_o =$	<input type="text" value="0.001"/>	m <sup>4</sup> /s <sup>3</sup>
momentum flux	$M_o =$	<input type="text" value="7.76"/>	m <sup>4</sup> /s <sup>2</sup>
discharge length scale	$L_Q =$	<input type="text" value="0.62"/>	m
momentum length scale	$L_M =$	<input type="text" value="165.57"/>	m

$$J_o = g'_o * Q_o \quad (> D: \text{positively buoyant})$$

$$M_o = U_o * Q_o$$

$$L_Q = (D^2 * \pi / 4)^{1/2} = Q_o / M_o^{1/2}$$

$$L_M = M_o^{1/2} / J_o^{1/2}$$

Figure 125: The second sheet of the discharge calculator for the Barka I (MSF) plant

The input data for the application of the discharge calculator to the Barka plants are given in Table 31. As the Barka II plant has been under construction during the working period of this report, only the estimated values have been used for the second scenario.

The first sheet of the discharge calculator for the Barka II (RO) plant (Figure 126) computes the outfall discharges plume as a negatively buoyant. The second sheet of the discharge calculator for the Barka II (RO) plant is given in Figure 127, and the third sheet in Figure 128.

Table 31: Input data for the application of the discharge calculator to the Barka plants

	Scenario I	Scenario II
Seawater intake temperature (°C)	24	25
Seawater intake salinity (ppt)	36	38
Desalination plant's capacity (m <sup>3</sup> /d)	91000	120000
Recovery rate (%)	40	50
Brine temperature	42	25
Power plant's cooling water (m <sup>3</sup> /h)	22005	59000
Blended temperature (°C)	32	32
Blended salinity (ppt)	36	45

### Flowrates & Effluent Characteristics

#### - ambient characteristics

ambient temperature	$T_a =$	25.00	°C
ambient salinity	$Sal_a =$	38.00	ppt
ambient density	$\rho_a =$	1025.28	kg/m <sup>3</sup>
ambient kin. viscosity	$\nu_a =$	9.41E-07	m <sup>2</sup> /s

annotations:

$T = 10$  to  $180^\circ\text{C}$   
 $Sal = 0$  to  $160$  ppt (ppt = g/kg)  
 allowed ranges for viscosity calculation:  
 $Sal = 0$  to  $160$  ppt,  $T = 10$  to  $180^\circ\text{C}$  (following El-Dessouky, Ettouney (2002))

#### - drinking water (permeate)

flowrate	$Q_{drink} =$	1.39	m <sup>3</sup> /s
recovery rate	$r =$	50	%
intake flowrate	$Q_{in} =$	2.78	m <sup>3</sup> /s

recovery rate:  
 percentage of intake water converted into permeate;  
 plant characteristic; following Lattemann:  $r = 40$ - $65\%$

#### - brine characteristics (effluent from desalination process)

plant effluent flowrate	$Q_{desal} =$	1.39	m <sup>3</sup> /s
temperature	$T_{desal} =$	25.00	°C
salinity	$Sal_{desal} =$	76.00	ppt
density	$\rho_{desal} =$	1054.15	kg/m <sup>3</sup>
substance concentration	$c_{desal} =$	20.00	ppm

ambient or  $1^\circ\text{C}$  above  
 with  $Sal_{drink} = 0$  ppt  
 e.g. coagulants, anti-scalants, ....

#### - blended effluent - external - (e.g. waste water or others)

flowrate	$Q_{effl,ex} =$	8.00	m <sup>3</sup> /s
temperature	$T_{effl,ex} =$	32.00	°C
salinity	$Sal_{effl,ex} =$	45.00	ppt
density	$\rho_{effl,ex} =$	1028.16	kg/m <sup>3</sup>

$Sal_{effl,ex} = 0$  to  $160$  ppt,  $T_{effl,ex} = 10$  to  $180^\circ\text{C}$

#### Final effluent characteristics:

flowrate	$Q_o =$	9.39	m <sup>3</sup> /s
effluent temperature	$T_o =$	30.96	°C
effluent salinity	$Sal_o =$	49.59	ppt
effluent density	$\rho_o =$	1031.98	kg/m <sup>3</sup>
buoyant acceleration	$g_o' =$	-0.06414	m/s <sup>2</sup>
-> negatively buoyant, ok!			
kin. viscosity	$\nu_o =$	8.47E-07	m <sup>2</sup> /s
substance concentration	$c_o =$	2.96	ppm

mean average  
 mean average  
 $g_o' = g * (|\rho_s - \rho_o|) / \rho_s$   
 $g_o' < 0$ : negatively buoyant,  $g_o' > 0$ : positively buoyant  
 allowed ranges for viscosity calculation:  
 $Sal = 0$  to  $160$  ppt,  $T = 10$  to  $180^\circ\text{C}$  (following El-Dessouky, Ettouney (2002))

Figure 126: The first sheet of the discharge calculator for the Barka II (RO) plant

## Discharge Characteristics

### - effluent characteristics

flowrate	$Q_o =$	<input type="text" value="9.39"/>	$m^3/s$
discharge density	$\rho_o =$	<input type="text" value="1031.98"/>	$kg/m^3$
kin. viscosity	$\nu_o =$	<input type="text" value="8.47E-07"/>	$m^2/s$

### - ambient characteristics

ambient density	$\rho_a =$	<input type="text" value="1025.28"/>	$kg/m^3$
buoyant acceleration	$g'_o =$	<input type="text" value="-0.06414"/>	$m/s^2$
offshore slope	$\theta_B =$	<input type="text" value="1"/>	$^\circ$

### - discharge characteristics

Choose a discharge angle (recommended: 45°):

discharge angle	$\theta_o =$	<input type="text" value="10"/>	$^\circ$
discharge angle ok!			
port discharge velocity	$U_o =$	<input type="text" value="5.00"/>	$m/s$
number of openings	$n =$	<input type="text" value="9"/>	
port diameter	$D =$	<input type="text" value="0.52"/>	$m$
dens. Froude Number	$Fr_o =$	<input type="text" value="27.50"/>	
Reynolds Number	$Re_o =$	<input type="text" value="3.04E+06"/>	

Checking of characteristic properties:

Diameter  $D$ : in required range, ok!

Froude Number  $Fr_o$ : in required range, ok!

Reynolds Number  $Re_o$ : in required range, ok!

Choose an appropriate port diameter (DN according to ISO standard):

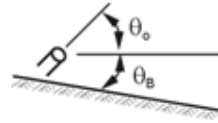
port diameter	$D =$	<input type="text" value="0.50"/>	$m$
---------------	-------	-----------------------------------	-----

### Final discharge characteristics:

port diameter	$D =$	<input type="text" value="0.50"/>	$m$
number of openings	$n =$	<input type="text" value="9"/>	
discharge angle	$\theta_o =$	<input type="text" value="10"/>	$^\circ$
flowrate (individual)	$Q_{o,ind.} =$	<input type="text" value="1.04"/>	$m^3/s$
port discharge velocity	$U_o =$	<input type="text" value="5.31"/>	$m/s$
dens. Froude Number	$Fr_o =$	<input type="text" value="29.67"/>	
Reynolds Number	$Re_o =$	<input type="text" value="3.14E+06"/>	
buoyancy flux	$J_o =$	<input type="text" value="-0.067"/>	$m^4/s^3$
momentum flux	$M_o =$	<input type="text" value="5.54"/>	$m^4/s^2$
discharge length scale	$L_Q =$	<input type="text" value="0.44"/>	$m$
momentum length scale	$L_M =$	<input type="text" value="13.97"/>	$m$

annotations:

$[0^\circ \leq \theta_B \leq 30^\circ]$  only integer!



$[0^\circ \leq \theta_o \leq 90^\circ]$  only integer!

recommended:  $U_o = 4-6$  m/s  
start with one opening!

$$Fr_o = U_o / (g'_o * D)^{1/2} = Q_o / (D^2 * \pi / 4) / (g'_o * D)^{1/2}$$

$$Re_o = U_o * D / \nu_o$$

required:

$0.1 \leq D \leq 1.0$

$Fr_o \geq 10$ , recommended:  $Fr_o = 20-25$

$Re_o > 4000$

$$J_o = g'_o * Q_o \quad (<0: \text{negatively buoyant})$$

$$M_o = U_o * Q_o$$

$$L_Q = (D^2 * \pi / 4)^{1/2} = Q_o / M_o^{1/2}$$

$$L_M = M_o^{3/4} / J_o^{1/2}$$

Figure 127: The second sheet of the discharge calculator for the Barka II (RO) plant

## Jet Properties

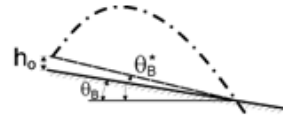
### - discharge & ambient characteristics

discharge angle	$\theta_o =$	<input type="text" value="10"/>	°
port height	$h_o =$	<input type="text" value="1.00"/>	m
in required range, ok!			
offshore slope	$\theta_B =$	<input type="text" value="10"/>	°
imaginary offshore slope	$\theta_B^* =$	<input type="text" value="10"/>	°
momentum length scale	$L_M =$	<input type="text" value="13.97"/>	m
dens. Froude Number	$Fr_o =$	<input type="text" value="29.67"/>	

annotations:

$h_o = 0\text{m}$  or  $h_o = 0.5\text{-}1.0\text{m}$

due to port height, not yet implemented



### - geometric jet properties (for discharge angles that are not a multiple of 15°: linear interpolation!)

	$Z_{max}/L_M$ (3%)	<input type="text" value="0.498"/>	} (taken from Fig. 2(a))	( $c/c_{max} = 3\%$ )
	$Z_{max}/L_M$ (25%)	<input type="text" value="0.391"/>		( $c/c_{max} = 25\%$ )
	$Z_{max}/L_M$	<input type="text" value="0.195"/>	} (taken from Fig. 4(a))	!port height not considered!
	$x_{max}/L_M$	<input type="text" value="0.981"/>		
	$z_i/L_M$	<input type="text" value="-0.491"/>		
	$x_i/L_M$	<input type="text" value="2.376"/>		
upper jet boundary	$Z_{max}$ (3%)	<input type="text" value="6.95"/>		m
	$Z_{max}$ (25%)	<input type="text" value="5.46"/>		m
maximum jet centerline	$Z_{max}$	<input type="text" value="2.72"/>		m
position	$x_{max}$	<input type="text" value="13.71"/>		m
jet centerline position at	$z_i$	<input type="text" value="-6.85"/>		m
the impingement point	$x_i$	<input type="text" value="33.19"/>		m
offshore location	$x \geq$	<input type="text" value="231.67"/>		m
local water depth	$H_{oo} \geq$	<input type="text" value="4.10"/>		m

$H_{oo} \geq 0.75Z_{max}$  (25%)

### Choose an appropriate outfall location:

offshore location	$x =$	<input type="text" value="240.0"/>	m
local water depth	$H_{oo} =$	<input type="text" value="4.24"/>	m

in required range,  
offshore location ok!

### - dilutions & concentration (for bottom slopes that are not a multiple of 10°: linear interpolation!)

minimum centerline	$S_m/Fr_o =$	<input type="text" value="0.17"/>	
dilution at $z_{max}$	$S_m =$	<input type="text" value="5.1"/>	
bulk dilution at	$S_i/Fr_o =$	<input type="text" value="0.88"/>	
impingement point	$S_i =$	<input type="text" value="26.1"/>	
substance concentration at the centerline of			
max. level of rise ( $z_{max}$ )	$c_m =$	<input type="text" value="0.58"/>	ppm
impingement point ( $z_i$ )	$c_i =$	<input type="text" value="0.11"/>	ppm

Fig. 2(b)

Fig. 4(b)

$S = c_o/c_c \rightarrow c_c = c_o/S$

Figure 128: The third sheet of the discharge calculator for the Barka II (RO) plant

## 6.1.7. CORMIX simulation for Barka plants

The beta-version of CORMIX (version 6.0) simulations are carried out for both the positive and negative buoyant plumes continuously being discharged from the Barka I (MSF) and Barka II (RO) plants. The outfall discharge point is located at 514 m offshore, and 8 m below the sea surface. The simulations will be terminated in zone of the boundary limits specified as the regulatory mixing zone (RMZ) at 300 m radius from the discharge point or the region of interest at 1500 m downstream.

## Scenario I

This scenario is used to represent a positively buoyant plume discharges from the Barka I (MSF) plant. The input data are summarized in Table 32.

Table 32: Input data for the CORMIX simulation of scenario I

CORMIX Checklist for Data Preparation – Version v6.0		
<b>PROJECT LEGEND</b>		
Project File Name: <u>Barka1.cmx (Scenario I)</u>	Design Case: <u>Single Port</u>	Date: <u>Jan 03 2010</u>
Site Name: <u>Barka I Plant</u>	Prepared By: <u>SCJ (Verified by MxZon)</u>	
<b>EFFLUENT DATA</b>		
<input checked="" type="checkbox"/> Non-Fresh Water Effluent Density	<input type="checkbox"/> Fresh Water Effluent Density	
Density $\rho_0$ : <u>1024.00</u> kg/m <sup>3</sup>	<input type="checkbox"/> Temperature $T_0$ : ..... °C	<input type="checkbox"/> Density $\rho_0$ : ..... kg/m <sup>3</sup>
Discharge Excess Concentration: <u>10.000</u> %	<input checked="" type="checkbox"/> Effluent Flowrate $Q_0$ : <u>0.001</u> m <sup>3</sup> /s	<input type="checkbox"/> Effluent Velocity $U_0$ : ..... m/s
<b>Pollutant Types</b>		
<input type="checkbox"/> Conservative	<input type="checkbox"/> Non Conservative: ..... /day	<input checked="" type="checkbox"/> Heated – Heat Loss Coefficient: <u>0.00</u> W/m <sup>2</sup> /°C
<input type="checkbox"/> Brine	<input type="checkbox"/> Sediment: Chunks: ..... % Sand: ..... % Coarse Silt: ..... % Fine Silt: ..... % Clay: ..... %	Total Sediment Concentration: ..... kg/m <sup>3</sup>
<b>AMBIENT GEOMETRY / FLOW FIELD DATA</b>		
Average Depth $H_a$ : <u>0.50</u> m	<input checked="" type="checkbox"/> Unbounded	<input type="checkbox"/> Bounded: Width BS: ..... m
Depth at Discharge $H_d$ : <u>0.00</u> m	Appearance: <input type="checkbox"/> Uniform <input type="checkbox"/> Slight Meander <input type="checkbox"/> Highly Irregular	
<input checked="" type="checkbox"/> Steady	<input type="checkbox"/> Unsteady	
<input type="checkbox"/> Ambient Flowrate $Q_a$ : ..... m <sup>3</sup> /s	Period: ..... hr Max Velocity $U_m$ : ..... m/s Tidal Velocity at this Time: $U_a$ : ..... m/s	
<input checked="" type="checkbox"/> Ambient Velocity $U_a$ : <u>0.00</u> m/s	<input type="checkbox"/> At Time: ..... hr Before Slack	<input type="checkbox"/> At Slack – $\Delta$ Time: ..... hr <input type="checkbox"/> At Time: ..... hr After Slack
<input type="checkbox"/> Single Slope	<input type="checkbox"/> Near & Far Slope	
Slope S: ..... %	<input type="checkbox"/> Near Shore Slope $S_1$ : ..... %	<input type="checkbox"/> Far Slope $S_2$ : ..... %
Near Shore Velocity: ..... m/s	<input type="checkbox"/> Near Shore Velocity $U_{a1}$ : ..... m/s	<input type="checkbox"/> Far Shore Velocity $U_{a2}$ : ..... m/s
Near Shore Darcy-Weisbach f: .....	<input type="checkbox"/> Near Shore Darcy-Weisbach $f_1$ : .....	<input type="checkbox"/> Far Shore Darcy-Weisbach $f_2$ : .....
<input type="checkbox"/> Manning's n: .....	<input checked="" type="checkbox"/> Darcy-Weisbach f: <u>0.005</u>	Wind Speed: <u>2.5</u> m/s
<b>AMBIENT DENSITY DATA</b>		
Water Body: <input type="checkbox"/> Fresh Water <input checked="" type="checkbox"/> Non-Fresh Water		
<input checked="" type="checkbox"/> Uniform	Fresh: <input type="checkbox"/> Temperature: ..... °C <input type="checkbox"/> Density $\rho_s$ : ..... kg/m <sup>3</sup>	Non-Fresh: Density $\rho_s$ : <u>1024.00</u> kg/m <sup>3</sup>
<input type="checkbox"/> Stratified	<input type="checkbox"/> Type A <input type="checkbox"/> Type B: Pycnocline Height: ..... m <input type="checkbox"/> Type C: Pycnocline Height: ..... m	Jump: ..... kg/m <sup>3</sup> /°C
	Density $\rho$ : At Surface $\rho_{as}$ : ..... kg/m <sup>3</sup> /°C	At Bottom $\rho_{ab}$ : ..... kg/m <sup>3</sup> /°C
<input type="checkbox"/> Brine & Sediment Only	Level 1 Density $\rho_1$ : ..... kg/m <sup>3</sup> Sub 1: ..... m	Level 2 Density $\rho_2$ : ..... kg/m <sup>3</sup> Sub 2: ..... m
<b>DISCHARGE GEOMETRY DATA</b>		
<b>CORMIX 1 – Single Port</b>	<b>CORMIX 2 – Multiport</b>	<b>CORMIX 3 – Surface Discharge</b>
Nearest Bank: <input type="checkbox"/> Left <input checked="" type="checkbox"/> Right	Nearest Bank: <input type="checkbox"/> Left <input type="checkbox"/> Right	Discharge Located: <input type="checkbox"/> Left <input type="checkbox"/> Right
Dist. to Nearest Bank: <u>510.00</u> m	<input type="checkbox"/> Unidirectional <input type="checkbox"/> Staged <input type="checkbox"/> Altern./ Vert.	Horiz. Angle $\sigma$ : ..... °
Vert. Angle $\theta_0$ : <u>30</u> °; Horiz. Angle $\sigma_0$ : <u>30</u> °	N <sup>o</sup> of openings: .....; Diffuser Length: ..... m	Local Depth at Discharge Outlet: ..... m
<input checked="" type="checkbox"/> Port Diameter $D_0$ : <u>0.30</u> m	Dist. to 1 <sup>st</sup> end-point $YB_1$ : ..... m	<input type="checkbox"/> Flush <input type="checkbox"/> Co-flowing
<input type="checkbox"/> Port Area $A_0$ : ..... m <sup>2</sup>	Dist. to 2 <sup>nd</sup> far end-point $YB_2$ : ..... m	<input type="checkbox"/> Protruding: Distance from Bank: ..... m
<b>Submerged</b>	Port Height $h_0$ : ..... m; Port Diameter $D_0$ : ..... m	<b>Discharge Outlet</b>
Port Height above Bottom $h_0$ : <u>1.0</u> m	Contraction Ratio: .....	<input type="checkbox"/> Channel: Width: ..... m; Depth $b_0$ : ..... m
<b>Above Surface</b>	<b>Angles (degrees)</b>	<input type="checkbox"/> Pipe: Diameter $D_0$ : ..... m
Port Height above Surface: ..... m	Vert. Angle $\theta$ : ..... °; Horiz. Angle $\sigma$ : ..... °	Bottom Invert Depth: ..... m
<input type="checkbox"/> Jet-like <input type="checkbox"/> Spray <input type="checkbox"/> Area	Align. Angle $\gamma$ : ..... °; Relat. Orient. Angle $\beta$ : ..... °	Local Bottom Slope at Chanel Entry: ..... °
Deflector Plate: <input type="checkbox"/> With or <input type="checkbox"/> Without	Nozzle Direction: <input type="checkbox"/> Same or <input type="checkbox"/> Fanned Out	
<b>MIXING ZONE DATA</b>		
<input checked="" type="checkbox"/> Non-Toxic Effluent		<input type="checkbox"/> Toxic Effluent
<input checked="" type="checkbox"/> WQ Standard: <u>1.0/0.00</u>	<input type="checkbox"/> No WQ Standard	CMC: ..... CCC: .....
<input checked="" type="checkbox"/> Mixing Zone Specified		<input type="checkbox"/> No Mixing Zone Specified
<input type="checkbox"/> Trajectory: ..... m	<input checked="" type="checkbox"/> Downstream Distance: <u>300.00</u> m	<input type="checkbox"/> Width: ..... % / m <input type="checkbox"/> Area: ..... %
Region of Interest: <u>1300.00</u> m	Grid Intervals for Display: <u>30</u>	

The near field region (NFR) is the zone of strong initial mixing, and it has no regulatory implication. As the effluent density from the Barka I (MSF) plant is less than the surrounding ambient density, the effluent plume is positively buoyant. The plume rises towards the surface and its bottom part is then deflected due to buoyant ambient spreading (Figure 129). The results predicted at the NFR boundary is summarized in Table 33.

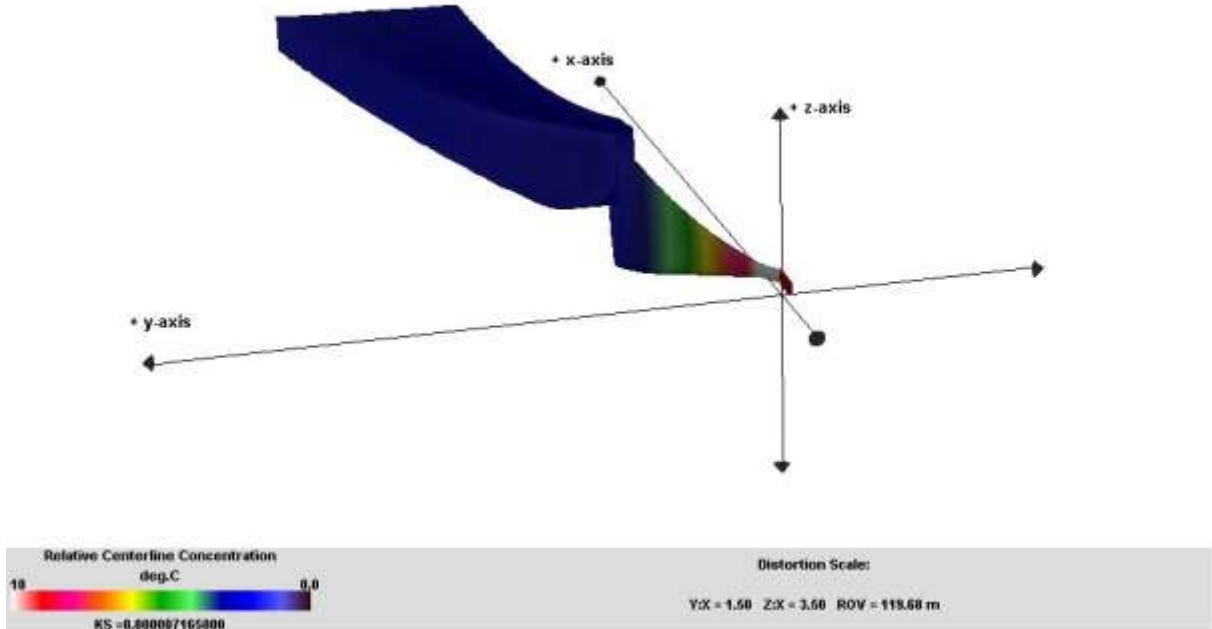


Figure 129: 3D view of the near field positively buoyant plume of scenario I

Table 33: NRF characteristics of scenario I

Temperature at the edge of NFR	0.50 °C above ambient
Dilution at the edge of NFR	19.8
NFR location (centerline coordinates)	X: 120m, Y: 38m, Z: 8m
NFR plume dimensions	Half-width: 13m, Thickness: 2.00m
Cumulative travel time	1120sec

The plume becomes vertically fully mixed at 1160 m downstream as the bottom plume attaches to the seabed, and as shown in Figure 130, after that the plume spreads due to passive ambient mixing in uniform ambient until it has reached the region of interest. The specified water quality standard has also been met within the RMZ, and the plume conditions at the boundary of RMZ are presented in Table 34.

Table 34: RMZ characteristics of scenario I

Temperature at the edge of RMZ	0.318451 °C above ambient
Dilution at the edge of RMZ	31.4
RMZ location (centerline coordinates)	X: 300m, Y: 37.86m, Z: 8m
RMZ plume dimensions	Half-width: 29.63m, Thickness: 2.51m
Cumulative travel time	2920.2312 sec

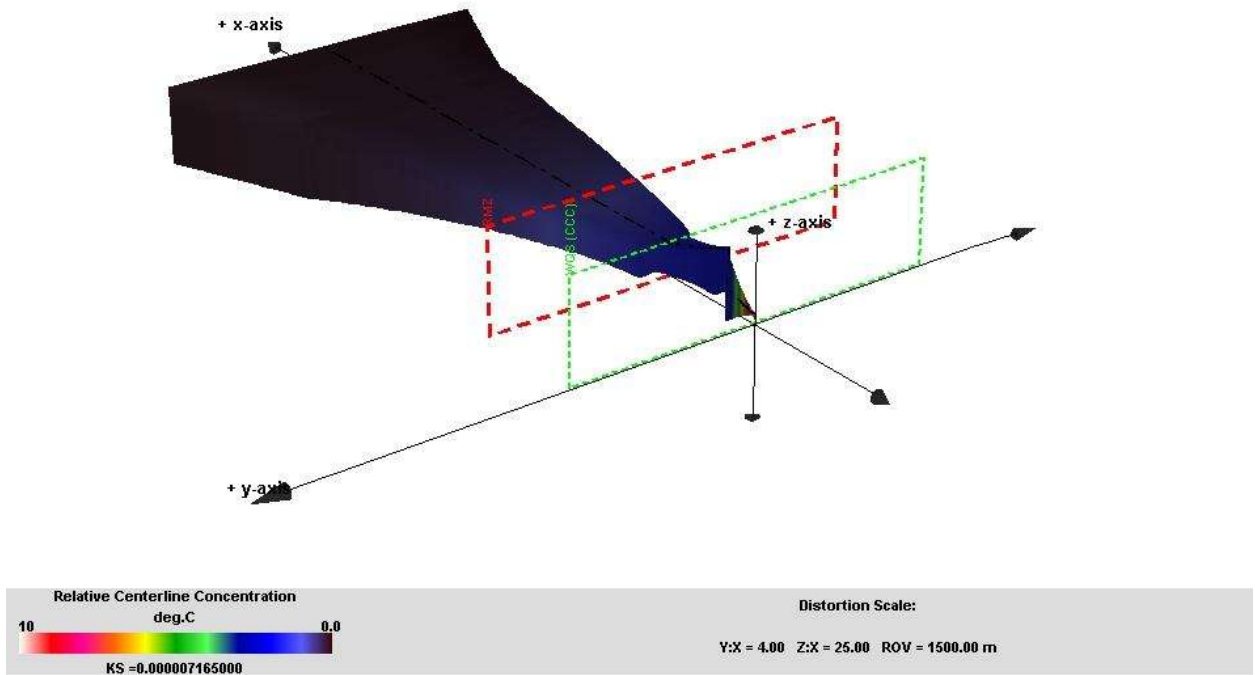


Figure 130: 3D view of the far field positively buoyant plume of scenario I

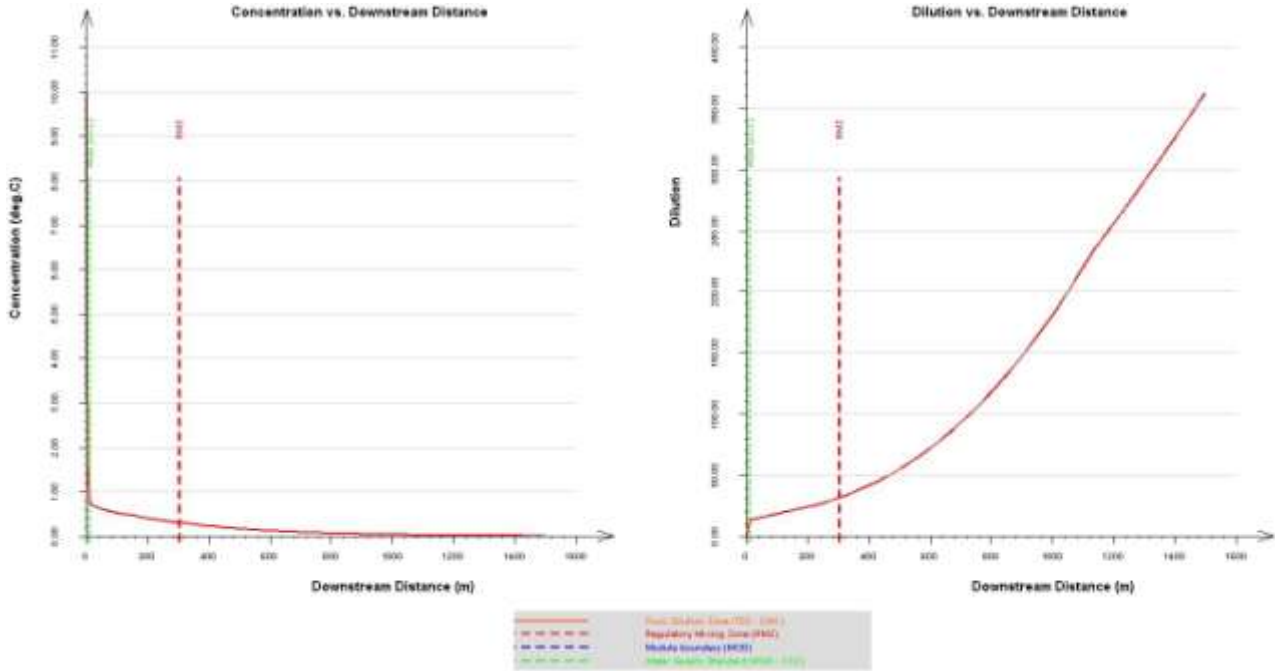


Figure 131: Temperature distribution (left) and dilution (right) downstream of scenario I

**Scenario II**

This scenario is used to represent a negatively buoyant plume discharges from the Barka II (RO) plant. The input data are summarized in Table 35.

Table 35: Input data for the CORMIX simulation of scenario II

CORMIX Checklist for Data Preparation – Version v6.0		
<b>PROJECT LEGEND</b>		
Project File Name: <u>Barka2.cmx (Scenario II)</u>	Design Case: <u>Single Port</u>	Date: <u>Jan 05 2010</u>
Site Name: <u>Barka 1+II (DC) Plant</u>	Prepared By: <u>SOB (Verified by Mizzi)</u>	
<b>EFFLUENT DATA</b>		
<input checked="" type="checkbox"/> Non-Fresh Water Effluent Density	<input type="checkbox"/> Fresh Water Effluent Density	
Density $\rho_0$ : <u>1007.00</u> kg/m <sup>3</sup>	<input type="checkbox"/> Temperature $T_0$ : ..... °C	<input type="checkbox"/> Density $\rho_0$ : ..... kg/m <sup>3</sup>
Discharge Excess Concentration: <u>100%</u>	<input checked="" type="checkbox"/> Effluent Flowrate $Q_0$ : <u>0.002</u> m <sup>3</sup> /s	<input type="checkbox"/> Effluent Velocity $U_0$ : ..... m/s
<b>Pollutant Types</b>		
<input checked="" type="checkbox"/> Conservative	<input type="checkbox"/> Non Conservative: ..... /day	<input type="checkbox"/> Heated – Heat Loss Coefficient: ..... W/m <sup>2</sup> /°C
<input checked="" type="checkbox"/> Brine	<input type="checkbox"/> Sediment: Chunks: ..... % Sand: ..... % Coarse Silt: ..... % Fine Silt: ..... % Clay: ..... % Total Sediment Concentration: ..... kg/m <sup>3</sup>	
<b>AMBIENT GEOMETRY / FLOW FIELD DATA</b>		
Average Depth $H_a$ : ..... m	<input checked="" type="checkbox"/> Unbounded	<input type="checkbox"/> Bounded: Width BS: ..... m
Depth at Discharge $H_d$ : <u>0.00</u> m	Appearance: <input type="checkbox"/> Uniform <input type="checkbox"/> Slight Meander <input type="checkbox"/> Highly Irregular	
<input checked="" type="checkbox"/> Steady	<input type="checkbox"/> Unsteady	
<input type="checkbox"/> Ambient Flowrate $Q_a$ : ..... m <sup>3</sup> /s	Period: ..... hr Max Velocity $U_m$ : ..... m/s Tidal Velocity at this Time $U_a$ : ..... m/s	
<input checked="" type="checkbox"/> Ambient Velocity $U_a$ : <u>0.10</u> m/s	<input type="checkbox"/> At Time: ..... hr Before Slack <input type="checkbox"/> At Slack – $\Delta$ Time: ..... hr <input type="checkbox"/> At Time: ..... hr After Slack	
<input checked="" type="checkbox"/> Single Slope	<input type="checkbox"/> Near & Far Slope	
Slope S: <u>0.0025 4%</u>	<input type="checkbox"/> Near Shore Slope $S_1$ : ..... % <input type="checkbox"/> Far Slope $S_2$ : ..... %	
Near Shore Velocity: <u>0.10</u> m/s	<input type="checkbox"/> Near Shore Velocity $U_{a1}$ : ..... m/s <input type="checkbox"/> Far Shore Velocity $U_{a2}$ : ..... m/s	
Near Shore Darcy-Weisbach f: <u>0.014</u>	<input type="checkbox"/> Near Shore Darcy-Weisbach $f_1$ : ..... <input type="checkbox"/> Far Shore Darcy-Weisbach $f_2$ : .....	
<input type="checkbox"/> Manning's n: .....	<input checked="" type="checkbox"/> Darcy-Weisbach f: <u>0.024</u>	Wind Speed: <u>0.0</u> m/s
<b>AMBIENT DENSITY DATA</b>		
Water Body: <input type="checkbox"/> Fresh Water <input checked="" type="checkbox"/> Non-Fresh Water		
<input checked="" type="checkbox"/> Uniform	Fresh: <input type="checkbox"/> Temperature: ..... °C <input type="checkbox"/> Density $\rho_a$ : ..... kg/m <sup>3</sup>	Non-Fresh: Density $\rho_a$ : <u>1024.00</u> kg/m <sup>3</sup>
<input type="checkbox"/> Stratified	<input type="checkbox"/> Type A <input type="checkbox"/> Type B: Pycnocline Height: ..... m <input type="checkbox"/> Type C: Pycnocline Height: ..... m Jump: ..... kg/m <sup>3</sup> /°C	
	Density $\rho$ : At Surface $\rho_{as}$ : ..... kg/m <sup>3</sup> /°C At Bottom $\rho_{ab}$ : ..... kg/m <sup>3</sup> /°C	
<input type="checkbox"/> Brine & Sediment Only	Level 1 Density $\rho_1$ : ..... kg/m <sup>3</sup> Sub 1: ..... m	Level 2 Density $\rho_2$ : ..... kg/m <sup>3</sup> Sub 2: ..... m
<b>DISCHARGE GEOMETRY DATA</b>		
<b>CORMIX 1 – Single Port</b>	<b>CORMIX 2 – Multiport</b>	<b>CORMIX 3 – Surface Discharge</b>
Nearest Bank: <input type="checkbox"/> Left <input checked="" type="checkbox"/> Right	Nearest Bank: <input type="checkbox"/> Left <input type="checkbox"/> Right	Discharge Located: <input type="checkbox"/> Left <input type="checkbox"/> Right
Dist. to Nearest Bank: <u>0.00</u> m	<input type="checkbox"/> Unidirectional <input type="checkbox"/> Staged <input type="checkbox"/> Altern./ Vert.	Horiz. Angle $\sigma$ : ..... °
Vert. Angle $\theta_0$ : <u>0.0</u> °; Horiz. Angle $\alpha_0$ : <u>0.0</u> °	N <sup>o</sup> of openings: .....; Diffuser Length: ..... m	Local Depth at Discharge Outlet: ..... m
<input checked="" type="checkbox"/> Port Diameter $D_0$ : <u>0.05</u> m	Dist. to 1 <sup>st</sup> end-point $YB_1$ : ..... m	<input type="checkbox"/> Flush <input type="checkbox"/> Co-flowing
<input type="checkbox"/> Port Area $A_0$ : ..... m <sup>2</sup>	Dist. to 2 <sup>nd</sup> far end-point $YB_2$ : ..... m	<input type="checkbox"/> Protruding: Distance from Bank: ..... m
<b>Submerged</b>	Port Height $h_0$ : ..... m; Port Diameter $D_0$ : ..... m	<b>Discharge Outlet</b>
Port Height above Bottom $h_b$ : <u>0.0</u> m	Contraction Ratio: .....	<input type="checkbox"/> Channel: Width: ..... m; Depth $b_0$ : ..... m
<b>Above Surface</b>	<b>Angles (degrees)</b>	<input type="checkbox"/> Pipe: Diameter $D_0$ : ..... m
Port Height above Surface: ..... m	Vert. Angle $\theta$ : ..... °; Horiz. Angle $\alpha$ : ..... °	Bottom Invert Depth: ..... m
<input type="checkbox"/> Jet-like <input type="checkbox"/> Spray <input type="checkbox"/> Area	Align. Angle $\gamma$ : ..... °; Relat. Orient. Angle $\beta$ : ..... °	Local Bottom Slope at Chanel Entry: ..... °
Deflector Plate: <input type="checkbox"/> With or <input type="checkbox"/> Without	Nozzle Direction: <input type="checkbox"/> Same or <input type="checkbox"/> Fanned Out	
<b>MIXING ZONE DATA</b>		
<input checked="" type="checkbox"/> Non-Toxic Effluent		<input type="checkbox"/> Toxic Effluent
<input checked="" type="checkbox"/> WQ Standard: <u>0.0%</u>	<input type="checkbox"/> No WQ Standard	CMC: ..... CCC: .....
<input checked="" type="checkbox"/> Mixing Zone Specified		<input type="checkbox"/> No Mixing Zone Specified
<input type="checkbox"/> Trajectory: ..... m	<input checked="" type="checkbox"/> Downstream Distance: <u>0.00</u> m	<input type="checkbox"/> Width: ..... % / m <input type="checkbox"/> Area: ..... %
Region of Interest: <u>100.00</u> m	Grid Intervals for Display: <u>50</u>	

In contrast to scenario I, the effluent plume is negatively buoyant and it will tend to sink at the seabed. The plume immediately becomes vertically fully mixed within NFR as it is discharged from the outfall (Figure 132), although it re-stratifies later on at a 92.62 m downstream. The results predicted at the NFR boundary is summarized in Table 36.

Table 36: NRF characteristics of scenario II

Concentration at the edge of NFR	2.3021 % above ambient
Dilution at the edge of NFR	43.4
NFR location (centerline coordinates)	X: 42.18m, Y: 48.38m, Z: -9.33m
NFR plume dimensions	Half-width: 6.37m, Thickness: 8m
Cumulative travel time	268.2532 sec

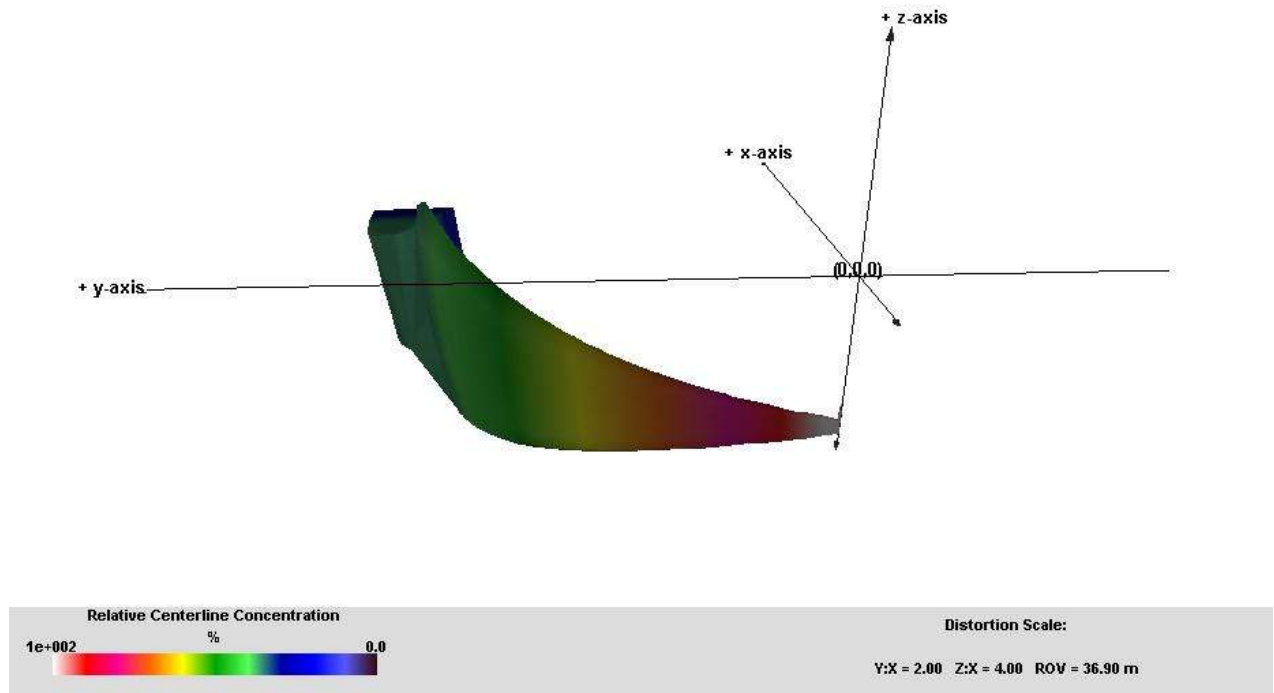


Figure 132: 3D view of the near field negatively buoyant plume of scenario II (origin is located at the surface)

The specified water quality standard has also been met within the RMZ, and the plume conditions at the boundary of RMZ are presented in Table 37. As the plume is attached to the seabed (Figure 133), it spreads due to density current down the slope without transition to the far field until it has reached the region of interest.

Table 37: RMZ characteristics of scenario II

Concentration at the edge of RMZ	0.008876 % above ambient
Dilution at the edge of RMZ	11266.9
RMZ location (centerline coordinates)	X: 300m, Y: 429.57m, Z: -20.49m
RMZ plume dimensions	Half-width: 39.73m, Thickness: 7.49m
Cumulative travel time	268.2532 sec

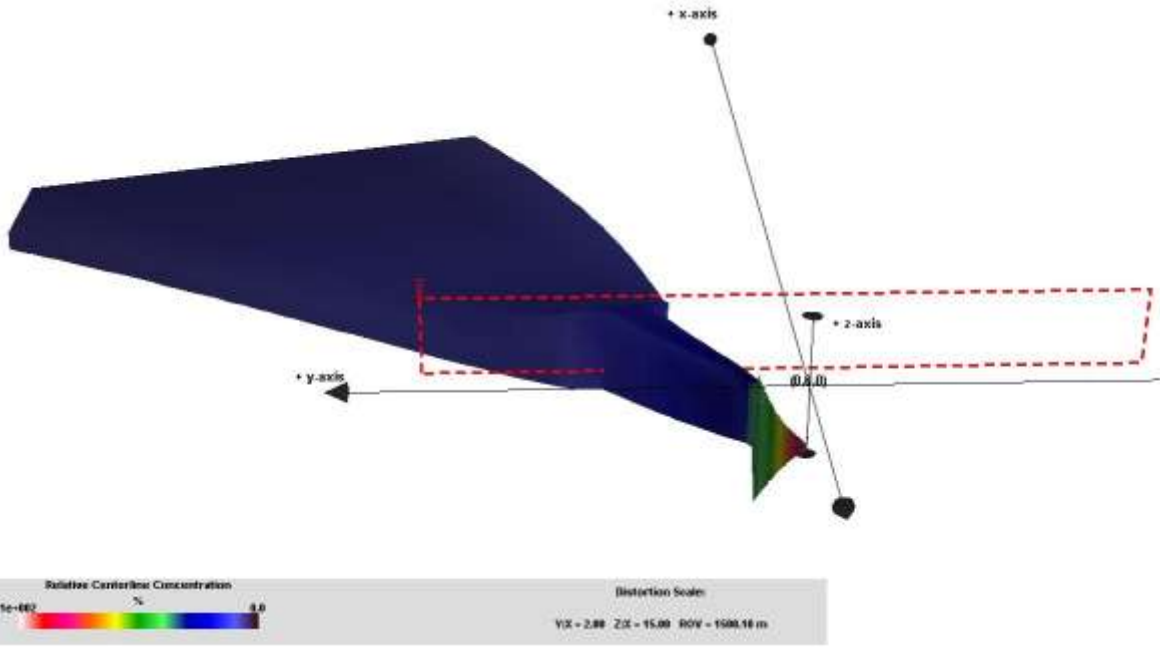


Figure 133: 3D view of the far field negatively buoyant plume of scenario II (origin is located at the surface)

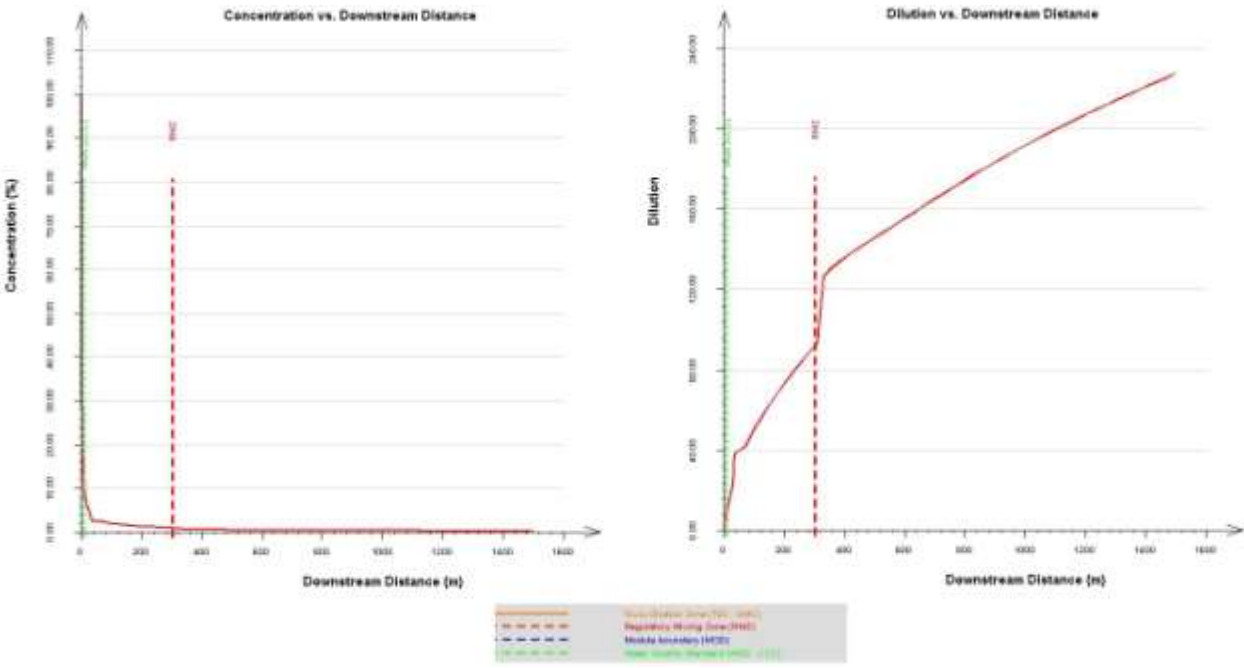


Figure 134: Concentration distribution (left) and (dilution) downstream of scenario II

The CORMIX simulation results show that the temperature rise is less than 0.4 °C and the salinity rise is less than 0.001 ppt at the edge of RMZ (300 m away from the outfall) under both scenarios. The maximum permissible limits by the Oman government are 1 °C and 2 ppt at 300 m from the outfall.

## 6.2. Theoretical case study for coupling analysis

The present coupling approach has been applied on the existing analysis of the planned waste water outfall in Cartagena, Colombia (Bleninger, 2006) with some modifications of the discharge conditions. Instead of waste water, a typical brine effluent of a RO plant ( $Q_o = 7 \text{ m}^3/\text{s}$ ) is discharged through a submerged single port. The ambient conditions are based on the field data for the Cartagena outfall following Bleninger (2006). The simulation time of one week was selected including 169 hourly time steps. This period contains current directions mainly oriented to the south-west with a range of about  $130^\circ$  with a mean velocity  $U_{a,mean} = 0.44 \text{ m/s}$  and a mean density  $\rho_{a,mean} = 1023.5 \text{ kg/m}^3$ . According to the ambient conditions, the effluent characteristics result in  $T_o = 27.7 \text{ }^\circ\text{C}$ ,  $Sal_o = 66.9 \text{ ppt}$ ,  $\rho_o = 1046.8 \text{ kg/m}^3$ . Further conditions illustrated in Figure 135 are the vertical angle of discharge  $\theta = 30^\circ$ , the port diameter  $D_o = 1.2 \text{ m}$ , the discharge velocity  $U_o = 6.19 \text{ m/s}$  and the discharge concentration  $C_o = 100\%$ . More details are listed in Niepelt (2007).

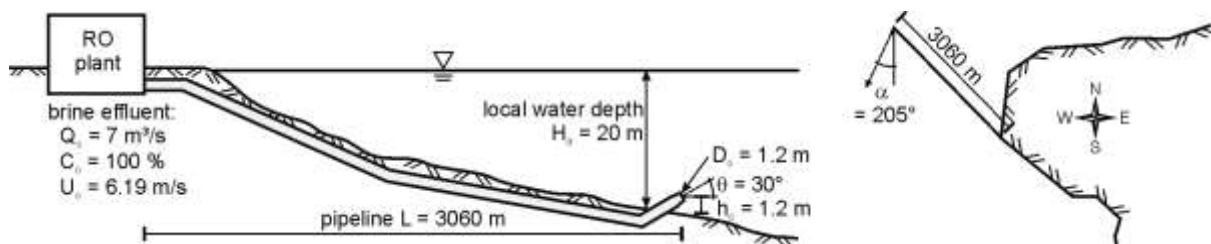


Figure 135: Sketch of the applied outfall design

In the far-field model the computational domain was chosen about 20km around the outfall location. A structured curvilinear grid was used for the horizontal discretization with higher resolution in the outfall region (Figure 136, left). In the vertical, a  $\sigma$ -grid with 13 layers was used. The cross-sectional views through the model domain are given on the right in Figure 136. The outfall is located in grid point M49 N51 in the layers 11 and 12.

### 6.2.1. Results of the near-field modeling

Over the whole simulation time, only two different flow characteristics were predicted. Two time steps (I and II) were selected which are representative for these two plume types visualized in Figure 137.

Depending on constant parameters ( $U_o$ ,  $Q_o$ ), the momentum flux  $M_o$  is identical for all time steps. The ambient density difference varies only slightly over time so that the buoyancy flux  $J_o$  is considered a constant. As a result, the jet/plume transition length scales  $L_M$  are the same, since  $L_M$  depends on  $M_o$  and  $J_o$ . These parameters result in:

$$\begin{aligned} \text{momentum flux:} \quad & M_o = 43.33 \text{ m}^4/\text{s}^2 \\ \text{buoyancy flux:} \quad & J_o = -1.56 \text{ m}^4/\text{s}^3 \quad (g_o' = -0.223 \text{ m/s}^2) \\ \text{jet/plume transition:} \quad & L_M = 13.53 \text{ m} \end{aligned}$$

The ambient velocity differs by 0.47 m/s. This leads to different plume-to-crossflow and jet-to-crossflow length scales:

time step I:		time step II:	
jet-to-crossflow:	$L_m = 10.88 \text{ m}$	• jet-to-crossflow:	$L_m = 47.35 \text{ m}$
plume-to-crossflow:	$L_b = 7.04 \text{ m}$	• plume-to-crossflow:	$L_b = 580.37 \text{ m}$
⇒ strong current:	$L_M/L_m > 1$	⇒ weak current:	$L_M/L_m < 1$

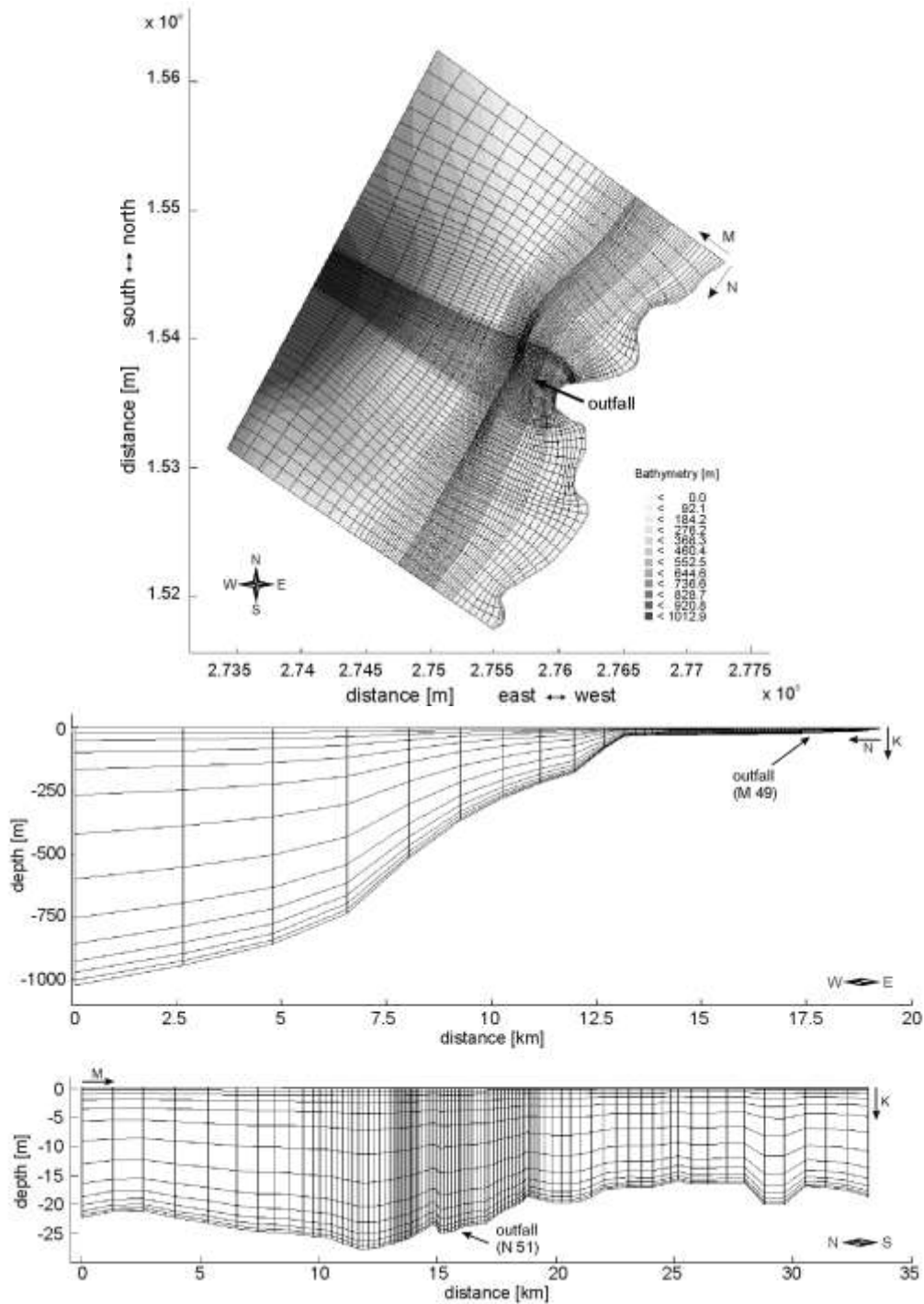


Figure 136: Computational domain of the far-field model. *Left*: Plan view of the numerical grid. *Right*: Cross-sectional views of the numerical grid: west ↔ east cross-section along N51 (top), south ↔ north cross-section along M49 (bottom)

As shown in Figure 137 the predicted flow class at time step I (occurring 34% of all calculated time steps) describes a plume which rises to a maximum height and then descends toward the bottom. Initially dominated by the effluent momentum, the plume gets strongly deflected by the predominant ambient current ( $L_M/L_m > 1$ ) after a short distance.

At time step II (occurring 66% of all time steps) the discharge strength dominates the flow. After some distance the plume gets deflected by the weak ambient current ( $L_M/L_m < 1$ ) and is vertically mixed over the full water depth.

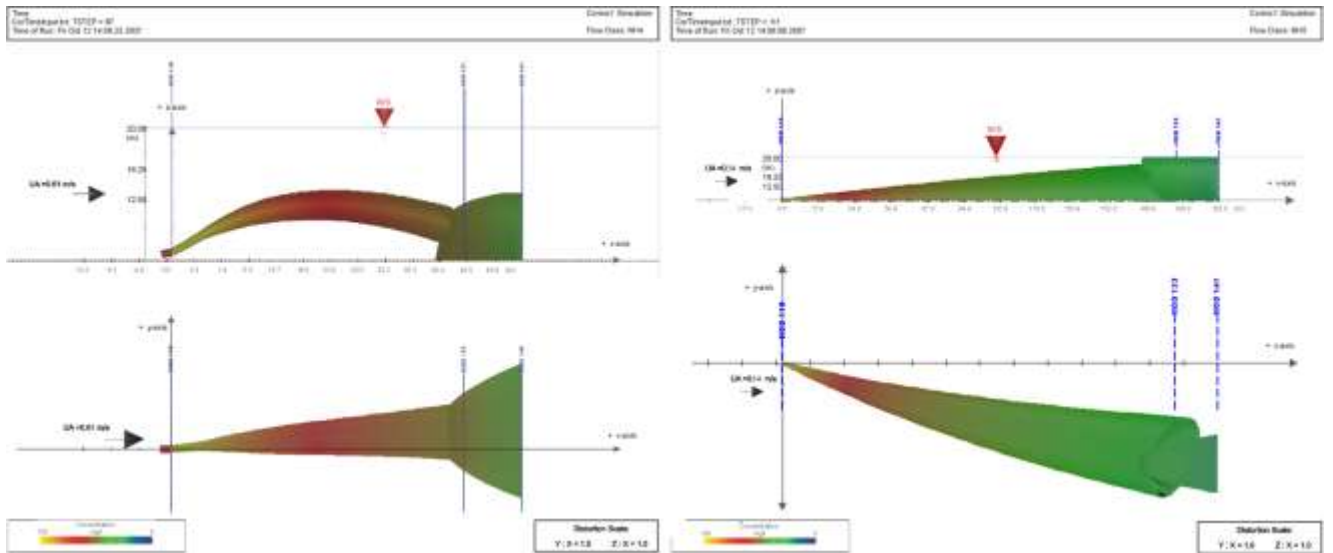


Figure 137: CORMIX plume visualizations for the time step I (left) and II (right)

Figure 138 shows the horizontal distribution of the endpoints of the near-field with their concentrations. Here, the two different plume characteristics are visible as well. In the near distance at about 50 m – representative shown at time step I – the plume gets less diluted ( $S \approx 18$ ) and concentrations of  $C = 4$  to  $5.87\%$  are expected. For the second flow class, higher dilution ( $S \approx 35-100$ ) is achieved so that the concentrations range from  $C = 1$  to  $4\%$ . The near-field has a range of 106 m to 757 m in mean flow direction and is spread over a distance of  $\pm 150$  m transversal to the mean flow. In the far-field model, the effluent will be discharged at the endpoints with respect to the width and the thickness of the plume.

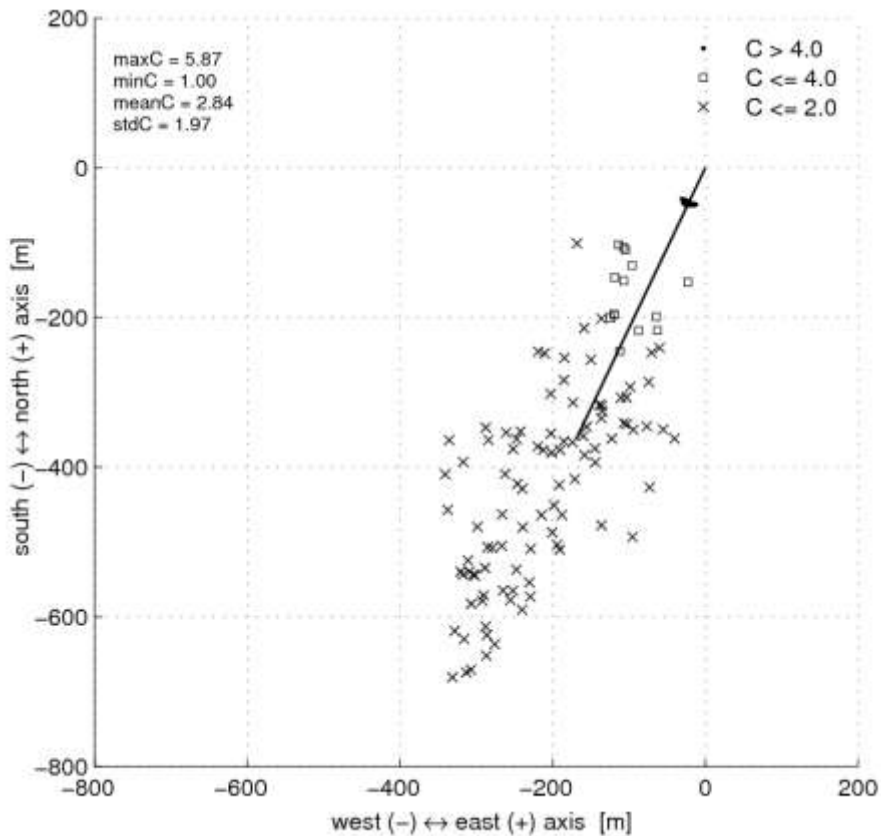


Figure 138: Scatter plot of the predicted endpoints of the near-field with their concentrations

## 6.2.2. Coupling configurations

In order to draw a comparison three coupling configurations were investigated (Figure 139):

### 1. no coupling

All results of CorTime are ignored.

⇒ Effluent discharges at the outfall location so that two cells are affected (Figure 139, 1<sup>st</sup> row).

### 2. vertical coupling

The vertical plume distribution computed with CorTime is considered while the determined near-field distance and the plume width are neglected.

⇒ Effluent discharges at the grid point of the outfall location, vertically distributed over the whole water depth or over layer 7 to 13. A uniform concentration distribution is assumed over the vertical (Figure 139, 2nd row).

### 3. full coupling

The plume size (thickness and width) and near-field distance determined with CorTime are considered.

⇒ Effluent discharges at the calculated endpoints of the near-field. In regards to the plume width 20 grid points are affected. The plume is vertically distributed over the whole water depth or over layer 7 to 13. A uniform concentration distribution is assumed over both the horizontal and the vertical (Figure 139, 3rd row).

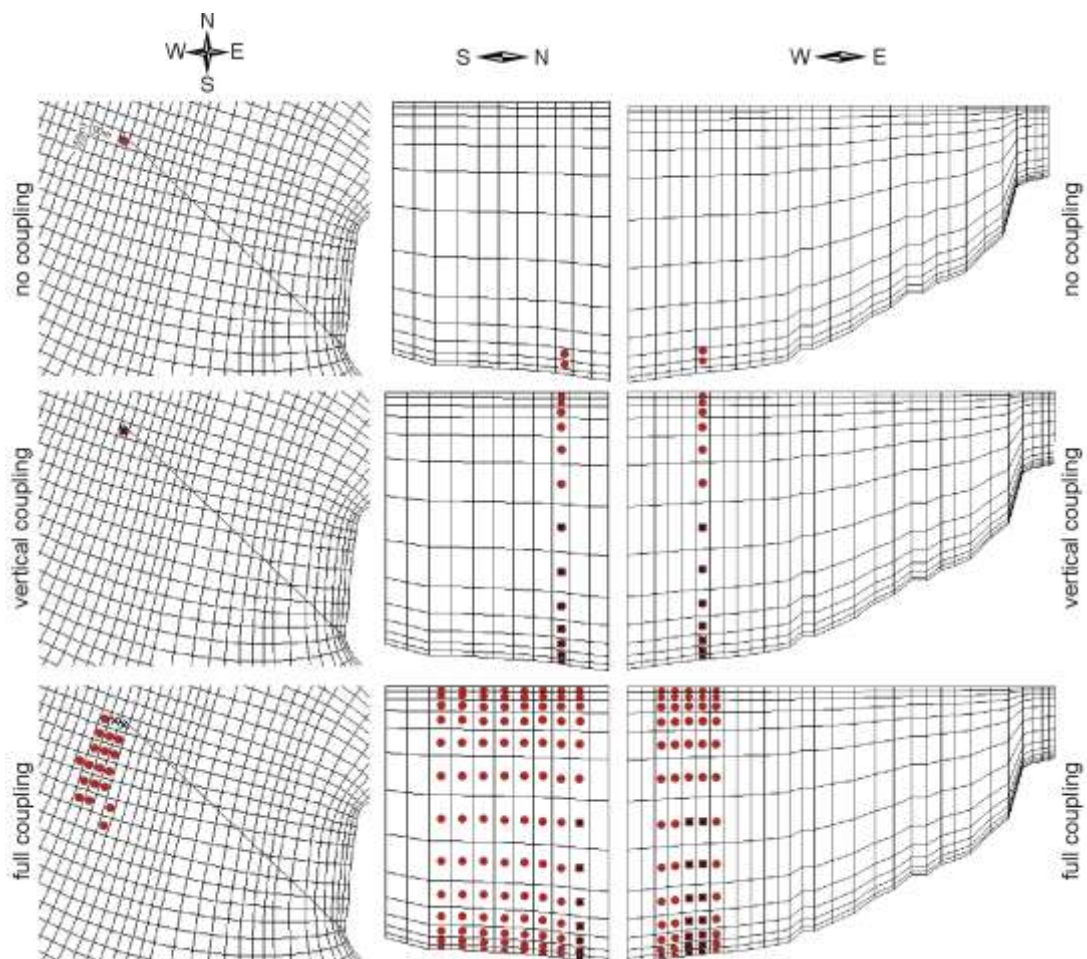


Figure 139: Distribution of the discharge locations for the three coupling configurations. Left: plan views, middle: south↔north cross-sections, right: east↔west cross-sections ●: discharge locations, ×: grid points where layer 7 to 13 are affected separately

### 6.2.3. Results of the (coupled) far-field modeling

For the analysis, the same time steps (I and II) as for the near-field analysis are considered. Further, three observation points (outfall, A and B) were regarded: the outfall is placed at the grid point of the outfall location, A is situated in 500 m, and B in 2300 m downstream of the outfall location in the mean flow direction.

Figure 140 and Figure 141 show maps for the three coupling configurations at the time steps I and II. Figure 141 shows the concentration distribution in layer 11 in which the outfall is located. Figure 142 displays cross-sectional views of the concentration distribution along the grid line M49. In the case of no coupling, a larger concentration scale is used. Figure 143 shows concentration profiles over the depth at the observation points outfall, A and B. Regarding the plan views given in Figure 141 at one time step, the plume looks similar for all coupling cases. The plume is travelling in the mean flow direction. Unsteady variations cause slight deflections and stretching of the plumes.

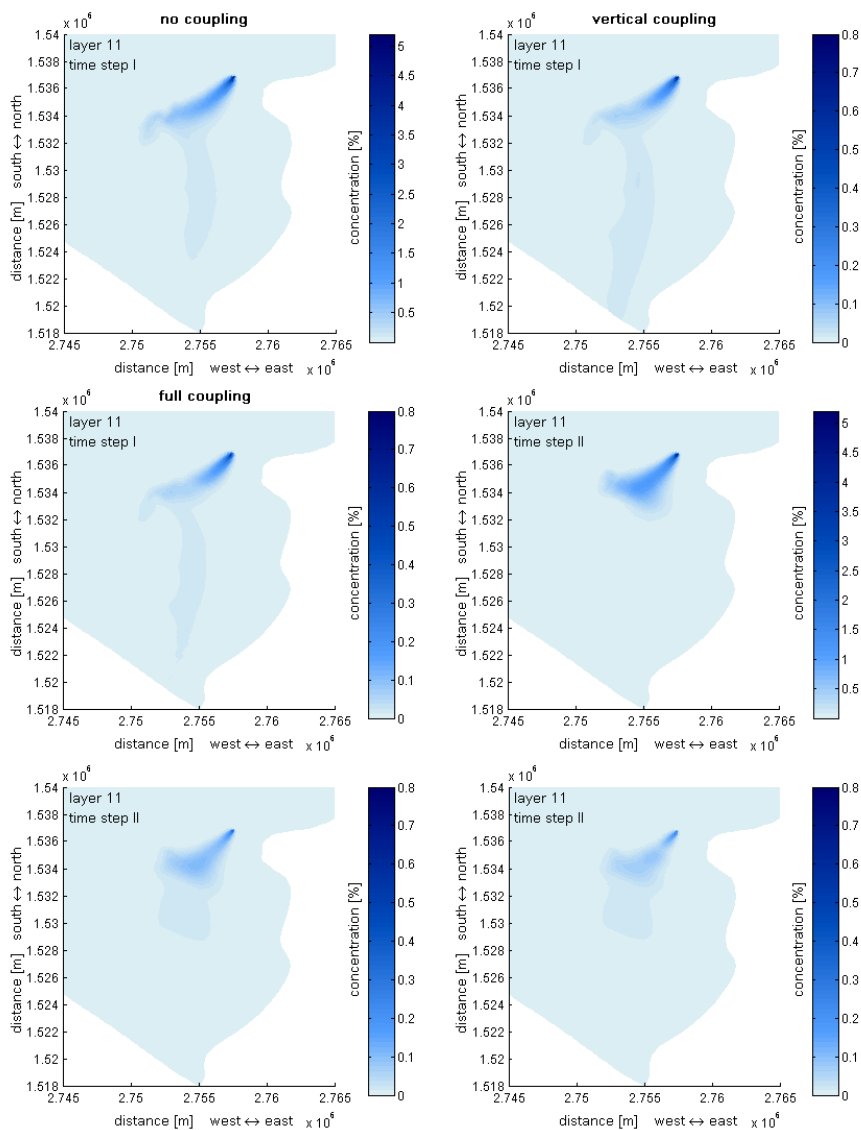


Figure 141: Plan views of the concentration distributions in layer 11 (height of outfall) for the three coupling configurations at time step I (top) and II (bottom). In the case of no coupling a larger concentration scale is used

A sharp distinction exists in the concentration of the plumes. If the effluent is discharged directly at the outfall location the concentration exceeds 5 % (no coupling). Considering at least the distribution over the vertical predicted by CorTime, the concentration amounts to less than 0.8 % (vertical and full coupling). In Figure 142 and Figure 143 the differences of the investigated coupling approaches are clearly visible. In the case of no coupling, the effluent is discharged at the height of the outfall location. The plume travels along the sea bed in layer 11 and 12 in the mean current direction. No vertical mixing occurs. The largest concentration (5.3 %) arises at the outfall location. While traveling further away from the source, the concentration decreases due to horizontal spreading.

For vertical and full coupling the shape of the plume is almost identical regarding the same time steps in the cross-sectional views. For the time step I the plume is distributed over layer 7 to 13. In time step II the plume is distributed over the whole water depth. Hence, the two different plume characteristics that were predicted with CorTime were transmitted correctly.

For the vertical coupling approach the largest concentration of about 0.74 % can be found at the outfall location. At the observation point A the concentration is reduced by almost half as in the case of no coupling. At the point B the plume concentrations are decreased to less than 0.05 %.

In the case of full coupling the highest concentration (0.26 %) occurs at the observation point A. The concentrations at the observation point B are lower than 0.04 %. Consequently, the concentrations resulting from vertical coupling are higher compared to the full coupling at each observation point.

That is because considering only the vertical plume distribution for the coupling, the effluent is continuously discharged in the grid point of the outfall location. Taking account of the predicted endpoint of the plume, the discharge location is not fixed in one point. As a result, the effluent concentration does not accumulate at the outfall location and is therefore lower in this grid point compared to the vertical coupling. Additionally, the sources are distributed in the transverse direction in the case of full coupling. That is why the concentration in point A and B are of minor value compared to vertical coupling since A and B are located in the mean flow direction.

However, at a distance of about 2300 m downstream from the outfall location, the concentration differences between the full and vertical coupling approaches are negligible.

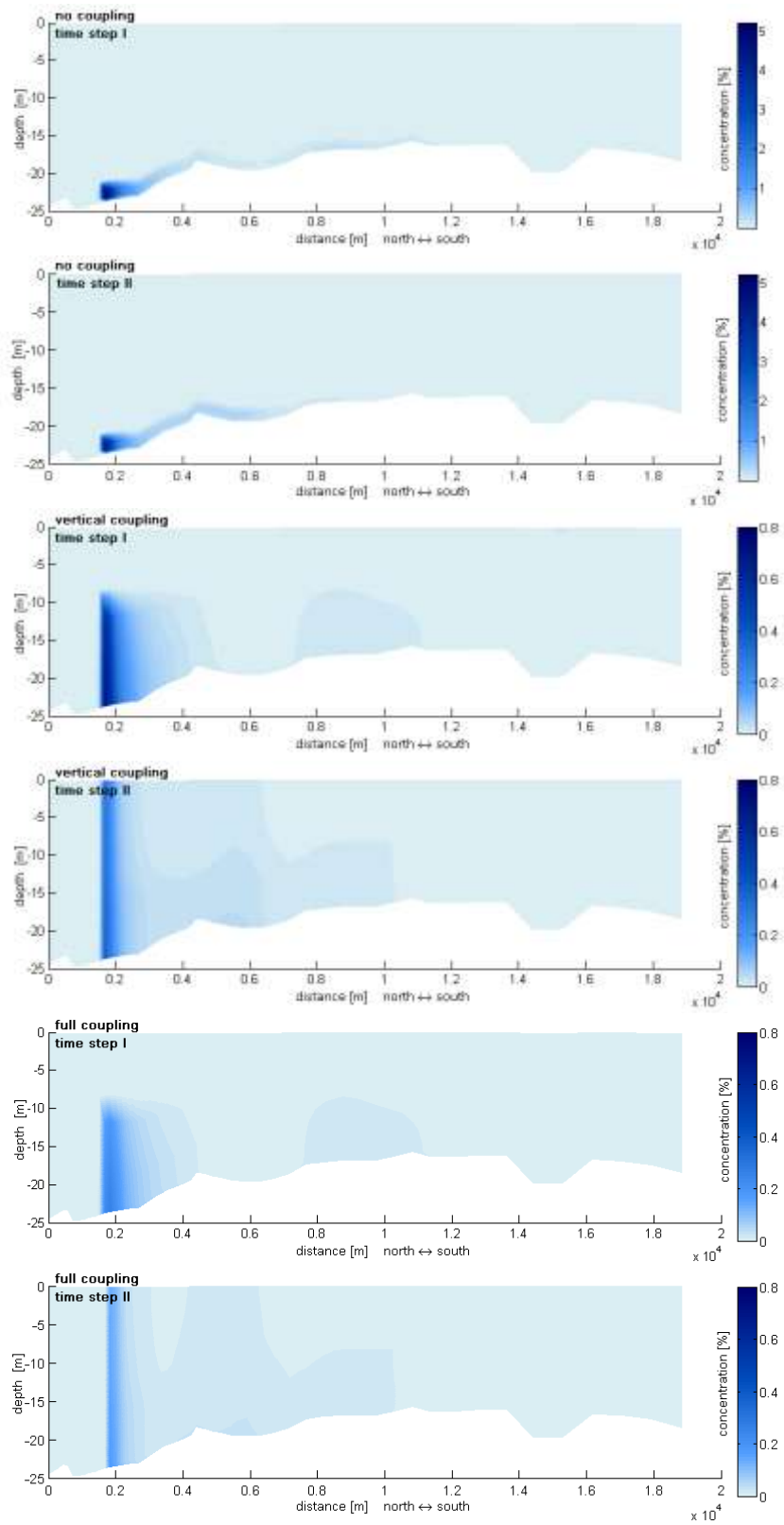


Figure 142: Concentration distributions in the cross-section along M49 for the three coupling configurations at time steps I and II. In the case of no coupling a larger concentration scale is used

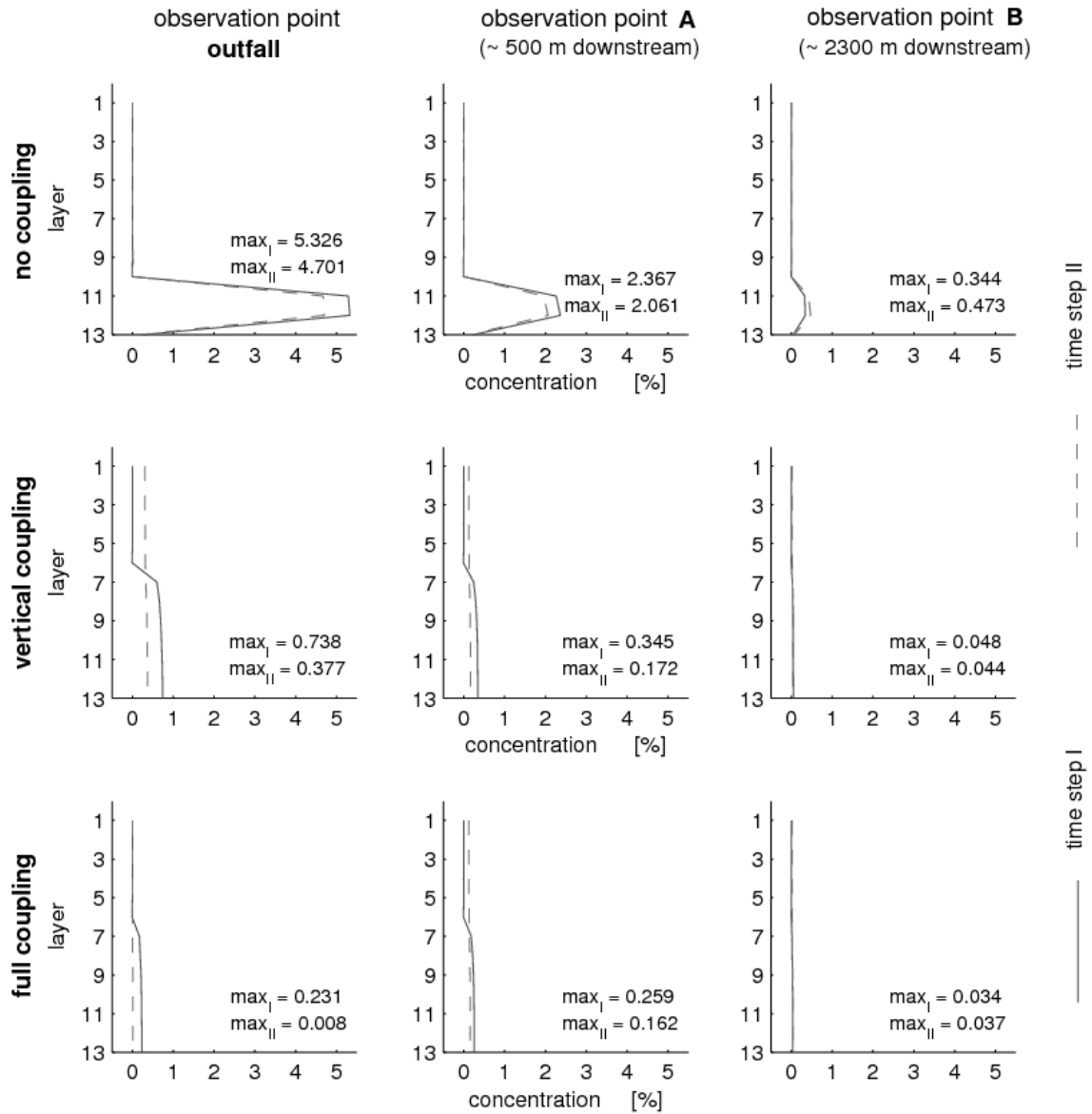


Figure 143: Concentration profiles at the observation points outfall, A and B for the three coupling configurations no, vertical and full coupling. Time steps: I and II

## 7. CONCLUSIONS

MSF and RO plants account for the highest share in global seawater desalination capacity. It was shown that the effluents of these plants have a variety of physical properties and chemical constituents which can be harmful for the marine environment. The impact intensity depends on the pollutant concentrations and loads as well as on the sensitivity of the respective coastal ecosystems. After consideration of toxicity, degradability and typical dosages, a ranking was developed which reflects the potential harmfulness of pollutants in desalination effluents. Chlorine, antiscalants and copper discharge as well as increased temperatures were classified as most critical in MSF effluents. For RO effluents, the high salinity, antiscalants and the membrane cleaning solutions containing several dangerous substances were identified to be the most critical pollutants. Reduction of these should have the highest priority for mitigation measures.

Efficient technologies exist to reduce the environmental impacts of desalination effluents and make sure that these technologies are not necessarily more costly than conventional systems. UF pretreatment and sponge ball systems provide more efficient pretreatment, better process control and enable the removal and reduction of the chemicals used in conventional MSF and RO plants. Sub-seabed intakes can be an equally efficient and ecologically beneficial pretreatment alternative, if the costs are properly assessed. Indispensable antiscalants can be replaced by more biocompatible alternatives. Copper pollution can be avoided by installing less costly duplex steels in MSF plants. The impact area of brine discharges is reduced by installing multiport diffusers and by optimising the discharge design.

The summary of existing environmental quality standards for planning and designing discharges showed that those are usually regulated by limiting pollutant levels in the reject streams at the point of discharge (effluent standards) and in the receiving environment (ambient standards). However, the review showed that regulation procedures must contain a clear mixing zone regulation for all point sources. The ambient standard values should apply outside and at the edge of the “mixing zone”, a spatially restricted region around the point source. This regulation pays attention to the physical fact that mixing processes in which a transition from the effluent standards to the ambient standards takes place occur only gradually and require a certain space. The actual dimensions of the mixing zone can be specified by simple directives from the authority depending on water body type and use or in ad-hoc procedures through an agreement between discharger and authority.

The various density differences between the brine and the receiving water represented by the buoyancy flux causes different flow characteristics of the discharge. The dense RO (reverse osmosis) effluent flow has the tendency to fall as a negatively buoyant plume. The MSF (multi-stage-flash) effluent is distinguished by a neutral to positive buoyant flux causing the plume to rise. It has been shown that multiport diffuser outfalls designed as efficient mixing devices installed at locations with high transport and purification capacities are capable to reduce environmental impacts significantly. Furthermore, it is evident that any discharge design requires field measurements and modelling applications to analyse and predict the impacts of such installations.

A spreadsheet calculator has been developed as a screening tool to define effluent properties and the initial estimated order of magnitude of the dilution of a chosen system. This calculator has proven to be very efficient in doing order of magnitude analysis and evaluating initial designs or existing systems.

For the actual design process two different hydrodynamic models were used for the prediction of either the near-field mixing (CORMIX) and/or the transport processes in the far-field (Delft3D). An optimized approach to couple both model types for brine discharge analysis has been developed. The coupling interface algorithm includes the transformation of the output data of the near-field model CORMIX into the input data for the far-field model Delft3D-FLOW. Based mainly on the theoretical case study (and not necessarily applies universally), the analysis of the concentration distributions shows the importance of model coupling. The far-field model can not simulate the strong mixing processes occurring in the near-field, particularly with regard to the vertical mixing. Thus, the vertical distribution of the plume needs to be calculated by the use of a near-field model and must then be transferred into the far-field model. Regarding the horizontal plume distribution of all coupling configurations, the plumes were passively advected by the ambient current and slowly mixed by the ambient turbulence in the same way. A horizontal coupling is considered to be unimportant since the concentration differences between the *vertical* and the *full coupling* are negligible. In addition, the dilutions resulting from the *vertical coupling* are lower compared to the *full coupling*. Hence, considering only the vertical distribution gives a conservative estimate regarding the mean flow direction. Thus, the coupling methodology allows for a considerably improved discharge assessment and an optimized environmental hydraulic design of the outfall structure.

Furthermore, model results allow for an optimized intake location to avoid recirculation. Also, interactions of different discharges, and consequences of different pre-treatment/operational schemes can be studied.

The results showed that the tools are readily applicable and improve the current state of the art for desalination brine discharge analysis. Dischargers, consultants and regulators are encouraged to apply these tools and to discuss the proposed modifications of existing regulations on one hand, and existing discharge systems on the other hand. Ongoing analysis showed that "cleaner" desalination is possible and feasible.

However, major works need to be done in the following fields, to further improve the presented approaches, and designs: Environmental Impact Studies need much more regional ecotoxicological studies, where local species characteristics are analyzed, and their vulnerability on local effluent characteristics are assessed. The numerical models for the near-field region require more validation studies in the laboratory, to improve the formulations after boundary impingement and further density spreading with the effect of ambient currents. The models for the far-field region require much more data on ambient currents, winds, and stratification, to allow for better specifications of boundary conditions. Such measurements complemented with modelling are highly valuable for further coastal zone management issues. And finally, field studies need to be undertaken to validate the presented methodologies and recommendations on a large scale, and including local, and regional features.

## 8. REFERENCES

- ABA Consultants (1992): Effects of Hyper-saline Water on Survival of *Olivella pycna* and *Dendraster excentricus*. Report to EIP Associates, Pasadena, CA
- Abdel-Jawad, M. and Al-Tabtabaei, M. (1999): Impact of current power generation and water desalination activities on Kuwaiti marine environment. Proceedings of IDA World Congress on Desalination and Water Reuse, San Diego, USA, 3, 231-240
- Abdul-Wahab, S.A. (2007): Characterization of water discharges from two thermal power/desalination plants in Oman. *Environ. Eng. Sci.* 24, 321-337
- Abdul-Wahab, S.A. (2008): A preliminary investigation into the environmental awareness of the Omani public and their willingness to protect the environment. *Am. J. Environ. Sci.* 4(1), 39-49
- Abdul-Wahab, S.A. and Jupp, B.P. (2009): Levels of heavy metals in subtidal sediments in the vicinity of thermal power/desalination plants: A case study. *Desalination* 244, 261-282
- Ahmed, M., Shayya, W.H., Hoey, D., Mahendran, A., Morris, R. and Al-Handaly, J. (2000): Use of evaporation ponds for brine disposal in desalination plants. *Desalination* 130, 155-168
- Akar, P.J. and Jirka, G.H. (1995): Buoyant spreading processes in pollutant transport and mixing. Part II: upstream spreading in weak ambient current. *J. Hydraul. Res.* 33(1), 87-100
- Alameddine, I. and El-Fadel, M. (2007): Brine discharge from desalination plants: a modeling approach to an optimized outfall design. *Desalination* 214, 241-260
- Al-Sahali, M. and Ettouney, H. (2007): Developments in thermal desalination processes: Design, energy, and costing aspects. *Desalination* 214, 227-240
- Alspach, B., Burch, R., Baudish, P., "Seawater Desalination in Australia: Water Supply Solutions without Environmental Cost", Proc. IDA World Congress – Atlantis, The Palm – Dubai, UAE November 7-12, 2009
- Altayaran, A.M. and Madany, I.M. (1992): Impact of a desalination plant on the physical and chemical properties of seawater, Bahrain. *Water Research* 26, 435-441
- ANZECC (2000): Australian and New Zealand Guidelines for Fresh and Marine Water Quality
- Argyrou, M. (1999): Impact of Desalination Plant on Marine Macrobenthos in the Coastal Waters of Dhekelia Bay, Cyprus, Department of Fisheries, Ministry of Agriculture, Natural Resources and Environment, 13 Aeolou Str., 1416 Nicosia, Cyprus
- Bay, S.M. (1993): Investigation of desalination plant toxicity, Southern California Coastal Water Research Project, 7171 Fenwick Lane, Westminster, CA 92683
- Birnbauer, W. (2007): Recycled water? We are not thirsty
- Bleninger, T. (2006): Coupled 3D hydrodynamic models for submarine outfalls: Environmental hydraulic design and control of multiport diffusers, Ph.D. Dissertation, Institute for Hydromechanics, University of Karlsruhe
- Bleninger, T. and Jirka, G.H. (2002): Outfalls database and information exchange. Proc. Intl. Conf. Marine Waste Water Discharges, MWWD 2002, Istanbul, Turkey
- Bleninger, T. and Jirka, G.H. (2004): Near- and far-field model coupling methodology for wastewater discharges. Lee, J.H.W. and Lam, K.L. (Eds.) Proc. 4<sup>th</sup> International Symposium on Environmental Hydraulics and 14<sup>th</sup> Congress of Asia and Pacific Division, International Association of Hydraulic Engineering and Research, Hong Kong, China
- Bleninger, T. and Jirka, G.H. (2008): Modelling and environmentally sound management of brine discharges from desalination plants. *Desalination* 221, 585-597
- Bleninger, T., Jirka, G.H. and Weitbrecht, V. (2006): Optimal discharge configuration for brine effluents from desalination plants, Proc. DME- Congress, Deutsche Meerwasser Entsalzung, Berlin

- Bleninger, T., Jirka, G.H., 2008, "Modelling and environmental sound management of brine discharges from desalination plants", *Desalination* Vol. 221/1-3 pp. 585-597
- Bleninger, T., Niepelt, A., Jirka, G.H., "Desalination plant discharge calculator", *Desalination and Water Treatment*, 13, 2010, 156-173
- Bleninger, Tobias. 2007. Coupled 3D hydrodynamic models for submarine outfalls: Environmental hydraulic design and control of multiport diffusers. 2007.
- Brooks, N.H. (1960): Diffusion of sewage effluent in an ocean current. Proc. 1<sup>st</sup> International Conference on Waste Disposal in the Marine Environment, University of California, Pergamon Press, New York
- Brooks, N.H. (1980): Synthesis of stratified flow phenomena for design of ocean outfalls. Proc. 2<sup>nd</sup> International Symposium on Stratified Flows, Trondheim, Norway, 809-831
- Brooks, N.H. (1984): Dispersal of wastewater in the ocean – a cascade of processes at increasing scales. Proc. Conf. Water for Resource Development, Coeur d'Alene
- Brooks, N.H. (1988): Seawater intrusion and purging in tunneled outfall. *Schweizer Ingenieur und Architect* 106(6), 156-160
- Brooks, N.H. and Koh, R.C.Y. (1965): Discharge of sewage effluent from a line source into a stratified ocean. Proc. XI Congress IAHR, Leningrad, paper No. 2.19
- Buceta, J.L., Gacia, E., Mas, J., Romero, J., Ruiz, J., Ruiz-Mateo, A. and Sanchez-Lizaso, J.L. (2003): Estudio de los efectos de incrementos de salinidad sobre la fanerogama marina *Posidonia oceanica* y su ecosistema, con el fin de prever y minimizar los impactos que pudieran causar los vertidos de aguas de rechazo de plantas desaladoras. *Ingenieria Civil* 132
- Buros, O.K. (2000): The ABCs of desalting, <http://www.idadesal.org/pdf/ABCs1.pdf>
- California American Water (2004): Seawater Desalination "White Paper". Monterey, California, USA
- California Coastal Commission (2004): Seawater Desalination and the California Coastal Act.
- Cannesson, N., Johnstone, P. M., Mitchell, M. A., Boerlage, S. F E., 2009: Community, Environmental and Marine Impact Minimisation at the Gold Coast Desalination Plant, Proc. IDA World Congress – Atlantis, The Palm – Dubai, UAE, November 7-12, 2009
- Carvalho, J.L.B., Roberts, P.J.W. and Roldao, J. (2002): Field observations of Ipanema beach outfall, *J. Hydraul. Eng.* 128(2), 151-160
- Christie, S., Bonn elye, V., "Perth, Australia: Two-year Feed Back on Operation and Environmental Impact", Proc. IDA World Congress – Atlantis, The Palm – Dubai, UAE November 7-12, 2009
- Cipollina, A., Brucato, A., Grisafi, F. and Nicosia, S. (2005): Bench scale investigation of inclined dense jets. *J. Hydraul. Eng.* ASCE 131, 1017-1022
- City of Carlsbad and Poseidon Resources (2005): Environmental Impact Report for the Carlsbad Seawater Desalination Facility
- Cooley, H., Gleick, P.H. and Wolff, G. (2006): Desalination, with a grain of salt. A California Perspective: Pacific Institute for Studies in Development, Environment and Security: Oakland, California
- COPPE (2000): SisBAHIA – Sistema de Base Hidrodinamica Ambiental, Documentacao tecnica. Universidade Federal de Rio de Janeiro
- CorTime (2008): v2.0 – User Instructions, September 29th 2008, MixZon Inc. ([www.mixzon.com](http://www.mixzon.com))
- Crisp, G., Rhodes, M. and Procter, D. (2007): Perth Seawater Desalination Plant – Blazing a Sustainability Trail. IDA World Congress on Desalination and Water Reuse, Maspalomas, Gran Canaria
- Damitz, B., Furukawa, D. and Toal, J. (2006): Desalination Feasibility Study for the Monterey Bay Region, Final Report prepared for the Association of Monterey Bay Area Governments (AMBAG)

- Davies, A.M., Jones, J.E. and Xing, J. (1997a): Review of recent developments in tidal hydrodynamical modeling. II: Turbulent Energy Models. *J. Hydraul. Eng.* 123(4), 293-302
- Davies, A.M., Jones, J.E. and Xing, J. (1997b): Review of recent developments in tidal hydrodynamical modeling. I: Spectral Models. *J. Hydraul. Eng.* 123(4), 278-
- Davis, A. (2006): *The Sydney Morning Herald*. [Online] 2006. [Cited: 08 02 2006.]
- Del Bene, J.V., Jirka, G.H. and Largier, J. (1994): Ocean brine disposal. *Desalination* 97, 365-372
- Del Bene, J.V., Jirka, G.H., and Largier, J. (1994), "Ocean brine disposal". *Desalination*, 97
- Delft Hydraulics (2001): *Delft3D User Interface, Capabilities and Applications*. Delft Hydraulics, Delft
- Delft3D-FLOW (2005): *Simulation of multi-dimensional hydrodynamic flows and transport phenomena, including sediments*. User Manual version 3.12, WL|Delft Hydraulics, Delft
- Department of Natural Resources and Mines (2003): *Desalination in Queensland*
- DLR, German Aerospace Centre (2007): *Concentrating solar power for seawater desalination*
- Dolnicar, S. and Schafer, A. (2007): *Desalination and recycling: Australians raise health, environment and cost concerns*. University of Wollongong, Australia
- Domenichini, P., Bazurro, N., Avanzini, C., Da Molo, E., Marchese, A., Ottonello, P. and Roccatagliata, E. (2002): *Outfall operation monitoring and environmental control: the experience of LIFE – Aquarius Project*. Proc. Marine Waste Water Discharges, MWWD 2002, Istanbul, Turkey
- Doneker, R. L., Jirka, G. H., Nash, J. D., (2004). Pollutant transport and mixing zone simulation of sediment density currents, *J. Hydraulic Engineering, ASCE*, 130 (4)
- Doneker, R.L. and Jirka, G.H. (1990): *CORMIX1: An Expert Systems for Hydrodynamic Mixing Zone Analysis of Conventional and Toxic Submerged Single Port Discharges*. Technical Report, De Frees Hydraulic Laboratory, School of Civil and Environmental Engineering, Cornell University
- Doneker, R.L. and Jirka, G.H. (1991): *Expert systems for design and mixing zone analysis of aqueous pollutant discharges*. *J. Water Resour. Planning and Management* 117(6), 679-697
- Doneker, R.L. and Jirka, G.H. (2007): *CORMIX User Manual: A Hydrodynamic Mixing Zone Model and Decision Support System for Pollutant Discharges into Surface Waters*, MixZon Inc., Portland, OR
- Doneker, R.L. and Jirka, G.H., 1991, "Expert Systems for Design and Mixing Zone Analysis of Aqueous Pollutant Discharges", *J. Water Resources Planning and Management*, 117, No.6, 679-697
- Doneker, R.L., Nash, J.D. and Jirka, G.H. (2004): *Pollutant transport and mixing zone simulation of sediment density currents*. *J. Hydraul. Eng. ASCE* 30 (4), 349-359
- DVWK (Deutscher Verband für Wasserwirtschaft und Kulturtechnik, now DWA) (1999): *Numerische Modelle von Flüssen, Seen und Küstengewässern*. Heft 127
- Einav, R., 2003, "Checking today's brine discharges can help plan tomorrow's plants", *Desalination and Water Reuse*, Vol. 13/1, 16-20
- Einav, R., Harussi, K. and Perry, D. (2002): *The footprint of the desalination processes on the environment*. *Desalination* 152, 141-154
- El-Dessouky and Ettouney (2002): *Fundamentals of Sea Water Desalination (Appendix A: Thermodynamic Properties)*
- El-Dessouky and Ettouney (2002): *Fundamentals of Sea Water Desalination (Appendix A: Thermodynamic Properties)*
- EU (2008): *Directive 2008/105/EC of the European Parliament on environmental quality standards in the field of water policy*
- Fernandez-Torquemada, Y. and Sanchez-Lizaso, J.L. (2005): *Effects of salinity on leaf growth and*

- survival of the Mediterranean seagrass *Posidonia oceanica* (L.) Delile. *Journal of Experimental Marine Biology and Ecology* 320, 57-63
- Fernández-Torquemada, Y., Loya, A., Mugica, Y., Sánchez-Lizaso, J.L., Templado, J., Calvo, M., Antoranz, A. and Cortés, J.M. (2007): Monitoring the Brine Discharge from a Desalination Plant in the Mediterranean, IDA World Congress on Desalination and Water Reuse, Maspalomas, Gran Canaria
- Fernandez-Torquemada, Y., Sanchez-Lizaso, J.L. and Gonzalez-Correa, J.M. (2005): Preliminary results of the monitoring of the brine discharge produced by the SWRO desalination plant of Alicante (SE Spain). *Desalination* 182, 395-402
- Fischer, H.B., List, E.J., Koh, R.C.Y., Imberger, J. and Brooks, N.H. (1979): *Mixing in Inland and Coastal Waters*, Academic Press, New York
- Fischer, H.B., List, E.J., Koh, R.C.Y., Imberger, J., and Brooks, N.H., 1979, „Mixing in Inland and Coastal Waters”, Academic Press, New York
- Freire, A. " Methodology to establish environmental mixing zones for outfall discharges in coastal waters based on a holistic approach", Research report, Universidad de Cantabria, E.T.S. Ingenieros de Caminos, Canales y Puertos, Dpto. de Ciencias y Tecnicas del agua y del medio ambiente, Grupo de Emisarios submarinos e hidraulica ambiental, September 2008
- Frew, W. (2005): The Sydney Morning Herald. [Online] 2005. [Cited: 14 12 2005.] <http://www.smh.com.au/news/national/city-desalination-plant-is-not-the-solution--poll/2005/12/13/1134236063939.html>
- Friocourt, Y., Lescinski, Jamie, Kleissen, F., " Brine Discharge Designs for Seawater Desalination Vessel: Combining Engineering and Environmental Constraints", Proc. IDA World Congress – Atlantis, The Palm – Dubai, UAE November 7-12, 2009
- Gacia, E., Invers, O., Manzanera, M., Ballesteros, E. and Romero, J. (2007): Impact of the brine from a desalination plant on a shallow seagrass (*Posidonia oceanica*) meadow. *Estuarine Coastal and Shelf Science* 72, 579-590
- Gameson, A.L.H. (1982): Investigations of sewage discharges to some British coastal waters. Chapter 5, Bacterial distributions. Part 4, Technical Report, Water Research Center
- GCD Alliance (2006): Material Change of Use Application ERA 16, 19 & 7, Gold Coast Desalination Project, <http://www.desalinfo.com.au/Environment.asp#Project>
- Genthner, K. (2005): Research and development in desalination – Current activities and demand. In Lecture Notes, DME Seminar, Berlin.
- Genthner, K., 2005, “Research and Development in Desalination – Current Activities and Demand”, in Lecture Notes, DME Seminar, Berlin, June 2005
- Glade, H. (2005): Design of seawater distillation plants. DME Seminar on the Introduction to Seawater Desalination, Berlin
- Global Water Intelligence (2004): *Desalination Markets 2005-2015: A global assessment and forecast*
- Goebel, O. (2005): Markets and desalination technologies in brief. DME Seminar on the Introduction to Seawater Desalination, Berlin
- Grace, R.A. (1978): *Marine Outfall Systems, Planning, Design, and Construction*. Department of Civil Engineering, University of Hawaii at Manoa, Honolulu, Prentice Hall, New Jersey.
- Gross, W.J. (1957): An analysis of response to osmotic stress in selected Decapod Crustacea. *Biological Bulletin* 112, 43-62
- Hassan, A.M., Al-Sofi, M.A.K., Al-Amoudi, A.S., Jamaluddin, A.T.M., Farooque, A.M., Rowaili, A., Dalvi, A.G.I., Kither, N.M., Mustafa, G.M. and Al-Tisan, I.A.R. (1998): A new approach to membrane and thermal seawater desalination processes using nanofiltration membranes. *Desalination* 118, 35-51
- HMR Consultants (2007): EIA Report for Barka Phase II Power and Desalination Project. SMN Barka Power, SAOC, Sultanate of Oman

- Hodgkiess, T., Oldfield, J.W., Hoepner, T., Ahmed, M. and Lattemann, S. (2003): Assessment of the Composition of Desalination Plant Disposal Brines, Project NO. 98-AS-026, Middle East Desalination Research Center (MEDRC)
- Holley, E.R. and Jirka, G.H., 1986, "Mixing and Solute Transport in Rivers", Field Manual, U.S. Army Corps of Engineers, Waterways Experiment Station, Tech. Report E 86 11
- Holley, E.R. and Jirka, G.H. (1986): Mixing and Solute Transport in Rivers. Field Manual, Waterways Experiment Station, U.S. Army Corps of Engineers, Technical Report E 8611
- Höpner, T. (1999): A procedure for environmental impact assessments (EIA) for seawater desalination plants. *Desalination* 124, 1-12
- Höpner, T. and Lattemann, S. (2008): Seawater desalination and the marine environment. European Desalination Society intensive course, Aquila, Italy
- Höpner, T. and Windelberg, J. (1996): Elements of environmental impact studies on coastal desalination plants. *Desalination* 108, 11-18
- IDA (2006): IDA Worldwide Desalting Plant Inventory, No. 19 in MS Excel format, Media Analytics Ltd., Oxford, UK
- IDA (2008): IDA Worldwide Desalting Plant Inventory, No. 20 in MS Excel format, Media Analytics Ltd., Oxford, UK
- IDA and GWI (2008): IDA Worldwide Desalting Plant Inventory, No. 20 in MS Excel format, Media Analytics Ltd., Oxford, UK
- Iso, S., Suizu, S. and Maejima, A. (1994): The lethal effect of hypertonic solution and avoidance of marine organisms in relation to the discharged brine from desalination plant. *Desalination* 97, 389-399
- Jenkins, S.A. and Wasyl, J. (2005): Hydrodynamic modeling of dispersion and dilution of concentrated seawater produced by the ocean desalination project at the Encina Power Plant, Carlsbad, Part II: Saline anomalies due to theoretical extreme case hydraulic scenarios
- Jirka, G. H. (2006). Improved discharge configurations for brine effluents from desalination plants, *J. Hydraulic Engineering*, ASCE, submitted
- Jirka, G.H. & Akar, P.J., 1991a, "Hydrodynamic Classification of Submerged Single-Port Discharges", *J. Hydraulic Engineer-ing*, ASCE, (117), 1095-1111, HY9
- Jirka, G.H. & Doneker, R.L., 1991b, "Hydrodynamic Classification of Submerged Multiport Diffuser Discharges", *J. Hydraulic Engineer-ing*, ASCE, (117), 1113-1128, HY9
- Jirka, G.H. (1979): Discussion of Roberts, P.J.W.: Line plume and ocean outfall dispersion. *J. Hydraul. Div. ASCE* 102(12), 1573-1575
- Jirka, G.H. (1982): Turbulent Buoyant Jets in Shallow Fluid Layers. In Rodi, W. (Ed.) *Turbulent Jets and Plumes*, Pergamon Press
- Jirka, G.H. (1994): Shallow jets. In Davies, P.A. and Valente, M.J. (Eds.): *Recent Advances in the Fluid Mechanics of Turbulent Jets and Plumes*. Kluwer Academics Publishers, Dordrecht
- Jirka, G.H. (2004), „Integral model for turbulent buoyant jets in unbounded stratified flows. Part 1: The single round jet”. *Environ. Fluid Mech.*, 4, 1-56
- Jirka, G.H. (2004): Integral model for turbulent buoyant jets in unbounded stratified flows. Part 1: The single round jet. *Environ. Fluid Mech.* 4, 1-56
- Jirka, G.H. (2006): Integral model for turbulent buoyant jets in unbounded stratified flows. Part 2: Plane jet dynamics resulting from multiport diffuser jets. *Environ. Fluid Mech.* 6, 43-100
- Jirka, G.H. (2008): Improved discharge configurations for brine effluents from desalination plants. *J. Hydraul. Eng.* 134, 116-120
- Jirka, G.H. and Akar, P.J. (1991): Hydrodynamic classification of submerged single port discharges. *J. Hydraul. Eng.* 117, 1113-1128
- Jirka, G.H. and Doneker, R.L. (1991): Hydrodynamic classification of submerged single port

- discharges. *J. Hydraul. Eng.* 117, 1095-1112
- Jirka, G.H. and Doneker, R.L. (2003): Discussion of Carvalho, J.L.B., Roberts, P.J.W. and Roldao, J.: Field observation of Ipanema beach outfall. *J. Hydraul. Eng.* 129(10), 823-826
- Jirka, G.H. and J.H.-W. Lee, 1994, "Waste Disposal in the Ocean", in "Water Quality and its Control", M. Hino (ed.), Balkema, Rotterdam
- Jirka, G.H. and Lee, J.H.-W. (1994): Waste Disposal in the Ocean, in "Water Quality and its Control", M. Hino (ed.), Balkema, Rotterdam
- Jirka, G.H., Abraham, G. and Harleman, D.R.F. (1976): An assessment of techniques for hydrothermal prediction. Department of Civil Engineering, MIT for US Nuclear Regulatory Commission, Cambridge
- Jirka, G.H., Adams, E. and Stolzenbach, K. (1981): Properties of surface buoyant jets. *J. Hydraul. Div. ASCE* 106(11)
- Jirka, G.H., and Doneker, R.L. (1991), "Hydrodynamic classification of submerged single port discharges". *J. Hydraul. Eng.*, 117, 1095-1112.
- Jirka, G.H., Bleninger, T., Burrows, R. and Larsen, T. (2004): Environmental Quality Standards in the EC-Water Framework Directive: Consequences for Water Pollution Control for Point Sources. European Water Management Online, European Water Association (EWA), [www.ewaonline.de](http://www.ewaonline.de)
- Jirka, G.H., Bleninger, T., Burrows, R., and Larsen, T., 2004, "Management of point source discharges into rivers. Where do Environmental Quality Standards in the new EC-Water Framework Directive Apply?", *Journal of River Basin Management*, Vol.2, 3
- Jirka, G.H., Doneker, R.L. and Hinton, S.W. (1996): User's manual for CORMIX: A hydrodynamic mixing zone model and decision support system for pollutant discharges into surface waters, U.S. Environmental Protection Agency, Tech. Rep., Environmental Research Lab., Athens, Georgia, USA
- Jirka, G.H., Doneker, R.L., and Hinton, S.W. (1996), "User's manual for CORMIX: A hydrodynamic mixing zone model and decision support system for pollutant discharges into surface waters", U.S. Environmental Protection Agency, Techn. Rep., Environmental Research Lab., Athens, Georgia, USA.
- Kastner, C. (2008): Meerwasserentsalzungsanlagen – Ableitung umweltrelevanter Standards. Diplomarbeit zur Erlangung des akademischen Grades Diplom-Geoökologin
- KEMA (2006): Quatargas trials EU's seawater chlorination Best Available Technique, Meeting the strict new standard, Information leaflet produced by KEMA, The Netherlands
- Kinnetic Laboratories Inc. (1999): Historical Review of Ocean Outfall Monitoring Program and Effects of Discharge on Marine Environment. Prepared for the City of Santa Cruz
- Krishna, H.J. (1989): Introduction to Desalination Technologies
- Kwarteng, A.Y., Dorvlo, A.S. and Yijaya Kumar, G.T. (2009): Analysis of a 27-year rainfall data (1977-2003) in the Sultanate of Oman. *Int. J. Climatol.* 29(4), 605-617
- Lahmeier International (2003): Water Desalination brochure
- Lamei, A., Von Münch, E., van der Zaag, P., "Environmental Impact and Economic Costs of Brine Disposal from RO Desalination Plants in Arid Coastal Regions", *Proc. IDA World Congress – Atlantis, The Palm – Dubai, UAE November 7-12, 2009*
- Lamparelli, C. (2003): Commissioning and monitoring challenges regarding ocean outfalls: San Paulo State Experience. *Proc. Submarine Outfalls: Design, Compliance and Environmental Monitoring, CETESB, San Paulo, Brazil*
- Latorre, M. (2005): Environmental impact of brine disposal on Posidonia seagrasses. *Desalination* 182, 517-524
- Lattemann, S. and Höpner, T. (2003), *Seawater Desalination: Impacts of Brine and Chemical*

- Discharge on the Marine Environment, Desalination Publications, L'Aquila, Italy
- Lattemann, S. and Höpner, T. (2008): Environmental impact and impact assessment of seawater desalination. *Desalination* 220, 1-15
- Lattemann, S. and Höpner, T., 2003, "Seawater Desalination: Impacts of Brine and Chemical Discharge on the Marine Environment", Desalination Publications, L'Aquila, Italy
- Law, A.W.K., Lee, C.C. and Qi, Y. (2002): CFD modeling of a multiport diffuser in an oblique current. *Proc. Marine Waste Water Discharges, MWWD 2002, Istanbul, Turkey*
- Le Page, S.D. (2005): Salinity Tolerance Investigations: A Supplemental Report for the Carlsbad, CA. Desalination Project
- Lee, J.H.W. and Cheung, V. (1990): Generalized lagrangian model for buoyant jets in current. *J. Environ. Eng. ASCE* 116(6), 1085-1105
- Lee, J.H.W. and Jirka, G.H. (1981): Vertical round buoyant jet in shallow water. *J. Hydraul. Div. ASCE* 107(12), 1651-1675
- Lee, J.H.W. and Neville-Jones, P. (1987): Initial dilution of horizontal jet in crossflow. *J. Hydraul. Eng. ASCE* 113(5), 615-629
- Malfeito, J.J., Diaz-Caneja, J., Farinas, M., Fernandez-Torrequemada, Y., Gonzalez-Correa, J.M., Carratala-Gimenez, A. and Sanchez-Lizaso, J.L. (2005): Brine discharge from the Javea desalination plant. *Desalination* 185, 87-94
- Mannaa, A.J.I. (1994): Environmental impacts of dual purpose plants. *Desalination and Water Reuse* 41, 46-49
- MEC Analytical Systems (2005): Toxicity testing of the concentrate discharge of the Carlsbad seawater desalination plant
- Mendez Diaz, M.M. and Jirka, G.H. (1996): Trajectory of multiport diffuser discharges in deep co-flow. *J. Hydraul. Eng. ASCE* 122(8), 428-435
- Mickley, M. (1995): Environmental considerations for the disposal of desalination concentrates. *Desalination and Water Reuse* 54, 56-61
- Mickley, M. (2006): Membrane Concentrate Disposal: Practices and Regulation. Mickley and Associates, sponsored by the US Department of Interior, Bureau of Reclamation, Agreement No. 98-FC-0054, 2006
- Mickley, M. (2006): Zero liquid discharge options for concentrate disposal.
- Miller, D. (2003): Bridging the gap: Desalination of recycled, brackish and ocean water. *Southwest Hydrology* 2(3).
- Miller, J.E. (2003): Review of water resources and desalination technologies. *Sand Unlimited Release*
- Miri, R. and Chouikhi, A. (2005): Ecotoxicological marine impacts from seawater desalination plants. *Desalination* 182, 403-410
- Moch, I. (2007): Better data and more awareness needed on discharges. *Desalination and Water Reuse* 17/1
- Morton, A.J., Callister, I.K. and Wade, N.M. (1996): Environmental impacts of seawater distillation and reverse osmosis processes. *Desalination* 108, 1-10
- Munk, F. (2008): Ecological and economic analysis of seawater desalination plants, Diploma thesis, Institute for Hydromechanics, University of Karlsruhe
- Munro, D. (1984): Sewage dilution between outfall and shore. *Public Health Engineer* 12(2), 113-114.
- Munro, D. and Mollowney, B.M. (1974): The effect of a bottom countercurrent and vertical diffusion on coliform concentrations at the shore due mainly wind-induced onshore currents. *Rapports et Proces-verbaux des Reunions Conseil International pour l'Exploration de la Mer* 167, 37-40
- Nash, J. D. (1995). Buoyant discharges into reversing ambient current, Master thesis, DeFrees Hydraulics Laboratory, Cornell University, Ithaca NY

- Nash, J.D. (1995): Buoyant discharges into reversing ambient current, Master thesis, DeFrees Hydraulics Laboratory, Cornell University, Ithaca NY
- National Hydrographic Office (2008): Oman Maritime Book 2009. Royal Navy of Oman
- Neves, M. and Neves, A. (1992): Descarga de Aguas Residuais no Mar. Exutores Submarinos. Actas do I Encontro da Engenharia Civil Ibero-Americana, Caceres, Espanha e Revista no 62 da Ordem dos Engenheiros
- Niepelt, A. (2007): Development of interfaces for the coupling of hydrodynamic models for brine discharges from desalination plants, Diploma thesis, Institute for Hydromechanics, University of Karlsruhe
- NRC (2008): Desalination: A National Perspective, Committee on Advancing Desalination Technology, Water Science and Technology Board, Division on Earth and Life Studies, National Research Council of the National Academies
- Okely, P.N., Antenucci, J.P. and Imberger, J. (2007): Field Investigation of the Impact of the Perth Seawater Desalination Plant Discharge on Cockburn Sound During Summer
- Okinawa Bureau for Enterprises (Anonymous): Environmental impact assessment report for the seawater desalination project in Okinawa, Japan, Executive summary
- Passavant Roedinger (2008): Membranverfahren. [Online] 2008. [Cited: 10 03 2008.] [http://www.passavant-roedinger.de/page/page\\_ID/288?PHPSESSID=f00bc6f9e0fb25ec78de228d1a110403](http://www.passavant-roedinger.de/page/page_ID/288?PHPSESSID=f00bc6f9e0fb25ec78de228d1a110403)
- Payo, A., Cortés, J.M., Molina, R., Effect of wind and waves on a nearshore brine discharge dilution in the east coast of Spain", *Proceedings of Intl. Conference and Exhibition on Desalination for the Environment, Clean Water and Energy, Organized by the European Desalination Society, Baden Baden, Germany, 17 - 20 May 2009*
- Pérez Talavera, J.L., Quesada Ruiz, J.J., "Identification of the mixing processes in brine discharges carried out in Barranco del Toro Beach, south of Gran Canaria (Canary Islands)", *Desalination* 139 (2001) 277–286
- Peters, T. (2005): Ultrafiltration und Module mit Offenkanal-Technik - Szenarien der chemikalienfreien Voraufbereitung von Meerwasserentsalzung. DME-Seminar: Wasservorbehandlung in der Meerwasserentsalzung
- Peters, T. and Pintó, D. (2006): Sub-seabed drains provide intake plus pretreatment. *Desalination and Water Reuse* 16
- Purnama, A. and Al-Barwani, H.H. (2006): Spreading of brine waste discharges into the Gulf of Oman. *Desalination* 195, 26-31
- Ragas, A.M.J. (2000): Uncertainty in Environmental Quality Standards, Doctoral dissertation, University of Nijmegen, The Netherlands
- Ragas, A.M.J., Hams, J.L.M. and Leuven, R.S.E.W. (1997): Selecting water quality models for discharge permitting, *European Water Pollution Control*, 7(5), 59-67
- Raventos, N., Macpherson, E. and Garcia-Rubies, A. (2006): Effect of brine discharge from a desalination plant on macrobenthic communities in the NW Mediterranean. *Marine Environmental Research* 62, 1-14
- RCJ, Royal Commission for Jubail and Yanbu. (1999): Royal Commission Environmental Regulations. Kingdom of Saudi-Arabia
- RFRD, Residents for Responsible Desalination. (2008): Huntington Beach desalination facts. [Online] 2008. [Cited: 08 02 2008.] [http://www.hbdesalfacts.org/html/public\\_opinion.html](http://www.hbdesalfacts.org/html/public_opinion.html)
- Ridge, M.M. (2002): Three-dimensional simulation of pollutant dispersion in coastal water. PhD thesis, Universitat Politècnica de Catalunya, Barcelona
- Roberts, P.J.W. (1979): Line plume and ocean outfall dispersion. *J. Hydraul. Div. ASCE* 105(4), 313-331

- Roberts, P.J.W. (1980): Ocean outfall dilution: Effects of Currents. J. Hydraul. Div. ASCE 106(5), 313-310
- Roberts, P.J.W. (1986): Engineering of ocean outfalls. In Kullenberg, G. (Ed.): The Role of Oceans as a Waste Disposal Option. NATO ASI series C 172, 73-109
- Roberts, P.J.W. (1990): Outfall design considerations. In Le Mehaute, B. and Hanes, D.M. (Eds.) The Sea: Ocean Engineering Science, Wiley-Interscience
- Roberts, P.J.W. (1996): Sea outfalls. In Singh, V.P. and Hager, W.H. (Eds.) Environmental Hydraulics, Kluwer
- Roberts, P.J.W. and Snyder, W.H. (1993): hydraulic model study for the Boston outfall: I. Riser configuration. J. Hydraul. Eng., 119(9), 970-987
- Roberts, P.J.W., Snyder, W.H. and Baumgartner (1989a): Ocean outfalls. I. Submerged waste field formation. J. Hydraul. Eng. 115(1), 1-25
- Roberts, P.J.W., Snyder, W.H. and Baumgartner (1989b): Ocean outfalls. II. Spatial evolution of submerged waste field. J. Hydraul. Eng. 115(1), 26-48
- Roberts, P.J.W., Snyder, W.H. and Baumgartner (1989c): Ocean outfalls. III. Effect of diffuser design on submerged waste field. J. Hydraul. Eng. 115(1), 49-70
- Rouse, H., Yih, C.S. and Humphreys, H.W. (1952): Gravitational convection from a boundary source. Tellus 4
- Rutherford, J.C. (1994): River Mixing, John Wiley, Chichester
- Rutherford, J.C., 1994, „River Mixing“, John Wiley, Chichester
- Salas, H. (1994): Emisarios submarinos, alternativa viable para la disposicion de aguas negras de ciudades costeras en America Latina. CEPIS (Centro Panamericano de Ingenieria Sanitaria) Lima, PE
- San Diego County Water Authority. (2004): Telephonic public opinion and awareness survey
- Sánchez-Lizaso, J.L., Romero, J., Ruiz, J., Gacia, E., Buceta, J.L., Invers, O., Fernández-Torquemada, Y., Mas, J., Ruiz-Mateo, A. and Manzanera, M. (2008): Salinity tolerance of the Mediterranean seagrass *Posidonia oceanica*: recommendations to minimize the impact of brine discharges from desalination plants. Desalination 221, 602–607
- Shams El Din, A.M., Aziz, S. and Makkawi, B. (1994): Electricity and water production in the Emirate of Abu Dhabi and its impact on the environment. Desalination 97, 373-388
- Signell, R.P., Jenter, H.L. and Blumberg, A.F. (2000): Predicting the Physical Effects of Relocating Boston's Sewage Outfall. US Geological Survey, Wood Hole, MA, USA
- Southwest Florida Water Management District (1997): Effects of the Disposal of Seawater Desalination Discharges on Near Shore Benthic Communities, University of South Florida
- Sultanate of Oman (2005): Ministerial Decision No: 159/2005, Promulgating the bylaws to discharge liquid waste in the marine environment, Ministry of Regional Municipalities, Environment and Water Resources
- Sydney Water, GHD, Fichtner. *Environmental assessment for Sydney's desalination project*, 2005.
- Talavera, J.L.P. and Ruiz, J.J.Q. (2001): Identification of the mixing processes in brine discharges carried out in Barranco del Toro Beach, south of Gran Canaria (Canary Islands). Desalination 139, 277-286
- Tampa Bay Water (2005): Public opinion survey
- Technology Review (2006): Desalination in Spain. MIT Enterprise, <http://www.technologyreview.com/microsites/spain/water/index.aspx#>
- Tetra Tech Inc. (2000): Ocean Circulation and Plume Dispersion Modeling Review, with Emphasis on Orange County Sanitation District's Offshore Outfall and Wastewater Plume. Orange County Sanitation District, California, USA [http://www.ocwatersheds.com/watersheds/pdfs/Ocean\\_Circulation\\_Plume\\_Dispersion\\_Model](http://www.ocwatersheds.com/watersheds/pdfs/Ocean_Circulation_Plume_Dispersion_Model)

ing.pdf

- Tettelbach, S.T. and Rhodes, E.W. (1981): Combined effects of temperature and salinity on embryos and larvae of the northern bay scallop *Argopecten irradians*. *Mar. Biol.* 63, 249-256
- Tolba, M.K. and Saab, N. (2006): Arab Public Opinion & the Environment: Report of 18 country survey
- Tsiourtis, N.X. (2001): Desalination and the environment. *Desalination* 141, 223-236
- UN ESCWA (2001): Water Desalination Technologies in the ESCWA member countries. UN Economic and Social Commission for Western Asia
- UNEP MAP (2003): Sea water desalination in the Mediterranean: Assessment and guidelines. MAP Technical Reports Series No. 139, United Nations Environment Programme (UNEP), Mediterranean Action Plan (MAP)
- UNESCO, 1981, "UNESCO Technical Papers in Marine Sciences 38: Background papers and supporting data on the Int. Equation of State of Seawater 1980", Paris, France
- UNESCO, 1991, "UNESCO Technical Papers in Marine Sciences 62: Salinity and density of SW: Tables for high salinities (42-50)", Paris, France
- US EPA (1994): Water Quality Standards Handbook: Second Edition. EPA 823-B-94-005a, Washington DC, USA
- US EPA (1998): Guidelines for Ecological Risk Assessment. EPA/630/R-95/002F, Risks Assessment Forum, US EPA, Washington DC, USA
- US EPA (2006): National Recommended Water Quality Criteria, National Center for Environmental Publications and Information, 11029 Kenwood Road, Cincinnati, Ohio 45242, USA. Available at <http://www.epa.gov/waterscience/criteria/wqctable/nrwqc-2006.pdf>
- USBRec (2003): Desalination and Water Purification Technology Roadmap - A report of the Executive Committee. US Bureau of Reclamation and Sandia National Laboratories, Denver, USA
- USGS (US Geological Survey) (2004): Huntington Beach Shoreline Contamination Investigation Phase III, Coastal Circulation and Transport Patterns: The Likelihood of OCSD's Plume Impacting the Huntington Beach Shoreline. Final Report 04-1019 by Noble, M. and Xu, J. (Eds.)
- Van der Bruggen, B. and Vandecasteele, C. (2002): Distillation vs. membrane filtration: overview of process evolutions in seawater desalination. *Desalination* 143, 207-218
- Violleau, D., Essis-Torne, H., Habarou, H., Croue, J.P. and Pontie, M. (2005): Fouling studies of a polyamide nanofiltration membrane by selected natural organic matter: An analytical approach. *Desalination* 173, 223-238
- von Medeazza, G.L.M. (2005): "Direct" and socially-induced environmental impacts of desalination. *Desalination* 185, 57-70
- Walker, D.I. (1989): Regional Studies – Seagrass in Shark Bay, the Foundations of an Ecosystem. In: Larkum AWD, McComb AJ, Sheperd SA (Eds), *Biology of Seagrasses – A Treatise on the Biology of Seagrasses with Special Reference to the Australian Region*. Elsevier, Amsterdam, pp. 182-210
- Wallingford, HR (2001): Barka power and desalination project phase I. Final bathymetric and marine survey report. HR Wallingford report EX4372
- Water Consultants Intl. (2006): Environmental Literature Review and Position Paper for Perth Seawater Desalination Plant Two and Sydney Seawater Reverse Osmosis Plant.
- Wec (2002): Perth metropolitan desalination proposal. Environmental protection statement, prepared by Welker Environmental Consultancy for Water Cooperation
- WFD (Water Framework Directive) (2000): Official Publication of the European Community, L327, Brussels

- WHO (2007): Desalination for safe water supply: Guidance for the health and environmental aspects applicable to desalination
- WHO (2008): Desalination for safe water supply, Guidance for the health and environmental aspects applicable to desalination. World Health Organization (WHO), Geneva, and Eastern Mediterranean Regional Office (EMRO), Cairo
- Winters, H., Isquith, I.R. and Bakish, R. (1979): Influence of desalination effluents on marine ecosystems. *Desalination* 30, 403-410
- Wolf, P.H., Siverns, S. and Monti, S. (2005): UF membranes for RO desalination pretreatment. *Desalination* 182, 293-300
- Wood, I.R., Bell, R.G. and Wilkinson, D.L. (1993): *Ocean Disposal of Wastewater*. World Scientific, Singapore
- Wood, I.R., R.G. Bell and D.L. Wilkinson, 1993, "Ocean Disposal of Wastewater", World Scientific, Singapore
- World Bank Group (1998): *Thermal Power: Guidelines for New Plants, from the Pollution Prevention and Abatement Handbook*. Download from: <http://www.ifc.org/ifcext/enviro.nsf/Content/EnvironmentalGuidelines>
- World Bank Group (1999): *Pollution Prevention and Abatement Handbook 1998. Toward Cleaner Production*, The World Bank Group Washington, D.C., in collaboration with the United Nations Environment Programme and the United Nations Industrial Development Organization
- World Bank Group (2007a): *Environmental, Health, and Safety Guidelines for Water and Sanitation*. Download from <http://www.ifc.org/ifcext/enviro.nsf/Content/EnvironmentalGuidelines>
- World Bank Group (2007b): *Environmental, Health, and Safety General Guidelines (EHS Guidelines)*. Download from <http://www.ifc.org/ifcext/enviro.nsf/Content/EnvironmentalGuidelines>
- WWF (2007): *Desalination: Option or distraction for a thirsty world?*
- Zhang, H. and Baddour, R.E. (1998), "Maximum penetration of vertical round dense jets at small and large Froude numbers". *J. Hydraul. Eng.*, 124(5), 550-553.
- Zhang, H. and Baddour, R.E. (1998), Maximum penetration of vertical round dense jets at small and large Froude numbers. *J. Hydraul. Eng.* 124(5), 550-553
- Zielke, W. and Mayerle, R. (1999): *Kustengewasser*, in Zielke, W. [Hrsg.]: *Numerische Modelle von Flüssen, Seen und Kustengewasser*, DVWK Schriften 127, Bonn

## APPENDIX C: Project Profile Form

The Principal Investigator shall provide a **Project Profile** as a separate document along with the final project report.

The purpose of a profile for each MEDRC research report is to give the busy desalination professional an overview of the full report. Profiles of all MEDRC projects' final reports are made available on the Center's web site and are provided to all individuals and organizations engaged in various desalination activities.

A completed Project Profile Form shall be submitted with the revised draft final project report. Please note that the final report itself will still contain an **Executive Summary**. In writing the Project Profile, the Principal Investigator may use few abbreviations, symbols, or equations. However, if such terms are used, their definitions should be clearly stated the first time they are mentioned.

The Profile is about two (2) pages of text in the format shown below.

### Project Profile Form

(Please provide the profile in Microsoft Word format as an attached file to an e-mail message.)

**Project Title:**

Environmental planning, prediction and management of brine discharges from desalination plants

**Project Number:**

07-AS-003

**Principal Investigator:**

Dr.-Ing. Tobias Bleninger  
Prof. G.H. Jirka, Ph.D.

Institut für Hydromechanik (IfH), Universität Karlsruhe, , Kaiserstr. 12, 76131 Karlsruhe, Germany, Tel.: +49 - 721 / 608-3687, Fax: +49 - 721 / 608-2202, E-mail: bleninger@ifh.uka.de , URL: www.ifh.uni-karlsruhe.de

**Research Partners:**

Dipl.-Ing. Anne Niepelt Research assistant at the IfH at the University Karlsruhe  
Dipl.-Wi.-Ing. Frank Münk, Diploma student of Engineering Economics in cooperation with the IfH at the University of Karlsruhe

Prof. Anton Purnama & Prof. Hamdi H. Al-Barwani, Sultan Qaboos University (SQU), Department of Mathematics and Statistics, P.O. Box 36, Al-Khod PC 123, Muscat, Sultanate of Oman, Tel: +968 2414 1425, Fax: +968 2441 3415, E-mail: hamdi@squ.edu.om, URL: www.squ.edu.om/sci/Math/

Prof. Robert L. Doneker MixZon Inc. and Department of Civil and Environmental Engineering, Portland State University, Oregon, USA, 1033 SW Yamhill Street, Suite 301, Portland, Oregon 97205-2539, USA, Tel.: +1 - 503 222 1022, Fax: +1 - 503 296 2354, E-mail: doneker@mixzon.com, URL: www.mixzon.com

Sabine Lattemann, M.Sc., Prof. Dr. Thomas Höpner, Dipl.biol.H.Brunken-Winkler, ARSU - Regional Planning and Environmental, Research group, Escherweg 1, 26121 Oldenburg, Germany, Tel.: +49 - 441 / 97174 - 97, Fax: +49 - 441 / 97174 - 73, E-mail: sabine.lattemann@icbm.de, URL: www.arsu.de

**Objectives:**

- (I) Identification of environmental impacts, regulatory frameworks and public concerns regarding brine effluent discharges
- (II) Elaboration of design nomograms
- (III) Development of hydrodynamic model interfaces for predicting brine effluent concentrations of key parameters in the marine environment by coupling a near-field mixing model with a far-field transport model
- (IV) Model application and validation for typical case studies
- (V) Management and realization of capacity building on environmental planning, prediction and management of brine discharges from desalination plants.

**Background:**

Sea water desalination plants discharge a concentrated brine effluent into coastal waters. Modern, large capacity plants require submerged discharges that ensure a high dilution in order to minimize harmful impacts on the marine environment. Existing design practice is limited to poor modeling concepts and a very heterogeneous or weak regulatory base. Stakeholder opinions vary from “negligible very localized impacts” up to major objections leading to significant project modifications and unnecessary delays.

**Highlights:**

Efficient technologies exist to reduce the environmental impacts of desalination effluents and ensure that these technologies are not necessarily more costly than conventional systems. One technology is multiport diffusers with an optimized discharge design.

Future amendments of the regulation procedures must contain a clear mixing zone regulation for all point sources. The ambient standards should apply outside and at the edge of the “mixing zone”, a spatially restricted region around the point source.

The analysis of the concentration distributions shows the importance of model coupling. The far-field model can not simulate the strong mixing processes occurring in the near-field particularly with regard to the vertical mixing. Thus, the vertical distribution of the plume needs to be calculated by the use of a near-field model and must then be transferred into the far-field model.

The coupling methodology, though simple, allows for an considerably improved discharge assessment.

**Approach:**

First, the identification of environmental impacts, regulatory frameworks and public concerns regarding brine effluent discharges. Second, the elaboration of easily applicable design nomograms as a basis for the first screening process within the assessment of brine discharges. Third, the development of hydrodynamic model interfaces for predicting brine effluent concentrations of key parameters in the marine environment by coupling a near-field mixing model for outfall design optimization with a far-field transport model for optimized outfall siting. Fourth, the model application and validation for typical case studies for the compilation of design recommendations with parallel improvement of design oriented input/output features. And fifth, the management and realization of capacity building activities.

**Results/Findings:**

Efficient technologies exist to reduce the environmental impacts of desalination effluents and ensure that these technologies are not necessarily more costly than conventional systems. One technology is multiport diffusers with an optimized discharge design.

Future amendments of the regulation procedures must contain a clear mixing zone regulation for all point sources. The ambient standards should apply outside and at the edge of the “mixing zone”, a spatially restricted region around the point source.

The analysis of the concentration distributions shows the importance of model coupling. The far-field model can not simulate the strong mixing processes occurring in the near-

field particularly with regard to the vertical mixing. Thus, the vertical distribution of the plume needs to be calculated by the use of a near-field model and must then be transferred into the far-field model.

The coupling methodology, though simple, allows for an considerably improved discharge assessment.

**Impact:**

The coupling methodology, though simple, allows for an considerably improved discharge assessment.

## APPENDIX D: Desalination Technologies

The most important desalination technologies can be divided into two process groups. *Thermal processes* use heat to evaporate water, leaving the salts behind in the brine. The thermal technology with the highest market share is Multi Stage Flash (MSF). *Membrane processes* use pressure or electricity to force water through a semi-permeable membrane which blocks salts and other dissolved solids. The main membrane technology is Reverse Osmosis (RO). Almost half of the global desalination capacity which includes all source waters like seawater, brackish water or river water is covered by Reverse Osmosis plants. MSF plants have the second largest share (Figure 144).

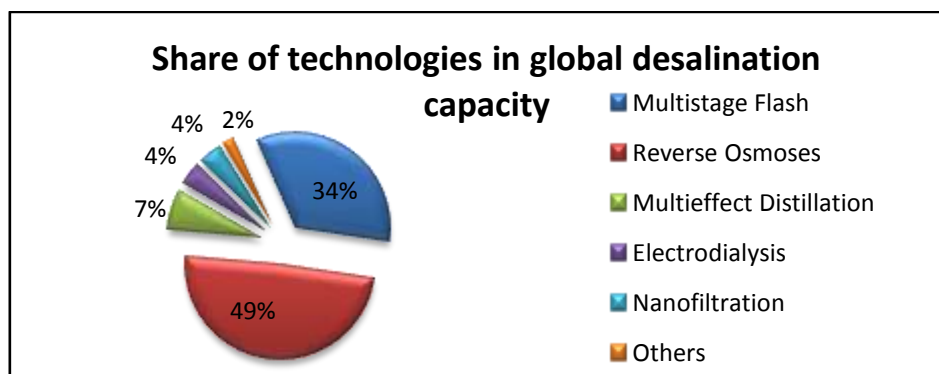


Figure 144: Global distribution of installed desalination capacity by technology (based on Höpner and Lattemann, 2008)

When only seawater desalination capacities are considered, MSF plants account for the highest share of the production (Figure 145). The share of RO plants has continuously increased in the last years and is predicted to catch up further in the future. The clear lead of MSF technology in the seawater sector is due to its strong predominance in the countries of the MENA (Middle East and North Africa) region (Höpner and Lattemann, 2008).

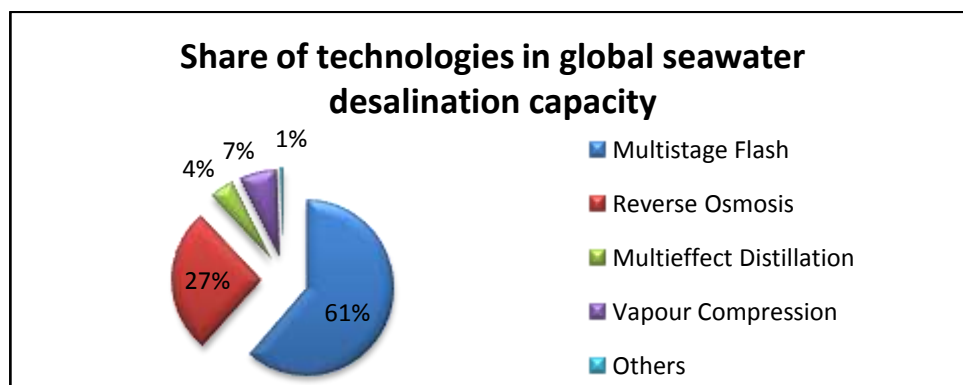


Figure 145: Global distribution of installed seawater desalination capacity by technology (based on Glade, 2005)

### Thermal technologies

Thermal processes, also called distillation processes, involve the evaporation and condensation of water. The main field of application is seawater desalination. Because of the high energy consumption, thermal desalination is mainly applied in countries with low energy prices and high energy resources. In most cases, thermal plants are operated in cogeneration



## Multi Effect Distillation (MED)

Multi Effect Distillation is the oldest desalination technology. MED units are usually built for capacities of 2,000-20,000 m<sup>3</sup>/d and the energy consumption amounts to around 15 kWh/m<sup>3</sup> (Al-Sahali and Ettouney, 2007).

The configuration is very similar to MSF. Seawater is boiled in several consecutive steps, called 'effects', at decreasing temperatures and pressures. In contrast to MSF, seawater is sprayed directly onto the heat exchanger tubes of each effect at the same time. The water evaporates and the generated vapour of one effect is transferred into the heat exchanger tubes of the following effect, where it condensates and causes more water to evaporate (Figure 147). A boiler generates the steam for the first effect and the vapour of the final stage is used to preheat the feed water. As the water does not evaporate from the bottom of the pressure chambers like in MSF units but directly on top of the heat transfer tubes, severe corrosion and scaling problems on the tubes are caused. Therefore the TBT must be reduced to values of around 70 °C. Because of these problems and the higher costs, MED lost competition against MSF in most applications (Miller, 2003), but is increasingly used again today due to the lower energy requirements and lower operating temperatures.

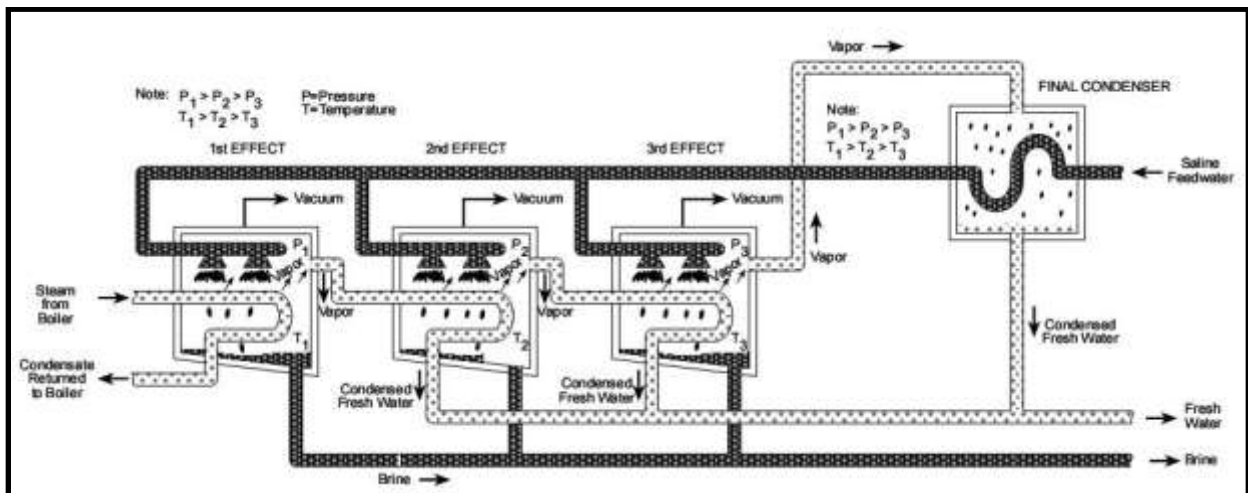


Figure 147: Schematic of the Multi Effect Distillation process with three effects (Buros, 2000)

## Vapour compression

In the case of vapour compression, the energy to evaporate the feed water is produced by compressing vapour with a mechanical or thermal compressor. The vapour enters the heat exchanger tubes and the pressure is decreased. At a certain pressure drop, the vapour condensates and latent heat is released. Thus, the feed water which is sprayed onto the tubes evaporates and more vapour is generated and compressed.

Vapour compression has a typical energy consumption of 7-12 kWh/m<sup>3</sup> which is lower than for other thermal processes. It is a very reliable technology and is mainly used for small desalination capacities of 3,000 m<sup>3</sup>/d or less. The reason for this is that each stage of the process needs its own compressor and compressors are expensive. Low cost compressors, however, cannot provide enough pressure to operate on several stages. Therefore, the process is most often limited to one or a few stages and restricted to small capacities.

## Membrane processes

In contrast to distillation, membrane processes are based on the separation of water and salts via a semi-permeable membrane. The *Reverse Osmosis* process uses pressure to separate the dissolved salts from the feed water. In the case of *Electrodialysis*, electricity is used. Reverse Osmosis can be applied for brackish and seawater sources. Many innovations and improvements in membrane efficiency and energy recovery have contributed to the accelerating distribution and growing popularity of Reverse Osmosis systems.

Nanofiltration plants, which are mostly used for brackish water desalination, apply the same technical principle as Reverse Osmosis plants and will not be separately discussed in this context.

## Reverse Osmosis (RO)

In the RO process, the feed water is pressurised by high pressure pumps to up to 80 bars and then passed through special membranes in an enclosed vessel. The membranes selectively block most dissolved solids including salts and let pure water pass. The blocked salts accumulate and are finally discharged. The amount of produced fresh water depends on the applied pressure and on the salt content of the feed water. The energy consumption increases with growing membrane pressure. By using recent methods of energy recovery, the energy consumption can be reduced to 3 kWh/m<sup>3</sup> (Buros, 2000). The typical components of an RO desalination system are illustrated in Figure 148.

Depending on the application and the feed water characteristics, several membrane materials and configurations can be applied. The first successful material on the market was *cellulose acetate*. Today a mix of cellulose di- and tri-acetate is usually used. However, synthetic polymer materials are increasingly replacing the natural cellulose membranes. This is mainly due to the better salt rejection and the higher durability of synthetic materials. Furthermore, polyamides resist to higher pH ranges and cope better with biological attacks and other feed water pollution. In contrast, they are very susceptible to chlorination.

The two most important membrane *configurations* are hollow thin fibre and spiral wound membranes. In the *hollow fibre* configuration, many thin fibre tubes (85 µm in diameter) are packed to bundles and placed inside a vessel. As the pressurised feed water flows into the vessel, it partly passes through the thin fibre structures and enters the tubes in a desalinated state. Due to the tiny spacing among the fibres tubes ( $\approx 25 \mu\text{m}$ ), particle trapping is a major danger. Therefore, the feed water quality has to be exactly controlled.

In the *spiral wound* configuration, thin membrane layers are wrapped around a collecting tube. The pressurised feed water is flowing in a spiral between the membrane layers. Portions of it are pushed through the membranes and enter the central collecting tube in a desalinated state. The remaining water concentrates and flows out as brine. Since spiral wound membranes are less loosely packed (several mm) they enable larger flux rates (membrane flux rates are defined as water volume per membrane area and time unit) and are less susceptible to particle trapping than hollow fibre configurations. Instead, the thin layers are more sensible to particle erosion and larger flux rates promote particle deposition (Krishna, 1989; Lattemann and Höpner, 2003).

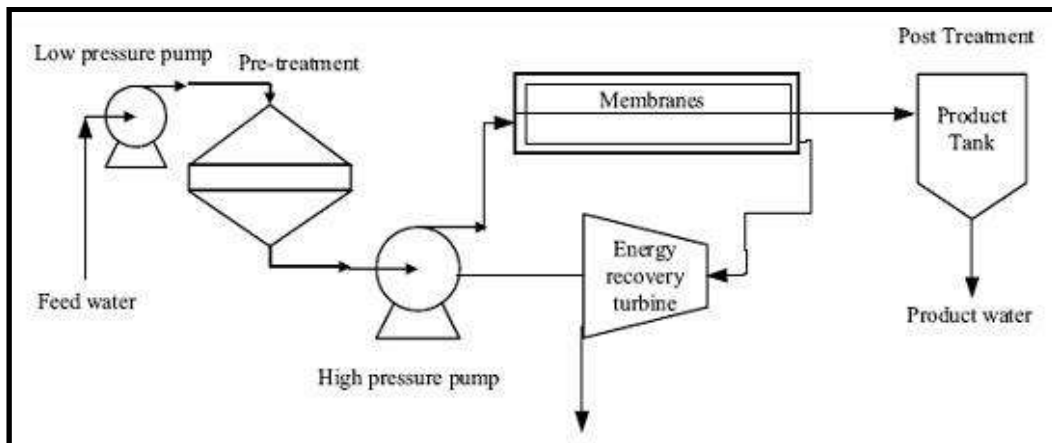


Figure 148: Major components of an RO desalination system (Munk, 2008)

## Electrodialysis (ED)

Most salts in water are ionic and thus can be deflected by an electric field. In an electrodialysis system the feed water flows into different chambers, divided by alternating cation and anion selective membranes (Figure 149). As voltage is connected, the anions are flowing towards the positive pole and the cations towards the negative pole. As the selective membranes are installed alternately, anions and cations can only pass one membrane and the next one is impenetrable. Thus, alternating chambers of concentrated and desalinated water are created which are extracted by different tube systems (Buros, 2000).

ED plants are mainly used for brackish water sources, since energy consumption is increasing proportionally with the salt concentration. As no pressure is applied and no water is streaming through the membranes, ED can handle higher levels of particle pollution than RO plants. Thus, less filtration and pretreatment is needed in ED systems (Miller, 2003).

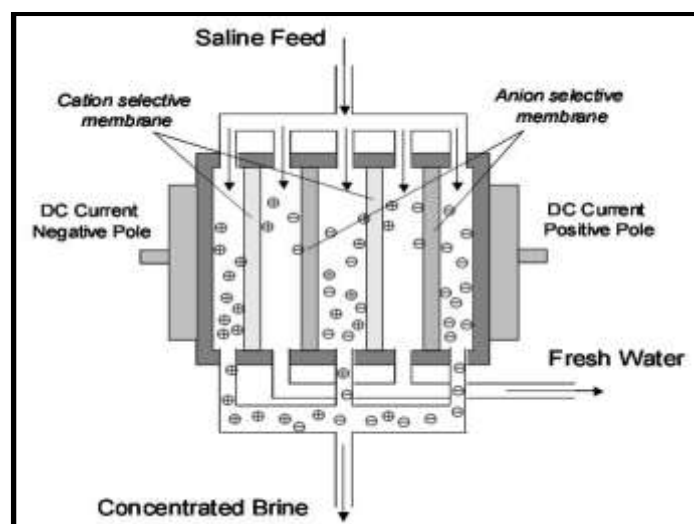
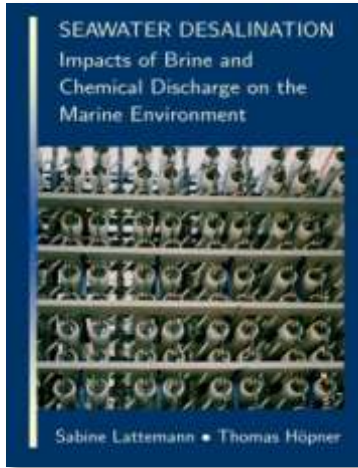


Figure 149: Schematic of the Electrodialysis process (Miller, 2003)

# APPENDIX E: Environmental Impacts

The following list provides a literature overview on the most relevant sources of *secondary* literature.



## Seawater Desalination - Impacts of brine and chemical discharges on the marine environment.

The book focuses on the chemical pretreatment and the chemical composition of desalination plant disposal brines and discusses the potential ecological impacts of the waste constituents. The book is based on a literature review of existing data. It contains maps of the Arabian Gulf and Red Sea, showing the locations of and the chemical loads discharged by the desalination plants. Special attention is given to the Arabian Gulf with the world's highest concentration of desalination plants.

S. Lattemann and T. Höpner (2003), Desalination Publications, L'Aquila, Italy, 142 p.

Inquiries: <http://www.desline.com/book.shtml>



## Environmental impact and impact assessment of seawater desalination

The paper was presented as a keynote at the EDS Conference on Desalination and the Environment in Halkidiki, Greece, in 2007. It can be regarded a short and updated version of the book "Seawater Desalination - Impacts of brine and chemical discharges on the marine environment" (see above).

S. Lattemann and T. Höpner, Desalination (2008) 220: 1-15

Reprint in Desalination and Water Reuse (2007) 17: Why we must have impact studies and mitigation. pp. 36-44

Download: <http://www.desline.com/articoli/8958.pdf>



## Desalination discharge databank

The discharge databank provides dosing, discharge and environmental data of individual substances/species in reject streams of desalination plants, based on a literature review of previous work, and classified into thermal and RO processes and including impact on bio-systems. It is a comprehensive collection of raw data (as of 2002).

Assessment of the Composition of Desalination Plant Disposal brines, Middle East Desalination Research Center (MEDRC) Research Project, No. 98-AS-026 (2002)

Download: [www.paua.de/Discharge\\_Databank.zip](http://www.paua.de/Discharge_Databank.zip) and [www.paua.de/Discharge\\_Databank\\_User\\_Information.zip](http://www.paua.de/Discharge_Databank_User_Information.zip)

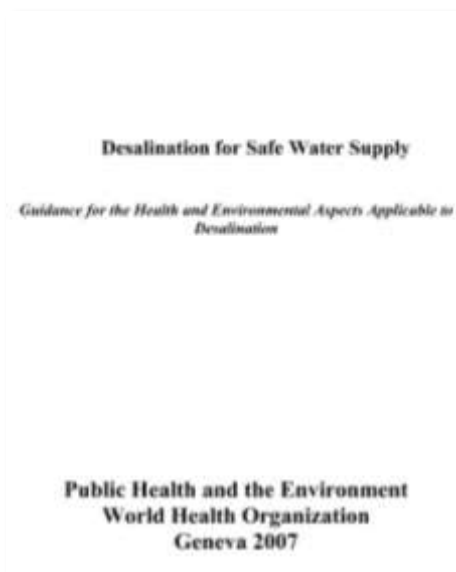


## **Seawater desalination in the Mediterranean, containing the Guidelines for Environmental Sound Management of Seawater Desalination Plants in the Mediterranean Region**

The UNEP/MAP report reviews the sea water desalination activities in the sea region as of 2002. It requires an update regarding the installed capacity, as a considerable growth of the desalination industry has taken place in the region since 2002. The guidelines for the brine disposal include a general review of potential impacts and recommendations for impact mitigations. The information is still accurate, but some more lessons have been learned since.

United Nations Environment Programme (UNEP), Coordinating Unit for the Mediterranean Action Plan (MAP), Marine Pollution Assessment and Control Programme (MED POL), MAP Technical Report No. 139, Athens, 2003.

Download: <http://195.97.36.231/acrobatfiles/MTSAcrobatfiles/mts139eng.pdf>



## **Desalination for safe water supply Guidance for the health and environmental aspects applicable to desalination**

The WHO developed this guidance in order to assist project designers and decision makers to anticipate and address all relevant concerns that may arise when undertaking a desalination project. The topic areas covered are: Technology – Engineering and Chemistry; Health – Toxicology of Contaminants and Nutritional Aspects; Sanitary and Marine Microbiology; Monitoring – Microbiological, Analytical Chemistry, Surveillance, Regulatory; and Environmental Effects and Impact Assessments.

World Health Organization, Public Health and the Environment, Geneva 2007 (draft),

expected publication: 2008 (English, Arabic)

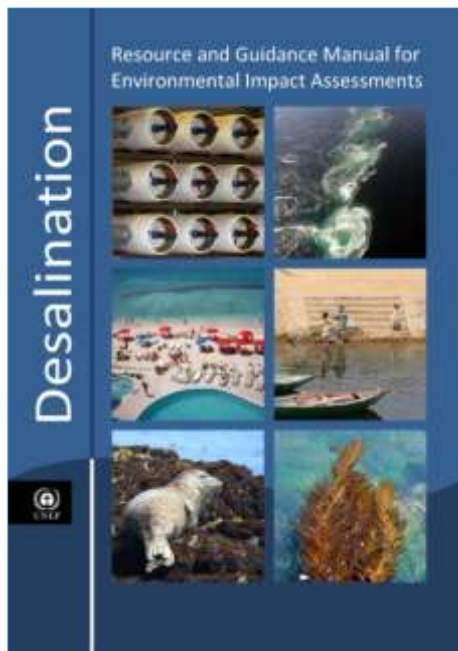
Related overview articles:

J. Cotruvo and S. Lattemann, WHO Guidance on Desalination, Desalination and Water Reuse (2008)

S. Lattemann, WHO Guidance on Desalination: Results of the Work Group on Environmental Impacts, Proceedings of the IDA World Congress on Desalination and Water Reuse, Maspalomas, Gran Canaria, 2007.

Project information site: [www.who.int/water\\_sanitation\\_health/gdwqrevision/desalination/en/](http://www.who.int/water_sanitation_health/gdwqrevision/desalination/en/)

Download (draft): [http://www.who.int/water\\_sanitation\\_health/gdwqrevision/desalination.pdf](http://www.who.int/water_sanitation_health/gdwqrevision/desalination.pdf)



### **Desalination. Resource and Guidance Manual for Environmental Impact Assessments**

The guidance document contains the complete results from the environmental working group of the WHO project "Desalination for safe water supply" (see above) and results from the research project "MEDINA" funded by the European Union within the Sixth Research Framework (see below). Part A of the document outlines a 10-step methodology for EIA studies of desalination and other water supply projects. Part B describes the scope and information requirements of EIA studies in the form of a "checklist". Part C gives an overview on the potential impacts of the discharges on the marine environment based on literature sources. The most comprehensive and most recent information source on environmental impacts to date.

United Nations Environment Programme (UNEP),  
Regional Office for West Asia (ROWA), Bahrain,  
Expected publication in 2008

<http://www.unep.org/bh/Publications/Type7.asp>

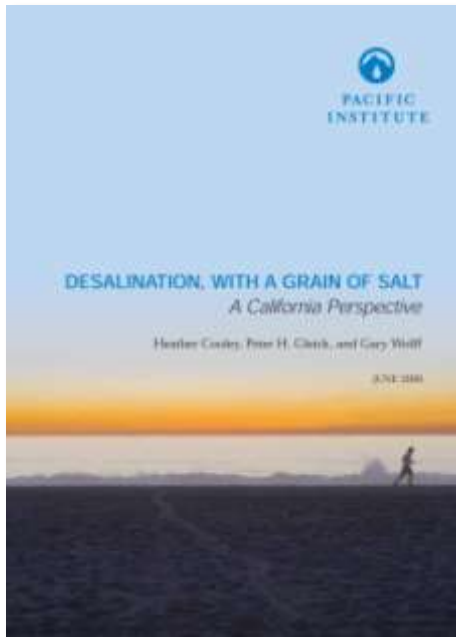


### **Desalination: A national perspective**

In this report, a 12-member group of experts from the United States performed a critical analysis of current state of the art desalination technologies, the potential for desalination to meet anticipated water supply needs in the United States, and the barriers to widespread implementation of desalination in the U.S., including an examination of environmental issues and cost of desalination, and alternative water supply options such as conservation. The report presents reasonable long-term goals for advancing desalination technology and provides recommendations for action and research. It identifies environmental impacts as one major focal point for future research activities.

Committee on Advancing Desalination Technology, Water Science and Technology Board, Division on Earth and Life Studies, National Research Council of the National Academies, The National Academies Press, Washington, D.C. 2008. The report was sponsored by the US Bureau of Reclamation and the U.S. Environmental Protection Agency.

Download: <http://www.nap.edu/catalog/12184.html>

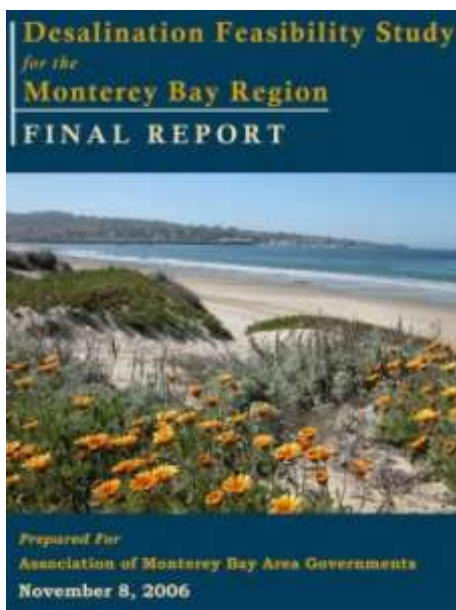


### **Desalination, with a grain of salt. A California Perspective**

In this controversially discussed study, the Pacific Institute provides a comprehensive overview of the history, benefits, and risks of desalination, and the barriers that hinder more widespread use of this technology in California. While some consider the report as a well-written comprehensive look at seawater desalination and its prospects for implementation in the State of California, others regard it as ‘anti-desal polemics’. The report is supposed to have some minor inaccuracies, but most references cited in the report are from recent and reputable sources.

H. Cooley, P. H. Gleick, G. Wolff, Pacific Institute for Studies in Development, Environment, and Security, Oakland, California, 2006.

Download: <http://www.pacinst.org/reports/desalination/index.htm>

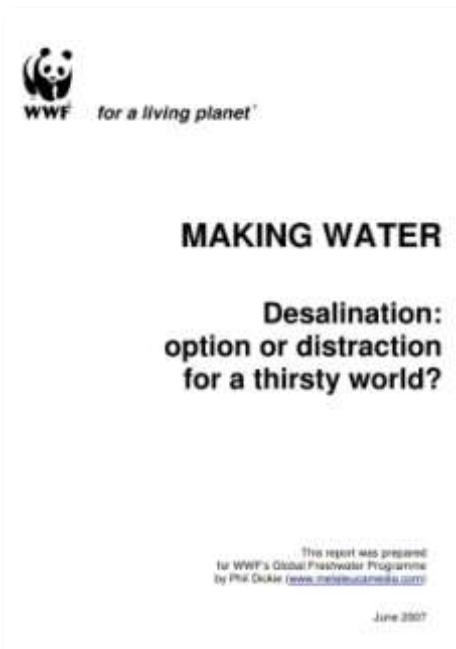


### **Desalination Feasibility Study for the Monterey Bay Region**

The study investigated the environmental, economic, and social impacts, both positive and negative, of seawater desalination project implementation in the context of the Monterey Bay region, California. It includes a baseline assessment of existing marine habitats in the Monterey Bay Region; an overview of the existing water supply situation in the Monterey Bay region and the role of desalination and other alternatives in future water supply portfolios; an analysis of the impacts related to brine discharge, entrainment and impingement, construction impacts, energy use and emissions, growth inducement, land use impacts; and an overview of the existing regulatory environment associated with desalination in the Monterey Bay Area.

B. Damitz, D. Furukawa, J. Toal, prepared for the Association of Monterey Bay Area Governments (AMBAG), 2006

[http://www.ambag.org/publications/reports/Desal%2006/AMBAG\\_FINAL\\_Desal\\_Study.pdf](http://www.ambag.org/publications/reports/Desal%2006/AMBAG_FINAL_Desal_Study.pdf)

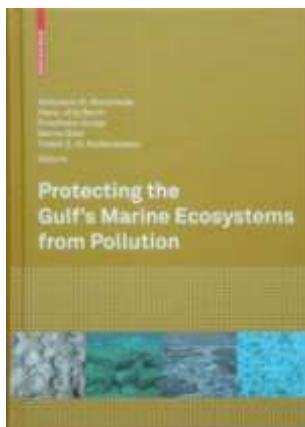


## **Making water. Desalination: option or distraction for a thirsty world?**

Similar to the Pacific Institute's report "Desalination, with a grain of salt" (see above), the World Wildlife Fund's report "Making water" has been discussed controversially and blemished as 'anti-desal polemics' by industry representatives. Phil Dickie, an award winning investigative journalist from Australia, prepared this critical review of worldwide desalination trends and potential environmental concerns related to the waste discharges and greenhouse gas emissions. The WWF's position is that desalination plants should only be constructed where they are found to meet a genuine need to increase water supply and are the best and least damaging method of augmenting water supply.

Phil Dickie ([www.melaleucamedia.com](http://www.melaleucamedia.com)), prepared for WWF's Global Freshwater Programme, 2007

Download: [www.wwf.org.au/publications/desalinationreportjune2007.pdf](http://www.wwf.org.au/publications/desalinationreportjune2007.pdf)



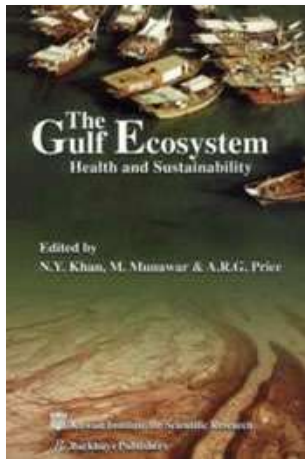
## **Protecting the Gulf's marine ecosystems from pollution**

The recently published book (2008) reviews the present sources and levels of land and sea-based pollution in the Gulf and assesses potential impacts on biota and ecosystems. It is an important source of information for environmental managers, researchers, administrators, and decision makers. The book comprises 16 articles, including different articles on oil pollution and one article on the **Impacts of seawater desalination plants on the marine environment of the Gulf.**

S. Lattemann and T. Höpner (2008), Impacts of seawater desalination plants on the marine environment of the Gulf, In: A. H. Abuzinada, H.-J. Barth, F. Krupp, B. Böer and T. Z. Al Abdessalaam (Eds.), Birkhäuser, Switzerland, 285 p.

Inquiries: <http://www.springer.com/>

Inquiries: <https://commerce.metapress.com/content/g3425m2t1335j148/resource-secured/?target=fulltext.pdf&sid=zto3v245bi3bfzip2tld5g45&sh=www.springerlink.com>

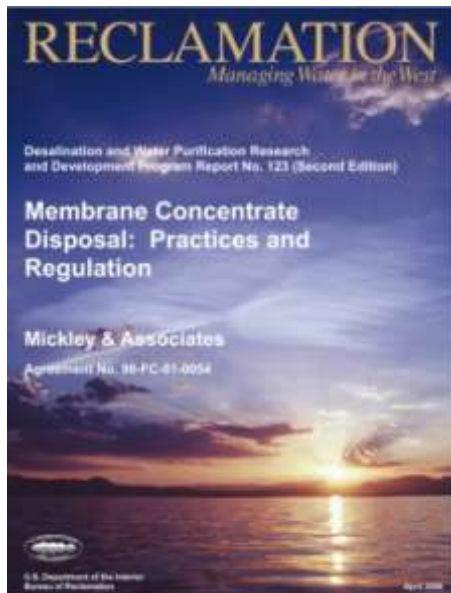


### The **Gulf Ecosystem: Health and Sustainability**

This book describes the bio-geo-physical setting of the Gulf ecosystem, the main sources of anthropogenic pollution including the oil and petroleum industry and the **power and desalination plants**, and other anthropogenic impacts such as habitat degradation, dredging and infilling, fishing and mariculture. It discusses the aquatic ecosystem health of the Arabian Gulf, identifies research and management needs and outlines legal and institutional frameworks.

**H. Khordagui (2002), Power and desalination plants, In:** N.Y. Khan, M. Munawar and A.R.G. Price (Eds.), Backhuys Publishers, Leiden, 510 p.

Inquiries: [http://www.aehms.org/gulfeco\\_toc.html](http://www.aehms.org/gulfeco_toc.html)



### **Membrane Concentrate Disposal: Practices and Regulation (Second Edition)**

The report is based on a detailed survey of 300 membrane plants providing a characterization of the membrane utility industry in general, and the concentrate and backwash disposal practices in particular. This included treatment of concentrate and backwash prior to disposal and disposal of cleaning wastes. Federal regulations were documented to provide the framework for a subsequent state-by-state review of disposal regulations. Design and cost issues associated with the various concentrate disposal options were discussed, and for four disposal options (deep well injection, spray irrigation, evaporation pond, and zero liquid discharge), preliminary level cost models were developed. A stand-alone executable database was developed to permit viewing, manipulation, and printing of the survey information. The report mainly focuses on inland brackish water membrane plants.

Mickley and Associates, Boulder, Colorado, Sponsored by the U.S. Department of the Interior, Bureau of Reclamation, Technical Service Center, Environmental Services Division, Water Treatment Engineering and Research Group, Denver, Colorado, Agreement No. 98-FC-81-0054, 2006.

Download: <http://www.usbr.gov/pmts/water/publications/reportpdfs/report123.pdf>

In the following, a short summary of the above listed literature is presented regarding major constituents and their impacts. A list summarizing reviewed information regarding environmental impact assessments can be found in Appendix F.

## **Antifouling additives**

The most commonly used antifouling additive is chlorine. It is a broad-effect agent and can have equally broad impacts on marine organisms. Moreover, chlorine is highly reactive and provokes dangerous chemical reactions, most importantly the halogenations of organic compounds. Both MSF and RO plants use chlorine or hyperchlorite to prevent fouling. A typical dosage is 2 mg/l. For shock chlorination, several times this value is added for a shorter period.

In RO plants using polyamide membranes, dechlorination of the feed water is carried out in order to protect the membranes. However, minor residual chlorine levels can still be present in the brine and the problem of the toxic halogenated organic compounds remains (Höpner, 1999). Sodiumbisulfite which is commonly used for dechlorination reacts to harmless products but may cause critical oxygen depletion if overdosed.

Nevertheless, the impacts of chlorine are more significant for MSF plants since usually no dechlorination is effected. Besides, MSF plants require larger feed water volumes which increase the loads of chlorine and its by-products. One can assume that 10-25 % of chlorine concentration in the feed water (equal to 200-500 µg/l) can approximately be measured in MSF effluents. Concentrations in the mixing zone of MSF plants were reported to be around 100 µg/l. The mixing zone is the area around the discharge location in which the brine and its constituents are diluted to ambient or given threshold values.

Chlorine is proven to be toxic at concentrations of a few micrograms only. The photosynthesis process of plankton can be seriously reduced at concentrations of only 20 µg/l. At levels of 50 µg/l the composition of marine organisms can change and their variety is reduced. The known lethal values for fish species range between 20 and several hundred µg/l (Lattemann and Höpner, 2003).

Halogenated organic compounds, most importantly trihalomethanes (THM), are typical by-products of chlorine addition and the result of reactions with hypochlorite. As in MSF effluents, THM can also be present in RO effluents if it has formed prior to the dechlorination process step. The concentrations are much lower than for chlorine but toxic concentrations might be reached. Moreover, the chronic effects of THM are not known and synergic effects must be taken into consideration. THM is proven to have carcinogenic effects on animals (Lattemann and Höpner, 2008).

## **Antiscaling additives**

*Polyphosphats* were the earliest antiscaling agents but are on the retreat because of two main disadvantages. Their stability is reduced at temperatures above 90 °C which makes them impractical for most thermal applications. Furthermore, polyphosphates are major macronutrients which can cause eutrophication. As a consequence, algae growth rates may soar, leading to deteriorating raw water quality, frequent filter problems and a growing need for antifouling agents.

Today the most commonly used agents are *polymeric antiscalants*, particularly the agent Belgard EV. Typical dosages are 2 mg/l. Only one study about Belgard EV has been carried out reporting that no accumulation in algae and fish was detected and that the agent is ecologically safe (Höpner, 1999). Toxic concentrations are usually by an order of magnitude of 1-3 higher than typical dosage levels. However, considerable loads are discharged into the seas. An estimated antiscalant load of almost 62,000 kg/d is discharged into the Arabian Gulf (cf. Appendix C). Thus, the degradability rate of antiscalants becomes of environmental interest. Belgard EV is only degraded by 18 % in 35 days. Other agents reach much better degradation in the same time, e.g. Flocon 100 (52 % in 35 days). Substances with good biodegradability should be chosen in order to avoid possible long term effects. Polymeric antiscalants might reduce the concentrations of essential trace metal ions in the seawater, but this process is still not entirely investigated (Höpner and Lattemann, 2008).

Some RO plants also use *sulphuric acid or hydrochloric acids* at 20-100 mg/l in order to avoid scaling, resulting in a feed water pH of 6-7. The acidic solution should be neutralised as far as possible prior to discharge to the sea (pH  $\approx$  8.3).

## **Antifoaming additives**

Commonly used antifoaming agents are polyglycols and fatty acids with typical dosages of about 0.1 mg/l. The dosage depends mainly on the raw water quality and its seasonally changing organic composition. Antifoaming additives are considered non-toxic. Polyglycols have a good biodegradability. They can transform into a polymerised state which is more persistent in the environment, but due to the low concentrations used in desalination plants, polyglycols are of little concern for the marine environment (Lattemann and Höpner, 2003).

## **Corrosion products and anticorrosive additives**

Heavy metal discharge as a consequence of corrosion is a main concern in MSF desalination plants because of the high temperatures involved. Depending on the materials used for the heat exchanger tubes and vessels, copper, nickel, iron, zinc and other heavy metals are corroded and discharged (Höpner, 1999). The prevailing alloy for the heat exchanger tubes is copper-nickel which has poor corrosion resistance and accounts for the highest heavy metal pollution in MSF plants. In RO plants, non-metal materials and stainless steel are predominating. There are traces of iron, nickel, chromium and molybdenum in the RO effluent, but the concentrations remain non-critical.

The average *copper* background concentration of the oceans lies at a minimum of 0.1  $\mu\text{g/l}$ . Copper concentrations in MSF effluents were reported in the range of 15-100  $\mu\text{g/l}$ . The tolerance towards copper pollution is not yet entirely known for all species. Copper can be toxic at higher concentrations, causing enzyme inhibition in organisms and reducing growth and reproduction (Miri and Chouikhi, 2005). Although the discharged concentrations can be high above natural levels in the mixing zone, the risk of acute toxicity is generally low.

Instead, there is a higher risk of accumulation and long term effects. Copper compounds tend to settle down and accumulate in the sediments. They can be absorbed by benthic organisms and even be transferred into the food chain eventually. With respect to bioaccumulation, the discharged loads instead of the concentrations become the main point of concern.

*Nickel* is contained by up to 30 % in the Cu-Ni heat exchanger alloys and is less toxic than copper. No real data exists about discharge concentrations, but they are believed to be much lower than that of copper. The U.S. Environmental Protection Agency (EPA) calls for a maximum concentration of 8.2 µg/l for long term exposure. With proper dilution at the discharge point, most effluents are likely to reach this level after a short area around the outfall. Nickel is quite mobile in water, but the majority of the load will accumulate in the sediments around the outfall. Adverse effects of accumulation cannot be excluded.

It should be kept in mind that the corrosion rates will most likely increase during the process of *acid cleaning* although no specific data is available. Additionally, low pH values make the discharged metals more mobile and thus more harmful for the environment.

Stainless steel materials comprise mainly of *iron* and lower rates of *chromium*, *nickel* and *molybdenum*. The toxicity and overall discharge concentrations are believed to be harmless. Concentrations might augment through pitting and failing process control.

One strategy used to fight corrosion is to reduce the oxygen levels of water during the desalination process. Sodiumbisulfite, the chemical also used for dechlorination in RO processes, can be applied as oxygen scavenger in MSF plants. In water, sulfite is oxidised to sulfate which is a harmless seawater component. Other corrosion inhibitors like benzotriazole are particularly used during chemical cleaning (Lattemann and Höpner, 2003).

## Coagulants

The need for coagulation of suspended solids is an RO-specific problem. Ferric chloride at dosages of 1-30 mg/l or polyelectrolytes like polyacrylamide at about 1-4 mg/l are usually added to the intake water in order to enhance coagulation. The dosages are correlated to the amount of suspended particles in the water. In most plants, the agglomerated particles are filtered by media filters and periodically backwashed into the sea (Table 2). However, most new projects in Australia, California or Spain nowadays treat the backwash water by dewatering and thickening and dispose of the sludge in a landfill.

Coagulants are non-toxic in the concentrations applied in RO plants. Iron is a natural seawater constituent and polyacrylamide is a non-priority pollutant. Problems are only posed by the possible disturbance of photosynthesis processes due to an increase in turbidity during backwash of the coagulated sludge and by coagulant enrichment in sediments. The Ashkelon RO plant in Israel (330,000 m<sup>3</sup>/d) doses 3 mg/l of ferrous coagulant and produces a highly turbid, red coloured effluent during backwash which is effected every hour for 10-15 minutes. This might be eased by treating or diluting the backwash with feed water prior to discharge. Land deposition of the filtered sludge is an alternative but adds an estimated 1-5 US-cents/m<sup>3</sup> to the water price (Höpner and Lattemann, 2008).

## Chemical cleaning substances

Despite all pretreatment measures, RO membranes and MSF tubing systems and boilers are cleaned periodically in order to remove residual deposits. Acidic solutions (pH 2-3) are used to remove metal oxides, scales and inorganic colloids. Alkaline solutions (pH 11-12) are applied for removal of biofilms as well as organic and inorganic colloids. The necessary

volumes of cleaning solutions are higher for MSF plants, which only perform acidic cleaning. It must be assumed that in most cases, the spent cleaning solutions are discharged into the sea without treatment. This should at least be done by gradually mixing the cleaning solution with the brine.

The extreme pH values of cleaning solutions can be a threat to the marine ecosystem depending on the discharged volumes and the degree of degradation at the discharge point. LC<sub>50</sub> mortality for certain fish species in an HCl solution of pH 2-2.5 is reached after 48 hours. Residual acidity and alkalinity are usually quickly neutralised by seawater.

Other threats are posed by the additives which are dosed to the cleaning solutions. These differ according to the desalination process. When it comes to MSF plants, the chemical impacts are comparatively low as only corrosion inhibitors like benzotriazole are dosed. The concentrations discharged into the sea are difficult to estimate because dosages and discharge methods for cleaning wastes are unknown. Benzotriazole has low toxicity but is quite persistent and slowly degraded in seawater. It tends to adsorb at suspended matter in an acidic environment and thus can accumulate in the sediments. The tendency for accumulation in organisms, however, is low.

With regard to the chemical cleaning process of RO membranes, a much more diverse and more harmful mix of chemicals is used. The agents commonly recommended by most membrane manufacturers are:

- disinfectants like formaldehyde and isothiazole
- sulfonate detergents like sodium dodecylsulfate (NA-DDS)
- complexing agents like Ethylene Diamine Tetraacetic acid (EDTA)

Disinfectants are biocides used to remove biological films from membranes and are acutely toxic for the marine environment. In the case of formaldehyde, LC<sub>50</sub> levels of only 0.1 mg/l were found for certain species.

Detergents are used for the removal of colloids. They disrupt the intercellular membrane system in organisms. Toxicity is in the middle range, with LC<sub>50</sub> levels of NA-DDS ranging between 1-10 mg/l for many marine species. Pretty good degradability at 80% in a couple of days is documented.

Complexing agents reduce the water hardness and remove scale deposits. EDTA has low toxicity but is poorly degradable at only 5% in three weeks.

Although the RO cleaning volumes are much lower than the MSF volumes, the toxicity of its constituents makes RO cleaning solutions far more dangerous for the marine ecosystem (Lattemann and Höpner, 2003; Höpner and Lattemann, 2008).

The main effluent characteristics of RO, MSF and MED plants are summarized in Table 3. The cooling waters produced by the MSF and MED process were considered in the table, but not dilution with additional cooling waters from co-located power plants or dilution with wastewater treatment plant effluents.

# APPENDIX F: Review of Environmental Impact Assessments

The following list summarizes the reviewed information mainly taken from the internet<sup>1</sup> regarding published environmental impact assessments. Those projects especially considered a strong public involvement for the permitting process. The review discusses mainly two aspects: Field and modeling studies for brine discharges, and Bioassay studies: salinity tolerance and toxicity studies.

## California

- City of Carlsbad Desalination Project, California:  
<http://www.carlsbaddesal.com/EIR.asp>
- City of Huntington Beach Desalination Project, California  
<http://www.surfcity-hb.org/citydepartments/planning/major/poseidon.cfm>

## Australia

- Perth Desalination Project  
[http://www.watercorporation.com.au/D/desal2\\_per.cfm](http://www.watercorporation.com.au/D/desal2_per.cfm)
- Sydney Desalination Project  
<http://www.sydneywater.com.au/EnsuringtheFuture/Desalination/>
- Adelaide Desalination Project  
<http://www.sawater.com.au/SAWater/WhatsNew/MajorProjects/ADP.htm>
- Penneshaw Desalination Plant  
<http://www.sawater.com.au/SAWater/Education/OurWaterSystems/Desalination.htm>
- Olympic Dam Desalination Plant  
<http://www.olympicdameis.com/eis/index.htm>
- Melbourne Desalination Project  
[http://www.ourwater.vic.gov.au/ourwater/governments\\_water\\_plan/desalination\\_plant](http://www.ourwater.vic.gov.au/ourwater/governments_water_plan/desalination_plant)
- Gold Coast Desalination Project  
<http://www.desalinfo.com.au/Environment.asp>

## Field and modeling studies for brine discharges

This section gives an overview on the existing field and modeling studies that were carried for desalination plant discharges. It should be understood as an update and amendment of the information that was analysed in previous literature reviews (book by Lattemann and Höpner, 2003) and MEDRC project “Assessment of the Composition of Desalination Plant Disposal Brines” (project 98-AS-026, Hodgkiess et al. 2003).

### For desalination plants with a capacity of 100,000 m<sup>3</sup>/d or more

- ▶ *Carlsbad SWRO plant, California (in planning)*

The U.S. *Navy Coastal Water Clarity Model* was used to analyze the dispersal and dilution of the combined discharge from the Encina Power Plant and the planned Carlsbad SWRO plant

---

<sup>1</sup> The list does not claim to be complete. Naturally, the overview can only include those studies that are available in the public domain and that were prepared and published in English.

located in Southern California under average and extreme conditions (City of Carlsbad and Poseidon Resources, 2005; Jenkins and Wasy1, 2005). Under average conditions, the concentrate from the desalination plant (about 50 mgd or 189,271 m<sup>3</sup>/d with a salinity of 67) will be combined with an average cooling water discharge (526 mgd or 1.9 million m<sup>3</sup>/d of ambient salinity, i.e. 33.5), which is reduced under extreme conditions (254 mgd or 0.96 million m<sup>3</sup>/d).

*Under average conditions*, the end-of pipe salinity would be 36.5. Beyond the zone of initial dilution, in 300 m distance from the point of discharge, the salinity would be reduced to 34.4 near the bottom and 34.0 in the mid-water column. Under *extreme conditions*, the end-of pipe salinity would be 39. In 300 m distance from the point of discharge, the salinity would be reduced to 38.2 near the bottom and 35.2 in the mid-water column.

Based on relevant literature data and plant-specific salinity tolerance investigations (see further below), it is concluded that operation of the plant under typical conditions would not result in salinity levels in excess of 36.2 in the zone of initial dilution, and that this would not substantially affect any marine species. Short-term and episodic salinity levels below 40 as potentially caused during extreme conditions would also not have a substantial effect on species within the study area.

► *Perth SWRO plant, Australia*

The Perth desalination plant (144,000 m<sup>3</sup>/d) is located in Cockburn Sound, Western Australia. The baseline studies for the plant included concentrate modeling, water and sediment quality, macrobenthic surveys, sediment oxygen demand and whole effluent toxicity testing (Crisp et al., 2007).

The Western Australian guidelines for fresh and marine waters specify that the median increase in salinity is to be less than 5 % from background, which in marine environments is a change of about  $\Delta S=1.5$  (Wec, 2002). The criteria for the concentrate discharge set by the Western Australia Environmental Protection Authority require that salinity would be within 1.2 units above or below ambient levels within 50 m of the discharge point and within 0.8 units of background levels within 1,000 m of the discharge point.

The modeling results<sup>2</sup> show that the desalination discharge, through the use of a diffuser, will influence salinity only in the immediate vicinity of the discharge and in a very limited manner, meeting the proposed water quality criteria. The small changes in salinity predicted to occur over a relatively small spatial scale are assumed not be detrimental to the water quality in Cockburn Sound where greater changes in salinity occur over larger areas naturally, on a daily and seasonal basis. Field testing during the first year of operation, included tracing an environmentally benign dye (Rhodamine) added to the plant discharge, showed that the desalination discharge rapidly mixes with the surrounding waters. Furthermore, a real-time telemetered monitoring system was established which provides feedback on dissolved oxygen levels, conductivity and temperature (Crisp et al., 2007).

---

<sup>2</sup> The models used have included: 3 dimensional (3D) hydrodynamic Environmental Fluid Dynamics Code (EFDC), 1D box model, 3D hydrodynamic and dispersion model MIKE 3 (Danish Hydraulics Institute), 3D numerical model Estuary, Lake and Coastal Ocean Model (ELCOM) and 3D Computation Aquatic Ecological Dynamics Model (CAEDM).

In an earlier literature study from 2002 (Wec, 2002), the capacity of the local marine fauna and flora to tolerate the predicted levels of salinity were evaluated, using one meta-literature source (Walker, 1989) that reviewed available information on seagrass communities in Shark Bay, Western Australia. Shark Bay is a sheltered embayment with salinities naturally higher than those of ambient seawater, which also harbours two seagrass species common to Perth's Coastal Waters, *Posidonia australis* and *Posidonia amphibolis*. Physiological investigations of these species found maximum growth rates at a salinity of 42.5, and the densest covers of seagrass meadow in the region occurred at salinities between 40 and 50. It is concluded that the existing data, though limited, indicates that seagrasses and benthic organisms are tolerant and may potentially benefit from salinity levels of 40. Due to the small salinity increases caused by the Perth desalination plants, it is furthermore concluded that direct or indirect adverse impacts on seagrass meadows, reef or bare sand environments and associated biota are not to be expected. First results extensive real-time monitoring in Cockburn Sound in combination with annual marine habitat mapping (Crisp et al., 2007; Okely et al., 2007) will help to detect any real changes in the macrobenthic communities.

### **For desalination plants with capacity of less than 100,000 m<sup>3</sup>/d**

#### ▶ *SWRO plant in Maspalomas, Gran Canaria*

The mixing processes of brine discharges from the Maspalomas II (25,000 m<sup>3</sup>/d) plant in the south of Gran Canaria were investigated (Talavera and Ruiz, 2001). The brine discharge of this desalination plant is carried out by means of two outfalls. The brine with a volume of 17,000 m<sup>3</sup>/d and a salinity of 90 is discharged via two outfalls with a diameter of 30 cm and 60 cm respectively, which extend about 300 m into the sea. The discharge depth is about 7 m. The location is characterized by a sandy seafloor where no seagrass beds are present, since the depth and the marine dynamics impede their development. A high initial dilution of the brine is observed: the salinity decreased from 75 (near the outlet) to about 38.5 (measured near the seabed) and 37 (measured near the surface) within 20 m from the outfall, with a decrease to almost ambient salinity values (37) within 100 m distance.

#### ▶ *SWRO plant in Blanes, Spain*

The effect of brine discharge from a desalination plant in Blanes, Spain, on macrobenthic communities were investigated (Raventos et al., 2006). The plant has a capacity of about 27,400 m<sup>3</sup>/d and a concentrate discharge of about 32,900 m<sup>3</sup>/d with a salinity of 60. The concentrate is discharged via a diffuser (perforated pipe). Salinity decreased quickly with distance from the pipe, being back to ambient values within 10 m distance from the outlet pipe. Two controls and one supposedly impacted location were selected and visual censuses were carried out by scuba divers 12 times before and 12 times after plant operating. No significant variations attributable to the brine discharge were found. This was explained by the rapid dilution of the brine and the high natural variability that is characteristic of this type of habitat (i.e. the sandy substratum), which is sufficiently large to be able to mask possible alterations caused by the discharge. However, any such alterations stayed within the system's own natural variability range. It was noted that the results of the study do not necessarily mean that the brine discharge had no direct effects on the populations present, but only that any such effects could not be discerned in a statistically significant manner on a short-term basis. The absence of any observed impact could also be the result of affected area size or species mobility, but apparent effects were also not observed for certain sessile species.

#### ▶ *SWRO plant in Javea, Spain*

The effect of brine discharge from a desalination plant in Javea, on the Mediterranean coast of Spain, were investigated in Malfeito et al. (2005). The desalination plant has a capacity of 28,000 m<sup>3</sup>/d, which will be raised to 42,000 m<sup>3</sup>/d in the future. The seawater is taken in through 10 beach wells, each with a depth of 200 m. The brine is diluted with seawater, which is specifically taken in for this purpose from a nearby river mouth, in order to reduce salinity below 45. The mixed brine and seawater then flow into a holding tank before being discharged into a channel through 16 diffuser heads. The channel flows into the sea. The salinity of the combined discharge was on average 39.5 and often reached values of 44, depending on the salinity of the river which is influenced by freshwater runoff. Four surveys (two in summer, two in winter) were carried out to assess the effects of the discharge on salinity in the channel and the nearby sea area. The salinity was measured in surface water, near the seabed and in sediment pore water. Surface water salinities were increased within the channel but not in the sea outside the channel mouth, whereas an increase in bottom and interstitial water was observed to a maximum of 300 m distance from the mouth of the channel into the sea under calm operations. Monitoring of a seagrass meadow “in the area surrounding the [...] channel” and two control sites was carried out over a two year period. It was concluded that seagrass dynamics in the potentially affected and the two control sites was very similar. The salinity increase in the potentially affected site and the distance to the channel mouth were not specified. From graphs it can be estimated that bottom salinity in the sea area surrounding the channel mouth ranged between 38 and 40, with ambient values of around 37 in 300 m distance.

► *SWRO plant in Alicante, Spain*

Preliminary effects of brine discharge from a desalination plant in Alicante, on the Mediterranean coast of Spain, were investigated (Fernandez-Torquemada et al., 2005). The plant has an installed capacity of 50,000 m<sup>3</sup>/d and operates at a recovery of 40 %, producing a brine discharge of 75,000 m<sup>3</sup>/d with a salinity of 68. The feedwater is taken from beachwells. Discharge takes place on the southern shore of the harbor, which has been previously impacted by other activities. Three surveys have been done over the course of one year, involving a sampling grid of more than 100 salinity sampling stations in the vicinity of the outfall. Salinity depth profiles taken in a distance of 2 km from the discharge point showed increased salinities of 38.5 in intermediate water layers (12 m) in August and near the bottom (16 m) in February and April. Horizontally, it was found that dilution is high in the near field and low dilution rates in the far field, with bottom water salinity increases higher than 0.5 above average up to 4 km distance from the outfall. Echinoderms and *Posidonia oceanica* meadows have been monitored in three locations (one in front of the discharge, and two controls in 2 km distance to the north and to the south). Preliminary results from the first year of monitoring the benthic fauna show that echinoderms have disappeared from the meadow in front of the discharge and the southern control site. No regression of the seagrass meadow is observed, but a lower vitality of plants near the discharge has been observed. As salinity increments measured in the meadow in front of the desalination plant discharge are close to the ones that have produced significant effects on *Posidonia* growth and survival in other studies (Buceta et al., 2003; Fernandez-Torquemada and Sanchez-Lizaso, 2005), long-term impacts are deemed possible.

► *SWRO plant in San Pedro del Pinatar (Murcia), Spain*

Monitoring results from a SWRO desalination in San Pedro del Pinatar (Murcia, SE Spain) were presented (Fernández-Torquemada et al., 2007). The plant started operation in May

2005, progressively increasing the number of lines in operation to a total of 9 with a maximum production of 65,000 m<sup>3</sup>/d at an average recovery rate of 44 %. The intake water is supplied by wells that were constructed by horizontally directed drilling. The concentrate has a salinity of about 70. The main discharge pipe, which has a length of 5 km and discharges at a water depth of 35 m, was completed 8 months later. Between start-up and completion of the pipe, the brine was provisionally diluted with seawater and discharged near the coastline at 2 m water depth. A monitoring program was established to investigate brine dispersal and potential effects on *Posidonia oceanica* meadows in this time period. The meadows appeared in 4 m water depth and approximately 200 m from the discharge point. The seabed in front of the discharge was characterized by sandy sediments with a few patches of rocks. Before the concentrate discharge, salinity oscillated between 37.5 and 38 in the upper limit of the meadow, which increased to more than 39 when the plant began operation in May. As a result, the dilution of the brine before discharge was increased. No changes in the biological communities (*Posidonia oceanica*, *Dendropoma petraeum* and echinoderms) were detected over the 8 months period of the provisional monitoring program. No information was given on the characteristics of the new discharge site in 35 m water depths and the mode of dilution of the discharge.

► *Desalination plants in Cyprus*

The impact of the Dhekelia SWRO plant on marine macrobenthos in the nearby coastal waters were investigated over a two year period (1997-1998) (Argyrou, 1999). The production capacity of the plant was increased from 20,000 m<sup>3</sup>/d to 40,000 m<sup>3</sup>/d in that time, with the facility discharging an equal amount of brine with a salinity of about 70. The concentrate was initially disposed of into the coastal area at a water depth of less than 0.5 m and then via an outfall at 200 m distance from the shore and at about 5 m water depth. Seasonal and spatial variations in salinity were observed in Dhekelia Bay, which is an enclosed bay with low dispersion rates. Salinities up to 50 were observed in a limited area around the outfall diffuser, with salinities decreasing to ambient values of 39 within 200 m around the outfall. Before discharge started, the area close to the outfall was characterized by rocky substrate dominated by forests of the brown macroalgae *Cystoseira barbata*, within which other species of macroalgae were found. Salinity increases seriously impacted the phytobenthic assemblage, with *Cystoseira* forests vanishing from the area around the point of discharge. High salinities also had effects on macrofauna composition in the vicinity of the outfall. While the benthic community prior to the concentrate discharge consisted of 27 % polychaetes, 27 % echinoderms, 26 % scaphopods and 20 % gastropods, the only remaining taxa after construction were polychaetes (71 %) and the gastrops (29 %). However, these results are based on short-term investigations and a continuation of the monitoring is recommended. According to Tsiourtis (2001), monitoring results carried out every 6 months for 4 years at the Dhekelia site have shown that the situation around the outfall point is steady and confined to an area within a radius of 200 m.

A larger SWRO plant was constructed in 2002 in Larnaca with a production capacity of 54,000 m<sup>3</sup>/d and a similar amount of brine. Following the experience in Dhkelia, the discharge pipe was constructed 1,500 m long and 25 m below the surface. According to Marina Argiro (Cyprus Department of Fisheries), the first measurements conducted in the site point to good dilution conditions (Einav et al., 2002).

**For desalination plants with a capacity of less than 10,000 m<sup>3</sup>/d**

► *SWRO plant on Antigua Island, Caribbean*

A comprehensive study was conducted for a small desalination plant on Antigua Island in the Caribbean. The facility has a capacity of 5,000 m<sup>3</sup>/d and produces about 6,800 m<sup>3</sup>/d of concentrate. The intake salinity is about 35, and the discharge salinity about 57. The site was chosen for its near shore benthic community, which included expansive areas of seagrass (*Thalassia*), coral heads, and typical tropical fish and invertebrate species. Biological and water quality data was collected before concentrate discharge to the study area began. The discharge increased salinities within 10 m from the discharge point. After 3 months, a weak positive correlation was observed between the intensity of the discharge plume and abundance of the algae *Dictyota dichotoma*, which may either be due to nitrogen enrichment in the plume, which may have attributed to the desalination process by the concentrating effect of the process, or nutrient increases associated with filter backflushing. After 6 months, abundances of *Dictyota dichotoma* were lower than during the previous survey. Besides this, no discernible effects of the concentrate on density, biomass, and production of seagrass, or on benthic fauna or pelagic fish species was observed during the surveys after 3 and 6 months (Southwest Florida Water Management District, 1997).

► *SWRO plant on Formentera, Balearic Islands, Mediterranean*

The impacts of brine discharges from a small RO plant on seagrass meadows (*Posidonia oceanica*) were investigated in Gacia et al. (2007) over a time period of 6 years. The plant has a maximum discharge rate of 2,000 m<sup>3</sup>/d during summer and receives feedwater from the groundwater table, which is potentially enriched in nutrients from agriculture. The discharge characteristics thus differed considerably from ambient seawater, with (on average) salinity values around 50, a reduced pH (7.5), and high concentrations of dissolved inorganic carbon, orthophosphate, nitrates and nitrites. Environmental samples were taken from three transects that were perpendicular to the coastline. Salinity along the “impacted” transect varied between 37.8 and 39.8, and along the two supposedly unaffected reference transects between 37.4 and 37.6. The sediment pore water showed a greater increase in salinity than the water column, as well as in some areas where water salinity was unaffected at the time of measurement. It was therefore assumed that the brine influence can extend beyond the areas of increased water column salinity. The authors observed no extensive decline of seagrass meadows, but the meadow near the brine discharge showed characteristics significantly different from those of the reference transects, such as increased nitrogen content in the leaves and deterioration in plant health (reflected by high frequencies of necrosis marks and low total non-structural carbohydrates) as well as a higher epiphyte load. It is concluded that the effects stem from two factors: increased nitrogen and hypersaline conditions. Based on the observations, a critical salinity threshold of 39.3 is established, which is in good agreement with the salinity threshold of 39.1 established by (Fernandez-Torquemada and Sanchez-Lizaso, 2005) for *P. oceanica* based on experimental results. A measured change in ecosystem integrity was the absence of echinoderms, holothurians and sea urchins, which are considered to be environmentally sensitive species based on laboratory findings.

The impacts of brine discharges on *Posidonia oceanica* were also investigated in a two year study involving laboratory (15 day tank experiments) and field investigations of effects caused by a SWRO pilot plant on Formentera. It seems that the results presented in the above study (Gacia et al., 2007) and the following results presented in (Latorre, 2005) are partly based on the same original study. Results are as follows:

- Salinities of about 50 caused 100 % mortality in 15 days. Salinities around 45 caused about 50 % mortality. Variable results were observed at salinities of 43, 42.9 and 40,

which caused 20 %, 55 % and 27 % mortality, respectively. In the laboratory experiments, mortality was also frequently observed in water of ambient salinity (on average 8.5 %).

- At salinities of 48-50, no plant growth was observed. At a salinity of 43, growth rates were 50 % of the growth rates at natural salinity. At a salinity of 40-41, growth rates were on average reduced by 14 % compared to ambient.
- Plants exposed to a salinity of 43 were able to recover when returned to normal conditions.
- Mortality and diminished growth are also observed when only the basal part of the plants was exposed to hypersaline water.
- The increased nutrient levels of the discharge were assumed to be the cause of some of the observed effects on the meadows.

It was recommended to avoid *Posidonia oceanica* meadows, or when avoidance is not possible, to dilute the discharge salinity appropriately so that it exceeds a value 38.5 in no more than 25 % of the time and a value of 40 in no more than 5 % of the time.

► *SWRO plant in Marina Coast, California*

The Marina Coast desalination plant in California, a small SWRO plant with 1,000 m<sup>3</sup>/d capacity, receives feedwater from a deep beach well constructed 18-24 m below the beach. The plant operates at 52 % recovery and discharges the concentrate into an injection well on the beach, where it is diluted through mixing with natural ground water, and finally diffuses into the turbulent surf zone. An ongoing monitoring program conducted for several years after the plant went online in 1996 detected no increase in the receiving waters due to brine discharge (Damitz et al., 2006; Kinnetic Laboratories Inc., 1999).

## **Bioassay studies: salinity tolerance and toxicity studies**

This section gives an overview on the available laboratory studies that were carried out for concentrate discharges. It should be understood as an update and amendment of the information that was analysed in previous literature reviews (book by Lattemann and Höpner, 2003) and MEDRC project “Assessment of the Composition of Desalination Plant Disposal Brines” (project 98-AS-026, Hodgkiess et al., 2003).

► *Studies conducted for the SWRO plant in Carlsbad, California (in planning)*

Salinity tolerance investigations (City of Carlsbad and Poseidon Resources, 2005; Le Page, 2005) were conducted to evaluate the effects of increased salinity on species commonly found in the discharge site of the proposed desalination project and species considered to be sensitive to environmental stress and those species.

In a first comparative study, a collection of 18 marine species was held in an aquarium that contained a blend of desalination plant concentrate and power plant effluent with a salinity of 36, which is equal to the salinity that would occur within the zone of initial dilution during 95 % of the time (ambient salinity is 33.5). Organisms were monitored and evaluated for overall health based on qualitative parameters (appearance, willingness to feed, activity, and gonad production in the urchins) and compared to a second set of organisms held in a control tank. The quantitative parameters measured were percent weight gain/loss and fertilization success of the purple sea urchin (*Strongylocentrotus purpuratus*). During the 5½ month test no mortality was encountered. All organisms remained healthy and showed normal activity

and feeding behavior at a salinity of 36. Concerning the quantitative tests, no statistical significant difference in weight gain/loss to the control group was observed, and sea urchin spawning and fertilization was also successful.

The second study was a salinity toxicity study in which selected species of concern (purple sea urchin *Stronglyocentrotus purpuratus*, sand dollar *Dendraster excentricus*, and red abalone *Haliotis rufescens*) were kept at salinities of 37, 38, 39, and 40 over a 19 day period. These species were chosen due to their known susceptibility to environmental stress and the objective was to capture the biological effects of increased salinity that might occur during extreme operating conditions in the zone of initial dilution. Survival rate was 100 % at the end of the test in all test salinities. General observations showed that all individuals were behaving normally.

In addition to the salinity tolerance investigations, a toxicity testing study was carried out (City of Carlsbad and Poseidon Resources, 2005; MEC Analytical Systems, 2005), using RO concentrate and diluting it with seawater to a salinity of 36. Standard bioassay test were performed on giant kelp *Macrocystis pyrifera* (48 hours germination and growth test), topsmelt *Atherinops affinis* (7 day survival using 10-day old larva) and red abalone *Haliotis rufescens* (48 hour post fertilization embryonic development test). The results indicate that under worst case discharge conditions, the blend of cooling water and RO concentrate will not exhibit acute or chronic toxicity.

Based on the salinity tolerance and toxicity investigations and results from relevant literature, it is concluded that no significant effects are expected from the operation of the SWRO plants under normal and extreme conditions. Species found in the southern California bight have geographical ranges that extend into sub-tropical waters, which have higher salinity and temperature values than those expected to occur during normal and extreme operating conditions of the proposed desalination plant. Thus, many species living in the project area naturally experience a salinity range that is comparable to or greater than what is predicted for the combined discharge. Fishes, plankton and other pelagic species will also have a shorter exposure time than applied in the tests (City of Carlsbad and Poseidon Resources, 2005; MEC Analytical Systems, 2005).

EPA (1998) recommendations state that, in order to protect wildlife habitats, salinity variation from natural levels should not exceed 4 from natural variation in areas permanently occupied by food and habitat forming plants when natural salinity is between 13.5 and 35. The food and habitat forming plants located in the vicinity of the proposed project are found in the subtidal hard bottom habitat located to the north and to the south of the discharge channel. As applied to the proposed project, operational conditions that do not elevate salinities above 38.4 (34.4 upper limit of the natural variation in salinity plus 4) in the subtidal hard bottom habitat would appear to be fully protective of the food and habitat forming plants living in the discharge field (City of Carlsbad and Poseidon Resources, 2005; MEC Analytical Systems, 2005).

► *Studies conducted for the SWRO plant in Santa Barbara, California*

To evaluate potential impacts of brine discharges from the Santa Barbara RO plant in California, three representative benthic species were exposed to elevated salinity levels (Bay, 1993). Salinity samples were produced by mixing hypersaline brine with laboratory seawater. Brine was produced by freezing and partially thawing laboratory seawater. It is concluded that the desalination waste brine is not toxic to amphipods, kelp spores, or sea urchin embryo at concentrations expected to occur in the field. The single test results were as follows:

- Spore germination and tube growth of the giant kelp *Macrocystis pyrifera* were tested in five different salinities ranging from 34.5 to 43 (the end-point of 43 was much higher than salinities predicted by a dilution model for the discharge site of the plant). During the 48-hour test, no statistically significant effects were observed, i.e. elevated salinity did not affect kelp spore germination or tube length. The highest germination percentage occurred at a salinity of 38.5, the lowest at 36.5. Germ tube length of kelp spores was highest at moderate salinities of 35.5 to 38.5 and lowest at the highest salinity of 43, but the effect was not significantly different from the control.
- Ten day tests with amphipods (*Rhepoxynius abronius*) exposed to salinities of 34.5 to 38.5 also did not indicate any salinity effects and survival was only slightly reduced in the higher salinity vessels.

48-hour salinity tests with sea urchin embryos produced variable results. A salinity of 36.5 produced a small response, but a severe response was produced at 38.5. Based on the modeling results for the Santa Barbara plant, which predict that salinities greater than 35 outside the zone of initial dilution will occur less than 10 % of the time, impacts on sea urchin embryo are not expected to occur in the field. The test, however, confirms sea urchin sensitivity, which is considered among the most sensitive of marine embryos (Bay, 1993). The next most sensitive species is the scallop, where embryo development decreased 40 % following a 20 % increase in salinity (Bay, 1993; Tettelbach and Rhodes, 1981).

▶ *Studies conducted by the University of Alicante, Spain*

The effects of salinity on leaf growth and survival of the Mediterranean seagrass *Posidonia oceanica* were investigated by short-term mesocosms experiments (Fernandez-Torquemada and Sanchez-Lizaso, 2005). Plants collected from shallow meadows at Alicante with an ambient salinity of 36.8 to 38 were placed in tanks of different salinities between 25 and 57 for 15 days. Leaf growth was at a maximum at salinities between 25 and 39 and decreased significantly at a salinity of 39.1 and above. No growth was observed at a salinity of 50. Plants also sustained significant mortality at a salinity above 42 and below 29, with 100 % mortality at a salinity of 50. Necrotic tissues were evident in treatments with salinities higher than 42.5 or lower than 33.4. Plants surviving at salinity below 46 for 15 days were able to regain growth when they were returned to normal seawater salinity. Epiphyte biomass was highly variable and did not show a clear response to salinity. The authors summarize that elevated salinity led to a significant reduction in leaf growth at an increase of 1 unit over ambient and increased mortality at an increase of 4 units over ambient. By comparison with salinity tolerance data for other seagrasses (*Amphibolis antarctica*, *Posidonia australis*, *Thalassia testudinum*, *Halodule wrightii*), the authors conclude that *Posidonia oceanica* is one of the most sensitive species to high salinity and that meadows may be adversely impacted by salinity increases associated with brine discharge from desalination plants.

▶ *Research program funded by ACSEGURA and CEDEX, Spain*

Different studies were conducted within a research program funded by ACSEGURA and CEDEX and the results published in several journal articles (Buceta et al., 2003; Fernandez-Torquemada and Sanchez-Lizaso, 2005; Fernandez-Torquemada et al., 2005; Gacia et al., 2007; Latorre, 2005; Sánchez-Lizaso et al., 2008). An overview article (Sánchez-Lizaso et al., 2008) summarizes the main findings from the research program which consisted of three parts:

- Experimental work in the laboratory: a number of *Posidonia oceanica* shoots were maintained in 300 l tanks during 15 days under different controlled salinity treatments (salinity range: 23–57) (see also Fernandez-Torquemada and Sanchez-Lizaso, 2005).
- Experimental work in the field: 1 m<sup>2</sup> surface plots located in a natural stand of *Posidonia oceanica* were treated in situ over a period of three months with two different concentrations of a hypersaline water discharge obtained from a pilot desalination plant constructed (salinity of 39.2 ± 0.8 corresponding to a 1.5 unit increase and 38.4 ± 0.3 corresponding to a 0.7 unit increase over ambient salinity of 37.7 ± 0.1).
- Field surveys: study of the long term impact of desalination plant discharge on a *Posidonia oceanica* meadow in the Balearic Islands (Island of Formentera, see also Gacia et al., 2007; Latorre, 2005).

*Experimental work in the laboratory:*

- A salinity of 39.1 and above had significant effects on plant vitality (leaf growth etc.). Results were basically the same when the whole plant or only the basal part of the plant was exposed to hypersaline water.
- A salinity of 40 and above had significant effects on plant mortality. A salinity of 45 caused 50 % mortality after 15 days exposure.
- In some cases, plants exposed to short hypersaline episodes were able to recover their normal growth after being returned to normal salinity.

Increased mortality of the mysid *Letomysis posidoniae* and the sea urchin *Paracentrotus lividus* (which are often found in the seagrass meadows) was observed at a salinity 40.5-41.

*Experimental work in the field:*

- Increased plant mortality and lower plant vitality was observed in plots with brine treatment compared to the plots without treatment.

*Field surveys:*

- In the nearest area to the point of discharge (salinities from 38.4 to 39.8), a significant reduction in leaf size, an overload of epiphytes, a higher nitrogen and phosphorous concentration in tissues and higher herbivore activity was observed compared to unaffected areas. The effects are probably caused by eutrophication.
- In the far field (salinities from 37.8 to 39.3), no eutrophication symptoms were observed. The meadow did not show differences in shoot densities compared to reference sites; however, changes in the structural pattern of the shoot distribution, an increase in the frequency of necrosis marks in the leaves, and a significant lower abundance of the accompanying macrofauna compared to reference meadows were observed. The effects are probably due to salinity stress.

*Overall conclusions:*

- Due to the high sensitivity of *Posidonia oceanica* and associated fauna to salinity increases, brine discharges into areas containing these ecosystems should be avoided.
- In case avoidance is not possible, salinity should not exceed 38.5 in any point of the meadow for more than 25 % of the observations on an annual basis and not more than 40 in any point of the meadow for more than 5 % of the observations on an annual basis.
- The salinity thresholds require verification by further studies and are only applicable to *Posidonia oceanica* of the Western Mediterranean region.

- ▶ *Bioassay studies summarized from secondary sources (original studies could not be obtained).*

Buceta et al. (2003) investigated the effects of brine on local *Posidonia* meadows. Salinity increases caused growth reduction, permanent leaf fall, appearance of necrosis in the tissues, structural pattern changes of the seagrass meadow, decreased abundance of the accompanying macrofauna and increased mortality rates. The sensitivity of fauna frequently found in the *Posidonia* meadows (in particular *Leptomysis posidoniae* and the sea urchin *Paracentrotus lividus*) has also been investigated. Mortality generally increased with salinity, with statistically significant effects at salinity of 40 and above, while for salinities close to 45, 50 % of the plants died within the first 15 days. It has been recommended that salinity thresholds should not be given in terms of a referential value but as frequency distribution: for instance, at no point in the meadow should the salinity surpass a salinity of 38.5 in over 25 % of the measurements, or 40 in over 5 % of the measurements (from von Medeazza, 2005) based on (Buceta et al., 2003). Due to the lack of long-term observations, uncertainty remains whether the observed effects would be accumulative or synergic in chronic situation. Season, temperature, depth variability and light availability as well as other environmental components probably also alter the observed reactions. For instance, plants of greater depth seem much more sensitive. Also, the detrimental contribution of the above mentioned chemical agents (sporadically or permanently found in the effluent brine) remain poorly quantified (von Medeazza, 2005).

Studies were conducted by Gross (1957) on the response of several species of decapod crustaceans to osmotic stress gradients, in order to assess their ability to osmoregulate. One of the test organisms was the sand crab *Emerita analoga*, an inhabitant of sandy beaches. The species was found to have a narrow range of salinity tolerance (stenohaline). Tests were run using seawater salinities of 50, 75, 90, 110, 125, and 150 ‰, corresponding to standard seawater salinities of 17, 26, 31, 38, 44, and 52, respectively. Animals placed in 50 ‰ (salinity of 17) and 150 ‰ (salinity of 52) seawater concentrations died within about two hours of immersion, while those placed in 75 ‰ (salinity of 26) to 125 ‰ (salinity of 44) seawater concentrations were able to survive as long as 24 hours, thus demonstrating some ability to tolerate changes for a period of time (from Damitz et al., 2006).

Bioassay studies were conducted by ABA Consultants (1992) for the Sand City Plant in California. The studies investigated the effects of saline water (using elevated salinity treatments of 33, 38, 43, and 48) on the survival of two shallow subtidal beach species, the olive snail *Olivella pycna* and the sand dollar *Dendraster excentricus* which occur in shallow subtidal sands of the Monterey Bay. It was found that salinity concentrations at some level between 43 and 48 would become lethal to young sand dollars (10-15 mm diameter) but not to olive snails (3-4 mm length). The authors discuss other pertinent studies and conclude that measuring chronic effects to growth and reproduction as well as survival may be a better indication of salinity toxicity and therefore require a longer test (from Damitz et al., 2006).

Another series of bioassay tests was conducted on Japanese littleneck clams (*Venerupis [Ruditapes] philippinarum*), juvenile sea bream (*Pagrus major*), and marbled flounder (*Pseudopleuronectes yokohamae*) (Iso et al., 1993), using hypertonic solutions made from a commercial salt mixture and aerated tap water (from Damitz et al., 2006).

- The clams showed unimpaired behavior in a salinity of 50 or less. Lethal effects were observed after 48 hours in a salinity of 60, and after 24 hours in a salinity of 70.

- The juvenile sea bream survived well in salinities of 45 or less. In a salinity of 50, 25 % died within 24 hours. In a salinity of 70, all fish died after 1 hour.
- In an avoidance experiment, researchers slowly pumped colored solutions of different salinity concentrations into the bottoms of tanks holding juvenile sea bream in water of normal (33) salinity, thereby creating two layers of water in the tanks. The sea bream behaved normally in water up to and including salinities of 40. Between salinities of 45 and 70 the fish spent less and less time in the higher salinity water. The fish did not enter water with a salinity of 100.

Hatchability of eggs of the marbled flounder was successful at salinities up to 60 but dropped to zero at a salinity of 70, however, hatchability was delayed with increasing salinity between 31 and 60. Marbled flounder larvae survived with no ill effects in salinities up to 50. At a salinity of 55, mortality began to occur after 140 hours. In salinities between 60 and 100, the number of dead larvae increased in shorter periods of time.

## **APPENDIX G: Capacity Building Materials**

Homepage [www.brinedis.net.ms](http://www.brinedis.net.ms), containing:

- Short course materials
- Model manuals
- Calculators
- Papers and reports